Pharmaciana
Vol.14, No.2, July 2024, Page. 109-120
ISSN: 2088 4559; e-ISSN: 2477 0256
DOI: 10.12928/pharmaciana.v14i2.27393

Study of kinetic and adsorption isotherm of ibuprofen on MCM-41 synthesized with rice husk

Olyvia Azzahra Putri Hartono[1], Frida Octavia Purnomo[1*], Dyah Ayuwati Waluyo[1] Tunas Alam[2], Mohammad Jihad Madiabu[3]

[1]Department of Pharmacy, Faculty of Health Sciences and Technology, Binawan University, Jl. Kalibata Raya - Dewi Sartika, No. 25-30, East Jakarta, DKI Jakarta, Indonesia
[2]Department of Pharmacy, STIKes Prima Indonesia, Jl. Raya Babelan, Kebalen, Babelan, Bekasi, Jawa Barat, Indonesia
[3]Department of Analytical Chemistry, Politeknik AKA Bogor, Jl.Pangeran Soegiri, Tanah Baru, Bogor, Indonesia

ABSTRACT

Rice husk is one of the abundant wastes, especially in agricultural countries. Rice husk waste has a silica content of 95.80%, where the silica content can be utilized to make an adsorbent. One of the adsorbents that can be made is Mobil Composition of Matter 41 (MCM-41), a material with a hexagonal structure with a surface area to adsorb ibuprofen. Based on the results of the research that has been done, MCM-41 synthesized with rice husk has the same characterization results as MCM-41 synthesized with commercial materials tetraethyl orthosilicate (TEOS). Fourier Transform Infrared Spectroscopy (FTIR) characterization results show the absorption peak is at wave number 1068.58 cm-1 which shows asymmetric Si-O-Si stretching vibrations and at 799.60 cm^{-1} region is symmetric Si-O-Si stretching vibrations. X-ray diffraction (XRD) characterization results show an hexagonal crystal form at $2\theta = 20^{o}$-30^{o}. Scanning Electron Microscope (SEM) characterization results show particle of 2,664 μm. Based on the results of the research that has been done MCM-41 synthesized from rice husk can adsorb ibuprofen with Langmuir isotherm approach and Pseudo Second Order kinetics, and the maximum adsorbing capacity is 34.48 mg/g.

Keywords: ibuprofen, langmuir isotherms, MCM-41, pseudo second order

Corresponding author:
Frida Octavia Purnomo
Department of Pharmacy, Faculty of Health Sciences and Technology, Binawan University
Jl. Kalibata Raya - Dewi Sartika, No. 25-30, East Jakarta, DKI Jakarta, Indonesia
Email: fridaoctavia@binawan.ac.id

INTRODUCTION

Ibuprofen is a type of Non-Steroidal Anti-Inflammatory Drug (NSAID) that is acidic and has cohesive properties greater than adhesive properties. In these properties, which causes ibuprofen to be difficult to contact with other substances, especially water, so that ibuprofen is also a little difficult to make in certain dosage forms. Absorption of ibuprofen is rapid through the stomach with maximum levels in plasma reached after 1-2 hours, with a half-life in plasma of about 2 hours (Juwita et al., 2015). In general, ibuprofen is adsorbed with polymers, forming a solid dispersion with polymers that can increase solubility in water, for example polyvinyl pyrrolidone (PVP) K30 (Hasanah et al., 2015) .

The application of kinetic models is very useful for understanding the process of reaction rates, changes in the concentration of a reactant. Based on the chemical reaction process, the kinetic model is expressed by the rate of change of the quality constant (k) and the reaction order (n). The value of the constant is a specific parameter that depends on each condition. The value of the reaction order is theoretically unlimited, but the value ranges from 0-2, and is used in kinetic modeling. Kinetic parameters are used as the main benchmark to determine the advantages and disadvantages of a reactant (Priyanto, 2009).

Based on research (Ahda, 2015), MCM-41 can be used to adsorb ibuprofen. By utilizing the large surface area and pore size of MCM-41, it is expected that ibuprofen will enter and spread throughout the pores and surface area of MCM-41. This causes the active site area of ibuprofen to increase, so that the half-life of ibuprofen is longer. MCM-41 has a basic composition including cetyltrimethylammonium bromide (CTAB), tetraethyl orthosilicate (TEOS), NaOH, and HNO_3. TEOS, which is the silica source of the MCM-41 component, can be modified by synthesizing rice husk into MCM-41 itself.

The synthesis of MCM-41 with controlled size and porous structure has been carried out at laboratory scale. MCM-41 is the first material analyzed by Mobil Corporation. It features hexagonal mesoporous arrays that can be used for various applications in biosensors, drug loading and other fields that require large surface areas and porous materials. The hexagonal sized pores in MCM-41 are an advantage to this material as it has the ability to perform drug adsorption processes (Amalia et al., 2020).

Adsorption is a state in which a substance (molecule or ion) is adsorbed on the surface of an adsorbent. The mechanism of adsorption is described as the process by which molecules initially present in solution physically attach to the surface of an adsorbent. Molecules are adsorbed when the adhesive force between the adsorbate and adsorbent is greater than the cohesive force of each molecule. The adsorption process occurs at the surface. The more molecules that hit the surface of the sorbent, the more molecules are adsorbed (Wijayanti & Kurniawati, 2019).

In agricultural countries, rice husk waste is very abundant. The current utilization of rice husk is mostly only used as fertilizer. Rice husk waste is one of the wastes that has the largest silica content. The dry weight of rice husk that has undergone complete combustion contains 87%-97% silica. In addition to the abundance of rice husk waste, silica can be obtained from rice husk very simply and at relatively low cost by alkaline extraction (Handayani et al., 2014)

MATERIALS AND METHOD

Materials

The tools used are thermometer, reagent bottle, measuring pipette, beaker, erlenmeyer, spatula, weighing bottle, separatory funnel, oven, magnetic stirrer, bulb, and analytical balance. Other instrumentation equipment are centrifuge (OREGON LC-04R), X-Ray Fluoresence (XRF) (Panalytical Epsilon 3 XLE), X-ray diffraction (XRD) (XPERT PRO PANalytical PW3040/60), Scanning Electron Microscope (SEM) (Hitachi SU-3500), Fourier Transform Infrared Spectroscopy (FTIR) (UATR PerkinElmer Frontier C90704 Spectrum IR Version 10.6.1), and spetrofotometri UV-Vis (THERMO SCIENTIFIC Genesys 50).

The materials used in this study were rice husk, ibuprofen (IOL Chemical), isopropyl alcohol

(Merck), CTAB (Cetyltrimethylammonium bromide) (Merck), Sodium Hydroxide (NaOH) (Merck), Sulfuric Acid (H_2SO_4) (Technical), Nitric Acid (HNO_3) (Technical), and distilled water.

Methods

Preparation of rice husk MCM-41 synthesis

Silica extraction from rice husk was carried out by mixing 80 grams of rice husk with 600 mL of 2 M HNO_3 solution in a beaker and then allowed to stand at room temperature for 24 hours. Then the rice husk was washed with distilled water until pH 7. The washed rice husk was then put into the melting furnace and burned in a muffle furnace at 600°C for 6 hours. As a result of this combustion, rice husk ash was obtained. XRF characterization was then conducted to see the silica content of the rice husk. XRF analysis is carried out to quickly determine the elemental composition of a material/sample (Amalia et al., 2020).

Synthesis of MCM-41 with rice husk

The synthesis of MCM-41 begins with the preparation of Natrium Silicate (Na_2SiO_3) solution based on research (Usgodaarachchi et al., 2021) which has been modified, carried out by dissolving 2 g of rice husk ash with 100 ml of 3.5 M NaOH, then stirring vigorously with a magnetic stirrer for 5 hours at 80°C. The resulting solution that has been obtained is then filtered with Whatman filter paper (No. 1) until there is a colorless thick solution, which is determined as a Na_2SiO_3 stock solution.

The formation of silica MCM-41 was then made by sol-gel technique. The contents of solution A mixing 2.4 g CTAB dissolved in a solution of 25 mL isopropyl alcohol and 25 mL distilled water. Na_2SiO_3 stock solution was added dropwise into solution A, with vigorous stirring using a magnetic stirrer at 60°C until froth was obtained in the solution. Then concentrated H_2SO_4 drop by drop was added to solution A which already appeared foam until it reached pH 4. Stirring with a magnetic stirrer is done to form a gel, then stored for 12 hours at room temperature. Silica was then rinsed with distilled water, then filtered. The silica residue was then dried at 80°C for 12 hours. The results from the oven were then crushed to be calcined at 550°C for 4 hours. (Usgodaarachchi et al., 2021).

Characterization of MCM-41

Characterization of MCM-41 was done by XRD and FTIR testing. XRD is used to identify crystallized or amorphous materials and measure the crystalline compounds formed (Wirawan et al., 2018). SEM was performed to see the morphological structure of the MCM-41 surface (Prasetyo et al., 2013). FTIR is performed to identify compounds, detect functional groups, and analyze the analyzed mixtures and samples (Sari & Fajri, 2018).

Preparation of ibuprofen calibration curve

The preparation of the ibuprofen calibration curve begins with the preparation of a parent solution, namely 1000 ppm ibuprofen in 100 ml isopropyl alcohol. Furthermore, a dilution of the standard solution with a concentration of 300 ppm - 700 ppm in 25 ml of isopropyl alcohol was made. After making the solution, the wavelength was determined, using a concentration of 400 ppm. After obtaining the wavelength, absorbance measurements can be made in spectrophotometry UV-Vis.

Adsorption isotherm of ibuprofen on MCM-41

The maximum adsorption capacity of MCM-41 towards ibuprofen is determined through adsorption isotherms, for that it is necessary to first determine the weight of the adsorbent and the optimum contact time of ibuprofen adsorbed with MCM-41 adsorbent. Based on the modified research (Apriyanti et al., 2018), the determination was carried out by making ibuprofen solutions with concentrations of 400 ppm, 500 ppm, and 600 ppm in isopropyl alcohol mixed with 0.05 g of MCM-41. The mixing results were then stirred using a magnetic stirrer for 30 minutes at room temperature, then measured the absorbance using a Spectrophotometry UV-Vis. To determine the adsorption pattern of ibuprofen solution on the surface of MCM-41 adsorbent, it was determined through

Langmuir and Freundlich adsorption isotherm models. Adsorption isotherms were used to determine the adsorption mechanism of MCM-41 on ibuprofen. Liquid solid phase adsorption belongs to the Freundlich and Langmuir isotherm types. Determination of the use of a suitable adsorption isotherm model for MCM-41 on ibuprofen can be known by looking at the correlation coefficient (R2) which is close to the value of 1 (Nafi'ah, 2016).

This adsorption isotherm process occurs when a single layer is formed, based on the assumption that particle capacity is independent of position or adjacent positions. The Langmuir isotherm was presented in equation (1).

$$W = \frac{a.b.Ce}{1 + b.Ce} \quad \text{.....(1)}$$

The equation (1) can be linearly reduced to equation (2):

$$\frac{Ce}{W} = \frac{1}{a}Ce + \frac{1}{a.b} \text{.....(2)}$$

Description:
W = Adsorption effectiveness (mg/g)
B = Langmuir constant (mg/L)
Ce = Equilibrium concentration (residual concentration)
a = Maximum adsorption capacity or power

This adsorption isotherm process occurs in many layers and shows weak bonding. Adsorption under these conditions is called physical adsorption. This adsorption model shows that multiple layers can form due to the uniform surface of the adsorbent. The Freundlich Isotherm equation can be formulated as equation (3).

$$W = KCe^{\frac{1}{n}} \text{.....(3)}$$

The linear form of the above equation can be changed by taking its logarithmic form (4):

$$Log\, W = Log\, K + \frac{1}{n} Log\, Ce \quad \text{.....(4)}$$

Description:
W = Adsorption effectiveness (mg/g)
K = Maximum adsorption capacity or power (mg/g)
N = Adsorption constant
Ce = Solute concentration in solution after adsorption equilibrium is reached (mg/L)

Kinetics of ibuprofen on MCM-41

The adsorption kinetics of MCM-41 with ibuprofen was evaluated based on the Pseudo First Order (PFO) and Pseudo Second Order (PSO) reaction equations. The treatment to determine the adsorption kinetics was carried out on a solution of ibuprofen with a concentration of 500 ppm in isopropyl alcohol mixed with 0.05 g of MCM-41, then observed through Spectrophotometry UV-Vis with a variation of observation time of 30 minutes, for 2 hours (Nafi'ah, 2016).

PFO modeling describes the adsorption mechanism with a fast rate with a short time span

(Priyanto, 2009). The PFO model can be calculated by the equation (5):

$$In\ (q_e - q_t) = In\ qe - k_t t \quad \text{.....(5)}$$

Description:
q_e and q_t = Amount of ibuprofen absorbed at equilibrium at a given time (mg/g)
k_1 = Pseudo first order rate constant (min^{-1})
t =Time (min)

PSO modeling describes the adsorption mechanism on a relatively long time span with a slow process (Priyanto, 2009). The PSO model can be calculated with the equation (6):

$$\frac{t}{qt} = \frac{t}{k_2 qe^2} + \frac{t}{qe} \quad \text{.....(6)}$$

Description:
q_e and q_t = Amount of ibuprofen absorbed at equilibrium at a given time (mg/g)
K_2 = Pseudo second order rate constant (min^{-1})
t = Time (min)

Data Analysis

Data analysis was carried out on the results of XRD characterization using Origin software. In the SEM characterization results, data analysis was carried out using Images-J, Origin, and Microsoft Excel software. Microsoft Excel was also used to analyze the results of adsorption kinetics and isotherms by looking at linearity (R^2).

RESULT AND DISCUSSION

XRD Characterization Results of MCM-41

In this study, XRD characterization was carried out to determine the composite results of MCM-41 material synthesized with rice husk. The composite results of this characterization can be seen at the 2θ angle read, measurements were taken from the range 2θ = 0°-100° with the diffractogram results shown in Figure 1. The peak of the diffractogram of the read characterization results is 2θ = 25.4993°, which proves that the MCM-41 material forms amorphous crystals with an increasingly regular crystal arrangement. The increasingly regular form of crystal arrangement is caused by the loss of CTAB surfactant. In addition, the loss of CTAB surfactant in the calcination process of MCM-41 synthesis also supports this material to have smaller unit cells (Hasanah et al., 2018).

The results of XRD characterization in the form of diffraction diffractogram peaks show amorphous and hexagonal material curve profiles. The amorphous curve profile is mentioned in research (Izzati et al., 2013) where the amorphous material curve shows a wide peak curve, as well as a hexagonal curve profile. Furthermore, it is mentioned in research (Asral et al., 2022) where the hexagonal structure curve shows long 2θ small peaks, as in Figure 1 with a range of 2θ = 20°-30° showing a wide curve peak. The number of rows of peaks from the characterization results depends on the number of atoms or ions contained in the unit cell of the material. The diffraction pattern of each crystalline solid is very distinctive and depends on the crystal lattice, unit parameters, and X-ray wavelength used.

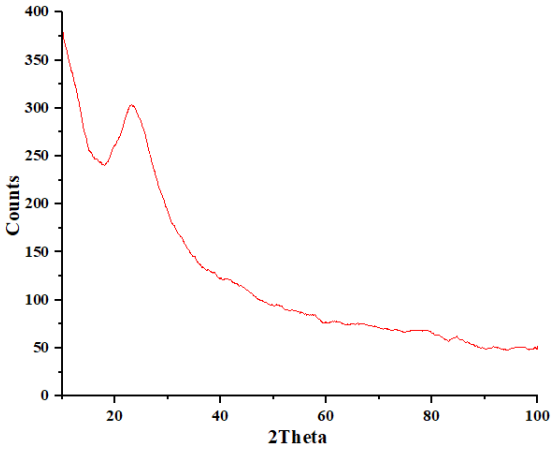

Figure 1. XRD characterization results of MCM-41

The amorphous hexagonal crystal shape in the XRD characterization results shows that the results of MCM-41 synthesis with rice husk are in accordance with the results of MCM-41 synthesis with commercial materials. Hexagonal crystals are characteristic of the shape of MCM-41, then amorphous crystals show that MCM-41 synthesized with rice husks has adsorption ability (Rahayu et al., 2020) .

FTIR characterization results of MCM-41

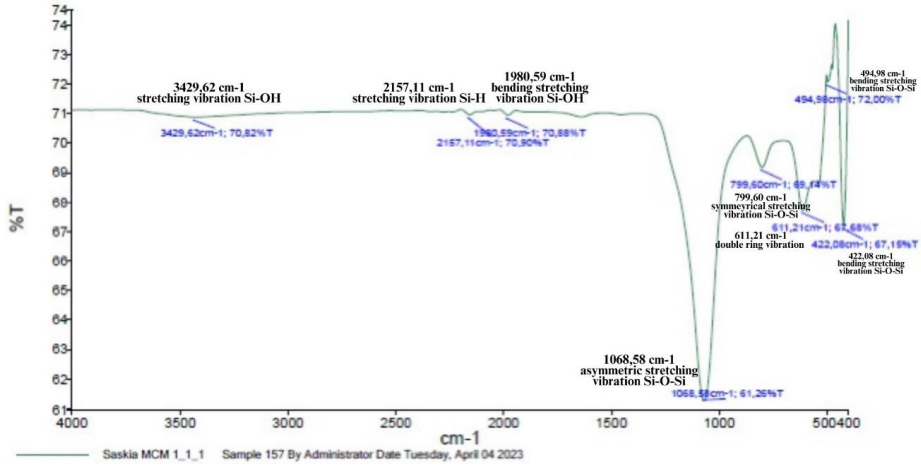

Figure 2. FTIR characterization results of MCM-41

In this study, FTIR characterization was carried out on MCM-41 material synthesized with rice husk, the absorption wave number in this characterization is 400 - 4000 cm^{-1} and the spectrum of the sample results is shown in Figure 2. FTIR results show typical absorption peaks for MCM-41 which has silica content, namely silanol (Si-OH) and siloxane (Si-O-Si). Some typical absorption spectra in silica materials are at 3429.62 cm^{-1} (Table 1) indicating the presence of asymmetric OH stretching vibrations from Si-OH (Rumiyanti et al., 2021). In the 2157.11 cm^{-1} region there is an absorption of Si-H stretching vibrations (Putrinesia et al., 2017). The bending stretching vibration of the Si-OH group of water is seen at 1980.59 cm^{-1} (Rumiyanti et al., 2021). The asymmetric Si-O stretching vibration of Si-O-Si is characterized by a wide and sharp peak at wave number 1068.58 cm^{-1} The same vibration also occurs in the 799.60 cm^{-1} region which indicates the symmetrical Si-O-Si stretching vibration (Hasanah et al., 2018).

Table 1. Vibration result of MCM-41

Wave Numbers (cm^{-1})	Indications
3429.62	Si-OH stretching vibrations
2157.11	Si-H bending vibration
1980.59	Si-OH bending stretching vibrations
1068.58	Si-O-Si asymmetric bending vibration
799.60	Si-O-Si symmetric bending vibration
611.21	Double ring vibration
494.98	Si-O-Si bending stretching vibration
422.08	Si-O-Si bending stretching vibration

In general, based on the FTIR results, the synthesized MCM-41 material with rice husk has a functional group match with MCM-41 synthesized with commercial materials. The results of the absorption peak in MCM-41 material are found at wave number 1068.58 cm^{-1} which shows asymmetric Si-O-Si stretching vibrations and in the 799.60 cm^{-1} region is a symmetrical Si-O-Si stretching vibration.

SEM characterization results of MCM-41

SEM characterization provides results in the form of three-dimensional images. The sample used for characterization in this study is MCM-41 synthesized from rice husk, with the results shown in Figure 3. The results of the characterization in Figure 3 are images of the morphological structure of the sample with a magnification of 1000x and voltage at 10 kV. Magnification and voltage used in characterization affect the clarity of the results.

In Figure 3 there are 2 views of the results seen from the same magnification and voltage, but from different detectors. The thing that distinguishes the image is the condition of the electrons that are not visible in Figure 3 (a) on the backscattered electron (BSE) detector, while in Figure 3 (b) the SE (secondary electron) detector the electrons are very clear. In research (Sujatno et al., 2017) explained the difference in appearance is due to the interaction of most of the electron beam managed to come back out, the electrons are referred to as BSE, a small part of the electrons enter the material then transfer most of the energy to the atomic electrons so that they bounce off the surface of the material, namely secondary electron (SE).

The results of SEM characterization on MCM-41 material synthesized with rice husk are hexagonal crystal morphology shape, where these results show the morphological shape that is in accordance with MCM-41 synthesized with commercial materials. The results of this characterization are then analyzed into digital data using Image-J digital data processing software, origin, and Microsoft excel to obtain particle distribution and size. Based on the results of the origin data analysis in Figure 3 (c), it can be obtained that the particle distribution of MCM-41 is well distributed, because it has R-Square (COD) = 0.99032. The average particle diameter size is analyzed using Microsoft excel, which can be seen that the average particle diameter size is 2.664 μm (Table 2).

Ibuprofen adsorption isotherm results with MCM-41

Quantitative determination of analyte concentrations in samples using chemical instruments can generally be done through calibration curves with acceptable linearity. A calibration curve is a straight-line (linear) graph showing the relationship between the concentration of the working solution, including blank values, and the proportional response of the instrument used (Wardhani & Nurbayanti, 2019).

The calibration curve was made on ibuprofen compounds that produce maximum absorbance at a maximum wavelength of 263.8 nm. Measurement of the wavelength of ibuprofen from isopropanol at 263.8 nm was then used as the basis for the appropriate wavelength to produce a calibration curve. The calibration curve for the relationship between the effect of ibuprofen concentration on absorbance showed linearity with a value of $R^2 = 0.9922$. These results indicate that concentration and absorbance

have a correlation. The linear regression equation follows the formula y = 0.0013 x - 0.0841. The equation has a slope of 1.434 and an intercept of 0.155 as shown in Figure 4

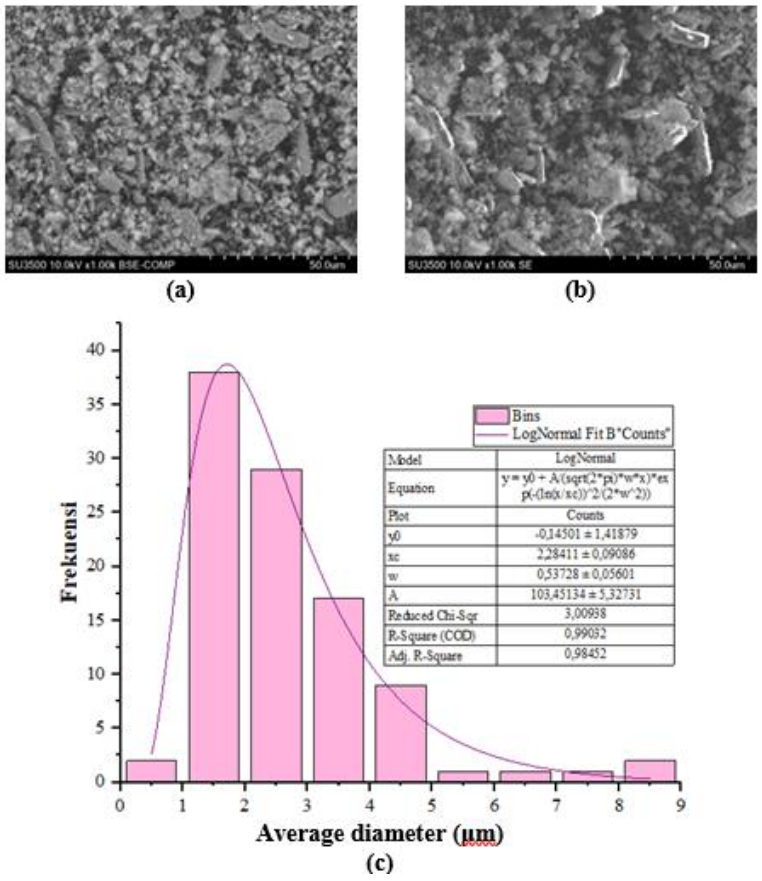

Figure 3. SEM characterization results of MCM-41 (a) detector BSE, (b) detector SE, (c) digital data analysis

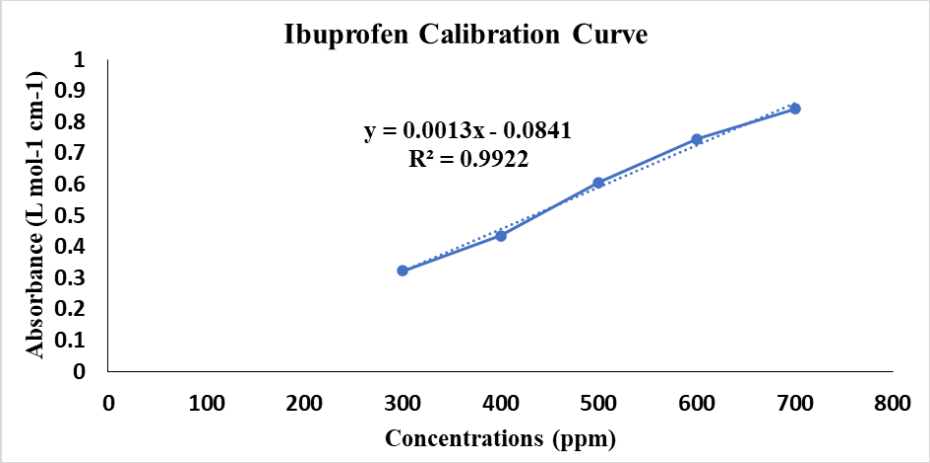

Figure 4. Ibuprofen calibration curve

Table 2. Average particle diameter calculation results

Sample	Average Diameter (µm)
MCM-41from Risk Husk	2.664

Ibuprofen adsorption isotherm results with MCM-41

Based on the calibration curve, the concentration range that can be used for adsorption isotherm testing is in the range of 300 ppm - 700 ppm. In this study, the ibuprofen concentrations used were 400 ppm, 500 ppm, and 600 ppm, while the amount of MCM-41 used was 0.05g. Adsorption isotherm measurements were carried out on UV-Vis spectrophotometry, the results of which can be seen in Figure 5 (a) and (b).

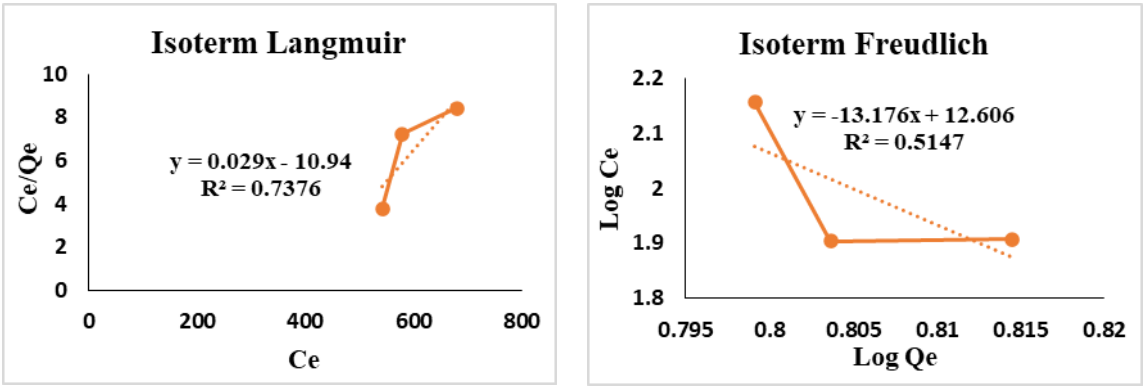

(a) **(b)**

Figure 5. Adsorption isotherm curve (a) Langmuir isotherm, (b) Freundlich isotherm

Based on the adsorption isotherm results in Figure 5 (a) and (b), it can be seen that the highest correlation coefficient (R^2) value is the Langmuir isotherm. This indicates that the adsorption of ibuprofen by MCM-41 has a Langmuir isotherm approach, with a maximum adsorption capacity of 34.48 mg/g. In previous research, which discussed the adsorption of tapioca liquid waste by MCM-41, the maximum capacity of absorption was 15.923 mg/g (Darmansyah et al., 2016). So that the adsorption of ibuprofen by MCM-41 synthesized from rice husk is better than the adsorption of tapioca liquid waste by MCM-41.

Langmuir isotherm is an adsorption process that occurs in a chemisorption monolayer. Chemisorption is the adsorption or attachment of molecules, ions or atoms to the surface to prevent the penetration of water molecules (Hasran et al., 2021). According to research (Nurhasni et al., 2014), on the Langmuir isotherm the adsorbent surface has homogeneous active sites that are proportional to the surface area. Each active site can only adsorb one adsorbate molecule so that adsorption will only be limited to the formation of a single layer (monolayer), while the Freundlich isotherm is a process that occurs by physisorption of many layers.

In this study ibuprofen is the adsorbate, and MCM-41 is the adsorbent. Based on the Langmuir isotherm approach, Ibuprofen is adsorbed with MCM-41 irreversibly where the absorbance increases, following the amount of adsorbent addition. The addition of MCM-41 as an adsorbent for ibuprofen, can form ibuprofen to be more stable absorption. In addition, the addition of MCM-41 to ibuprofen can also increase the surface area of ibuprofen (Jamburidze et al., 2019). The large particle surface area causes the particle contact surface with water to be large so that the solubility of particles in water increases (Ferdiansyah et al., 2018).

Results of ibuprofen adsorption kinetics with MCM-41

In this study, the concentration of ibuprofen used was 500 ppm, with the amount of MCM-41 addition used being 0.05 g. Measurement of adsorption kinetics was carried out on UV-Vis spectrophotometry, the results of which can be seen in Figure 6 (a) and (b).

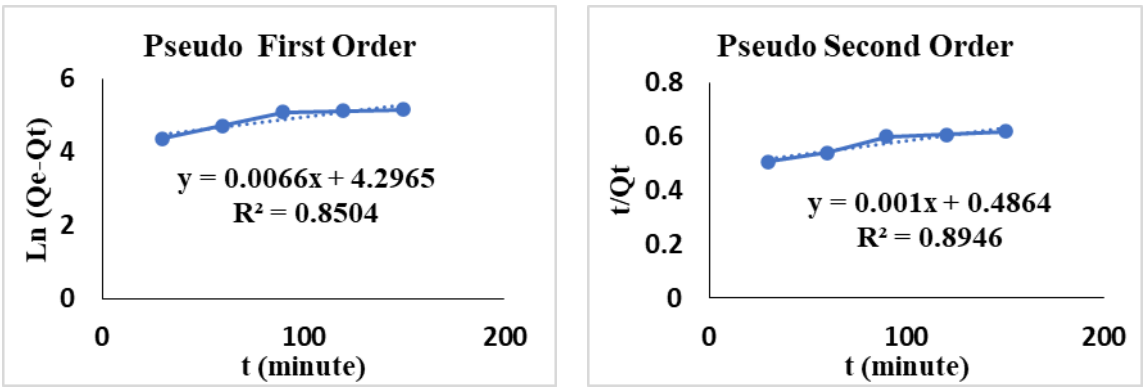

(a) **(b)**

Figure 6. adsorption kinetics curves (a) pseudo first order, (b) pseudo second order

Based on the results of adsorption kinetics in Figures 6 (a) and (b), it can be seen that the highest correlation coefficient (R^2) value is in Pseudo Second Order. This indicates that the kinetics of ibuprofen adsorption by MCM-41 has an approach to the Pseudo Second Order. In previous studies, which discussed the adsorption of methylene green with MCM-41 also showed the same approach, namely Pseudo Second Order (Alardhi et al., 2020).

The Pseudo Second Order adsorbs kinetics model can be used to predict the speed of transfer from the adsorbate solution to the designed adsorbent (Kurniawati et al., 2016). The Pseudo Second Order kinetics model is modeling based on the ability of absorption in the solid phase with the chemisorption mechanism being the controlling factor of adsorption speed (Nuansa & Istyanti, 2013). The Pseudo Second Order kinetics model depends on the adsorption capacity of each solid phase. If it is assumed that the adsorption capacity is proportional to the number of active sites on the adsorbent (Kurniawati et al., 2016).

Based on the Pseudo Second Order approach, ibuprofen adsorption with MCM-41 has a long contact time, following the amount of adsorbent addition (Revellame et al., 2020). This is related to the Langmuir isotherm approach, where the absorbance of ibuprofen also increases in Pseudo Second Order kinetics. The Pseudo Second Order kinetics model is a suitable kinetics model for ibuprofen because the adsorption process can be applied to the process at any time (Revellame et al., 2020).

CONCLUSION

Rice husk that has been activated with HNO_3 has a high silica content so that it can be utilized for the synthesis of MCM-41 which can be used for ibuprofen adsorption. Based on the results of FTIR characterization, MCM-41 material synthesized with rice husk has an absorption peak at wave number 1068.58 cm^{-1} which shows asymmetric Si-O-Si stretching vibrations and in the 799.60 cm^{-1} region is symmetrical Si-O-Si stretching vibrations. In XRD characterization, it is proven that the crystal form of MCM-41 is amorphous hexagonal which has been proven in the analysis where in the $2\theta = 20^o$-30^o area the shape of the curve widens and other small peaks. In the SEM analysis that has been through digital data processing, it is mentioned that the particles are well distributed, with an average particle size of 2.664. Ibuprofen adsorption kinetics model with MCM-41 synthesized with rice husk is pseudo second order model. The adsorption isotherm of Ibuprofen with MCM-41 synthesized with rice husk is Langmuir isotherm, with the maximum capacity of Ibuprofen adsorption with MCM-41 of 34.48 mg/g.

REFERENCES

Ahda, M. (2015). Aplikasi silika Mcm-41 sebagai material berpori dalam adsorpsi ibuprofen. *Media Farmasi*, *Vol 12*(No.2), 152–163. https://doi.org/10.12928/mf.v12i2.3754

Alardhi, S. M., Alrubaye, J. M., & Albayati, T. M. (2020). Adsorption of methyl green dye onto

MCM-41: Equilibrium, kinetics and thermodynamic studies. *Desalination and Water Treatment*, *179*, 323–331. https://doi.org/10.5004/dwt.2020.25000

Amalia, R. F., Purwaningsih, H., Susanti, D., & Pratiwi, V. M. (2020). Analisis pengaruh rasio pelarut etanol terhadap kinerja nanopartikel silika mesopori dari sekam padi sebagai material pengantar obat. *Jurnal Teknik ITS*, *9*(1), 66–71. https://doi.org/10.12962/j23373539.v9i1.50395

Apriyanti, H., Candra, I. N., & Elvinawati, E. (2018). Karakterisasi isoterm adsorpsi dari Ion Logam Besi (Fe) pada tanah di Kota Bengkulu. *Alotrop*, *2*(1), 14–19. https://doi.org/10.33369/atp.v2i1.4588

Asral, S. S. T., Adfa, M., & Yudha, S. (2022). *Perkembangan sintesis MCM-41 berbasis sumber daya alam dan aplikasinya: sebuah telaah pustaka*. *2*(1), 122–127. https://doi.org/10.33369/rjna.v2i1.24444

Darmansyah, D., Ginting, S., Ardiana, L., & Saputra, H. (2016). Mesopori MCM-41 sebagai adsorben: kajian kinetika dan isotherm adsorpsi limbah cair tapioka. *Jurnal Rekayasa Kimia & Lingkungan*, *11*(1), 10–16. https://doi.org/10.23955/rkl.v11i1.4228

Ferdiansyah, R., Putri, Y. D., Hamdani, S., & Julianto, A. (2018). Peningkatan Kelarutan dan Disolusi Ibuprofen melalui Pembentukan Mikropartikel Metode Emulsification-Ionic-Gelation menggunakan Polivinil Alkohol (PVA) sebagai Polimer Tripolifosfat (TPP) sebagai Agen Crosslink. *Indonesian Journal of Pharmaceutical Science and Technology*, *4*(3), 118. https://doi.org/10.15416/ijpst.v4i3.13864

Handayani, P. A., Nurjanah, E., & Rengga, W. D. P. (2014). Pemanfaatan limbah sekam Padi menjadi Silika Gel. *Jurnal Bahan Alam Terbarukan*, *3*(2), 55–59. https://doi.org/10.15294/jbat.v3i2.3698

Hasanah, N., Sutarni, & Kunarti, E. S. (2018). Characteristic study of the MCM-41 Modified with Zn by Direct Synthesis. *JKPK (Jurnal Kimia Dan Pendidikan Kimia)*, *3*(3), 183. https://doi.org/10.20961/jkpk.v3i3.22808

Hasanah, U., Ardana, M., & Rusli, R. (2015). Pengaruh PH medium terhadap disolusi ibuprofen dengan metode dispersi padat. *Prosiding Seminar Nasional Kefarmasian*, *1*, 5–6. https://doi.org/10.25026/mpc.v1i1.15

Hasran, M. A. R., Imam, D. N. A., & Sunendar, B. (2021). Addition of Rice Husk Nanocellulose To the Impact Strength of Resin Base Heat Cured. *Journal of Vocational Health Studies*, *4*(3), 119. https://doi.org/10.20473/jvhs.v4.i3.2021.119-124

Izzati, H. N., Nisak, F., & Munasir. (2013). Sintesis dan karakterisasi kekristalan Nanosilika berbasis pasir Bancar. *Inovasi Fisika Indonesia*, *2*(03), 19–22.

Jamburidze, A., Huerre, A., Baresch, D., Poulichet, V., De Corato, M., & Garbin, V. (2019). Nanoparticle-Coated Microbubbles for Combined Ultrasound Imaging and Drug Delivery. *Langmuir*, *35*(31), 10087–10096. https://doi.org/10.1021/acs.langmuir.8b04008

Juwita, D. A., Noviza, D., & Erizal, D. (2015). Perbandingan efek antipiretik antara Ibuprofen dengan campuran Ibuprofen dan Kafein. *Jurnal Farmasi Indonesia*, *7*(4), 223–227.

Kurniawati, P., Wiyantoko, B., Kurniawan, A., & Purbaningtias, T. E. (2016). Kinetic study of Cr(VI) Adsorption on Hydrotalcite Mg/Al with Molar Ratio 2:1. *Eksakta*, *13*(1–2), 11–21. https://doi.org/10.20885/eksakta.vol13.iss1-2.art2

Nafi'ah R. (2016). Kinetika Adsorpsi Pb (II) dengan Adsorben Arang Aktif dari Sabut Siwalan. *Jurnal Farmasi Sains Dan Praktis*, *I*(2), 28–37.

Nuansa, C. G., & Istyanti, D. T. (2013). *Kinetika Adsorpsi Kolesterol Daging Kambing Kinetika Adsorpsi Kolesterol Daging Kambing Menggunakan Adsorben Kitosan Dan Karbon Aktif*. *2*(2), 18–24.

Nurhasni, Hendrawati, & Saniyyah, N. (2014). Sekam padi untuk menyerap ion logam tembaga dan timbal dalam air limbah. *Jurnal Kimia Valensi*, *4*(1), 36–44.

Prasetyo, A., Nafsiati, R., Kholifah, S. N., & Botianovi, A. (2013). Analisis permukaan zeolit alam Malang yang mengalami modifikasi pori dengan uji Sem-Eds. *Sainstis*. https://doi.org/10.18860/sains.v0i0.2306

Priyanto, G. (2009). Aplikasi Model Kinetika Dalam Pengembangan Produk Baru. *Dinamika*

Penelitian BIPA, *20*(35).

Putrinesia, M. I., Nurlina, & Rahmalia, W. (2017). Sintesis dan karakterisasi komposit polianilin / silika gel. *Jurnal Kimia Khatulistiwa*, *6*(2), 89–95.

Rahayu, Y. S., Astuti, Y., & Prasetya, E. F. (2020). Identifikasi ekstasi/MDMA menggunakan analisis tes warna dan gas Chromatography-Mass Spectrometry (GCMS). *Jurnal Sains Dan Edukasi Sains*, *3*(2), 38–45. https://doi.org/10.24246/juses.v3i2p38-45

Revellame, E. D., Fortela, D. L., Sharp, W., Hernandez, R., & Zappi, M. E. (2020). Adsorption kinetic modeling using pseudo-first order and pseudo-second order rate laws: A review. *Cleaner Engineering and Technology*, *1*(October), 100032. https://doi.org/10.1016/j.clet.2020.100032

Rumiyanti, L., Destiana, C., Oktaviani, R., Sembiring, S., Syafriadi, & Juliasih, N. L. G. R. (2021). Pengujian gugus fungsi Silika berbasis sekam padi dengan variasi suhu & konsentrasi Cetyltrimethylammonium Bromide sebagai bahan baku Mesoporous Silica. *Jurnal Teori Dan Aplikasi Fisika*, *9*(2), 153–158. https://doi.org/10.23960/jtaf.v9i2.2727

Sari, N. W., & Fajri, M. Y. (2018). Analisis fitokimia dan gugus fungsi dari ekstrak etanol Pisang Goroho Merah (Musa Acuminate (L)). *Indonesian Journal of Biotechnology and Biodiversity*, *2*(1), 30–34.

Sujatno, A., Salam, R., Bandriyana, B., & Dimyati, A. (2017). Studi Scanning Electron Microscopy (Sem) Untuk Karakterisasi Proses Oxidasi Paduan Zirkonium. *Jurnal Forum Nuklir*, *9*(1), 44. https://doi.org/10.17146/jfn.2015.9.1.3563

Usgodaarachchi, L., Thambiliyagodage, C., Wijesekera, R., & Bakker, M. G. (2021). Current research in green and sustainable chemistry synthesis of mesoporous silica nanoparticles derived from rice husk and surface-controlled amine functionalization for ef fi cient adsorption of methylene blue from aqueous solution. *Current Research in Green and Sustainable Chemistry*, *4*(March), 100116. https://doi.org/10.1016/j.crgsc.2021.100116

Wardhani, D. S., & Nurbayanti, I. (2019). Uji linieritas kurva kalibrasi deret standar N-NH3 pada rentang konsentrasi yang berbeda secara Spektrofotometri. *Buletin Teknik Litkayasa Akuakultur*, *17*(1), 5–8.

Wijayanti, I. E., & Kurniawati, E. A. (2019). Studi Kinetika Adsorpsi Isoterm Persamaan Langmuir dan Freundlich pada Abu Gosok sebagai Adsorben. *EduChemia (Jurnal Kimia Dan Pendidikan)*, *4*(2), 175. https://doi.org/10.30870/educhemia.v4i2.6119

Wirawan, R., Wibowo, M. A., Mahyarudin, & Rahmayanti, S. (2018). Uji aktivitas antibakteri minyak atsiri kulit Jeruk Pontianak (Citrus nobilis Lour. var . microcarpa) terhadap bakteri Staphylococcus epidermidis. *Jurnal Cerebellum*, *4 (2)*, 1025–1036.

Pharmaciana
Vol.14, No.2, July 2024, Page. 121-132
ISSN: 2088 4559; e-ISSN: 2477 0256
DOI: 10.12928/pharmaciana.v14i2.28097

Controlled release kinetics of furosemide from chitosan matrix tablets with hydroxypropyl methylcellulose phthalate coated

Samran[1*], Suprianto[1], Sumardi[1], Ahmad Hafizullah Ritonga[1], Melati Yulia Kusumastuti[2]

[1]Institut Kesehatan Medistra Lubuk Pakam, Deli Serdang,
Jl. Sudirman No. 38, Petapahan, Lubuk Pakam District, Deli Serdang Regency, Sumatera Utara, Indonesia
[2]Sekolah Tinggi Ilmu Kesehatan Indah Medan,
Jl. Saudara Ujung No.113-129, Sudirejo II, Medan, Sumatera Utara, Indonesia

Submitted: 30-12-2023 ***Reviewed: 03-04-2024*** ***Accepted: 20-04-2024***

ABSTRACT

Sustained-release dosage forms were critical in drug delivery, ensuring controlled and prolonged release for optimal therapeutic outcomes. Chitosan (CH) has become pivotal in sustained-release tablet formulation due to its biocompatibility and mucoadhesive properties. This study aims to explore the release kinetics of furosemide (FS) from CH matrix tablets in a concurrent medium. The formulation involves a core tablet and coated tablet, with CH matrix as a binder and Hydroxypropyl Methyl Cellulose Phthalate (HPMCP) as a film-coated for the core tablet, and both are made using the wet granulation method. Assessment parameters include tablet hardness, disintegration, and FS release profiles across various media, analyzed using spectrophotometric methods to comprehend drug release kinetics with multiple models such as zero-order, first-order, Higuchi, and Korsmeyer-Peppas employed. In the press-coated tablet comprising core tablet CH as matrix uncoated with 20 mg CH per tablet core, a zero-order release pattern emerged in the pH 1.2 medium within 0-2 h, which displayed first-order release kinetics within 2-6 h and 6-16 h in concurrent media of pH 5.8 and 7.4. Notably, a zero-order release pattern emerged in the pH 1.2 medium within 0-2 h. Press-coated tablets incorporating CH matrix with HPCMP coated (CH-HPCMP), also containing 20 mg CH per tablet, exhibited diverse drug release kinetics. These tablets showed Korsmeyer-Peppas, zero-order, and first-order kinetics in pH 1.2, 5.8, and 7.4, respectively. The study suggests that a Press-coated tablet incorporating CH-HPMCP is suitable as the candidate for sustained-release formulations. The observed versatility in release kinetics across varying pH environments underscores the potential adaptability of these formulations in addressing diverse therapeutic needs.

.

Keywords: press-coated tablet, controlled release, furosemide, chitosan, HPCMP

Corresponding author:
Samran
Faculty of Pharmacy, Institut Kesehatan Medistra Lubuk Pakam
Jl. Sudirman No. 38, Petapahan, Lubuk Pakam District, Deli Serdang Regency, Sumatera Utara, Indonesia
Email: samranamatrejo@gmail.com

INTRODUCTION

In disease therapy, conventional preparations are often administered three times a day. This approach releases drugs from the matrix, is absorbed, and promptly enters systemic circulation (Murugesan et al., 2020; Sharma et al., 2019). Conventional drug delivery systems (CDDS) had limitations: poor absorption from the target site, poor bioavailability, high first-pass metabolism, fluctuations in plasma drug levels, premature excretion from the body, repeated dosing, and high dumping dose (Adepu & Ramakrishna, 2021). However, advancements in science and technology have prompted pharmacists to modify drug release systems to overcome CDDS (Jain, 2020; Sharma et al., 2019). Currently, drug release does not occur instantly but is controlled through a matrix system. This system is utilized in developing drug release from solid dosage forms with sustained, prolonged, or time-based release methods (Jain, 2020; Murugesan et al., 2020). Controlled-release products promise more optimal disease therapy by regulating drug levels in plasma, reducing side effects, and controlling fluctuations in drug levels, albeit at higher costs (Mandhar & Joshi, 2015; Mehta et al., 2021). This development often involves various additives to create controlled-release preparations. Generally, these additives act as protective matrices to slow down drug release gradually (Hanna & Saad, 2019; Qu & Luo, 2020). The nature of these additives as protective agents influences the characteristics of controlled dosage forms (Sacco et al., 2018). It can adhere to various drug release kinetics models such as zero order, first order, Higuchi, and Korsemeyer-Peppas. Ideally, the model follows zero-order drug release kinetics to ensure stable drug levels in plasma (Murugesan et al., 2020; Suprianto, 2016).

Matrices based on various polymer types like polyethylene (PE), polyvinyl chloride (PVC), ethyl cellulose (ES), and polyacrylate (PA) are mixed with drugs and printed into tablets, allowing controlled drug diffusion (Mehta et al., 2021; Sharma et al., 2019). Drug release behavior from controlled dosage forms can be enhanced using hydrophilic matrices such as methylcellulose (MC), hydroxypropyl methylcellulose (HPMC), hydroxypropyl cellulose (HPC), xanthan gum (XG), sodium alginate (SA), carbomer (CB), and chitosan (CH). Lipid groups also play a role in creating controlled preparations, for instance, a combination of carnauba wax with stearyl alcohol or stearic acid (Pathak et al., 2023).

Biodegradable and non-biodegradable polymer-based matrices are crucial in controlled product development (Kamaly et al., 2016; Mehta et al., 2021). These matrices can degrade by enzymes or non-enzymes, becoming metabolizable monomers, such as glycolic acid (GA), lactic acid (LA), and ethylene vinyl acetate (EVA) (Wu et al., 2020; Yadav et al., 2021). Additionally, hydrogel matrices also contribute significantly to controlled product development, for example, hydroxyethyl methacrylate polymer (HEMA), vinyl alcohol (VA), vinylpyrrolidone (VP), ethylene oxide (EO), and acrylamide (AA) (Yadav et al., 2021). One frequently used substance is chitosan, derived from the deacetylation of chitin found in crustacean shells. Chitosan is a cationic polymer generated from D-glucosamine replication with N-acetyl-D-glucosamine through glycosidic bonds (Sacco et al., 2018; Wu et al., 2020). Due to its good biocompatibility, non-toxicity, biodegradability, low production cost, and abundant natural availability, chitosan finds extensive use in controlled preparation development (Idacahyati et al., 2020; Shao et al., 2015). Chitosan's ability to control drug release via gel formation has been studied (Liu et al., 2018; Shariatinia & Jalali, 2018). Studies have shown that the optimal combination of CH-MC (600 mg: 20 mg) demonstrates potential as a controlled-release preparation (Suprianto, 2016). The drug release profile of theophylline using CH-CMC tablets exhibited first-order kinetics and the Higuchi model (Murugesan et al., 2020; Suprianto, 2016). CH-SA, CH-CB, and CH-HPMC have also been investigated as potential controlled preparations with various drugs (Guarnizo-Herrero et al., 2021; Li et al., 2015; Zhang et al., 2018).

HPMCP coating effectively delays drug release, while the CH-HPMCP combination successfully enhances release with reduced polymer use. To formulate an appropriate release profile, this research focuses on developing a controlled drug release system using CH as a matrix tablet, HPMCP as a coating film, and furosemide (FS) as a model drug. The objective of this study is to explore the release kinetics of FS from CH matrix tablets with or without an HPMCP layer, as well as to understand the drug release profile in different media using UV spectrophotometry.

MATERIALS AND METHOD

Materials

Furosemide (FS) was obtained from PT. Kimia Farma Tbk, Jakarta, Indonesia. Pharmaceutical-grade magnesium stearate, lactose, talcum, and Manihot starch are obtained from PT. Brataco, Jakarta, Indonesia. Chemical materials such as acetic acid, acetone, sodium chloride, hydrochloric acid, potassium dihydrogen phosphate (KH_2PO_4), sodium hydroxide, and hydroxypropyl methylcellulose phthalate (HPMCP) are obtained from Merck, Darmstadt, Germany. Chitosan (CH) is derived from the solid waste of swallow shrimp (*Metapenaeus monoceros*) and obtained from Medan Industrial Estate, Medan, Indonesia.

Methods

Core tablet preparation

CH powder was placed into a porcelain cup, then an acetic acid 1% solution was added and stirred until it formed a gel. Next, lactose and FS were added to a mortar and ground until homogeneous. The CH gel was added to the mortar while continuously grinding until it formed a solid mass. This solid mass was granulated using a 10-mesh sieve, dried at a temperature of 60°C for 4 h, then re-granulated using a 12-mesh sieve, lubricated with talcum and magnesium stearate, and compressed into core tablets with a single punch machine (Erweka) with a diameter of 6 mm. The core tablets with the slowest release in medium pH 1.2, 5.8, and 7.4 were selected for coating film with HPMCP solution. Press-coated tablets consisted of a core and coated tablets that were compressed with a diameter of 10 mm. The press-coated tablet formula was shown in Tabel 1. These core tablets that exhibited controlled release were coated with HPMCP as a border.

Table 1. The Press-coated tablet formula

Component		Formula				
		A	**B**	**C**	**D**	**E**
Core tablet (mg)	Furosemide (FS)	65	65	65	65	65
	Chitosan (CH)	-	5	20	40	60
	Lactose	62	57	42	22	2
	Talcum	2	2	2	2	2
	Magnesium stearate	1	1	1	1	1
Coated tablet (mg)	Furosemide (FS)	35	35	35	35	35
	Chitosan (CH)	10	10	10	10	10
	Lactose	20	20	20	20	20
	Talcum	300	300	300	300	300
	Magnesium stearate	3	3	3	3	3
	Furosemide (FS)	2	2	2	2	2
Total Mass (mg)		500	500	500	500	500

Coated tablet granule preparation

CH powder was placed into a porcelain cup, then an acetic acid 1% solution was added and stirred until it formed a gel. Lactose, starch, and FS were placed into the mortar and ground until homogeneous. The CH gel was added to the mortar while continuously grinding until homogeneous, forming a compact mass. This compact mass was granulated using a 10-mesh sieve, dried in an oven at 60°C for 4 h, and then re-granulated using a 12-mesh sieve, lubricated with talcum and magnesium stearate. The coated tablet granule was used for bottom and top coating on a press-coated tablet, and the formulation was provided in Table 1.

Coating of the core tablet

2.0 g of HPMCP were dissolved in 50 mL of acetone. The core tablets were dipped into the HPMCP solution three times and then dried in an oven at 50°C for 30 min.

Press-coated tablet manufacturing

160 mg of the coated granules (bottom coated) were loaded into the die, and then the core tablet was placed on the granule surface in the center. After that, 160 mg of the coated granules (top coated) were put into the die and then compressed into Press-coated tablets using a single punch machine (Erweka). Each formulation was conducted using the same method.

Dissolution Medium Manufacturing

The dissolution medium was manufactured without enzymes, following the method outlined in the Indonesian Pharmacopoeia Edition IV. In the production of the artificial gastric medium, 2.0 g of sodium chloride (p) was dissolved in 7.0 mL of hydrochloric acid (p), after which the pH was adjusted to 1.2 by the addition of hydrochloric acid (p) and subsequent dilution with distilled water to achieve a total volume of 1000 mL. For the artificial duodenum medium, a mixture of 250 mL of potassium dihydrogen phosphate 0.2 M and 18 mL of sodium hydroxide 0.2 N was prepared and diluted with sufficient free water carbon dioxide to make a total volume of 1,000 mL. Similarly, the artificial small intestine medium was created by placing 250 mL of potassium dihydrogen phosphate 0.2 M into a volumetric flask containing 195.5 mL of sodium hydroxide 0.2 M, followed by dilution with water to 1,000 mL. The pH of this solution was measured as 7.4 using a pH meter.

Evaluation of furosemide press-coated tablet

The CH matrix FS preparations were assessed for tablet hardness, friability, and disintegration employing a Hardness Tester (Strong Cobb, Erweka), Friabilator (Roche, Erweka), Disintegration Tester (Copley), and dissolution (Dissolution Tester, Erweka).

Dissolution studies

The dissolution test was carried out using a type 2 dissolution apparatus (paddle), with a medium of 900 mL pH 1.2 (artificial gastric medium), 5.8 (artificial duodenum medium), and 7.4 (artificial small intestine medium), temperature 37 ± 0.5 ºC with a rotation speed of 50 rpm. At certain time intervals of 0.08, 0.25, 0.50, 0.75, 1, 2, 4, 5, 6, 7, and 8 h, 5.0 mL samples were taken and replaced with an equal medium solution to keep the volume constant. Dissolution tests in simultaneous medium were browned for 0-2 h in the artificial stomach medium, 2-6 h in the artificial duodenum medium, and 6-16 h in the artificial intestinal fluid. The sample solution was filtered and analyzed with spectrophotometry (UV Probe 1800 Shimadzu, λ = 276 nm). The FS release was calculated using the regression equation. The replications of this FS release are carried out six times.

Drug release kinetics analysis

The kinetic model was extensively utilized to analyze controlled tablet matrix drug release (Damodharan, 2020; Moroney & Vynnycky, 2021). Dissolution data were utilized to ascertain the release kinetics models, encompassing zero-order, first-order, Higuchi, and Korsmeyer-Peppas models (Arafat et al., 2021; Damodharan, 2020; Moroney & Vynnycky, 2021; Suprianto, 2016).

RESULT AND DISCUSSION

Evaluation of furosemide tablets

The press-coated tablets were prepared by the wet granulation method. Press-coated tablets were tested for content uniformity, weight, hardness, friability disintegration, and dissolution. The results are shown in Table 2. The tablets provided physical content that met the Indonesian Pharmacopoeia edition IV requirements regarding the uniformity of content, weight, hardness, friability, disintegration, and dissolution. The results showed that increasing the concentration of CH led to a significant decrease ($p<0.05$) in hardness, disintegration time, and an increase in tablet friability. The volume of glacial acetate solvent 1 % used to develop chitosan remains constant, so the higher the chitosan level, the less perfect the chitosan development, so the binding capacity decreases. As a result, hardness also decreases,

and disintegration time increases. The concentration of chitosan that can bind the mass well was 20 mg in formula C because chitosan expands perfectly in 1% acetic acid so that it could bind the mass well. While Formulas D and E contain 40 mg and 60 mg chitosan, the chitosan did not expand completely, and the ability of binding capacity decreased (Aranaz et al., 2021; Pardo-Castaño & Bolaños, 2019).

Table 2. Evaluation results data of tablet formulations

Formula	Hardness (n=5)	Weight (n=20)	Friability (n=20)	Disintegration (n=6)	Drug content (n=10)
A	5.05 ± 0.130	501.2 ± 0.130	0.45 ± 0.020	0.92 ± 0.021	98.93 ± 0.108
B	4.50 ± 0.100	499.4 ± 0.090	0.42 ± 0.006	0.75 ± 0.018	99.31 ± 0.121
C	4.11 ± 0.020	500.7 ± 0.050	0.35 ± 0.008	0.63 ± 0.015	101.02 ± 0.106
D	4.05 ± 0.150	498.5 ± 0.170	0.31 ± 0.013	0.34 ± 0.008	98.87 ± 0.112
E	3.97 ± 0.090	501.9 ± 0.240	0.20 ± 0.002	0.28 ± 0.005	99.29 ± 0.103

Furosemide release profile of Press-coated tablet

The analysis of FS release from press-coated tablet which uncoated core tablet was depicted in Figure 1 (1). FS delineates a swifter release from the coated tablet than the core tablet under a pH 1.2 medium. So that the coated tablet functions as an initial dose, while FS in the core tablet functions as a maintenance dose, ensuring a continuous drug release from the Press-coated tablet. Press-coated tablet with a coated tablet contains CH and starch, renowned for their swelling properties, facilitating easy breakdown into particles and hastening FS solubility. The FS released from the press-coated tablet, which the core tablet coated with HPMCP shown in Figure 1 (2), which elucidates how the HPMCP coating modifies the FS release pattern from the Press-coated tablet by reducing the quantity of FS released from the core tablet with CH as matrix and the HPMCP as film-coated.

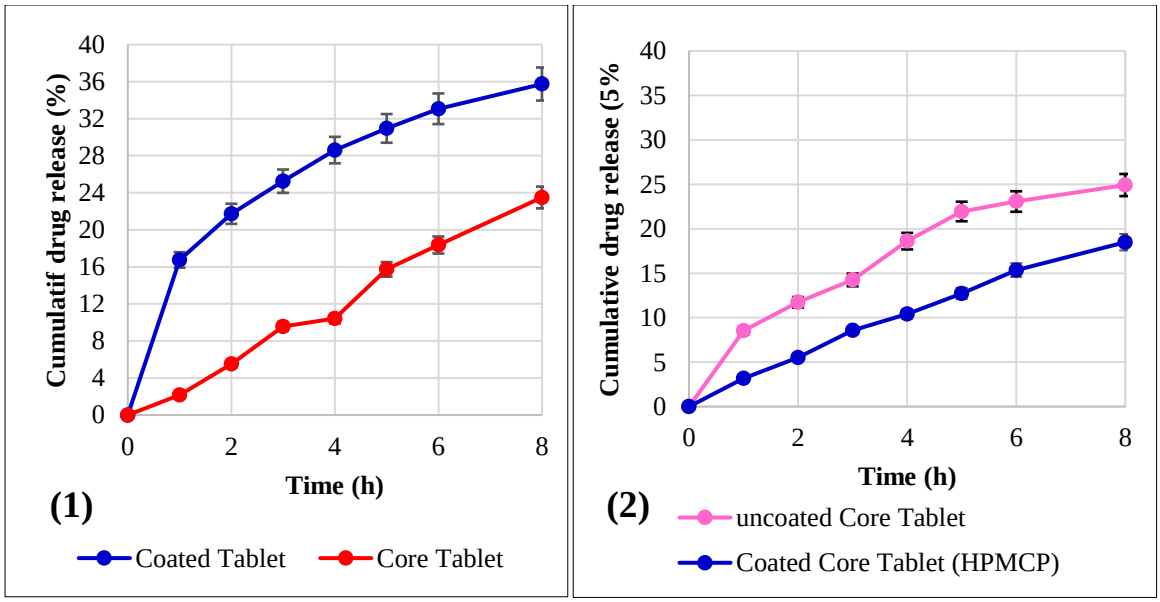

Figure 1. FS release from coated and core tablets uncoated (1), uncoated and coated core tablets (2)

The press-coated tablet consists of a core and a coated tablet. The core tablet was uncoated and coated with HPMCP. The core tablet in formula C showed the best-controlled release at pH 1.2 (Figure 2 (1)), 5.8 (Figure 3 (1)), and 7.4 (Figure 4 (1)), so it was chosen to be film coated with HPMCP.

Figure 2 (1) and Figure 2 (2) delineate the FS release profile from the CH matrix in a pH 1.2 medium. These figures explicate that with an elevation in CH concentration, FS release intensifies owing to the expansion of CH in the acidic pH 1.2 environment (Li et al., 2021; Moradi et al., 2023). Figure 2 (2) exhibits a relatively higher FS release than Figure 2 (1), attributed to the presence of FS in the coating formula, prompting immediate tablet disintegration and FS dissolution. The escalated CH concentration in the core tablets accelerates FS release as CH swells in the acidic pH 1.2 medium.

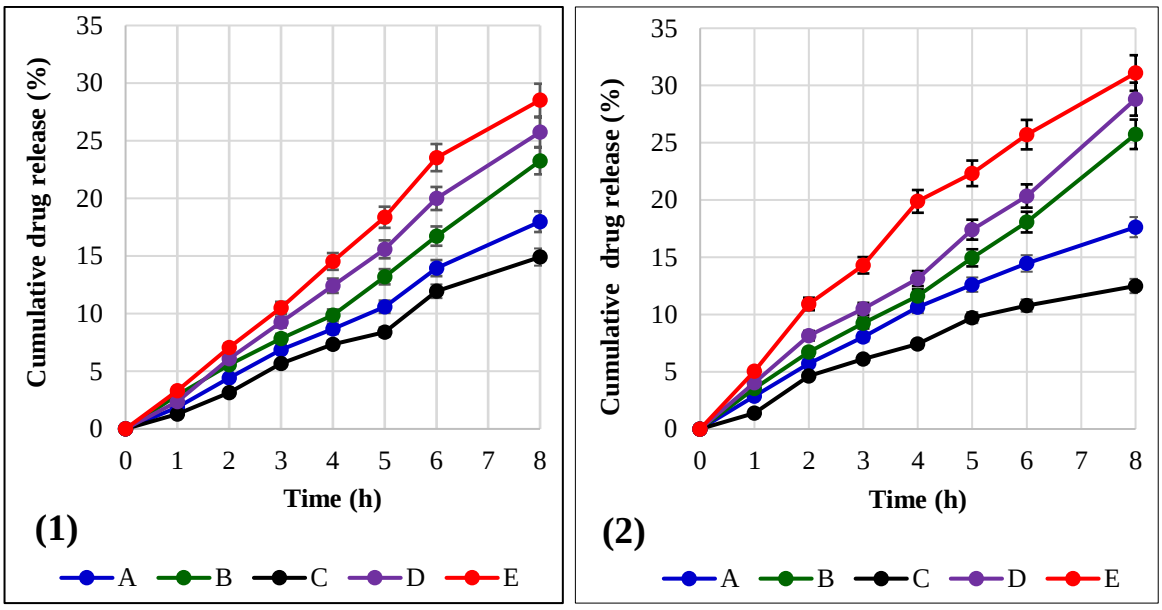

Figure 2. FS release of core tablet (1) and press-coated (2) in medium pH 1.2

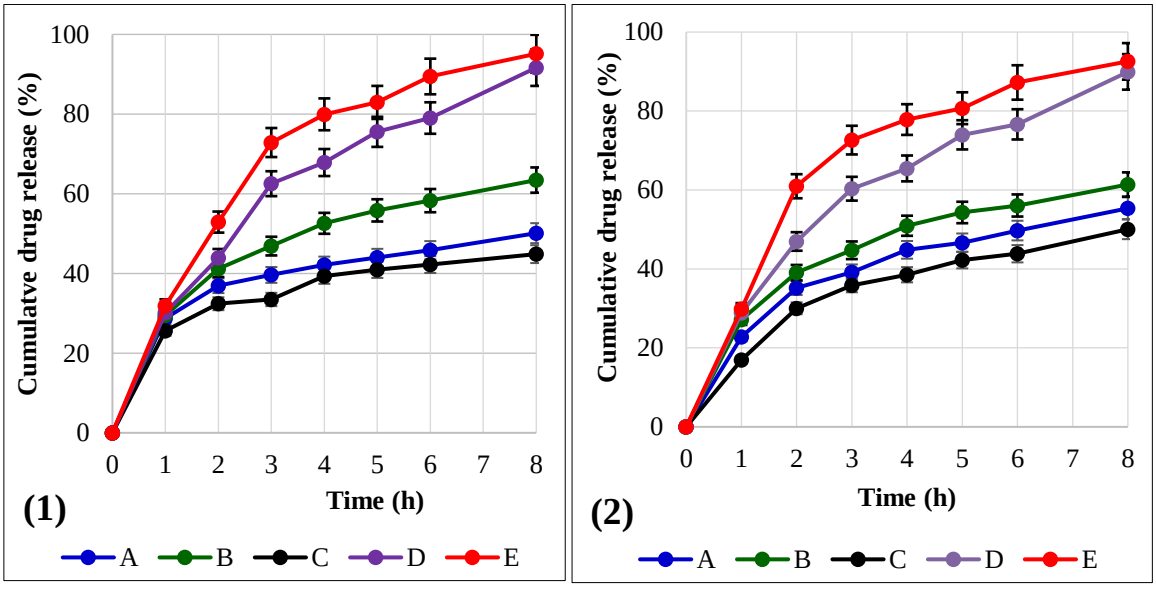

Figure 3. FS release of core tablet (1) and press-coated (2) in medium pH 5.8

Figure 3 (1) and Figure 3 (2) portray the FS release pattern from the CH matrix in a pH 5.8 medium. These figures manifest that higher CH concentrations correspond to faster FS release at pH 5.8 compared to pH 1.2. Elevated CH concentrations expedite FS release due to augmented swelling power, resulting in rapid tablet disintegration into particles and FS liberation. Prior studies have also highlighted CH's disintegrating properties (Moradi et al., 2023; Shiyan et al., 2021), underscoring that increased CH content augments tablet disintegration into particles, facilitating FS release into the dissolution medium. Conversely, formula A core tablets lacking CH and developer exhibit slower FS dissolution due to limited fluid penetration. Formula C core tablets coated with HPMCP exhibit the slowest dissolution rate. HPMC effectively constrains FS release from the CH matrix employed in the formula. The distinction in release profiles between the core tablet and the pre-coated tablet emanates from the release of a charged dose in pre-coated tablets before expansion, inducing the protective tablet to fragment into particles, thereby augmenting FS dissolution, giving the impression that pre-coated tablets release more FS.

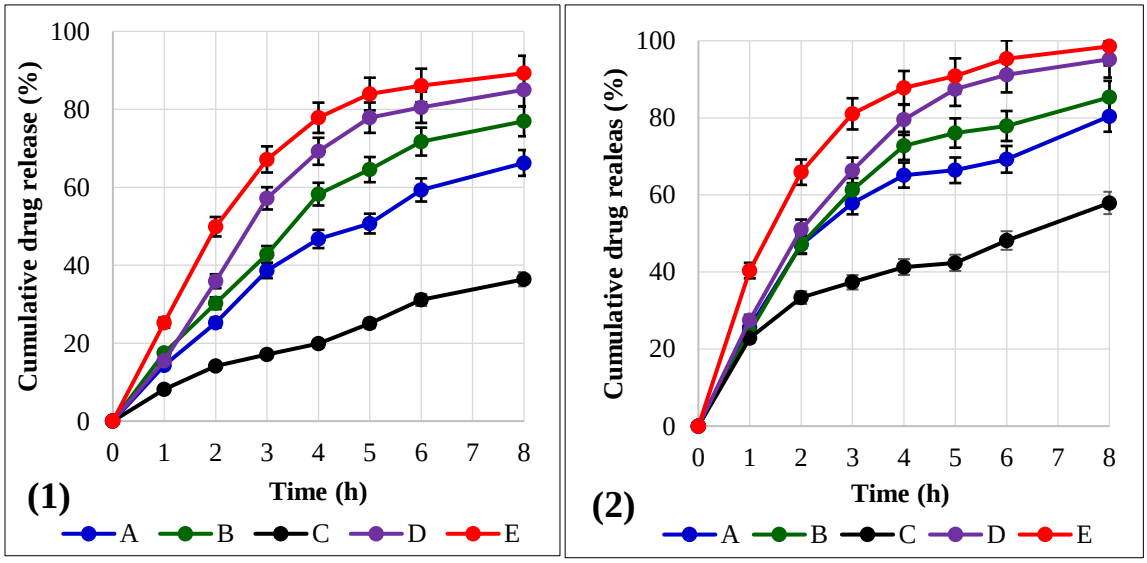

Figure 4. FS release of core tablet (1) and press-coated (2) in medium pH 7.4

Figure 4 (1) and Figure 4 (2) illustrate the FS release profile from the CH matrix at pH 7.4. These figures explicate that an augmented CH concentration expedites FS release due to heightened swelling power, leading to rapid tablet disintegration into particles and FS dissolution in the dissolution medium. Previous studies have emphasized CH's role as a disintegrant (Anisa et al., 2022; Shiyan et al., 2021), signifying its contribution to tablet disintegration into particles poised for FS release into the dissolution medium.

Effect of medium pH on drug release

The drug release profile consisted of commercial press-coated tablet, coated tablet, and core tablet film coated with HPMCP in the pH of medium simultaneous pH 1,2; 5,8 and 7,4 was depicted in Figure 5.

The observed trend indicates that the release of FS at pH 5.8 and 7.4 surpasses the release at pH 1.2. This behavior was attributed to FS being a weak acid (with a pKa of 3.9), resulting in limited solubility in an acidic medium like pH 1.2. Conversely, FS demonstrates enhanced solubility in a slightly acidic medium (pH 5.8), facilitating its release as the HPMCP expands without hindering FS dissolution. At pH 7.4, FS displays significantly high solubility, yet the expansion of HPMCP marginally restrains the dissolution process. These findings are consistent with previous research utilizing CH as a matrix, where

the release of the drug at pH 1.2 was slower compared to pH 6.8 (Shiyan et al., 2021; Suprianto, 2016). Figure 5 illustrates the minimal release of FS in C-coated HPMCP when subjected to simultaneous dissolution in an acidic medium. The coating aims to safeguard the core tablet from degradation within the intestine.

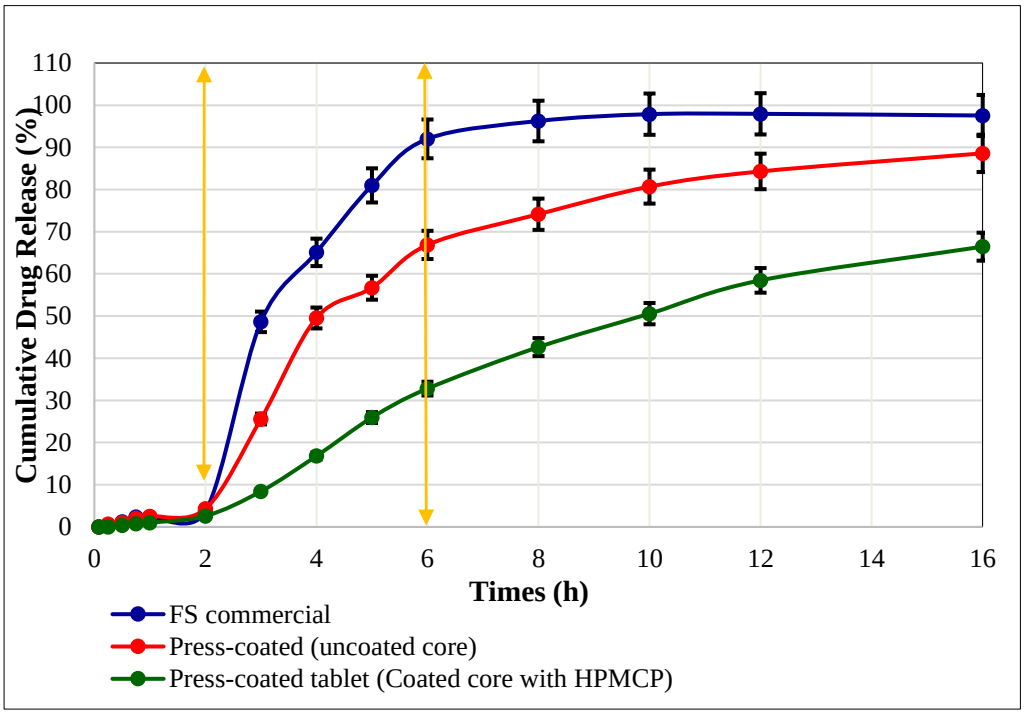

Figure 5. FS release of Furosemide commercial, Press-coated tablet with uncoated core tablet and Press-coated tablet with film coated core tablet in simultaneous medium pH 1.2, 5.8, and 7.4

Drug release kinetics in three mediums

The comprehensive analysis of FS release kinetics from the CH matrix across three different mediums is presented in Table 3, encompassing zero, first, and Higuchi order models alongside Korsmeyer-Peppas models. FS release kinetics was determined at intervals of 0-2, 2-6, and 6-16 h. The correlation coefficients of each model serve as pivotal indicators for determining the FS release kinetics model from the CH Matrix (Arafat et al., 2021; Damodharan, 2020; Suprianto, 2016). Furthermore, Formula C, constituting a core tablet coated with HPMCP, exhibits an unpredictable kinetic model across acidic (pH 1.2), slightly acidic (pH 5.8), and basic (pH 7.4) mediums, conforming to first-order models, Higuchi, and Higuchi, respectively. The coating process does not guarantee mastery over the kinetic model's consistency across various dissolution mediums, as it remains contingent upon the physicochemical properties of the adjuvant utilized within the tablet matrix (Qu & Luo, 2020; Yadav et al., 2021). Notably, except for formula D, the kinetic model governing FS release from the CH matrix in a pH 7.4 medium predominantly adheres to Higuchi's order.

Release kinetics on simultaneous medium

The kinetic model governing the release of FS from the CH matrix in the simultaneous medium is detailed in Table 4. This determination of the kinetic model stems from a comprehensive assessment of correlation coefficients associated with each model, as established in prior studies (Damodharan, 2020;

Moroney & Vynnycky, 2021; Suprianto, 2016). Additionally, this determination is based on the time span analysis, which correlates with the transit time within the gastrointestinal tract (Kali et al., 2022).

During the initial 0-2 hour period, the release of FS from both CH and commercially available matrix tablets at pH 1.2 exhibited no discernible difference. This lack of differentiation arises due to the significantly low solubility of FS at pH 1.2, which is attributed to its nature as a weak acid (pKa = 3.9) (Soni et al., 2021). Consequently, the FS dissolution assay conducted at pH 1.2 was extended for 2 hours, aligning with an approximate transit time of 2 hours within the stomach (Kali et al., 2022). The findings in Table 4 illustrate that the kinetics governing drug release within the 0-2 hour window adhere to the Higuchi, Korsmeyer-Peppas, and zero-order models for each respective product.

The dissolution test conducted on FS in a simultaneous medium at pH 5.8 for 4 hours corresponds to the anticipated drug transit time within the intestine, estimated between 2 to 6 hours. Analysis of the release profile revealed that the C-coated formulation exhibited a notably slower release rate than other variants, indicating that HPMCP coating impeded FS release from the CH matrix (Kali et al., 2022). Conversely, the non-coated C formulation showed a faster release, solely relying on the ability of CH to expand and diffuse FS into the dissolution medium, albeit still slower than the release rate of commercial FS. HPMCP C-coated tablets exhibit insolubility in the pH 5.8 medium; however, FS release occurs due to the formation of pores by HPMCP, allowing liquid penetration into the tablet's core and subsequent dissolution of FS. The FS release kinetics primarily followed first-order kinetics, except for the C-coated tablets, which exhibited zero-order kinetics, indicating a constant release rate of FS at pH 5.8 from these specific tablets, as detailed in Table 4. During 6 to 16 hours, the release of FS from CS matrix tablets was observed in a simultaneous medium at pH 7.4. Figure 5 highlights the absence of FS release from commercial tablets, while uncoated and HPMCP-coated CH matrix tablets exhibited FS release in the study. Notably, the dissolution rate of coated C was slower than that of non-coated C, underscoring the substantial role played by HPMCP coating in facilitating FS release from the tablets. Further insights into release kinetics are provided in Table 4. Moreover, at pH 7.4 in the simulated medium, both types of tablets exhibited first-order release kinetics. It emphasizes that the release of FS depends not only on the matrix components and HPMCP coating employed in the preparation of controlled formulations but also on the concentration of FS within the tablet a critical factor influencing release behavior (Shiyan et al., 2021; Soni et al., 2021).

Table 3. Model of drug release kinetics in three medium

pH	Formula	Correlation coefficient (R)				Kinetic Model
		N	S	H	K	
1.2	A	0.9862	0.9919	0.9512	0.9959	K
	B	0.9946	0.9874	0.8911	0.9942	N
	C	0.9668	0.9722	0.9427	0.9485	S
	D	0.9946	0.9879	0.8995	0.9924	N
	E	0.9785	0.9906	0.9560	0.9884	S
5.8	A	0.6793	0.8920	0.9769	0.9707	H
	B	0.7788	0.8920	0.9728	0.9807	K
	C	0.7016	0.9003	0.9797	0.9468	H
	D	0.8073	0.9817	0.9926	0.9793	
	E	0.8344	0.9765	0.9522	0.8849	S
7.4	A	0.8295	0.9519	0.9726	0.9313	
	B	0.8367	0.9638	0.9667	0.9296	H
	C	0.8533	0.9289	0.9835	0.9753	
	D	0.8534	0.9638	0.9711	0.9474	
	E	0.7511	0.9955	0.9473	0.9164	S

Notes: Zero order (N); First Order (S); Order of Higuchi (H); Order of Korsmeyer-Peppas (K)

Table 4. Release kinetics model of chitosan matrix tablet FS on simultaneous medium

pH	Formula	Correlation coefficient (R)				Kinetic Model
		N	S	H	K	
1.2	A	0.9862	0.9919	0.9512	0.9959	K
	B	0.9946	0.9874	0.8911	0.9942	N
	C	0.9668	0.9722	0.9427	0.9485	S
	D	0.9946	0.9879	0.8995	0.9924	N
	E	0.9785	0.9906	0.9560	0.9884	S
5.8	A	0.6793	0.8920	0.9769	0.9707	H
	B	0.7788	0.8920	0.9728	0.9807	K
	C	0.7016	0.9003	0.9797	0.9468	H
	D	0.8073	0.9817	0.9926	0.9793	
	E	0.8344	0.9765	0.9522	0.8849	S
7.4	A	0.8295	0.9519	0.9726	0.9313	
	B	0.8367	0.9638	0.9667	0.9296	H
	C	0.8533	0.9289	0.9835	0.9753	
	D	0.8534	0.9638	0.9711	0.9474	
	E	0.7511	0.9955	0.9473	0.9164	S

Notes: Zero order (N); First Order (S); Order of Higuchi (H); Order of Korsmeyer-Peppas (K)

CONCLUSION

The HPMCP-coated and non-coated CH matrix core tablets exhibit promising potential as controlled preparations with planned release. Release kinetics analysis indicates that the non-coated CH matrix core tablets follow a first-order release pattern at pH 5.8 and pH 7.4 within the periods of 2-6 hours and 6-16 hours, while at pH 1.2 within the initial 0-2 hours, the release switches to zero order. On the other hand, the HPMCP-coated CH matrix core tablets demonstrate more complex release kinetics, following the Korsmeyer-Peppas order pattern at pH 1.2 in the initial 0-2 hours, then transitioning to zero order and first order within the periods of 2-6 hours and 6-16 hours. At pH 5.8 and 7.4, the release follows zero order and first order sequentially across various periods. These findings depict the potential application of these tablets in controlled drug delivery with tailored release profiles adaptable to different environmental conditions and time requirements.

REFERENCES

Adepu, S., & Ramakrishna, S. (2021). Controlled drug delivery systems: current status and future directions. *Molecules*, *26*(19), 5905. https://doi.org/10.3390/molecules26195905

Anisa, A., Rahmah, E., & Putri, U. S. (2022). Diffusion rate of quercetin from chitosan-TPP nanoparticles dispersion of onion (Allium cepa L.) ethanol extract in medium phosphate buffer pH 7.4. *Pharmaciana*, *12*(1), 94–102. https://doi.org/10.12928/pharmaciana.v12i1.21585

Arafat, M., Sarfraz, M., Bostanudin, M. F., Esmaeil, A., Salam, A., & AbuRuz, S. (2021). In vitro and in vivo evaluation of oral controlled release formulation of BCS class i drug using polymer matrix system. *Pharmaceuticals*, *14*(9), 929. https://doi.org/10.3390/ph14090929

Aranaz, I., Alcántara, A. R., Civera, M. C., Arias, C., Elorza, B., Heras Caballero, A., & Acosta, N. (2021). Chitosan: An overview of its properties and applications. *Polymers*, *13*(19), 3256. https://doi.org/10.3390/polym13193256

Damodharan, N. (2020). Mathematical modelling of dissolution kinetics in dosage forms. *Research Journal of Pharmacy and Technology*, *13*(3), 1339–1345. https://doi.org/10.1016/j.ijpharm.2013.04.044

Guarnizo-Herrero, V., Torrado-Salmerón, C., Torres Pabón, N. S., Torrado Durán, G., Morales, J., & Torrado-Santiago, S. (2021). Study of different chitosan sodium carboxymethyl cellulose proportions in the development of polyelectrolyte complexes for the sustained release of

clarithromycin from matrix tablets. *Polymers*, *13*(16), 2813. https://doi.org/10.3390/polym13162813

Hanna, D. H., & Saad, G. R. (2019). Encapsulation of ciprofloxacin within modified xanthan gum-chitosan based hydrogel for drug delivery. *Bioorganic Chemistry*, *84*, 115–124. https://doi.org/10.1016/j.bioorg.2018.11.036

Idacahyati, K., Amalia, Y., & Lestari, T. (2020). Decreased total cholesterol levels in rats administered with chitosan from Green mussel (Perna viridis L.) shells. *Pharmaciana*, *10*(2), 157–166. https://doi.org/10.12928/pharmaciana.v10i2.13976

Jain, K. K. (2020). An Overview of Drug Delivery Systems. In *drug delivery systems. methods in molecular biology* (Third Edit),1–54. Humana Press Inc. https://doi.org/10.1007/978-1-4939-9798-5_1

Kali, G., Knoll, P., & Bernkop-Schnürch, A. (2022). Emerging technologies to increase gastrointestinal transit times of drug delivery systems. *Journal of Controlled Release*, *346*, 289–299. https://doi.org/10.1016/j.jconrel.2022.04.016

Kamaly, N., Yameen, B., Wu, J., & Farokhzad, O. C. (2016). Degradable controlled-release polymers and polymeric nanoparticles: mechanisms of controlling drug release. *Chemical Reviews*, *116*(4), 2602–2663. https://doi.org/10.1021/acs.chemrev.5b00346

Li, C., Fang, K., He, W., Li, K., Jiang, Y., & Li, J. (2021). Evaluation of chitosan-ferulic acid microcapsules for sustained drug delivery: Synthesis, characterizations, and release kinetics in vitro. *Journal of Molecular Structure*, *1227*, 129353. https://doi.org/10.1016/j.molstruc.2020.129353

Li, L., Li, J., Si, S., Wang, L., Shi, C., Sun, Y., Liang, Z., & Mao, S. (2015). Effect of formulation variables on in vitro release of a water-soluble drug from chitosan–sodium alginate matrix tablets. *Asian Journal of Pharmaceutical Sciences*, *10*(4), 314–321. https://doi.org/10.1016/j.ajps.2014.09.002

Liu, H., Wang, C., Li, C., Qin, Y., Wang, Z., Yang, F., Li, Z., & Wang, J. (2018). A functional chitosan-based hydrogel as a wound dressing and drug delivery system in the treatment of wound healing. *RSC Advances*, *8*(14), 7533–7549. https://doi.org/10.1039/C7RA13510F

Mandhar, P., & Joshi, G. (2015). Development of sustained release drug delivery system: a review. *Asian Pac. J. Health Sci*, *2*(1), 179–185. https://doi.org/10.21276/APJHS.2015.2.1.31

Mehta, M., Keerthy, H. S., & Yadav, R. P. (2021). Sustained release matrix tablet: an overview. *Asian Journal of Pharmaceutical Research and Development*, *9*(3), 112–117. https://doi.org/10.22270/ajprd.v9i3.954

Moradi, G., Heydari, R., Zinadini, S., & Rahimi, M. (2023). Chitosan-furosemide/pectin surface functionalized thin film nanofiltration membrane with improved antifouling behavior for pharmaceutical wastewater treatment. *Journal of Industrial and Engineering Chemistry*, *124*, 368–380. https://doi.org/10.1016/j.jiec.2023.04.031

Moroney, K. M., & Vynnycky, M. (2021). Mathematical modelling of drug release from a porous granule. *Applied Mathematical Modelling*, *100*, 432–452. https://doi.org/10.1016/j.apm.2021.07.023

Murugesan, S., Gowramma, B., Lakshmanan, K., Reddy Karri, V. V. S., & Radhakrishnan, A. (2020). Oral modified drug release solid dosage form with special reference to design; an overview. *Current Drug Research Reviews*, *12*(1), 16–25. https://doi.org/10.2174/2589977511666191121094520

Pardo-Castaño, C., & Bolaños, G. (2019). Solubility of chitosan in aqueous acetic acid and pressurized carbon dioxide-water: Experimental equilibrium and solubilization kinetics. *The Journal of Supercritical Fluids*, *151*, 63–74. https://doi.org/10.1016/j.supflu.2019.05.007

Pathak, R., Bhatt, S., Punetha, V. D., & Punetha, M. (2023). Chitosan nanoparticles and based composites as a biocompatible vehicle for drug delivery: A review. *International Journal of Biological Macromolecules*, *253*, 127369. https://doi.org/10.1016/j.ijbiomac.2023.127369

Qu, B., & Luo, Y. (2020). Chitosan-based hydrogel beads: preparations, modifications and applications in food and agriculture sectors–a review. *International Journal of Biological Macromolecules*, *152*, 437-448. https://doi.org/10.1016/j.ijbiomac.2020.02.240

Sacco, P., Furlani, F., De Marzo, G., Marsich, E., Paoletti, S., & Donati, I. (2018). Concepts for Developing Physical Gels of Chitosan and of Chitosan Derivatives. *Gels*, *4*(3), 67. https://doi.org/10.3390/gels4030067

Shao, Y., Li, L., Gu, X., Wang, L., & Mao, S. (2015). Evaluation of chitosan–anionic polymers based tablets for extended-release of highly water-soluble drugs. *Asian Journal of Pharmaceutical Sciences*, *10*(1), 24–30. https://doi.org/10.1016/j.ajps.2014.08.002

Shariatinia, Z., & Jalali, A. M. (2018). Chitosan-based hydrogels: Preparation, properties and applications. *International Journal of Biological Macromolecules*, *115*, 194–220. https://doi.org/10.1016/j.ijbiomac.2018.04.034

Sharma, D., Dev, D., Prasad, D. N., & Hans, M. (2019). Sustained release drug delivery system with the role of natural polymers: a review. *Journal of Drug Delivery and Therapeutics*, *9*(3-s), 913-923. https://doi.org/10.22270/jddt.v9i3-s.2859

Shiyan, S., Marketama, M., & Pratiwi, G. (2021). Optimization transdermal patch of polymer combination of chitosan and HPMC-loaded ibuprofen using factorial designs. *Pharmaciana*, *11*(3), 406–415. https://doi.org/10.12928/pharmaciana.v11i3.19935

Soni, S., Jain, V., Jain, S. K., & Khangar, P. K. (2021). Formulations of sustained release matrix tablets of Furosemide using natural and synthetic polymers. *Journal of Drug Delivery and Therapeutics*, *11*(5), 105–109. https://doi.org/10.22270/jddt.v11i5.5122

Suprianto. (2016). Analisis kinetika pelepasan teofilin dari granul matriks kitosan. *Jurnal Ilmiah Manuntung*, *2*(1), 70–80. https://doi.org/10.51352/jim.v2i1.50

Wu, Y., Rashidpour, A., Almajano, M. P., & Metón, I. (2020). Chitosan-based drug delivery system: applications in fish biotechnology. *Polymers*, *12*(5), 1177. https://doi.org/10.3390/polym12051177

Yadav, R. P., Sheeba, F. R., Sharma, M., Bhargav, A., Kumar, Y., & Patel, A. K. (2021). The role of matrix tablet in oral drug delivery system. *Asian Journal of Pharmaceutical Research and Development*, *9*(2), 80–86. https://doi.org/10.22270/ajprd.v9i2.930

Zhang, X., Gu, X., Wang, X., Wang, H., & Mao, S. (2018). Tunable and sustained-release characteristics of venlafaxine hydrochloride from chitosan–carbomer matrix tablets based on in situ formed polyelectrolyte complex film coating. *Asian Journal of Pharmaceutical Sciences*, *13*(6), 566–574. https://doi.org/10.1016/j.ajps.2018.01.004

Pharmaciana
Vol.14, No.2, July 2024, Page. 133-146
ISSN: 2088 4559; e-ISSN: 2477 0256
DOI: 10.12928/pharmaciana.v14i2.28242

Inhibition breast carcinogenesis via PI3K/AKT pathway using bioactive compounds of Strychnine tree (*Strychnos nux-vomica*): *in silico* study

Aulia Ayu Rispriandari[1], Sarmoko[2*], Joko Setyono[3], Sindhu Wisesa[4]
[1]Master of Biomedicine Programme, Faculty of Medicine, Universitas Jenderal Soedirman
Jl. Gumbreg, Mersi, Purwokerto, Indonesia
[2]Pharmacy Department, Faculty of Science, Institut Teknologi Sumatera
Jl. Terusan Ryacudu, Way Huwi, Lampung, Indonesia
[3]Department of Biochemistry, Faculty of Medicine, Universitas Jenderal Soedirman
Jl. Gumbreg, Mersi, Purwokerto, Indonesia
[4]Department of Anatomy, Faculty of Medicine, Universitas Jenderal Soedirman
Jl. Gumbreg, Mersi, Purwokerto, Indonesia

Submitted: 18-01-2024 ***Reviewed: 31-03-2024*** ***Accepted: 29-06-2024***

ABSTRACT

Breast cancer poses a significant global health challenge, with a notable prevalence in Indonesia. Given the intricate nature of breast cancer progression and classification, precise treatment strategies are imperative, particularly targeting signaling pathways like PI3K/AKT, pivotal in cell growth, proliferation, survival, and apoptosis. Bioactive compounds from the Strychnine tree demonstrate potential in enhancing apoptotic effects and inhibiting breast carcinogenesis. This potential is explored through *in silico* studies. This research aims to analyze potential targets of Strychnine tree compounds, along with binding energy and stability between ligands and receptors. Employing bioinformatics target analysis, molecular docking, and molecular dynamics simulation, the study reveals AKT1 as a potential target of Strychnine tree compounds. These compounds inhibit AKT1 at both active and allosteric sites, displaying notably low binding energy scores. For example, brucine exhibits a binding energy of -10.83 kJ/mol at the active site, surpassing the standard capivasertib. However, lupeol, with a binding energy of -11.14 kJ/mol, falls short of the MK-2206 standard at the allosteric site. Molecular dynamics simulations expose fluctuations in parameters like RMSD, RMSF, and binding energy within the initial 5 ns. In conclusion, Strychnine tree compounds, such as brucine and lupeol, showcase potential AKT1 inhibition at both active and allosteric sites, enhancing apoptotic effects. However, the stability of these compounds in binding to their receptors within the first 5 ns of the simulation warrants further investigation for prolonged interactions.

Keywords: PI3K/AKT pathway, AKT1, strychnine tree compounds, target analysis, molecular docking, molecular dynamics

Corresponding author:
Sarmoko
Pharmacy Department, Faculty of Science, Institut Teknologi Sumatera
Jl. Terusan Ryacudu, Way Huwi, Lampung, Indonesia
Email: sarmoko@fa.itera.ac.id

INTRODUCTION

Breast cancer is a major global health issue, with a notable proportion of cases reported from Indonesia. According to a research published by the International Agency for Research on Cancer (IARC), 16.6% of all new instances of cancer in Indonesia are breast cancer, out of a total of 396,914 cases. The report also shows the percentage of deaths due to breast cancer in Indonesia to be 9.6%. IARC also reports that breast cancer patients worldwide, including in Indonesia, are predominantly women over the age of 40 (Global Cancer Observatory 2020; Global Cancer Observatory 2021).

The intricate nature of breast cancer's progression and classification necessitates precise treatment strategies that target the signaling pathways involved in breast carcinogenesis, one of them being the PIP3K/AKT pathway. A key component of cell development, proliferation, survival, and apoptosis is the PI3K/AKT pathway. Research on the application of targeted therapy on the PI3K/AKT pathway is also substantial. The utilization of bioactive chemicals obtained from plants, such as those from the strychnine tree, has been increasingly investigated in the development of medications for breast cancer (Martorana et al., 2021; Saraswati & Agrawal, 2013; Victor et al., 2016; Yuan et al., 2023; Zhu et al., 2022).

The Strychnine tree (*Strychnos nux-vomica*) is known to contain compounds such as alkaloids, iridoid glycosides, triterpenoids, and organic acids like strychnine, brucine, adenosine, lupeol, catechol, and maltol that have the potential to inhibit breast carcinogenesis (Chen et al., 2014; Enkhtaivan et al., 2015; Joy et al., 2016; Saraswati & Agrawal, 2013; Victor et al., 2016; Zhang et al., 2012). The majority of the Strychnine tree's anti-cancer studies have been carried out both in vitro and in vivo. Additional study is required to assess the pharmacological processes, efficacy, precise receptor targets, and stability of receptor interactions of strychnine tree substances, notwithstanding the encouraging results of these studies on their anti-cancer activities. Further research is crucial to create formulations that are safer and more effective (Eldahshan & Abdel-Daim, 2015; Guo et al., 2018; Lu et al., 2020).

Numerous studies have been carried out using *in silico* technology to find and develop new medications, including those for breast cancer. Through *in silico* research, predictions can be made about the activity of a compound with receptor targets involved in cellular biological processes and the pathways related to that activity (De Vivo et al., 2016; Hermawan, et al., 2021; Hermawan, et al., 2021; Hermawan, et al., 2021; Roy et al., 2022; Roy et al., 2016). *In silico* research has proven to complement the development of new, specific, and safe drugs in the pharmaceutical field The predictive results of these *in silico* studies can serve as hypotheses for further research, especially in the field of oncology.

The research by Zhou et al. (2020) indicates that *Strychnos nux-vomica* has the potential as an anticancer agent by binding to several potential targets such as AKT1, EGFR, ALB, MAPK1, EGF, VEGFA, CCND1, SRC, Jun, Casp3, HSP90AA1, ESR1, MAPK8, and FN1. However, this study did not analyze the potential binding of strychnine tree compounds to these receptor targets or the stability of compound-protein interactions. Another study using strychnine tree compounds was conducted by Reynaldi & Setiawansyah (2022), indicating that the compounds strychnine, brucine, and secoxyloganin from the plant *Strychnos lucida* R.Br have the potential to bind to the estrogen α receptor but have affinity energies no better than 4-hydroxytamoxifen. However, this study did not conduct potential target analysis beforehand. The finding by Zhou et al. (2020) and Reynaldi & Setiawansyah (2022) indicate that certain strychnine tree chemicals may block receptors connected to the PI3K/AKT pathway, thus further we is needs to be conducted.

Based on the above considerations, we are interested in conducting *in silico* research on compounds from strychnine trees that may prevent breast cancer by blocking the PI3K/AKT pathway. We will explore potential targets, binding energies, and the stability of ligand-receptor interactions for compounds such as strychnine, brucine, adenosine, lupeol, catechol, and maltol. These compounds are primarily found in the seeds of the strychnine tree and are available in databases. Through the PI3K/AKT pathway, they may be able to prevent breast cancer.

MATERIALS AND METHOD

Materials

The hardware used in this research included a Lenovo ThinkPad T460s laptop with an Intel Core i7 6th gen processor, 8 GB RAM, 256 GB SSD, and Windows 10. The software used includes applications such as Cytoscape, Autodock tools/MGL tools, MarvinSketch, YASARA Dynamics, YASARA View, and Biovia Discovery Studio Visualizer. Additionally, web servers such as http://stitch.embl.de, https://string-db.org/, https://bioinfogp.cnb.csic.es/tools/venny/, https://www.ncbi.nlm.nih.gov/, http://www.swisstargetprediction.ch/, and https://pubchem.ncbi.nlm.nih.gov/ were utilized. The compounds investigated in this study were strychnine, brucine, adenosine, lupeol, catechol, and maltol from the strychnine tree.

Methods

Potential target analysis

The search for Direct Target Proteins (DTP) of active compounds from *S. nux-vomica* was conducted using STITCH (http://stitch.embl.de). The search for Indirect Target Proteins (ITP) of active compounds from S. nux-vomica was performed using STRING (https://string-db.org/). Target proteins not found in STITCH and STRING were searched using Swiss Target Prediction (http://www.swisstargetprediction.ch/). Breast cancer gene targets were searched using the National Center for Biotechnology Information (NCBI) database (https://www.ncbi.nlm.nih.gov/). Potential Target Therapeutic Genes (PTTG) were identified using Venn diagrams on the Venny 2.1 server (https://bioinfogp.cnb.csic.es/tools/venny/). A Protein-Protein Interaction (PPI) Network was constructed using STRING (https://string-db.org) with a confidence score > 0.7 and visualized using the Cytoscape software. Genes with a degree score greater than 10 were analyzed using the CytoHubba plugin (Brown et al., 2015; Chin et al., 2014; Daina et al., 2019; Hanif, et al., 2021; Kuhn et al., 2014; Liao et al., 2019; Szklarczyk et al., 2015).

Molecular docking simulation

The RCSB PDB (https://www.rcsb.org/) provided the target proteins. Before conducting molecular docking simulations, validation was performed using native ligands obtained from PDB (PDB ID: 3MVH for active site and PDB ID: 3O96 for allosteric site). Ligands obtained from https://pubchem.ncbi.nlm.nih.gov/ in sdf format were converted to pdb format using https://cactus.nci.nih.gov/translate/. Ligand files were opened in the MarvinSketch application and their conformers were calculated using the MMFF9 force field Modified (Hanif et al., 2020; Surya & Praveen, 2021). With Biovia Discovery Studio Visualizer, the receptor from RCSB PDB was prepared. Next, using the Autodock Tools program, the native ligand was docked to the target receptor in order to look for 3D conformations. The studied result is shown as RMSD, and a value of less than 2 Å is accepted as indicative of a reliable molecular docking outcome. Using the Autodock Tools tool, the test compounds were docked to the target protein taking into account the binding site grid box size in Angstrom as well as the center of mass coordinates of the structure. Each compound's binding energy value was determined using the LGA parameter. Using the DS Biovia tool, the result with the lowest possible binding energy was chosen for additional amino acid residue visualization and analysis. Modified from Tapiory et al. (2020), Al-Khodairy et al. (2013), Rizvi et al. (2013) and Zardecki et al. (2016).

Molecular dynamics simulation

YASARA Dynamics software was used for molecular dynamics simulations, employing AMBER14 as the force field. Na^+ and Cl^- ions were added for neutralization at physiological pH 7.4. The TIP3P water model was used for the solvation step. Preparation steps included minimization and heating to 310K. For 5 ns, simulations with a time step of 2.5 fs were run in an NPT ensemble at constant temperature and pressure, followed by a production step for 100 ps. The results of RMSD, RMSF, and binding energy were analyzed using Ms. Excel (Ouassaf et al., 2021).

Data Analysis

The data analysis employed is descriptive analysis to illustrate and elucidate data from bioinformatics target analysis, molecular docking, and molecular dynamics simulations of the strychnine tree in inhibiting AKT1 in breast carcinogenesis.

RESULT AND DISCUSSION

In silico studies on bioactive compounds from the strychnine tree can demonstrate how these bioactive compounds may be able to stop breast cancer from developing by blocking the PI3K/AKT pathway. This *in silico* study encompasses the search for potential targets, molecular docking simulations, and molecular dynamics simulations.

Potential target analysis

After obtaining target proteins from STITCH, STRING, and Swiss Target Prediction, an analysis was conducted to obtain PTTG (Potential Therapeutic Target Gene). The results indicated that out of 654 target proteins and 5326 breast cancer genes, 369 PTTGs were obtained (Figure 1). These results led to the construction of a proein-protein interaction network using STRING for additional analysis. Cytoscape was used to find the top 10 hub genes with CytoHubba plugin. According to the analysis, the top 10 hub genes are those with the highest level of interaction. Bioinformatics target analysis shows that bioactive compounds from the strychnine tree have the potential to interact with target proteins, including TP53, AKT1, GAPDH, IL6, CTNNB1, EGFR, ESR1, INS, SRC, and PTEN (Figure 2).

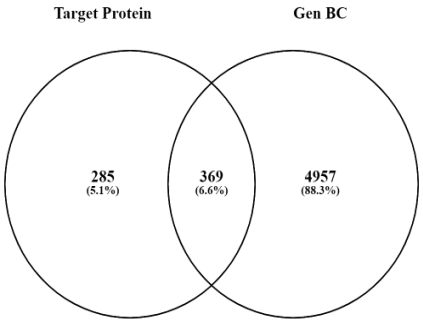

Figure 1. Results of PTTG (Potential Therapeutic Target Gene) of bioactive compounds from the strychnine tree

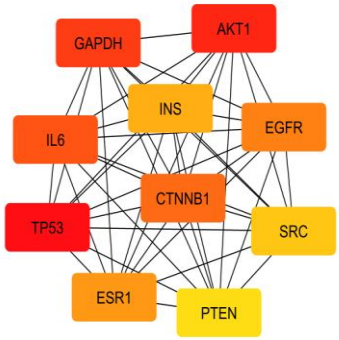

Figure 2. Top 10 genes that interact most intensely from Cytoscape analysis.

Explanation: TP53 (Tumor Protein 53), AKT1 (Serine/Threonine Kinase 1), GAPDH (Gyceraldehyde 3-Phosphate Dehydrogenase), IL-6 (Interleukin-6), CTNNB1 (Catenin (Cadherin-Associated Protein) Beta 1), EGFR

(Epidermal Growth Factor Receptor), ESR1 (Estrogen Receptor 1), INS (Insulin), SRC (Protein Kinase Src), PTEN (Phosphatase and Tension homolog deleted on chromosome ten)

The analysis results with Cytoscape indicate that the more intense the red color formed, the stronger the potential of that protein as a target for bioactive compounds. This is based on the degree of interaction between proteins and compounds obtained from databases like STITCH, STRING, and Swiss Target Prediction, which predict protein-compound, protein-protein and compound-compound interactions based on supporting information and evidence from text mining, experiments, databases, co-expression, neighborhood, gene fusion, and co-occurrence (Chin et al., 2014; Kuhn et al., 2014; Szklarczyk et al., 2015).

Targeting TP53 as a direct target protein (DTP) indicates a strong association with bioactive compounds derived from the strychnine tree. TP53 is a target protein obtained from STITCH, which analyzes the potential interactions between compounds and proteins. The results obtained indicate that TP53 has a strong potential interaction with compounds from the strychnine according to the supporting information that is currently accessible (Hermawan et al., 2020; Kuhn et al., 2014). However, TP53 as a tumor suppressor gene (TSG) has a high mutation rate, making it less suitable as a drug target (Bull & Doig, 2015; Giacomelli et al., 2018; Gonzalez-Garcia & Mlachila, 2017). Therefore, the next potential target for inhibiting breast cancer development is *AKT1*. This finding suggests that this putative target is connected to the PI3K/AKT pathway (Martorana et al., 2021).

Interfering with AKT can increase apoptosis and negatively impact cell growth, proliferation, and survival by disrupting the PI3K/AKT/mTOR signaling pathway. Cell growth and survival are decreased by AKT inhibition, which controls a number of protein molecules and transcription factors including mTOR, cyclin D, and CDK4/6. AKT also regulates mTOR, 4E-BP1, eIf4E, and P70S6K1, which can reduce cell proliferation. Moreover, AKT regulates Bad, Bcl-2, and Bcl-xL to enhance apoptosis (Dong et al., 2021; Fusco et al., 2021; Hein et al., 2014; Liu et al., 2020; Tapia et al., 2014). Protein AKT1 was then used as the receptor target in molecular docking simulations.

Molecular docking simulation

To comprehend how the ligand and receptor interact, as well as to anticipate the binding energy or affinity, molecular docking simulation was used (Pantsar & Poso, 2018). Since AKT1 is a crucial component of multiple signaling pathways involved in cell growth, proliferation, survival, and metabolism, targeting it is one tactic to slow the advancement of breast cancer (Hua et al., 2021; Martorana et al., 2021; Zhu et al., 2022). On the active and allosteric locations, molecular docking simulations were run. The PDB file 3MVH was utilized by the active site with the standard drug capivasertib, while the allosteric site used the PDB file 3O96 with the standard drug MK-2206. Both active and allosteric sides showed validation results with RMSD below 2 Å. represents the binding energy of the native ligand at -11.22 kJ/mol when it binds to AKT1 at the active site. The binding energy of the standard, capivasertib, is -10.56 kJ/mol. With a binding energy of -10.83 kJ/mol, brucine is the strychnine tree compound with a higher binding energy than the standard compound. At the allosteric site, the natural ligand having a binding energy of -12.82 kJ/mol with AKT1. The binding energy of the used standard, MK-2206, is -11.39 kJ/mol. Lupeol, with a binding energy of -11.14 kJ/mol, is the strychnine tree compound with the lowest value binding energy, while still not much better than the standard. Different types of interactions between ligands and receptors affect the magnitude of affinity energy (Arthur et al., 2021).

Ionic, hydrogen bonding, hydrophobic, and Van Der Waals interactions are a few examples of the chemical interactions that have a substantial impact on binding energy. Phi (π) interactions can stabilize ligand conformations and facilitate the insertion of ligand structures into the binding pocket on the receptor protein, whereas carbon hydrogen bonds are weak interactions. High hydrogen bonding is known to contribute significantly to the low binding energy produced (Arthur et al., 2021; Pantsar & Poso, 2018). Brucine and capivasertib compounds have one hydrogen bonding interaction each, at residues Lys158 and Glu228, respectively (Figure 3). While lupeol has one hydrogen bonding

interaction at residue Ser205, MK-2206 has two hydrogen bonding interactions at residues Tyr272 and Ser205 (Figure 4).

Table 1. Results of molecular docking simulation for the active and allosteric sites of AKT1 in the strychnine tree compound

Compound	Binding Energy (kJ/mol)	
	Active Site	Allosteric Site
Native	-11.22	-12.82
Capivasertib	-10.56	-
MK-2206	-	-11.39
Strychnine	-10.19	-9.34
Brucine	-10,83	-10.04
Adenosine	-6.90	-5.76
Lupeol	-9.71	-11.14
Catechol	-4.89	-4.43
Maltol	-4.81	-4.46

Note: Native compound = compound obtained from PDB binding with protein. Standard drug for active site= capivasertib. Standard drug for allosteric site= MK-2206

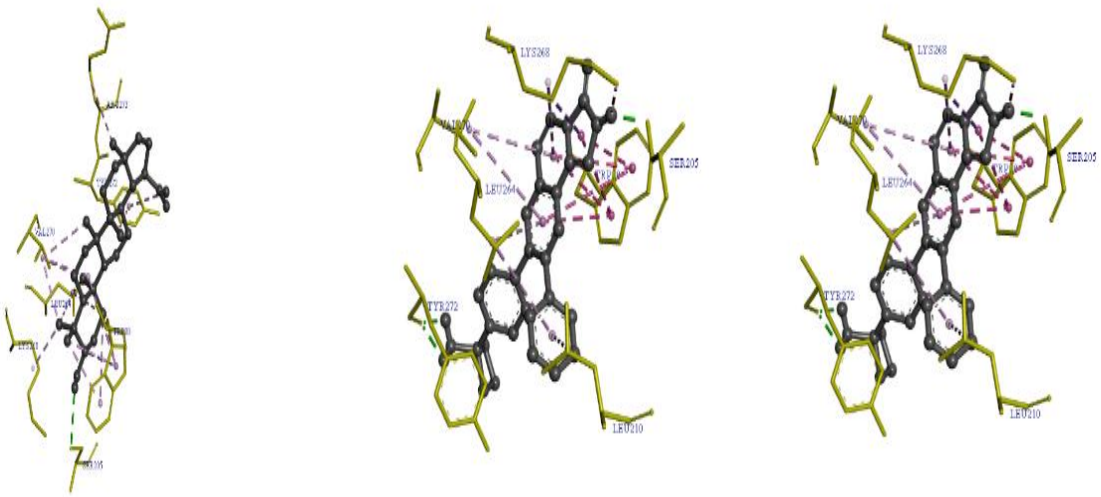

(A) **(B)** **(C)**

Figure 3. Molecular docking simulation results with AKT1 protein at the active site. (A) Native compound (B) Standard capivasertib. (C) Compound brucine

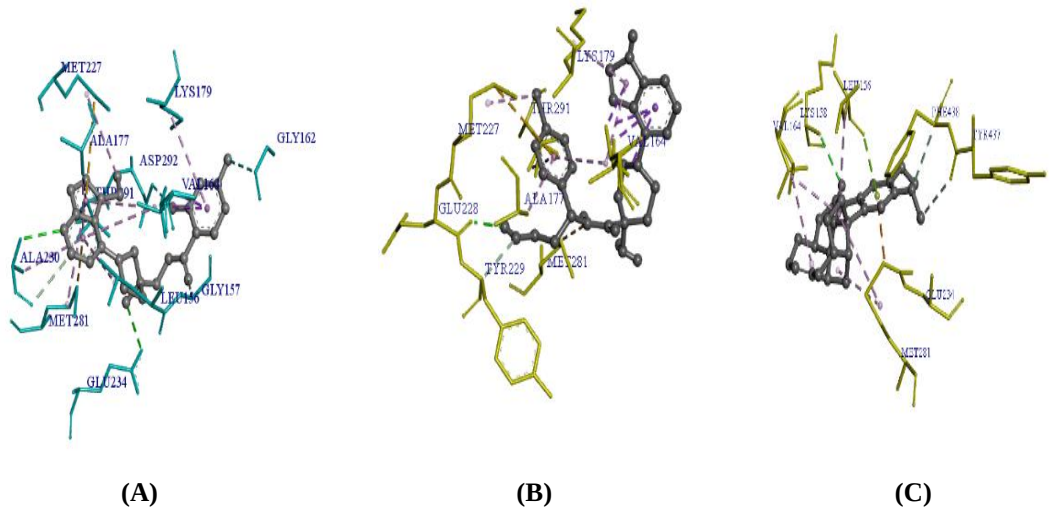

(A) **(B)** **(C)**

Figure 4. Molecular docking simulation results with AKT1 protein at the allosteric site. (A) native compound. (B) standard MK-2206. (C) compound lupeol

By competing via ATP to bind to AKT at the ATP binding site, inhibitors can inhibit AKT through the active site. Inhibition of AKT by the inhibitor can also occur through the allosteric site by targeting the PH domain and then maintaining AKT in an inactive form by preventing the protein from migrating to the plasma membrane where activation by the upstream kinase occurs (Andrikopoulou et al., 2022). Active site inhibitors have high potential but may have side effects, requiring dose restrictions. Some active site inhibitors of AKT that have been studied are capivasrtib (AZD5363) and ipatasertib (GDC0068), which have undergone clinical trials phases I and II. The efficacy of allosteric inhibitors in clinical studies is still modest despite their greater selectivity and lack of competition. MK-2206 and miransertib (ARQ092) are two examples of AKT allosteric inhibitors. Research suggests that these inhibitors can reduce side effects and toxicity (Landel et al., 2020; Mundi et al., 2016). The interaction between bioactive compounds from the strychnine tree and AKT1 will then be further analyzed for stability through molecular dynamics simulations.

Molecular dynamics simulation

Next, employing YASARA Dynamics software, the outcomes of molecular docking were used to analyze molecular dynamics simulations. In order to gather data regarding the temporal dynamics of interactions between ligands and proteins as well as binding sites, molecular dynamics simulations were run. Furthermore, these simulations were run in a setting that replicated human physiological parameters in order to ascertain the stability of the relationships between these two molecules (Chairunisa et al., 2023; Ivanova et al., 2018). Trajectory analysis employed Root Mean Square Deviation (RMSD), Root Mean Square Fluctuation (RMSF), and binding energy.

The use of molecular dynamics simulation time varies depending on the type of research. In drug development studies, some molecular dynamics research uses a time period of 20 ns to depict the stability of interactions between ligands and receptors. Other studies also utilize longer times such as 50 ns, 70 ns, 100 ns, up to 200 ns to illustrate the stability of ligand-receptor interactions (Al-Karmalawy et al., 2021; Castro et al., 2008; Fakih et al., 2021; Mohimani et al., 2017; Sakkiah et al., 2013; Wang et al., 2022). However, according to Ouassaf et al. (2021), simulations are conducted for a period of 5 ns to depict the potential of a compound as a drug candidate.

The RMSD evaluations show how a protein alters from its starting structural shape to its final position (Aier et al., 2016). Within the range of 0.514-2.127 Å, the average RMSD of the native (1.577 Å) and capivasertib (1.710 Å) at the active site of AKT1 is lower than the normal RMSD (1.758 Å) and brucine

(1.772 Å). The average RMSD under normal conditions falls within the ligand RMSD range, i.e., 1,577-1,772 Å. The average normal RMSD on the allosteric site (2.070 Å) is lower than the RMSD of lupeol (2.231 Å) within the range of 0.718-2.527 Å. Meanwhile, the average normal RMSD on the allosteric side falls within the ligand RMSD range, i.e., 1.882-2.231 Å (Figure 5A & 5B). Generally, normal RMSD values are higher than when the protein binds to the ligand, indicating that the chemical interactions between the ligand and protein stabilize the interaction of these two molecules. The mean normal RMSD within the ligand's range However, RMSD indicates that the interaction between the ligand and the protein it bonds to has a negligible impact on the stability of protein structure (Kalasariya et al., 2022; Weng et al., 2021).

Amino acid residue fluctuations on the protein during simulation are demonstrated by the RMSF analysis (Kalasariya et al., 2022). The RMSF values at the active site of AKT1 range from 0.72-1.09 Å for Val164 residues and 0.54-0.78 Å for Met281 residues. For Val164 residues, the RMSF of brucine is higher than the normal RMSF. The allosteric site RMSF ranges from 0.740-1.860 Å for Lys268 residues, 0.520-1.590 Å for Trp80 residues, 0.710-1.140 Å for Leu264 residues, 0.740-1.1370 Å for Val270 residues, and 0.750-1.930 Å for Ser205 residues. In general, the allosteric site RMSF under normal conditions is higher than the ligand RMSF, except for Ser205, Leu264, and Val270 residues where the RMSF of lupeol is higher. MK-2206 RMSF at Val270 residues also has a higher value than its normal RMSF (Figure 5C & 5D). The results of RMSF analysis at the active and allosteric sites show varied outcomes. Higher RMSF values indicate that amino acid residues do not have strong interactions at the amino acid binding site with their ligands, indicating suboptimal binding between them. Nonetheless, the low RMSF values obtained are less than 2 Å, suggesting that the ligand and its protein still have a strong level of binding (De Vita et al., 2021; Umar et al., 2023).

Binding energy provides information on the binding affinity formed during the simulation period. The free binding energy (ΔG) that is derived from the combined potential energy of the protein, ligand, and ligand, along with the solvation energy of all three, is known as binding energy (Chen et al., 2015; Riandono & Istyastono, 2023). The results of binding energy analysis at the active site of AKT1 are less favorable within the 5 ns timeframe. The binding energy values within the 5 ns timeframe are negative, with average binding energy values successively -157.001 kJ/mol, -199.920 kJ/mol, and -194.716 kJ/mol for native, capivasertib, and brucine. Similarly, the analysis of binding energy at the allosteric site of AKT1 is less favorable within the 5 ns timeframe, where the binding energy values within the 5 ns timeframe are negative, with average binding energy values successively -47.485 kJ/mol, -69.797 kJ/mol, and -23.752 kJ/mol for native, MK-2206, and lupeol **(**Figure 5E & 5F**).** The results of molecular dynamics analysis indicate low stability between the bioactive compounds from the strychnine tree and the AKT1 protein. Factors influencing this include instability in the initial binding mode, mismatched force field parameters, and the limited simulation time, suggesting that new stability may occur after 5 ns (Kalasariya et al., 2022; Liu et al., 2017).

Simulations of molecular dynamics was out with distinct proteins for the allosteric site (PDB ID: 3O96) and the active site (PDB ID: 3MVH). Overall, molecular dynamics simulation results show that the stability of protein conformations during the simulation period is largely unaffected by the ligand-protein interaction, both at the active and allosteric sites (Kalasariya et al., 2022; Weng et al., 2021). The ligand and its protein bind relatively strongly, as evidenced by the RMSF values at the active and allosteric sites (De Vita et al., 2021; Umar et al., 2023). At the conclusion of the simulation, if the values are still changing, there may be a chance that conformational changes have occurred, indicating less stable connections between the ligand and the receptor. This implies that longer simulation times would be required to get better results because the anticipated stability might not materialize for up to 5 ns (Aier et al., 2016; Kalasariya et al., 2022). Less stable interactions with the AKT1 protein are shown by the examination of the energies of all ligands. Positive binding energy values yield positive results in binding energy analysis utilizing YASARA software (Chen et al., 2015).

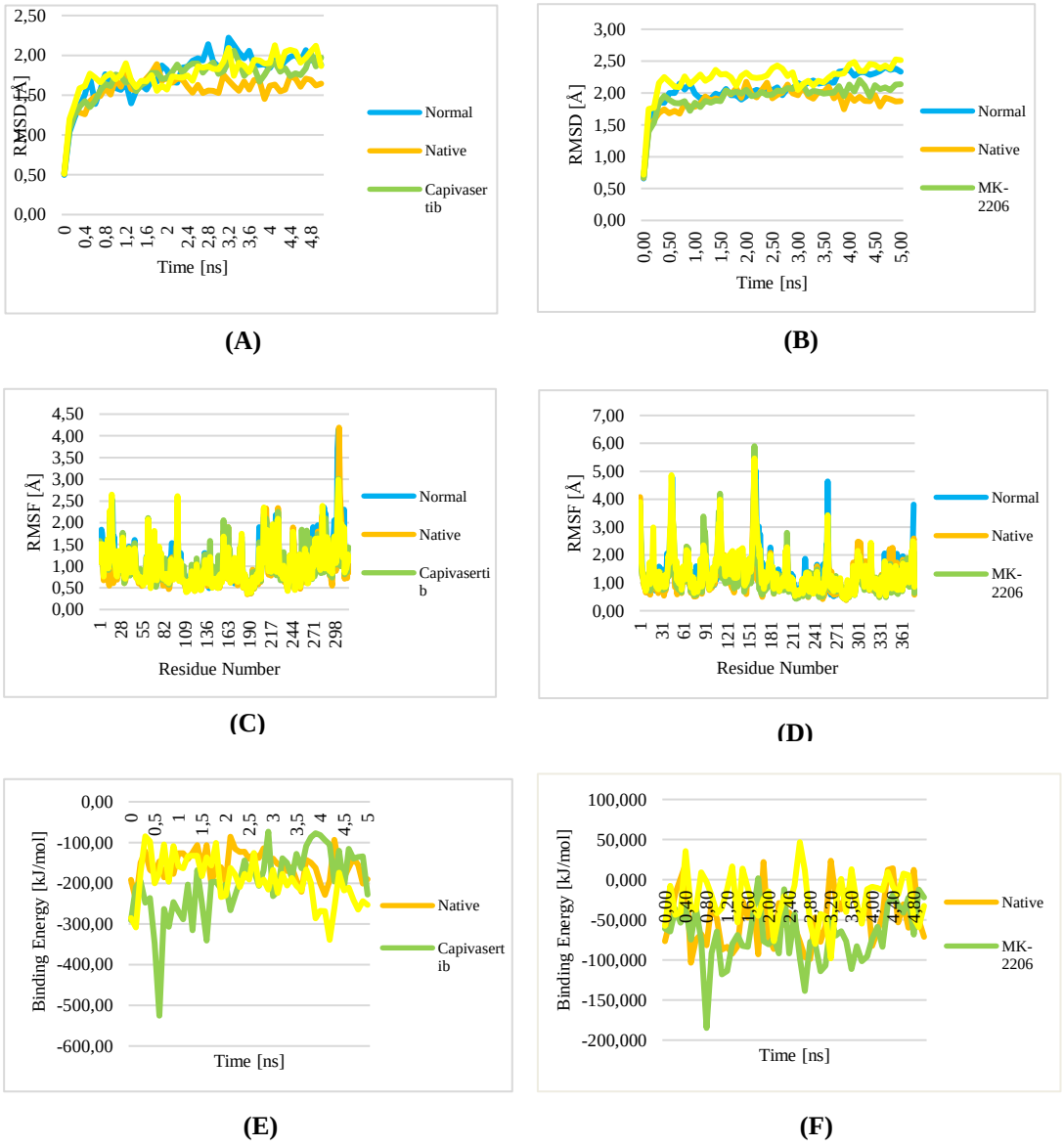

Figure 5. Results of molecular dynamics simulation with AKT1 protein and strychnine tree compounds. (A) analysis result of AKT1 RMSD on the active site. (B) analysis result of AKT1 RMSD on the allosteric site. (C) analysis result of AKT1 RMSF on the active site. (D) analysis result of AKT1 RMSF on the allosteric site. (E) analysis result of AKT1 binding energy on the active site. (F) analysis result of AKT1 binding eEnergy on the allosteric site

Explanation: Normal: when the protein is not bound to any ligand

CONCLUSION

The potential of bioactive compounds from the strychnine tree (*Strychnos nux-vomica*) can be demonstrated by *in silico* and molecular dynamics research to inhibit breast cancer development through the PI3K/AKT pathway by targeting AKT1. This has the potential to reduce cell proliferation, migration, angiogenesis, and metastasis, as well as enhance apoptotic effects. AKT1 protein inhibition is feasible at both the active and allosteric sites. However, the stability of the interaction between bioactive

compounds from the strychnine tree and AKT1 still shows less favorable results due to the limitations of the tools used, resulting in a simulation time of only 5 ns. Further research is needed using a 20 ns or more time frame for molecular dynamics simulation. To further corroborate the results of this investigation, in vitro and in vivo experiments can be carried out.

ACKNOWLEDGEMENT

No particular grant from a public, private, or nonprofit organization was given for this research. This journal article is written based on the research findings of a thesis conducted at Faculty of Medicine, Master of Biomedicine Programme, Universitas Jenderal Soedirman. The author would like to express gratitude to Dr. Muhammad Salman Fareza, S.Si., M.Si and Dr. dr. Gita Nawantantrini, Sp.PA., M.Kes for their contributions in reviewing and providing valuable input for this research.

REFERENCES

Global Cancer Observatory. (2021). World Health Organization in International Agency for Research on Cancer: Indonesia - Globocan 2020. Retrieved March 17, 2022, from https://gco.iarc.fr/today/fact-sheets-populations

Global Cancer Observatory. (2020). World Health Organization in International Agency for Research on Cancer: Breast - Globocan 2020. Retrieved May 21, 2022, from https://gco.iarc.fr/today/data/factsheets/cancer/20-Breast-fact-sheet

Aier, I., Varadwaj, P. K., & Raj, U. (2016). Structural insights into conformational stability of both wild-type and mutant EZH2 receptor. *Scientific Reports*, *6*(September), 1–10. https://doi.org/10.1038/srep34984

Al-Karmalawy, A. A., Dahab, M. A., Metwaly, A. M., Elhady, S. S., Elkaeed, E. B., Eissa, I. H., & Darwish, K. M. (2021). Molecular Docking and Dynamics Simulation Revealed the Potential Inhibitory Activity of ACEIs Against SARS-CoV-2 Targeting the hACE2 Receptor. *Frontiers in Chemistry*, *9*(May). https://doi.org/10.3389/fchem.2021.661230

Al-Khodairy, F. M., Kalim, M., Khan, A., Kunhi, M., Pulicat, M. S., Akhtar, S., & Arif, J. M. (2013). *In silico* prediction of mechanism of erysolin-induced apoptosis in human breast cancer cell lines. *American Journal of Bioinformatics Research*, *2013*(3), 62–71. https://doi.org/10.5923/j.bioinformatics.20130303.03

Andrikopoulou, A., Chatzinikolaou, S., Panourgias, E., Kaparelou, M., Liontos, M., Dimopoulos, M. A., & Zagouri, F. (2022). "The emerging role of capivasertib in breast cancer." *Breast*, *63*(March), 157–167. https://doi.org/10.1016/j.breast.2022.03.018

Arthur, D. E., Akoji, J. N., Sahnoun, R., Okafor, G. C., Abdullahi, K. L., Abdullahi, S. A., & Mgbemena, C. (2021). A theoretical insight in interactions of some chemical compounds as mTOR inhibitors. *Bulletin of the National Research Centre*, *45*(1). https://doi.org/10.1186/s42269-021-00525-x

Brown, G. R., Hem, V., Katz, K. S., Ovetsky, M., Wallin, C., Ermolaeva, O., Tolstoy, I., Tatusova, T., Pruitt, K. D., Maglott, D. R., & Murphy, T. D. (2015). Gene: A gene-centered information resource at NCBI. *Nucleic Acids Research*, *43*(D1), D36–D42. https://doi.org/10.1093/nar/gku1055

Bull, S. C., & Doig, A. J. (2015). Properties of protein drug target classes. *PLoS ONE*, *10*(3), 1–44. https://doi.org/10.1371/journal.pone.0117955

Castro, J. R. M., Fuzo, C. A., Degrève, L., & Caliri, A. (2008). The role of disulfide bridges in the 3-D structures of the antimicrobial peptides gomesin and protegrin-1: A molecular dynamics study. *Genetics and Molecular Research*, *7*(4), 1070–1088. https://doi.org/10.4238/vol7-4gmr507

Chairunisa, F., Safithri, M., Andrianto, D., Kurniasih, R., & Irsal, R. A. P. (2023). Molecular docking of red betel leaf bioactive compounds (Piper crocatum) as lipoxygenase inhibitor. *Indonesian Journal of Pharmaceutical Science and Technology*, *10*(2), 90. https://doi.org/10.24198/ijpst.v10i2.38934

Chen, D. E., Willick, D. L., Ruckel, J. B., & Floriano, W. B. (2015). Principal component analysis of binding energies for single-point mutants of hT2R16 bound to an agonist correlate with experimental

mutant cell response. *Journal of Computational Biology*, *22*(1), 37–53. https://doi.org/10.1089/cmb.2014.0192

Chen, J., Qu, Y., Wang, D., Peng, P., Cai, H., Gao, Y., Chen, Z., & Cai, B. (2014). Pharmacological evaluation of total alkaloids from nux vomica: Effect of reducing strychnine contents. *Molecules*, *19*(4), 4395–4408. https://doi.org/10.3390/molecules19044395

Chin, C. H., Chen, S. H., Wu, H. H., Ho, C. W., Ko, M. T., & Lin, C. Y. (2014). cytoHubba: Identifying hub objects and sub-networks from complex interactome. *BMC Systems Biology*, *8*(4), 1–7. https://doi.org/10.1186/1752-0509-8-S4-S11

Daina, A., Michielin, O., & Zoete, V. (2019). SwissTargetPrediction: updated data and new features for efficient prediction of protein targets of small molecules. *Nucleic Acids Research*, *47*(W1), W357–W3664. https://doi.org/10.1093/nar/gkz382

De Vita, S., Chini, M. G., Bifulco, G., & Lauro, G. (2021). Insights into the ligand binding to bromodomain-containing protein 9 (BRD9): A guide to the selection of potential binders by computational methods. *Molecules*, *26*(23). https://doi.org/10.3390/molecules26237192

De Vivo, M., Masetti, M., Bottegoni, G., & Cavalli, A. (2016). Role of molecular dynamics and related methods in drug discovery. *Journal of Medicinal Chemistry*, *59*(9), 4035–4061. https://doi.org/10.1021/acs.jmedchem.5b01684

Dong, C., Wu, J., Chen, Y., Nie, J., & Chen, C. (2021). Activation of PI3K/AKT/mTOR pathway causes drug resistance in breast cancer. *Frontiers in Pharmacology*, *12*(March), 1–16. https://doi.org/10.3389/fphar.2021.628690

Eldahshan, O. A., & Abdel-Daim, M. M. (2015). Phytochemical study, cytotoxic, analgesic, antipyretic and anti-inflammatory activities of Strychnos nux-vomica. *Cytotechnology*, *67*(5), 831–844. https://doi.org/10.1007/s10616-014-9723-2

Enkhtaivan, G., Maria John, K. M., Ayyanar, M., Sekar, T., Jin, K. J., & Kim, D. H. (2015). Anti-influenza (H1N1) potential of leaf and stem bark extracts of selected medicinal plants of South India. *Saudi Journal of Biological Sciences*, *22*(5), 532–538. https://doi.org/10.1016/j.sjbs.2015.01.011

Fakih, T. M., Wisnuwardhani, H. A., Dewi, M. L., Ramadhan, D. S. F., Hidayat, A. F., & Prayitno, R. (2021). Simulasi dinamika molekuler senyawa asam ferulat dan turunannya dari kulit buah Nanas (Ananas comosus) sebagai inhibitor enzim tirosinase. *Jurnal Sains Farmasi & Klinis*, *8*(2), 208. https://doi.org/10.25077/jsfk.8.2.208-220.2021

Fusco, N., Malapelle, U., Fassan, M., Marchiò, C., Buglioni, S., Zupo, S., Criscitiello, C., Vigneri, P., Dei Tos, A. P., Maiorano, E., & Viale, G. (2021). PIK3CA mutations as a molecular target for hormone receptor-positive, HER2-negative metastatic breast cancer. *Frontiers in Oncology*, *11*(March), 1–9. https://doi.org/10.3389/fonc.2021.644737

Giacomelli, A. O., Yang, X., Lintner, R. E., McFarland, J. M., Duby, M., Kim, J., Howard, T. P., Takeda, D. Y., Huong Ly, S., Kim, E., Gannon, H. S., Hurhula, B., Sharpe, T., Goodale, A., Fritchman, B., Steelman, S., Vazquez, F., Tsherniak, A., Aguirre, A. J., … Genet Author manuscript, N. (2018). Mutational processes shape the landscape of TP53 mutations in human cancer HHS Public Access Author manuscript. *Nat Genet*, *50*(10), 1381–1387. https://doi.org/10.1038/s41588-018-0204-y.Mutational

Gonzalez-Garcia, J., & Mlachila, M. (2017). Beyond the headlines. *Finance and Development*, *54*(2), 48–50. https://doi.org/10.3917/reco.566.1275

Guo, R., Wang, T., Zhou, G., Xu, M., Yu, X., Zhang, X., Sui, F., Li, C., Tang, L., & Wang, Z. (2018). Botany, Phytochemistry, Pharmacology and Toxicity of Strychnos nux-vomica L.: A Review. *American Journal of Chinese Medicine*, *46*(1), 1–23. https://doi.org/10.1142/S0192415X18500015

Hanif, A. U., Lukis, P. A., & Fadlan, A. (2020). Pengaruh minimisasi energi MMFF94 dengan MarvinSketch dan Open Babel PyRx pada penambatan molekular turunan oksindola tersubstitusi. *Alchemy*, *8*(2), 33–40. https://doi.org/10.18860/al.v8i2.10481

Hein, A. L., Ouellette, M. M., & Yan, Y. (2014). Radiation-induced signaling pathways that promote cancer cell survival (Review). *International Journal of Oncology*, *45*(5), 1813–1819. https://doi.org/10.3892/ijo.2014.2614

Hermawan, A., Ikawati, M., Istighfari, R., Khumaira, A., Putri, H., Putri, I., Meta, S., & Anggraini, H. (2021). Identification of potential therapeutic target of naringenin in breast cancer stem cells inhibition by bioinformatics and in vitro studies. *Saudi Pharmaceutical Journal*, *29*(1), 12–26. https://doi.org/10.1016/j.jsps.2020.12.002

Hermawan, A., Putri, H., Hanif, N., & Ikawati, M. (2021). *Integrative bioinformatics study of tangeretin potential targets for preventing metastatic breast cancer*. *2021*

Hermawan, A., Putri, H., & Utomo, R. Y. (2020). Functional network analysis reveals potential repurposing of β-blocker atenolol for pancreatic cancer therapy. *DARU, Journal of Pharmaceutical Sciences*, *28*(2), 685–699. https://doi.org/10.1007/s40199-020-00375-4

Hermawan, A., Putri, H., & Yudi, R. (2021). Exploration of targets and molecular mechanisms of cinnamaldehyde in overcoming fulvestrant - resistant breast cancer : a bioinformatics study. *Network Modeling Analysis in Health Informatics and Bioinformatics*, *9*. https://doi.org/10.1007/s13721-021-00303-9

Hua, H., Zhang, H., Chen, J., Wang, J., Liu, J., & Jiang, Y. (2021). Targeting Akt in cancer for precision therapy. *Journal of Hematology and Oncology*, *14*(1), 1–25. https://doi.org/10.1186/s13045-021-01137-8

Ivanova, L., Tammiku-Taul, J., García-Sosa, A. T., Sidorova, Y., Saarma, M., & Karelson, M. (2018). Molecular Dynamics Simulations of the Interactions between Glial Cell Line-Derived Neurotrophic Factor Family Receptor GFRα1 and Small-Molecule Ligands. *ACS Omega*, *3*(9), 11407–11414. https://doi.org/10.1021/acsomega.8b01524

Joy, A. L. M., Appavoo, M. R., & Mohesh, M. I. G. (2016). Antiangiogenic activity of Strychnos nux vomica leaf extract on chick chorioallantoic membrane model. *Journal of Chemical and Pharmaceutical Research*, *8*(1), 549–552. http://jocpr.com/vol8-iss1-2016/JCPR-2016-8-1-549-552.pdf

Kalasariya, H. S., Patel, N. B., Gacem, A., Alsufyani, T., Reece, L. M., Yadav, V. K., Awwad, N. S., Ibrahium, H. A., Ahn, Y., Yadav, K. K., & Jeon, B. H. (2022). Marine Alga ulva fasciata-derived molecules for the potential treatment of SARS-CoV-2: An *in silico* Approach. *Marine Drugs*, *20*(9), 1–38. https://doi.org/10.3390/md20090586

Kuhn, M., Szklarczyk, D., Pletscher-Frankild, S., Blicher, T. H., Von Mering, C., Jensen, L. J., & Bork, P. (2014). STITCH 4: Integration of protein-chemical interactions with user data. *Nucleic Acids Research*, *42*(D1), 401–407. https://doi.org/10.1093/nar/gkt1207

Landel, I., Quambusch, L., Depta, L., & Rauh, D. (2020). Spotlight on AKT: current therapeutic challenges. *ACS Medicinal Chemistry Letters*, *11*(3), 225–227. https://doi.org/10.1021/acsmedchemlett.9b00548

Liao, Y., Wang, J., Jaehnig, E. J., Shi, Z., & Zhang, B. (2019). WebGestalt 2019: gene set analysis toolkit with revamped UIs and APIs. *Nucleic Acids Research*, *47*(W1), W199–W205. https://doi.org/10.1093/nar/gkz401

Liu, K., Watanabe, E., & Kokubo, H. (2017). Exploring the stability of ligand binding modes to proteins by molecular dynamics simulations. *Journal of Computer-Aided Molecular Design*, *31*(2), 201–211. https://doi.org/10.1007/s10822-016-0005-2

Liu, R., Chen, Y., Liu, G., Li, C., Song, Y., Cao, Z., Li, W., Hu, J., Lu, C., & Liu, Y. (2020). PI3K/AKT pathway as a key link modulates the multidrug resistance of cancers. *Cell Death and Disease*, *11*(9). https://doi.org/10.1038/s41419-020-02998-6

Lu, L., Huang, R., Wu, Y., Jin, J. M., Chen, H. Z., Zhang, L. J., & Luan, X. (2020). Brucine: a review of phytochemistry, pharmacology, and toxicology. *Frontiers in Pharmacology*, *11*(April), 1–6. https://doi.org/10.3389/fphar.2020.00377

Martorana, F., Motta, G., Pavone, G., & Motta, L. (2021). *AKT Inhibitors : New Weapons in the Fight Against Breast Cancer ? 12*(April), 1–13. https://doi.org/10.3389/fphar.2021.662232

Mohimani, H., Gurevich, A., Mikheenko, A., Garg, N., Nothias, L.-F., Ninomiya, A., Kentaro Takada, P. C. D., & Pevzner, P. A. (2017). Molecular Dynamics for all. *Physiology & Behavior*, *176*(3), 139–148. https://doi.org/10.1016/j.neuron.2018.08.011.Molecular

Mundi, P. S., Sachdev, J., McCourt, C., & Kalinsky, K. (2016). AKT in cancer: new molecular insights and advances in drug development. *British Journal of Clinical Pharmacology*, *110*, 943–956. https://doi.org/10.1111/bcp.13021

Ouassaf, M., Belaidi, S., Mogren Al Mogren, M., Chtita, S., Ullah Khan, S., & Thet Htar, T. (2021). Combined docking methods and molecular dynamics to identify effective antiviral 2, 5-diaminobenzophenonederivatives against SARS-CoV-2. *Journal of King Saud University - Science*, *33*(2), 101352. https://doi.org/10.1016/j.jksus.2021.101352

Pantsar, T., & Poso, A. (2018). Binding affinity via docking: fact and fiction. *Molecules*, *23*(8), 1DUMMY. https://doi.org/10.3390/molecules23081899

Reynaldi, M. A., & Setiawansyah, A. (2022). Potensi anti-kanker payudara tanaman songga (Strychnos lucida R.Br): Tinjauan interaksi molekuler terhadap reseptor estrogen-α *in silico*. *Sasambo Journal of Pharmacy*, *3*(1), 30–35. https://doi.org/10.29303/sjp.v3i1.149

Riandono, F. D., & Istyastono, E. P. (2023). Molecular dynamics simulations of the Stk630921 Interactions To Interleukin-17a. *International Journal of Applied Pharmaceutics*, *15*(1), 250–255. https://doi.org/10.22159/ijap.2023v15i1.46369

Rizvi, S. M., Shazi, S., & Mohd., H. (2013). A simple click by click protocol to perform docking : *EXCLI Journal*, *12*, 831–857

Roy, A., Anand, A., Garg, S., Khan, M. S., Bhasin, S., Asghar, M. N., & Emran, T. Bin. (2022). Structure-Based *in silico* Investigation of Agonists for Proteins Involved in Breast Cancer. *Evidence-Based Complementary and Alternative Medicine*, *2022*. https://doi.org/10.1155/2022/7278731

Roy, N., Davis, S., Narayanankutty, A., Nazeem, P. A., Babu, T. D., Abida, P. S., Valsala, P. A., & Raghavamenon, A. C. (2016). Garlic phytocompounds possess anticancer activity by specifically targeting breast cancer biomarkers - an *in silico* study. *Asian Pacific Journal of Cancer Prevention*, *17*(6), 2883–2888

Sakkiah, S., Arooj, M., Kumar, M. R., Eom, S. H., & Lee, K. W. (2013). Identification of inhibitor binding site in human sirtuin 2 using molecular docking and dynamics simulations. *PLoS ONE*, *8*(1). https://doi.org/10.1371/journal.pone.0051429

Saraswati, S., & Agrawal, S. S. (2013). Brucine, an indole alkaloid from strychnos nux-vomica attenuates VEGF-induced angiogenesis via inhibiting VEGFR2 signaling pathway in vitro and in vivo. *Cancer Letters*, *332*(1), 83–93. https://doi.org/10.1016/j.canlet.2013.01.012

Surya, R. U., & Praveen, N. (2021). A molecular docking study of SARS-CoV-2 main protease against phytochemicals of Boerhavia diffusa Linn. for novel COVID-19 drug discovery. *Virus Disease*, *32*(1), 46–54. https://doi.org/10.1007/s13337-021-00683-6

Szklarczyk, D., Franceschini, A., Wyder, S., Forslund, K., Heller, D., Huerta-Cepas, J., Simonovic, M., Roth, A., Santos, A., Tsafou, K. P., Kuhn, M., Bork, P., Jensen, L. J., & Von Mering, C. (2015). STRING v10: Protein-protein interaction networks, integrated over the tree of life. *Nucleic Acids Research*, *43*(D1), D447–D452. https://doi.org/10.1093/nar/gku1003

Tapia, O., Riquelme, I., Leal, P., Sandoval, A., Aedo, S., Weber, H., Letelier, P., Bellolio, E., Villaseca, M., Garcia, P., & Roa, J. C. (2014). The PI3K/AKT/mTOR pathway is activated in gastric cancer with potential prognostic and predictive significance. *Virchows Archiv*, *465*(1), 25–33. https://doi.org/10.1007/s00428-014-1588-4

Tapiory, A. A., Octavia Pertiwi, K., Fadilla, K., Reyhanditya, D., & Fatchiyah, F. (2020). In-Silico Analysis of Methoxyl Pectin Compounds from Banana Peels as HMG-CoA Reductase Inhibitor Complexes. *JSMARTech*, *1*(2), 46–50. https://doi.org/10.21776/ub.jsmartech.2020.001.02.5

Umar, K., Zothantluanga, J. H., Luckanagul, J. A., Limpikirati, P., & Sriwidodo, S. (2023). Structure-based computational screening of 470 natural quercetin derivatives for identification of SARS-CoV-2 Mpro inhibitor. *PeerJ*, *11*, 1–27. https://doi.org/10.7717/peerj.14915

Victor, D., Doss, A., Doss, V. A., Maddisetty, P., & Sukumar, M. (2016). Biological active compounds with various medicinal values of Strychnos Nux-vomica – A Pharmacological summary. *J Global Trends Pharm Sci*, *7*(1), 3044–3047

Wang, X., Chen, Y., Zhang, S., & Deng, J. N. (2022). Molecular dynamics simulations reveal the selectivity mechanism of structurally similar agonists to TLR7 and TLR8. *PLoS ONE*, *17*(4 April), 1–18. https://doi.org/10.1371/journal.pone.0260565

Weng, Y. L., Naik, S. R., Dingelstad, N., Lugo, M. R., Kalyaanamoorthy, S., & Ganesan, A. (2021). Molecular dynamics and *in silico* mutagenesis on the reversible inhibitor-bound SARS-CoV-2 main protease complexes reveal the role of lateral pocket in enhancing the ligand affinity. *Scientific Reports*, *11*(1), 1–22. https://doi.org/10.1038/s41598-021-86471-0

Yuan, Y., Long, H., Zhou, Z., Fu, Y., & Jiang, B. (2023). *PI3K – AKT-Targeting Breast Cancer Treatments : Natural Products and Synthetic Compounds*. 1–23.

Zardecki, C., Dutta, S., Goodsell, D. S., Voigt, M., & Burley, S. K. (2016). RCSB protein data bank: a resource for chemical, biochemical, and structural explorations of large and small biomolecules. *Journal of Chemical Education*, *93*(3), 569–575. https://doi.org/10.1021/acs.jchemed.5b00404

Zhang, J. Y., Li, N., Hu, K., & Tu, P. F. (2012). Chemical constituents from processed seeds of Strychnos nuxvomica. *Journal of Chinese Pharmaceutical Sciences*, *21*(2), 187–191. https://doi.org/10.5246/jcps.2012.02.025

Zhou, Yang, & Wang. (2020). Network pharmacology-based investigation for predicting active ingredients and potential targets of *Strychnos nux-vomica* L. in treating multiple myeloma [preprint]. Available at Research Square [https://doi.org/10.21203/rs.3.rs-97494/v1]

Zhu, K., Wu, Y., He, P., Fan, Y., Zhong, X., Zheng, H., & Luo, T. (2022). *PI3K / AKT / mTOR-Targeted Therapy for Breast Cancer*. 1–20

Pharmaciana
Vol.14, No.2, July 2024, page. 147-156
ISSN: 2088 4559; e-ISSN: 2477 0256
DOI: 10.12928/pharmaciana.v14i2.28242

Antioxidant, analgetic, and anti-inflammatory activity test of purple leaf ethanol extract (*Graptophyllum pictum* L. Griff) *in vitro* and *in vivo*

Sisca Ocvinta[1], Niluh Puspita Dewi[2*], Indah Kurnia Utami[2], Darmayanti[1], Syafika Alaydrus[2], Wawang Anwarudin[3]
[1]*Undergraduate Pharmacy Study program, STIFA Pelita Mas Palu*
Jl. Wolter Monginsidi, No. 106A Lolu Sel., Palu Sel, Palu City, Central Sulawesi, Indonesia
[2]*Department of Pharmacology, Clinical Pharmacy and Conmunity, STIFA Pelita Mas Palu*
Jl. Wolter Monginsidi, No. 106A Lolu Sel., Palu Sel., Palu City, Central Sulawesi, Indonesia
[3]STIKES Muhammadiyah Kuningan, Cigugur, Kuningan,
Jl. Raya Cigugur No. 28 Kuningan, Kabupaten Kuningan, West Java, Indonesia

Submitted: 12-06-2024 ***Reviewed: 01-07-2024*** ***Accepted: 23-07-2024***

ABSTRACT

Purple leaves (*Graptophyllum pictum* L. Griff) are one plant that is widely used as a medicine. Purple leaves have pharmacological activities that can be used as medicine, including antioxidants, anti-inflammatory, antidiabetic, analgesics, immunomodulators, antihemorrhoids, and antibacterial. The objective of this study was to determine the antioxidant properties of ethanol extract from purple leaves as well as its properties as an analgesic and anti-inflammatory against Wistar rats. Antioxidant activity was measured using the DPPH method with quercetin as a comperation in vitro the in vivo study of 25 Wistar rats was divided into 5 groups consisting of 5 animals each, namely normal control, positive control, negative control, treatment group with a dose of 50 mg/kg BW and treatment group with a dose of 100 mg/kg BW. The analgetic activity test was conducted by the writhing test method, while anti-inflammatory activity was measured by measuring the percentage of inflammatory volume using a mercury plethysmometer. The data was analyzed using the One-way ANOVA SPSS software program. The results showed that antioxidant activity showed an IC_{50} value of 72.312 ± 24.406 μg/mL (strong antioxidant). Meanwhile, in the analgetic test, the highest percentage of analgesic effectiveness was found at a dose of 100 mg/kg BW with a value of 129.64% and showed anti-inflammatory activity at a dose of 100 mg/kg BW with a percentage decrease in edem volume of 28.73% at the sixth hour.

Keywords: antioxidant, analgesic, anti-inflammatory, *Grapthophyllum pictum* (L.) Griff

Corresponding author:
Niluh Puspita Dewi
Pelita Mas Palu College of Pharmaceutical Sciences,
Jl. Wolter Monginsidi, No. 106A Lolu Sel., Palu Sel, Palu City, Central Sulawesi, Indonesia
Email: niluhpuspitadewi978@gmail.com

INTRODUCTION

Antioxidants are compounds that have the ability to neutralize free radicals, which harm body cells and result in many health issues, including inflammation (Kurniawati et al., 2020). While Inflammation is the complex biological response of blood vessel tissue to stimuli that cause damage. Furthermore, there is a correlation between inflammation and pain, which is linked to alterations in membranes, vascular permeability, and protein denaturation (Gunathilake et al., 2018). Pain is an unpleasant sensory and emotional experience for the sufferer, which is related to (threat) tissue damage. Mechanical, chemical, or physical stimulation that injure tissues can result in pain. Additionally, several chemicals known as pain mediators, including prostaglandins, histamine, bradykinin, and leukotriene, can be released in response to stimulation (Yane & Handayani, 2019).

Traditional medicine is a medicine made from ingredients or a combination of ingredients obtained from plants or minerals that have not been processed in the form of pure substances. People use traditional medicine for prevention, recovery, and health improvement. Traditional medicine is an alternative treatment that has been accepted in various countries. Traditional medicine in general uses plants, one of which is purple leaves (*Graptophyllum pictum* (L). Griff) (Triyandi et al., 2021).

Purple leaves are a plant that can be used for medicine. Purple leaves have 3 types of plant varieties, namely purple leaves, green leaves, and white mottled leaves. Purple leaves have pharmacological activities that can be used as medicines, including antioxidants (improving the deterioration of cells in the body), anti-inflammatory (reducing or suppressing inflammation), antidiabetic (lowering blood glucose levels), analgesics (relieving pain), immunomodulators (increasing the work of the immune system in the body), antihemorrhoids (treating symptoms and complaints of hemorrhoids), and antibacterial (as an antiseptic) (Sartika & Indradi, 2021). Flavonoids, tannins, alkaloids, steroids, saponins, alcohols, and calcium oxalate are the secondary metabolite compounds of purple leaves. This content has many benefits so it is widely used as medicine by the community (Rachim et al., 2021). In previous research, purple leaf infusion contained moderate antioxidants with an IC_{50} value of 125.09 µg/mL (Salim, 2018). In other research, purple leaves at a dose of 4.5 mg/200 g BW had a greater ability than a dose of 1.125 mg/kg BW to provide anti-inflammatory effects (Triyandi et al., 2021). In line with other research, purple leaf extract has the greatest analgesic activity at a dose of 12 mg/kg BW (Nhadira et al, 2019).

The purpose of this study was to determine the antioxidant activity of purple leaf ethanol extract (*Graphtophyllum pictum* (L.) Griff) in vitro using the DPPH method and to determine its effectiveness as an analgesic and anti-inflammatory against Wistar rats.

MATERIALS AND METHOD

Collection and authentication of plant material

Graphtophyllum pictum (L.) Griff was collected in Gunung Sari Village, Pasangkayu Regency, and authenticated by botanists from UPT. Suber of Sulawesi Biodiversity (Herbarium Celebense) with number 98/UN.28.UPT-SDHS/LK/2023 at Tadulako University.

Methods

Extract preparation

The preparation of purple leaf ethanol extract was carried out by maceration method using 96% ethanol solvent. Simplicia powder was weighed 1,000 grams and then extracted using a 96% ethanol solvent of 6 liters divided into 3 vessels. Maceration is carried out for 3x24 hours in a room that is protected from direct sunlight and is at room temperature with several times stirring. After obtaining the results of maceration, it is filtered on filter paper and then filtrate is obtained. After obtaining the filtra, it is then concentrated using rotavapor at a temperature of 70ºC and in a waterbath at 60ºC until a thick extract is obtained, then the yield is calculated (Elmitra et al., 2019).

$$\%\ Ectract = \frac{\text{weight of ectract obtained (g)}}{\text{weight of ectracted material (g)}} x\ 100\% \quad \text{.....(1)}$$

DPPH solution preparation

Antioxidant activity is determined by the DPPH free radical method. DPPH 0.004% b/v solution is made by dissolving 0.004 gram DPPH Crystals in 100 mL ethanol Pro Analyst (Antarti & Lisnasari, 2018).

Preparation of quartz comparative solution

The raw solution was made at a concentration of 100 ppm of quartz by weighing 10 mg of quartz in 100 mL of ethanol (for the calibration curve) with concentrations of 2,4,6,8 and 12 ppm (Sari et al., 2021).

Determining of maximum wavelength

A total of 1 mL of quartz cetin solution is pipetted into the cuvette then 1 mL of DPPH 0.004% b/v solution is added and homogenized After that, the absorption of the solution is read using a UV-Vis spectrophotometer at the maximum wavelength (400-800 nm) (Maulydya et al., 2023).

OT (operating time) determination

The determination of the Operating Time for the test material was carried out by pipetting 1000 µL of quartz cetin solution into the cuvette, then adding 1000 µL of DPPH 0.004% b/v solution. After that, read the absorption of the solution using a UV-Vis spectrophotometer every 5 minutes until the 30th minute with the maximum wavelength (Agustiarini & Wijaya, 2022).

Control solution absorbance measurement

Take 1 mL of DPPH 0.004% b/v solution then add 1 mL of ethanol solution pro Analyst and then homogenize. Then read the absorption using a UV-Vis spectrophotometer at a maximum wavelength with ethanol as a blank (Agustiarini & Wijaya, 2022).

Measurement of antioxidant activity of quartz comparator

Dilution was carried out from the 1000 ppm quartz master solution into 20, 40, 60, 80, and 100 ppm, each taking 1 mL then added with DPPH 0.004% b/v as much as 1 mL, then left to sit during the OT obtained and then read the absorption with a UV-VIS spectrophotometer at a maximum wavelength repeated 3 times (Agustiarini & Wijaya, 2022).

Measurement of antioxidant activity of purple leaf ethanol extract

Sample testing uses several concentrations, namely 20; 40; 60; and 80 ppm. Each sample was taken as much as 1000 µL then 200 µL DPPH 0.004% b/v was added, then incubated during the operating time of each sample. Then measure absorbance at the maximum wavelength and then record the absorbance value obtained at each concentration. Then observe the comparison with quartz as a comparison. The percentage of inhibition or inhibitor can be calculated using the Formula 2: (Prasetyo et al., 2021).

$$\%\ inhibition = \frac{\text{abs.control} - \text{abs.sample}}{\text{abs.control}} x\ 100\% \text{.....(2)}$$

Preparation of CMC Na colloidal solution

Sodium carboxymethyl cellulose (Na CMC) was weighed as much as 0.5 grams of Na.CMC was sprinkled into a mortar filled with hot water as much as 10 mL. Let stand for a homogeneous period, then pour into a 100 mL measuring flask, and add aquadest to the limit mark (Triyandi et al., 2021).

Purple leaf extract suspension manufacturing

Purple leaf extract (*Graptophyllum pictum* (L) Griff) was weighed to make a suspension with 0.2 grams (dose 50 mg/kg BW) and 1 gram (dose 100 mg/kg BW) respectively. Furthermore, 0.5% Na CMC is added to each extract and the volume is sufficient to 25 mL, then beaten until homogeneous (Suryandari et al., 2021).

Manufacturing of mefenamic acid suspension

Mefenamic Acid tablets as many as 1 tablet were crushed until smooth using a lump and weighed as much as 0.0036 g. Then it is suspended with Na CMC that has been made and the volume is enough to 100 mL with aqua dest (Wardani et al., 2020).

Preparation of diclofenac sodium suspension

Weigh 100 mg of diclofenac sodium, then add aquadest to a volume of 25 mL. Take the solution as much as 11.81 mL, put it in a jar then add 0.5% Na CMC and homogenize, and put it in a measuring flask enough with aquadest until the volume is 25 mL. Volume of each 2.5 mL/200 g BW rat (Triyandi et al., 2021).

Carrageenan suspension preparation

1% carrageenan is obtained by suspending 1 gram of carrageenan and then homogenizing it in 0.9% sodium chloride then putting it into a 10 mL measuring flask to be sufficient to the limit mark on the measuring flask (Triyandi et al., 2021).

Test animals

This study uses an experimental method with a group random design, using 50 white rats have been approved by the ethics committee of Tadulako University with an approval number of 1795/UN28.1.30/KL/2024. The test animals used had inclusion criteria, namely male sex, rat weight of 100-200 grams, about 2-3 months old, healthy, active movement, normal behavior and activities, and macroscopic no anatomical and morphological abnormalities (BPOM RI, 2020).

Analgesic testing

This study used 25 rats and was grouped into 5, namely; normal control (no treatment), negative control group (Na CMC 0.5%), positive control group (mefenamic acid), and treatment group (purple leaf ethanol extract at a dose of 50 mg/kg BW and purple leaf ethanol extract at a dose of 100 mg/kg BW, each group was filled with 5 rats. Before the experiment was carried out for 18 hours, the rats were not fed. To stimulate the occurrence of squirting, acetic acid induction is carried out and then observed to find out the number of squirting every 5 minutes until the 30th minute. The number of squirms in each group was averaged and the percentage of analgetic protection in each group was calculated. The analysis was carried out to find out the differences in all treatment groups. The research data on the sigmun method in the form of the cumulative number of squirts in each treatment group was used to calculate the squirt protection and % of analgetic effectiveness with the formula (Sasongko et al., 2016).

$$\% \text{ writhing movement protection} = 100-(P/K \times 100\%)$$

Information:

P = Average cumulative number of experimental groups per individual

K = Number of cumulative squirms of the control group, mean cumulative number of squirms of rats, and percent. protection of squirms from all treatment groups

$$\% \text{ Analgetic activity} = \frac{\%protection\ of\ test\ material}{\%\text{acetic acid protection}} \times 100\% \quad \text{.....(3)}$$

Anti-inflammatory testing

This study used 25 rats and was grouped into 5, namely; normal control (no treatment), negative control group (Na CMC 0.5%), positive control group (sodium diclofenac), and treatment group (purple leaf ethanol extract at a dose of 50 mg/kg BW and purple leaf ethanol extract at a dose of 100 mg/kg BW, each group was filled with 5 rats. Before the experiment, the Wistar rats were not fed for 18 hours. Each mouse was weighed and the left leg was marked as the limit for measuring inflammation. Next, the leg was inserted into a plestimometer and the initial volume (Vo) of the rat's leg was recorded. Then, reagentation induction was carried out on the soles of the rats' feet to stimulate edema. After 1 hour of inflammation is measured as Inflammation volume after a certain time (Vt) and each test group is given treatment on an oral basis. Measurements are carried out for 6 hours and are measured once every 1 hour. Then the percentage of inflammation for each dose of the test substance is calculated with the formula percent of inflammation (Rikomah et al., 2019):

$$\% \text{ Inflammation} = \frac{(Vt-Vo)}{Vo} \times 100\%$$

Information:
Vt = Volume of inflammation after a certain time
Vo = Initial volume of the foot

Statistical analysis

The data from the test observation results will be statistically analyzed with One-way ANOVA with a confidence level of 95%, first, a normality test and a homogeneity test are carried out. If the results are not normally distributed and homogeneous, they will then be analyzed using the Kruskal Wallis nonparametric test to find out the significant difference with the $p<0.05$ value selected as the significance level. If there is a significant difference, the Man-Whitney test is carried out. Data classification was carried out using the SPSS V.29 software program.

RESULT AND DISCUSSION

Antioxidant activity

The antioxidant activity of purple leaf extract was carried out using the DPPH method. The concentration of antioxidant compounds that can inhibit the activity of DPPH free radicals by 50%. The smaller the IC_{50} value, the greater the antioxidant activity. $IC_{50\ was}$ obtained using the formula Y= bx+a based on linear regression (Maulydya et al., 2023).

Figure 1 shows the results of quercetin and purple leaf ethanol extract in inhibiting DPPH. The results of quercetin with a linear equation obtained an IC_{50} value of 66.26 ± 23.93 µg/mL, it can be said that quercetin has strong antioxidant activity and can inhibit DPPH free radicals. Meanwhile, in the testing of purple leaf ethanol extract, three repetitions were carried out for each concentration, and data on the standard value of the division was obtained by substituting in a linear equation IC_{50} value of 72.312 ± 24.406 µg/ml was obtained, this shows that purple leaf extract contains strong antioxidants so that the sample can inhibit of DPPH free radicals.

Based on the IC_{50} value, it can be stated that quercetin and purple-leaf ethanol extract both contain antioxidants, but the IC_{50} value in quercetin is lower than that of purple-leaf ethanol extract. This is because quercetin itself is a pure antioxidant that is often used as a comparison (Kammoda et al., 2021). In the meantime, secondary metabolites including alkaloids, sitosterols, glycosides, saponins, steroids, phenolic compounds, tannins, and flavonoids including anthocyanins and leucoanthocyanins have been found to be present in purple leaves (Disi et al., 2023). In the phenolic and flavonoid groups, it can donate or give hydrogen atoms to DPPH free radicals so that it can form a stable DPPH compound. The hydroxy group in phenol compounds is not the only one that affects the ability to dampen free radicals but is also influenced by the position or location of the group, and the presence of a 4-oxo group in its basic framework (Sartika & Indradi, 2021). The content of flavonoid compounds in purple leaves is a low-

molecular compound with high antioxidant properties. Flavonoids produce large amounts of simple phenolic acids, which can fight free radicals and enhance antioxidant effects (Rajeshwaran et al., 2021).

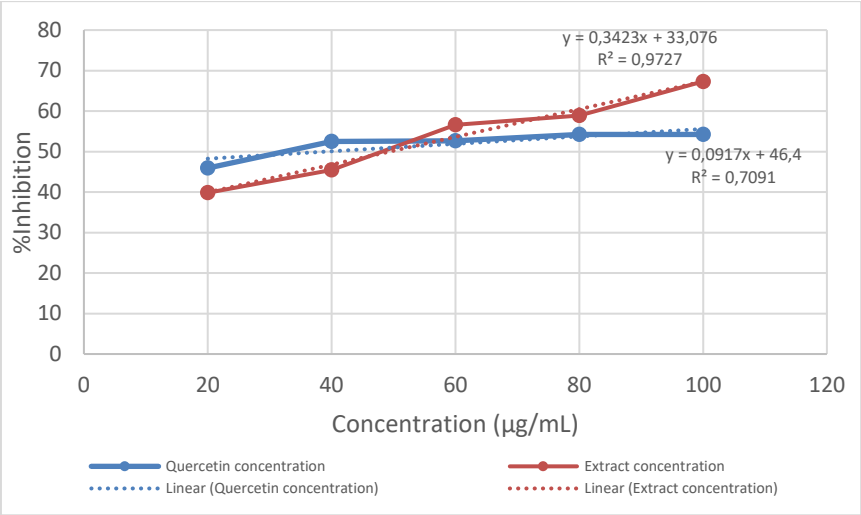

Figure 1. Antioxidant activity of quercetin and *Grapthophyllum* extract

Analgetic test results

In the analgetic activity test, the Writhing test method with chemical stimulation was used, namely Acetic Acid by injecting rats to stimulate pain. This method was chosen because it can trigger the release of arachidonic acid from phospholipid tissue through cyclooxygenase and form prostaglandin, causing pain. From the test, the recorded data included the accumulation of the activity of the Wistar rats observed every 5 minutes for 30 minutes. The data was used to calculate the percentage of analgetic power and the presentation of the protective power that appeared to determine the percentage of analgetic effects.

The 1% acetic acid inducer provides a painful effect, which is indicated by the presence of wriggling or contractions in the abdominal area of rats shown in Table 1. The results of the analgetic effect test showed a decrease in the average number of writhing in rats included in the positive control group by giving mefenamic acid of 3.6 mg/kg BW and the extract group with doses of 50 mg/kg BW and 100 mg/kg BW when compared to the negative control. This shows that both extract control (50 mg/kg BW and 100 mg/kg BW) and positive control (mefenamic acid) can reduce wriggling in rats. The smaller the average number of squirms shown by the group of rats, the better the analgesic effect (Darmayanti et al., 2020).

The percentage of analgetic power protection is used to determine the decrease in the number of squirming, the higher the amount of protection, the smaller the number of squirming that occurs. So that the *Grapthophyllum* extract given is able to withstand the pain stimulus of acetic acid in the pain response. Protection percentage data can be seen in Table 2, This test uses the Mann-Whitney further test because the data is not normally distributed and homogeneous. Based on the results obtained from the presentation of the largest analgesic power protection or close to the percentage of protection in the positive control group, there was a dose of 100 mg/kg BW in the extract group 80.23%, which means that at a dose of 100 mg/kg BW, it is effective in providing analgesic effects. Meanwhile, the comparison of doses of 50 mg/kg BW and 100 mg/kg BW was obtained without a statistically significant difference where 50 mg/kg BW extract had a greater variation than 100 mg/kg BW extract.

Table 1. The average number of writhing movements of animals induced 1% acetic acid and treated by *Graptophyllum* extract

Time (minute)	Writhing movement average ±					*p value*
	Normal group	Negative group	Mefenamic acid	Extract 50 mg/kg BW	Extract 100 mg/kg BW	
5	0 ± 0.00	3.4 ± 0.10	1 ± 0.70	1.2 ± 0.40	0.4 ± 0.50	0.001
10	0 ± 0.00	2.4 ± 0.50	1 ± 0.00	1.0 ± 0.70	0.4 ± 0.50	0.001
15	0 ± 0.00	2.2 ± 0.80	1.6 ± 0.50	1.4 ± 1.10	0.4 ± 0.50	0.004
20	0 ± 0.00	1.8 ± 0.40	0.4 ± 0.50	1.2 ± 0.80	0.6 ± 0.50	0.005
25	0 ± 0.00	1.6 ± 0.50	0.2 ± 0.40	0.6 ± 0.90	0.4 ± 0.50	0.012
30	0 ± 0.00	2.0 ± 0.70	0.8 ± 1.10	0.2 ± 0.40	0.4 ± 0.50	0.010

Exp: Value *p value* Obtained from *Kruskal-wallis Test* where the value *p<0,05* There is a significant difference

Table 2. The average percent of analgetic protection of animal induced by 1% acetic acid and treated with *Graptophyllum* extract

Group	% Analgetic protection ± SD	*P value*
Negative Group	0 ± 0,000^	0.003
Positive Group	61.89 ± 13.11	
Dosage extract 50 mg/Kg BW	56.38 ± 24.07^	
Dosage extract 100 mg/kg BW	80.23 ± 5.53^*	

Note : *= significant difference with negative control (p <0,05). ^ = not significantly different from the positive control. The p-value is obtained from the Kruskal-Wallis Test where the value p <0.05 is a significant difference

The percentage test results were carried out to prove that purple leaf ethanol extract has the ability as an analgetic drug, statistical data analysis can be seen in Table 3. The results of statistical analysis with the Kruskal-Wallis Test produced a significant value (P<0.05) which showed that the average percentage of analgetic was significantly different. The results showed that the positive control group and the 50 mg/kg BW extract group showed no significant difference in analgetic effects, while the extract group dose of 100 mg/kg BW had a significant difference. The larger the dose given, the greater the activity, so the dose of 100 mg/kg BW has a stronger analgetic activity than mefenamic acid.

Table 3. Analgetic activity percentage of *Grapthophyllum* extract compared to mefenamic acid as positive control

Group	%Analgetic activity ±	*P value*
Positive group	100 ± 0.000	0.044
Dosage extract 50 mg/Kg BW	91.11 ± 38.886	
Dosage extract 100 mg/kg BW	129.64 ± 89.40	

Exp: The p-value was obtained from the Kruskal-Wallis test where the p<0.05 value was significantly different

From the test results, it can be seen that the positive control and purple leaf ethanol extract (doses of 50 mg/kg BW and 100 mg/kg BW) both have analgetic effects. Mefenamic acid itself has the ability to inhibit the enzyme cyclooxygenase (COX) which plays a role in forming prostaglandins. Meanwhile, in ethanol extract, purple leaves have analgetic activity. Especially in alkaloid compounds and flavonoids in purple leaves have anti-inflammatory and analgetic content, this is related to the content of flavonoids whose mechanism of action inhibits the action of the cyclooxygenase enzyme (Nhadira et al., 2019). The enzyme cyclooxygenase functions in stimulating the release of pain mediator, prostagladin (Darmayanti et al., 2020). In line with reports stating that phytoconstituents such as flavonoids,

alkaloids, tannins, and steroids have significant analgetic activity after the process of separation of compounds in plants (Yimer et al., 2020).

Anti-inflammatory test results

Artificial inflammation was performed for anti-inflammatory testing, by injecting 1% Carrageenan into the soles of the rats' feet so it can cause swelling. Carrageenan is a sulfated polysaccharide derived from red seaweed plants and plays a role in the formation of udem in the acute inflammatory model. The volume of inflammation was measured before and after administration of the test material. The tool used to measure the volume of inflammation is a plestimometer.

The comparator used is sodium diclofenac where sodium diclofenac is one of the drugs that has an anti-inflammatory effect and is often used as a comparative control in studies regarding anti-inflammatory tests. In addition, diclofenac sodium has the ability to be absorbed quickly in the body and has low side effects compared to other anti-inflammatory drugs (Suryandari et al., 2021). NSAID are a bunch whose component of activity restrains the chemical cyclooxygenase 2 (COX-2) in creating prostagladin (an provocative arbiter) in tissues (Amran only et al., 2018).

In Figure 2, it can be seen that the positive control and extract control groups experienced a significant reduction in edema compared to the negative control. The largest decrease in edema volume occurred in the control of the extract at a dose of 100 mg/kg BW where the decrease occurred constantly from the first hour to the sixth hour. Meanwhile, in positive control, it was produced with a significant decrease in edema volume. In the control dose of 50 mg/kg BW experienced a lower decrease, while in the negative control, the increase in edema was quite long.

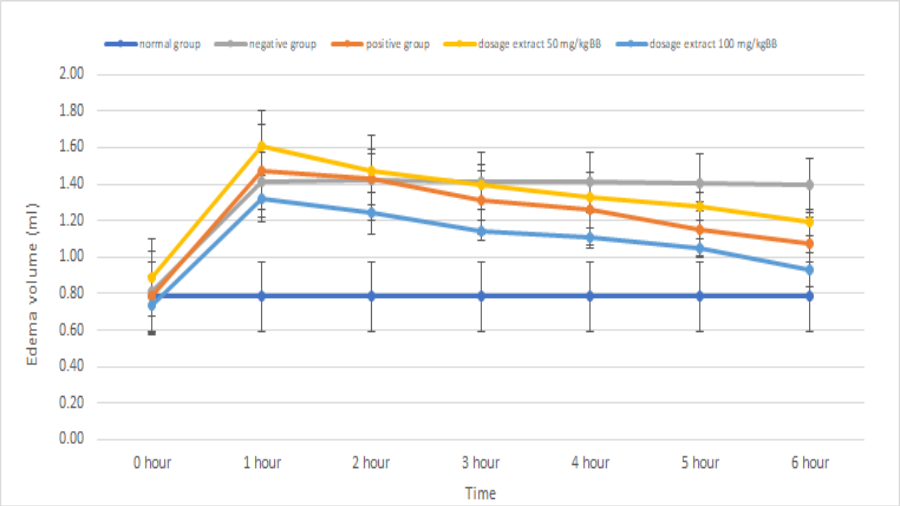

Figure 2. The average decrease in edema volume of carrageenan induced rat treated by *Grapthophyllum* extract

To determine the percentage of reduction in rat foot edema, it can be seen in Table 4 where the positive control and the dose of 50 mg/kg BW did not have a significant difference, while at the dose of 100 mg/kg BW, there was a significant difference and and it can be interpreted as a dose of 100 mg/kg BW had a fairly high anti-inflammatory activity.

From the analysis of statistical data using the ANOVA, it was shown that the positive control (sodium diclofenac) produced no significantly different anti-inflammatory effect with a noticeable volume of rat leg edema at the observation period ($P>0.05$) and this finding is in line with the general function of diclofenac sodium in reducing inflammation by blocking the enzyme cyclooxygenase by converting arachidonic acid into prostaglandins which are mediators of inflammation (Mandang et al., 2022). Purple

leaf ethanol extract with a dose of 50 mg/kg BW and a dose of 100 mg/kg BW also experienced a significant decrease in the volume of rat leg edema during the entire observation period (P>0.05). Alkaloids, flavonoids, tannins, saponins, steroids, alcohols, and calcium oxalate are the contents of purple leaf compounds. The complex and different substance causes purple to clear out to have an anti-inflammatory impact. Flavonoids are one of the compounds that are able to inhibit the cyclooxygenase and lipooxygenase pathways. Alkaloid compounds also have an anti-inflammatory role in preventing the formation of prostagladin (Rachim et al., 2021).

Table 4. Average percentage of decrease in edema volume of carrageenan induced rat treated by *Grapthophyllum* extract

Time (hour)	Average percent decrease in edema ± SD				*p value*
	Negative group	Positive group	Dosage extract 50 mg/kg BW	Dosage extract 100 mg/kg BW	
1	84.73 ± 48.065	90.52 ± 20.434	86.23 ± 28.660	86.53 ± 46.793	0.966
2	85.84 ± 47.443	85.62 ± 19.323	71.89 ± 33.548	74.76 ± 41.331	0.900
3	84.73 ± 48.065	70.27 ± 15.713	63.40 ± 35.790	60.87 ± 32.586	0.709
4	84.73 ± 48.065	64.35 ± 21.154	55.61 ± 32.631	55.24 ± 31.503	0.515
5	83.30 ± 45.687	50.11 ± 17.496	50.16 ± 32.467	46.94 ± 27.134	0.274
6	81.70 ± 46.989	39.94 ± 19.400	41.13 ± 37.703	28.73 ± 15.665	0.093

Exp: The *p-value* was obtained from the ANOVA One-way *test where the* p>0.05 *value* was no significant difference.

CONCLUSION

It can be stated that purple leaves (*Graptophyllum pictum* L Griff) have a strong antioxidant activity. The IC value was 72.312 ± 24.406 µg/ml. Purple leaf ethanol extract can also provide analgesic and anti-inflammatory effects with an effective dose of 100 mg/kg BW.

ACKNOWLEDGEMENT

The author thanks the campus of STIFA Pelita Mas Palu for facilitating the Analysis laboratory to complete antioxidant research and the Biopharmaceutical laboratory to complete analgetic and anti-inflammatory research.

REFERENCES

Agustiarini, V., & Wijaya, D. P. (2022). Uji aktivitas antioksidan ekstrak etanol-air (1:1) Bunga Rosella (*Hibiscus sabdariffa* L.) dengan metode DPPH (1,1-difenil-2-pikrilhidrazil). *Jurnal Penelitian Sains*, *24*(1), 29. https://doi.org/10.56064/jps.v24i1.679

Amran, N., Ma'ruf, D., Sari, I. W., Djide, N., & Kabo, P. (2018). Uji analgetik dan antiinflamasi ekstrak etanol 70% daun beruas laut (*Scaevola taccada* (Gaertn.)Roxb) pada tikus putih (Rattus novergicus). *Media Farmasi*, *XIV*(April), 59–64.

Antarti, A. N., & Lisnasari, R. (2018). Uji aktivitas antioksidan ektrak ethanol daun Family Solanum menggunakan metode reduksi radikal nebas DPPH. *JPSCR : Journal of Pharmaceutical Science and Clinical Research*, *3*(2), 62. https://doi.org/10.20961/jpscr.v3i2.15378

BPOM RI. (2020). Peraturan badan pengawas obat dan makanan tentang pedoman uji toksisitas praklinik secara in vivo. *Journal of Chemical Information and Modeling*, *53*(9), 1–207.

Darmayanti, N. P. O., Artini, N. P. R., & Budhi Setiawan, P. Y. (2020). Uji aktivitas analgetik ekstrak etanol 96% daun Belimbing Wuluh (*Averrhoa bilimbi* L.) dengan metode geliat pada Mencit Putih (*Mus musculus* L) galur swiss webster. *Widya Kesehatan*, *2*(2), 30–34. https://doi.org/10.32795/widyakesehatan.v2i2.963

Disi, M. Z. A., Usia, M. A., & Harbelubun, N. (2023). Uji aktivitas antioksidan ekstrak etanol daun Ungu (*Graptophyllum pictum* L.) dengan metode DPPH. *Jurnal Kieraha Medical*, *5*, 41–47.

Elmitra, Apriyanti, O., & Sepriani, T. L. (2019). Ujie fektivitas antiinflamasi ekstrak etanol daun Cabe Rawit (*Solanum frutescens*.L) pada Mencit Jantan (Mus muscullus) dengan metode induksi caraagenan. *Jurnal Akademi Farmasi Prayoga*, *4*(2), 2–12.

Gunathilake, K. D. P. P., Ranaweera, K. K. D. S., & Rupasinghe, H. P. V. (2018). In vitro anti-inflammatory properties of selected green leafy vegetables. *Biomedicines*, *6*(4), 1–10. https://doi.org/10.3390/biomedicines6040107

Kamoda, P.M.D.A., Nindatu, M., Kusadhiani, I., Astuty, E., Rahawarin, H., & Asmin, E. (2021). Uji aktivitas antioksidan alga cokelat saragassum sp. dengan metode 1,1- difenil-2-pikrihidrasil (dpph). *Patimura Medical Review*, *3*(April), 60–72.

Kurniawati, A., Praharani, D., & Handoko, G. V. (2020). Effectiveness of *Graptophyllum pictum* (L.) griff leaves extract toward porphyromonas gingivalis adhesion to neutrophils. *Malaysian Journal of Medicine and Health Sciences*, *16*(4), 60–66.

Mandang, M., Patala, R., Farmasi, J. T.-F. J., & 2022, U. (2022). Uji efek ekstrak etanol daun Pandan wangi terhadap histopatologi ginjal tikus putih diinduksi streptozotocin. *Jfarma.Org*, *1*.

Maulydya, C. E., Yuniarti, R., Dalimunthe, G. I., & Nasution, H. M. (2023). Analisis aktivitas antioksidan teh daun Jamblang (*Syzygium Cumini* (L.) Skeels) dengan metode DPPH (1,1-Diphenyl-2-Picrylhydrazyl). *Farmasainkes: Jurnal Farmasi, sains, dan Kesehatan*, *2*(2), 189–200. https://doi.org/10.32696/fjfsk.v2i2.1890

Nhadira, N., Rahminawati, M., Rustiani, E., & Dwiputri, F. (2019). Perbandingan efektivitas analgetik ekstrak etanol dan air daun ungu pada Mencit (*Mus musculus* L.). *Fitofarmaka Jurnal Ilmiah Farmasi*, *9*(2), 103–108.

Prasetyo, E., Kiromah, N. Z. W., & Rahayu, T. P. (2021). Uji aktivitas antioksidan menggunakan metode DPPH (2,2-difenil-1-pikrilhidrazil) terhadap ekstrak etanol kulit Buah Durian (*Durio zibethinnus* L.) dari Desa Alasmalang Kabupaten Banyumas. *Jurnal Pharmascience*, *8*(1), 75. https://doi.org/10.20527/jps.v8i1.9200

Rachim, S. A., Kurniawati, A., & Pudji Astuti. (2021). The effect of Purple leaf extract (*Graptophyllum pictum* L. Griff) to the amount of fibroblast in Gingiva Rat Wistar induced by Porphyromonas gingivalis. *Denta*, *14*(2), 94–100. https://doi.org/10.30649/denta.v14i2.7

Rajeshwaran, N., Ramamurthy, J., & Rajeshkumar, S. (2021). Evaluation of antioxidant and anti inflammatory activity of grape seed oil infused with silver nanoparticles an in vitro study. *International Journal of Dentistry and Oral Science*, *8*(7), 3318–3322. https://doi.org/10.19070/2377-8075-21000676

Rikomah, S. E., Elmitra, & Mauri, A. O. (2019). Effectiveness test of anti-inflammation of ethanol-extracted cream of *Graptophyllum pictum* L . Griff on White Male Mice (*Mus musculus*). *Der Pharmacia Lettre*, *11*(2), 59–66.

Salim, R. (2018). Antioxidant activity test of purple leaf infusion with DPPH method (1,1-diphenyl-2-picrylhydrrazyl). *Journal of Catalyst* ,3(2),153. https://doi.org/10.22216/jk.v3i2.3372

Sari, F., Kurniaty, I., & Susanty. (2021). Aktivitas antioksidan ekstrak daun jambu biji (*Psidium guajava* L) sebagai zat tambah pembuatan sabun cair. *Jurnal Konversi*, *10*(1), 7.

Sartika, S., & Indradi, R. B. (2021). Berbagai aktivitas farmakologi tanaman Daun Ungu (*Graptophyllum pictum* L. Griff). *Indonesian Journal of Biological Pharmacy*, *1*(2), 88. https://doi.org/10.24198/ijbp.v1i2.37531

Sasongko, H., Sugiyarto, S., Efendi, N. R., Pratiwi, D., Setyawan, A. D., & Widiyani, T. (2016). Analgesic activity of ethanolic extracts of Karika Leaves (*Carica pubescens*) in vivo. *JPSCR : Journal of Pharmaceutical Science and Clinical Research*, *1*(2), 83. https://doi.org/10.20961/jpscr.v1i2.1938

Suryandari, S. S., De Queljoe, E., & Datu, O. S. (2021). Uji aktivitas antiinflamasi Ekstrak Etanol Daun Sesewanua (*Clerodendrum squamatum* Vahl.) Terhadap Tikus Putih (Rattus norvegicus L.) Yang Diinduksi Karagenan. *Pharmacon*, *10*(3), 1025–1032.

Triyandi, R., Rokiban, A., & Setia Pratiwi MS, C. (2021). Fraksi air ekstrak daun Wungu (*Graptopphyllumpictum* L.) sebagai antiinflamasi terhadap Tikus putih jantan. *JFL: Jurnal Farmasi Lampung*, *9*(1), 1–9. https://doi.org/10.37090/jfl.v9i1.325

Wardani, H. A., Adnan, J., & Musawir, S. (2020). Uji efek analgetik ekstrak daun binahong (*Anredera cordifolia* (Ten) Steenis) kombinasi daun afrika (*Vernonia amygdalina* Del) terhadap mencit jantan putih (Mus musculus). *Jurnal Farmasi Pelamonia*, 44–48.

Yane, D. K., & Handayani, S. R. (2019). Uji aktivitas analgetik ekstrak etanol daun Inggu (*Ruta angustifolia* [l.] Pers) Pada Tikus Putih Jantan. *Journal Syifa Sciences and Clinical Research*, *1*(2), 57–69. https://doi.org/10.37311/jsscr.v1i2.2662

Yimer, T., Birru, E. M., Adugna, M., Geta, M., & Emiru, Y. K. (2020). Evaluation of analgesic and anti-inflammatory activities of 80% methanol root extract of echinops kebericho m. (asteraceae). *Journal of Inflammation Research*, *13*, 647–658. https://doi.org/10.2147/JIR.S267154

Pharmaciana
Vol.14, No.2, July 2024, Page. 157-163
ISSN: 2088 4559; e-ISSN: 2477 0256
DOI: 10.12928/pharmaciana.v14i2.28249

Acute toxicity of the intranasal administration of *Anredera cordifolia* extract in Wistar Rats

Asti Widuri[1*], Rifki Febriansah[2]
[1]Department of Otorhinolaryngology Head and Neck Surgery, Faculty of Medicine and Health Sciences, Universitas Muhammadiyah Yogyakarta, Yogyakarta, Brawijaya Road, Kasihan, Bantul, Yogyakarta Indonesia
[2]Department of Pharmacy, Faculty of Medicine and Health Sciences, Universitas Muhammadiyah Yogyakarta, Brawijaya Road, Kasihan, Bantul, Yogyakarta Yogyakarta, Indonesia

Submitted: 12-02-20242 ***Reviewed: 26-03-2024*** ***Accepted: 29-06-2024***

ABSTRACT

Anredera cordifolia (AC) known as the binahong plant in Indonesia has been commonly used for traditional medicine since the ancients. AC contains secondary metabolites such as flavonoids that have anti-oxidative, anti-inflammatory, anti-mutagenic, and anti-carcinogenic properties. Many flavonoids compound that has anti-inflammatory activity have the potential for the treatment of nasal inflammatory such as allergic rhinitis. This study aims to evaluate the preclinical safety of acute intranasal administration of AC extract in Wistar rats with mortality, clinical changes, blood laboratory, and body weight evaluation. Acute toxicity using the intranasal irrigation administration of AC extract was evaluated on 30 female Wistar rats, divided into five rats for control, and each five of doses 5%, 10%, 25%, 50%, and 75%. We perform blood laboratory after administration and observation for 14 days for the incidence of mortality and signs of toxicity such as tremors, hypoactivity, irregular respiration, and bodyweight loss. The AC extract intranasal administration doses at 5, 10, 25, 50, and 75 did not show mortality, or treatment-related adverse events and did not show significantly changes in blood profile. Based on the study the AC extract was found safe until 75% for nasal administration in Wistar rats.

Keywords: *Anredera cordifolia*, toxicity, nasal administration, anti-inflammatory

Corresponding author:
Asti Widuri
Department of Otorhinolaryngology Head and Neck Surgery, Faculty of Medicine and Health Sciences
Universitas Muhammadiyah Yogyakarta
Brawijaya Road, Kasihan, Bantul, Yogyakarta, Indonesia
Email: astiwiduri@gmail.com

INTRODUCTION

Anredera cordifolia (Ten.) Steenis (AC) is a plant that comes from the Basellaceae family which used for medical purposes since ancient Indonesia, a country rife with biodiversity (Rofida, 2010). Phytochemical content found in AC were terpenoids, steroids, glycocide, flavonoids, saponin, and alkaloids had pharmacology activities (Alba et al., 2020; Kočevar et al., 2013).

Some scientific research has reported the pharmacological activity of AC as antibacterial (Leliqia et al., 2017; Sari et al., 2020), antifungal, antivirus, antidiabetes, antihypertensive, vasodilator, hypolipidemic, antioxidant (Rajathi & Suja, 2017), gastroprotective, hepatoprotective, cytotoxic, antiinflammatory (Sutrisno et al., 2016), analgetic and wound healing (Hanafiah et al., 2019).

Inflammation is an important biological response in various diseases including allergic rhinitis. *Anredera cordifolia* is reported to contain bioactive compounds of flavonoids for anti-inflammatory activities. It has been reported that AC posses the anti-inflammatory by inhibits inflammatory mediators including TNF-α, IL-1β, IL-6, and nitric oxide (Laksmitawati et al., 2017).

The longtime treatment for allergic rhinitis control is challenging from several aspects such as the first pass metabolism, unwanted side effects, patient inconvenience, and high cost (Hossenbaccus et al., 2020; Licari et al., 2019). The intranasal drug is one of the options to resolve the problems and has higher bioavailability (Laffleur & Bauer, 2021; Keller et al., 2022). Nowadays intranasal drug administration is commonly used for the treatment of local inflammatory diseases including allergic rhinitis. The advantages of nasal drug application were rapid absorption, quick local effect, prevention of first-pass metabolism, reduced systemic side effects, avoid drug damage in the Gastrointestinal Track (GIT), and better compliance or comfort for the patient (Keller et al., 2022).

This study aims to evaluate the preclinical safety of acute intranasal administration of AC extract in laboratory Wistar rats.

MATERIALS AND METHOD

Materials

Thirty adult female Wistar rats nulliparous and nonpregnant (120-200 gram) were fed adaptively for acclimatized a week at laboratory before the experiment. All rats were placed in 5 divided cages, in a temperature-controlled, humidity-controlled, and light controlled experimental environment. Rats were fed on pelleted feed and provided pure potable water with steel sipper tubes. The whole research process was conducted at the experimental animal research laboratory of Laboratorium Penelitian dan Pengujian Terpadu (LPPT) Gadjah Mada University. The study protocol was approved by the Ethics Committee of Universitas Muhammadiyah Yogyakarta no. 071/EC-KEPK FKIK UMY/XII/2021.

Binahong leaves used in this study came from the Hargobinangun Pakem Sleman Yogyakarta area, which was determined by CV Merapi Farma Herbal. AC leaf extract is done by maceration method using 96% ethanol. The maceration process is carried out 5 times, and the results filtered and evaporated using a rotary vacuum evaporator. The concentration of extract used was 5 %, 10%, 25%, 50%, and 75% with sterile aquadest solvent.

Methods

This procedure was modification of OECD Acute Inhalation Toxicity Testing, evidence toxicity is a general term describing clear signs of toxicity following the administration of a test chemical. The animals are exposed to the test chemical in the nose only single exposure method and this approach not only using death/moribundity as endpoint but also evident clinical signs of toxicity at one of a series of fixed dose levels. The acute toxicity study of AC extract was performed with the nasal administration. The doses of 5, 10, 25, 50, and 75% AC extract were instilled intranasal in each group of five Wistar rats and control group with saline isotonic. The rats were observed for 2 weeks for any incident of mortality or signs of toxicity.

Before and one day after intranasal administration the rat's olfactory function is tested by measuring the time to find food under a layer of bedding, its procedure according to the buried food test relies on the animal's natural tendency the ability to smell odors for foraging (Thakurdesai, 2021). We also collected blood samples for laboratory evaluations and measured the body weight.

RESULT AND DISCUSSION

The rats nervus olfactorius function test relies on the animal's natural ability to find the food palette hidden under a layer of bedding. The effect of extract binahong on the olfactory system was carried out before initiation of treatment and one day after the procedure, the recorded result of time to find the food was 241.49 seconds and 316.92 seconds, there was an increasing time to find the food palette but the was none rat anosmia so the AC extract not toxic for the olfactory nerves. More details can be seen in Table 1.

Table 1. Results of olfactory function test data before and after intranasal administration of *Anredera cordifolia* extract

	Before treatment (seconds) Mean ± SD	After treatment (seconds) Mean ± SD
Control group NaCl 0.9%	298.44 ± 26.01	46,45 ± 2,35
Group of 5% AC extract	167.97 ± 28.01	508,98 ± 425,69
Group of 10% AC extract	222.90 ± 65.93	666,56 ± 130,98
Group of 15% AC extract	189.52 ± 118.76	53,41 ± 16,21
Group of 50% AC extract	353.25 ± 391.28	231,56 ± 179,80
Group of 75% AC extract	216.89 ± 90.70	394,54 ± 481,07

The acute study at intranasal administration dose until 75% extract AC did not reveal any mortality or abnormal clinical signs in female Wistar rats see Table 2.

Table 2. The acute toxicity symptoms and death of rats after intranasal administration of *Anredera cordifolia* extract

Nasal Irigation	Sample Number	Toxic Symptom	Death
Control NaCl 0.9%	5	0	0
5% extract AC	5	0	0
10% extract AC	5	0	0
25% extract AC	5	0	0
50% extract AC	5	0	0
75% extract AC	5	0	0

No significant body weight loss was observed during the 14-day observation post dosing period, and in the observation of body weight in rats, there was no significant weight gain compared to the control group and there was no dose response increasing see Figure 1.

The blood profile associated with a human health status, the effects of AC extract were also evaluated in Wistar rat's blood profile after nasal administration as showed in Table 3.

The results of the hematological measurement of Wistar rats were analyzed statistically using one way ANOVA method did not show any significant differences between the control group and all dose groups, with each significant value for WBC p=0.612, RBC p=0.262, PLT p=0.267, HB p=0.072, HCT p=0.186, MCV p=0.366, MCH p=0.243, MCHC p=0.227.

Allergic rhinitis (AR) is an inflammatory disease of the nasal mucosa, caused by a hypersensitivity reaction mediated by immunoglobulin E after repeated allergen exposure (Small et al., 2018). Symptoms

of AR include runny nose, sneezing, nasal congestion, itchy nose, and sometimes accompanied by complaints of itchy, red eyes and tears. Allergic Rhinitis can cause symptoms of respiratory tract obstruction during sleep and become a risk factor for other diseases including chronic rhinosinusitis, asthma, and otitis media (Bousquet et al., 2020). Allergic Rhinitis is the most common chronic respiratory disease, with prevalence varying between regions and environmental conditions ranging from 10-40% of the total population (Savouré et al., 2022). Symptoms of AR are generally harmless but cause a decrease in quality of life, sleep disturbances, work/school performance and the treatment costs a lot (Bjermer et al., 2019).

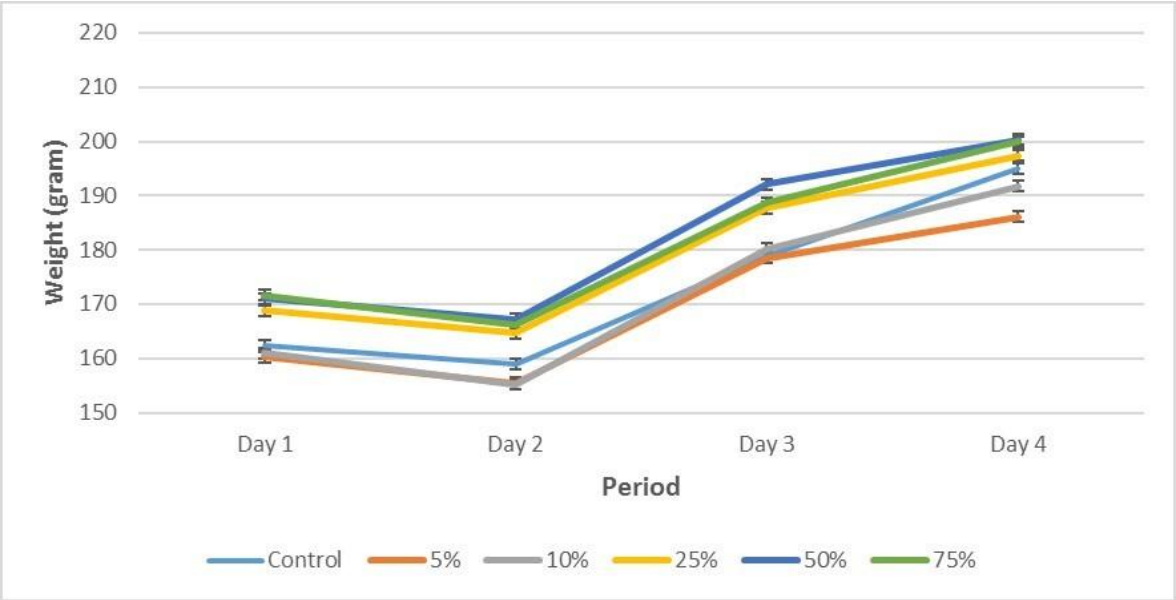

Figure 1. The comparisons of body weight in rats control and intranasal irrigation with extract AC

Table. 3. Blood Profile measurement after *Anredera cordifolia* extract nasal administration

	Control (*mean* ± SD)	**Dose 5% (*mean* ± SD)**	**Dose 10% (*mean* ± SD)**	**Dose 25% (*mean* ± SD)**	**Dose 50% (*mean* ± SD)**	**Dose 75% (*mean* ± SD)**
WBC (10^3)	10.18 ± 1.55	10.42 ± 2.19	9.38 ± 1.68	8.70 ± 1,54	10.14 ± 1.46	9.72 ± 1.50
RBC (10^6)	6.39 ± 0.41	6.83 ± 0.54	6.33 ± 0.29	6.26 ± 0.37	6.52 ± 0.47	6.11 ± 0.64
PLT (10^3)	1070.6 ± 93.91	950.8 ± 77.89	983.8 ± 79.79	975.0 ± 65.04	969.4 ± 59.64	963.8 ± 106.74
HB	13.32 ± 0.61	14.98 ± 1.41	13.64 ± 0.66	13.78 ± 0,74	14.30 ± 1,04	13.28 ± 1.03
HCT (%)	41.04 ± 1.92	44.38 ± 3.56	41.32 ± 1.77	40.84 ± 2.06	42.04 ± 2.85	39.66 ± 3.77
MCV (fL)	-64.30 ± 1.19	-64.98 ± 0.44	-65.32 ± 0.73	-65.24 ± 0.57	-64.40 ± 1.20	-64.94 ± 0.91
MCH	-20.90 ± 0.77	-21.94 ± 0.77	-21.56 ± 0.36	-22.0 ± 0.77	-21.94 ± 1.07	-21.80 ± 0.74
MCHC	32.46 ± 0.94	33.76 ± 1.30	33.0 ± 0.72	33.76 ± 1.03	34.04 ± 1.46	33.54 ± 0.79

The current management of RA includes education, allergen avoidance, pharmacology, immunotherapy, biology, and probiotics (Zhang et al., 2021). The clinical practice therapy guide was developed by Allergic Rhinitis and its Impact on Asthma (ARIA) by means of integrated services

utilizing social media, mobile health, and multidisciplinary services (Linton et al., 2021). Intranasal steroids are recommended as the first choice for controlling the symptoms of moderate-severe persistent allergic rhinitis, but there were a few incidences of adverse effects such as epistaxis, headache, taste disorder, and pharyngitis. There the potential of AC medical used as an anti-inflammatory agent for allergic rhinitis needs safety evaluation using international guidelines before administration in humans (Sasmito et al., 2017).

Preliminary safety evaluation or acute toxicity test of AC extract after nasal administration in this study showed no death, no abnormal clinical signs, no decreasing body weight, and blood profile significant changes of all concentrations compared to the control group. The results are necessary for the development of AC extract in order to be phytomedicine for nasal administration. The result showed nasal irrigation with 75% extract binahong safe and relatively not hazardous, it is consistent with Salasanti et al. (2014) that reported *Anredera cordifolia* leaf extract ethanol LD50 was greater than 15 g/kg body weight. Repeated oral treatment of ethanol extract of A. cordifolia leaves for 90 days at doses of 0.1, 0.4, and 1 g/kg body weight did not result in any deaths, changed the behavior of the rats, affected their blood profile or biochemistry parameters, and was not hazardous to their organs (Salasanti et al., 2014).

Similar to the research of Ramadhan et al. (2023), AC extraction, formulated with transdermal binahong leaf extract patches using a formula that includes hydroxypropylmethylcellulose, (polymer), glycerol (plasticizer), oleic acid (enhancer) and tween 80 (enhancer), is safe and does not cause death in mice. The transdermal patches of AC 30% and 47% had the effect of reducing blood glucose levels in rats that had been induced by insulin but were not significantly different. Another evidence for the safety of AC also in topical application, which reported that ethanol extract preparation of 70 % AC leaf on Wistar rat did not cause a death with observation for 14 days. So AC has met the standard of safety according to Indonesian Herbal Phamacopoeia (Samirana et al., 2018)

CONCLUSION

This present study reported the safety of intranasal acute administration of extract AC without any effect on nervus olfactory function and blood profile in laboratory female Wistar rats. The maximum dose of 75% concentration did not find mortality or sign of toxicity or practically non-toxic.

REFERENCES

Alba, T. M., de Pelegrin, C. M. G., & Sobottka, A. M. (2020). Ethnobotany, ecology, pharmacology, and chemistry of *Anredera cordifolia* (Basellaceae): A review. *Rodriguesia*, *7*. https://doi.org/10.1590/2175-7860202071060

Bjermer, L., Westman, M., Holmström, M., & Wickman, M. C. (2019). The complex pathophysiology of allergic rhinitis: Scientific rationale for the development of an alternative treatment option. *Allergy, Asthma and Clinical Immunology*, *15*(1), 1–15. https://doi.org/10.1186/s13223-018-0314-1

Bousquet, J., Anto, J. M., Bachert, C., Baiardini, I., Bosnic-Anticevich, S., Walter Canonica, G., Melén, E., Palomares, O., Scadding, G. K., Togias, A., & Toppila-Salmi, S. (2020). Allergic rhinitis. *Nature Reviews Disease Primers*, *6*(1). https://doi.org/10.1038/s41572-020-00227-0

Hanafiah, O. A., Abidin, T., Ilyas, S., Nainggolan, M., & Syamsudin, E. (2019). Wound healing activity of binahong (*Anredera cordifolia* (Ten.) Steenis) leaves extract towards NIH-3T3 fibroblast cells. *Journal of International Dental and Medical Research*, *12*(3), 854–858.

Hossenbaccus, L., Linton, S., Garvey, S., & Ellis, A. K. (2020). Towards definitive management of allergic rhinitis: Best use of new and established therapies. *Allergy, Asthma and Clinical Immunology*, *16*(1), 1–17. https://doi.org/10.1186/s13223-020-00436-y

Keller, L. A., Merkel, O., & Popp, A. (2022). Intranasal drug delivery: Opportunities and toxicologic challenges during drug development. *Drug Delivery and Translational Research*, *12*(4), 735–757. https://doi.org/10.1007/s13346-020-00891-5

Kočevar, N., Glavač, I., & Kreft, S. (2013). Chemistry and Biological Activities of Flavonoids: An Overview. *The Scientific World Journal*, *58*(4), 145–148. https://doi.org/10.2307/j.ctt1w0ddx8.35

Laffleur, F., & Bauer, B. (2021). Progress in nasal drug delivery systems. *International Journal of Pharmaceutics*, *607*(August), 120994. https://doi.org/10.1016/j.ijpharm.2021.120994

Laksmitawati, D. R., Widyastuti, A., Karami, N., Afifah, E., Rihibiha, D. D., Nufus, H., & Widowati, W. (2017). Anti-inflammatory effects of Anredera cordifolia and piper crocatum extracts on lipopolysaccharide-stimulated macrophage cell line. *Bangladesh Journal of Pharmacology*, *12*(1), 35–40. https://doi.org/10.3329/bjp.v12i1.28714

Leliqia, N. P. E., Sukandar, E. Y., & Fidrianny, I. (2017). Antibacterial activities of Anredera Cordifolia (Ten.) V. Steenis leaves extracts and fractions. *Asian Journal of Pharmaceutical and Clinical Research*, *10*(12), 175–178. https://doi.org/10.22159/ajpcr.2017.v10i12.21503

Licari, A., Castagnoli, R., Tosca, M. A., Marseglia, G., & Ciprandi, G. (2019). Personalized therapies for the treatment of allergic rhinitis. *Expert Review of Precision Medicine and Drug Development*, *4*(5), 275–281. https://doi.org/10.1080/23808993.2019.1681896

Linton, S., Burrows, A. G., Hossenbaccus, L., & Ellis, A. K. (2021). Future of allergic rhinitis management. *Annals of Allergy, Asthma & Immunology*, *127*(2), 183–190. https://doi.org/10.1016/j.anai.2021.04.029

Rajathi, P., & Suja, S. (2017). Biomimetic synthesis, characterization and evaluation of antioxidant, antimicrobial efficacy of silver nanoparticles using anredera cordifolia leaf extract. *Asian Journal of Pharmaceutical and Clinical Research*, *10*(4), 329–334. https://doi.org/10.22159/ajpcr.2017.v10i4.16819

Ramadhan, G. P., Wahyuningsih, I., & Widyaningsih, W. (2023). Development of transdermal patch preparations binahong leaf extract (Anredera cordifolia (Ten.) Steenis) and antihyperglycemia test in rats. *Pharmaciana*, *13*(2), 224. https://doi.org/10.12928/pharmaciana.v13i1.24602

Rofida, S. (2010). Studi Etnobotani dan Etnofarmakologi Umbi Binahong (Anredera cordifolia (Ten) Steenis). *Farmasains : Jurnal Farmasi Dan Ilmu Kesehatan*, *1*(1). https://doi.org/10.22219/far.v1i1.429

Salasanti, C. D., Sukandar, E., & Fidrianny, I. (2014). Acute and sub chronic toxicity study of ethanol extract of anredera cordifolia (Ten.) v. Steenis leaves. *International Journal of Pharmacy and Pharmaceutical Sciences*, *6*, 348–352.

Samirana, P. O., Pratiwi, D. M. N., Musdwiyuni, N. W., Andhini, D. A. A., Mahendra, A. N., & Yadnya-Putra, A. G. R. (2018). Uji Pendahuluan Toksisitas Akut Dermal Sediaan Salep Ekstrak Etanol 70% Daun Binahong (*Anredera Scandens* (L.) Moq.) Terstandar. *Jurnal Kimia*, 180. https://doi.org/10.24843/JCHEM.2018.v12.i02.p14

Sari, M. K., Tumangger, B. S., Sorbakti, B. J., Helmalia, F., & Fadhliani. (2020). Effectiveness of the binahong leaf extract (Anredera cordifolia) in devoting bacterial growth Vibrio cholerae in vitro. *IOP Conference Series: Materials Science and Engineering*, *725*(1), 1–6. https://doi.org/10.1088/1757-899X/725/1/012073

Sasmito, W. A., Wijayanti, A. D., Fitriana, I., & Sari, P. W. (2017). Pengujian Toksisitas Akut Obat Herbal Pada Mencit Berdasarkan Organization for Economic Co-operation and Development (OECD). *Jurnal Sain Veteriner*, *33*(2). https://doi.org/10.22146/jsv.17924

Savouré, M., Bousquet, J., Jaakkola, J. J. K., Jaakkola, M. S., Jacquemin, B., & Nadif, R. (2022). Worldwide prevalence of rhinitis in adults: A review of definitions and temporal evolution. *Clinical and Translational Allergy*, *12*(3), 1–10. https://doi.org/10.1002/clt2.12130

Small, P., Keith, P. K., & Kim, H. (2018). Allergic rhinitis. *Allergy, Asthma and Clinical Immunology*, *14*(s2), 1–11. https://doi.org/10.1186/s13223-018-0280-7

Sutrisno, E., Ketut Adnyana, I., Sukandar, E. Y., Fidrianny, I., & Aligita, W. (2016). Anti-inflammatory study of *Anredera cordifolia* leaves and *Centella asiatica* herbs and its combinations using human red blood cell-membrane stabilization method. *Asian Journal of Pharmaceutical and Clinical Research*, *9*(5), 78–80. https://doi.org/10.22159/ajpcr.2016.v9i5.11973

Thakurdesai, P., & Deshpande, P. (2021). Preclinical safety evaluation of acute and subacute intranasal administration of polyphenols-based Cinnamon Bark extract in Laboratory Rats. *Pharmacognosy Journal*, *13*(6s), 1621–1631. https://doi.org/10.5530/pj.2021.13.209

Zhang, Y., Lan, F., & Zhang, L. (2021). Advances and highlights in allergic rhinitis. *Allergy*, *76*, 3383–3389. https://api.semanticscholar.org/CorpusID:236989687

Pharmaciana
Vol.14, No.2, July 2024, Page. 164-172
ISSN: 2088 4559; e-ISSN: 2477 0256
DOI: 10.12928/pharmaciana.v14i2.27665

Demographics, knowledge, and attitudes toward fe supplementation for stunting prevention at public health center, Ciamis-Indonesia

Andriana Sari*, Reni Meyleni
Department of Pharmacology and Clinical Pharmacy, Faculty of Pharmacy, Universitas Ahmad Dahlan, Jl. Prof. Dr. Soepomo, S.H, Warungboto, Umbulharjo, Yogyakarta, Indonesia

Submitted: 21-11-2023 ***Reviewed: 26 -03-2024*** ***Accepted: 11-07-2024***

ABSTRACT

Stunting has been linked to malnutrition in children from prenatal to before five years old, a condition with 24% prevalence, according to the 2021 Indonesian Nutrition Status Survey. Ciamis (West Java, Indonesia) reported 2,334 cases (3.4%) of stunting problems in 2022. The government has introduced Fe tablets to pregnant women, but this specific intervention can only be effective if accompanied by their adequate knowledge and positive perception of its usefulness, which can be influenced by their experience, education level, and sociocultural environment. This study aimed to determine the relationship between demographic characteristics and knowledge and attitudes toward Fe supplementation. This quantitative research adopted the analytical survey and cross-sectional designs and used demographics, knowledge, and attitudes questionnaires as the research instruments. Cluster sampling in the operational area of the Sadananya Public Health Center in Ciamis obtained 151 respondents. Data were analyzed using a chi-square test in SPSS. Results show that the majority of the sample size had low knowledge (118 respondents; 77.6%) and less positive attitudes (103; 67.8%) toward Fe supplementation. There was a significant relationship between age and knowledge (p=0.044), while none was observed between knowledge and education (p=0.100) and obstetric history (p=0.057). Moreover, age, education, and obstetric history were not statistically related to attitudes toward Fe supplementation (p=0.645, 0.951, 0.792). This studi concluded that there was a significant relationship between age ad knowledge, but there was no significant relationship between education and history of pregnancy with knowledge. Moreover, there was no significant relationship between demographic characteristics.

Keywords: Demographic characteristics, knowledge, attitudes, Fe supplements

Corresponding author:
Andriana Sari
Department of Pharmacology and Clinical Pharmacy, Faculty of Pharmacy, Universitas Ahmad Dahlan
Jl.Prof. Dr. Soepomo, S.H, Warungboto, Umbulharjo, Yogyakarta, Indonesia
Email: andriana@pharm.uad.ac.id

INTRODUCTION

Stunting is a condition related to nutritional intake that particularly stems from malnutrition in pregnant women, causing impaired growth with the height-for-age measurement showing a z-score or standard deviation of <-2 (WHO, 2020). The Indonesian Nutrition Status Survey explained that the prevalence of stunting achieved 27.7% in 2019 and 24.4% in 2021 (Indonesia Ministry of Health, 2021). Ciamis is one of the many regencies in West Java, Indonesia, that is dealing with impaired growth issues in children. Based on a preliminary study by Ciamis Health Services, the prevalence of stunting among toddlers was 6.4% in 2020 and continuously decreased to 4.9% in 2021 and 3.4% in 2022. Based on these percentages, 20 villages have been designated as the priority loci for reducing stunting in 112 under-five children, and some are parts of the operational area of the Sudananya Public Health Center (Ciamis Health Services, 2022).

Stunting incidence occurs in the first 1,000 days after conception, and the influencing factors may comprise socioeconomic status, food intake, maternal nutrition, infectious diseases, micronutrient deficiencies, and the environment (Ramayulis et al., 2018). Micronutrients include minerals (e.g., iron and folic acid) and vitamins. Iron (Fe) deficiency causes anemia in pregnant women and low birth weight (LBW), which are risk factors for stunting. Another contributing factor is that little attention is given to whether or not pregnant women extensively understand health and nutrition before, during, and after giving birth. Stunting can be prevented most effectively during pregnancy and the first two years of children's life (Ramayulis et al., 2018). The government has implemented special intervention services that encourage pregnant women to receive Fe supplements to immediately reduce the number of stunting incidence (Indonesia Ministry of Health, 2018).

For the above reasons, it is imperative to assess knowledge and attitudes toward Fe supplementation among pregnant women to achieve the government's goals of reducing stunting rates. Demographic characteristics, e.g., level of education, experience, and sociocultural environment, have been linked to the acquisition and development of knowledge, attitudes, and behavior (Notoatmodjo, 2012). In addition, the operational area of the Sadananya Public Health Center is far from public facilities. Therefore, this research was designed to analyze if and to what extent the demographic characteristics of expectant mothers related to their knowledge and attitudes toward Fe supplementation as an effort to prevent stunting in this operational area.

MATERIALS AND METHOD

Materials

The research tool was an ordinal survey questionnaire adopted from Azzahra (2014), which comprised demographic data including age, education and Obstetric history, 10 items knowledge of Fe benefits, and 10 items attitudes toward Fe supplementation. The knowledge and attitude questionnaires were tested for validity through expert judgment in the fields of psychology and pharmacy, followed by a Pearson product-moment correlation test (r) on 30 pregnant women outside the research respondents. This test showed that each questionnaire item is valid, i.e., measuring the data it is supposed to, because r count > r table (r=0.3610). Moreover, a further reliability test revealed that both questionnaires are reliable instruments to measure knowledge and attitudes because their Cronbach's alpha coefficients were 0.783 and 0.712, or greater than 0.6.

Methods

This quantitative research used the analytical survey and cross-sectional designs to describe the relationship between demographic characteristics and knowledge and attitudes toward Fe supplementation for stunting prevention. The research population was pregnant women who met these two inclusion criteria: currently taking Fe supplement tablets and living in the operational area of the Sadananya Public Health Center, Ciamis Regency, Indonesia (including Mekarjadi, Sukajadi, Mangkubumi, Bendasari, Werasari, Sadananya, Gunungsari, Tanjungsari Villages). However, those with a history of kidney failure and anemia were omitted (exclusion criteri). From the research population, 152 respondents were selected using cluster sampling including Sukajadi (19.7% of the respondents), Werasari (23.7%), Tanjungsari (14.5%), Sadananya (26.3%), and

Bendasari (15.8%). The number of respondents fulfill the requirement of minimum sample size of 151 from calculations using the Lameshow formula.

Data Analysis

Data were analyzed univariately and bivariately using the SPSS v.25 program for IOS (Iphone Operating System). The univariate analysis aimed to determine demographic characteristics, level of knowledge, and attitudes toward Fe supplementation. Then, the bivariate analysis using a chi-square test assessed the relationship between these variable pairs: demographics-knowledge and demographics-attitude. Each relationship would be concluded as statistically significant if p-value < 0.05.

RESULT AND DISCUSSION

This research was conducted from May 6 to June 26, 2023, with ethical clearance number 2805/KEP-UNISA/IV/2023. In total, 152 respondents in the operational area of the Sadananya Public Health Center met the inclusion and exclusion criteria. They were pregnant women who came to the public clinics in these villages for consultation: Sukajadi (19.7% of the respondents), Werasari (23.7%), Tanjungsari (14.5%), Sadananya (26.3%), and Bendasari (15.8%).

Demographic characteristics

According to the Indonesian Ministry of Health, age can be divided into three stages: adolescence (17–25 years old), early adulthood (26-35), and late adulthood (36–45) (Al Amin & Juniati, 2017). This study combined the early and late adulthoods into one category: adults. As seen in Table 1, more than half of the respondents (58.6%) belonged to the adult group. However, another research focusing on Fe supplementation found that the sampled pregnant women were predominantly in the 17–25 age group (94.3%) compared to those aged 26–35 (Darmawati et al., 2023).

Table 1. Distribution and frequency of the respondents based on demographic characteristics

Variable	Frequency (N)	Percentage (%)
Age		
Adolescents (17–25 years old)	63	41.4
Adults (26–45 years old)	89	58.6
Education		
Nine years of compulsory education*	77	50.7
> Nine years of education	75	49.3
Obstetric history (gravidity)		
G1–2	97	63.8
≥G3	55	36.2
Level of knowledge		
Good	34	22.4
Poor	118	77.6
Attitude type		
Positive	49	32.2
Negative	103	67.8

Notes: *primary and lower secondary education

The attained education is a correlate of knowledge level. About half of the respondents (50.7%) had received primary and lower secondary education (i.e., SD and SMP). Meanwhile, a previous study in Gunung Tua Village (Mandailing Natal, North Sumatra, Indonesia) found that a large

share of the sampled pregnant women (46.66%) had completed their higher secondary education (i.e., SMA) (Aryunita, 2022). The contradictory sample profiles are probably due to the different incomes of the respondents' parents and levels of access to schools and other educational facilities.

In addition, the majority of the respondents had an obstetric history of G1–2 (63.8%). This means they were currently pregnant and already had 0 (G1) to 1 previous pregnancy (G2). In contrast, the largest proportion of respondents in another research on knowledge of Fe tablets had been pregnant more than once or had multigravida (80.5%) (Kadir et al., 2021).

Knowledge and attitudes toward Fe supplementation

Levels of knowledge

Knowledge is the result of a person's sensing or learning of objects through their senses (Notoatmodjo, 2012). The more often an individual receives information, the higher their level of knowledge. Good knowledge provides the stems for good ways of thinking or feeling, including positive attitudes. For this reason, knowledge is believed to be a strong contributing factor in the success of stunting prevention measures.

Table 1 shows that a large share of the respondents (77.6%) did not know the usefulness of Fe supplements in preventing stunting. This finding differs from another research in Sleman (Yogyakarta, Indonesia), which reported that young women had good knowledge of this benefit (Rizkiana, 2022). There are several factors responsible for the differences or variations in the knowledge level, for example, proximity to urban areas, methods for or capability of understanding ideas, and educational attainment. Further information on which aspects of knowledge the respondents were familiar with is presented in Table 2.

Table 2. Responses to questions on knowledge of Fe supplementation

Question	Response	
	False (%)	True (%)
Definition of anemia	23.0	77.0
Benefits of blood supplement tablets	55.3	44.7
How to take blood supplement tablets	31.6	68.4
Signs of anemia	18.4	81.6
The impact of anemia on pregnancy	40.8	59.2
The number of blood supplement tablets that pregnant women are recommended to take	53.9	46.1
The recommended time for pregnant women to start taking blood supplement tablets	77.6	22.4
Anemia prevention	11.2	88.8
Anemia monitoring	48.0	52.0
The long-term impact of anemia	37.5	62.5

The respondents had good knowledge of anemia prevention (88.8%) but were unfamiliar with when to start taking blood supplement tablets (22.4%). Pregnant women are recommended to take the supplements in the second trimester when blood hemoglobin levels are at their lowest (Indonesia Ministry of Health, 2018). Moreover, only about half of the respondents were fully cognizant of the benefits and the number of blood supplement tablets they should take (44.7% and 46.1%, respectively). Blood supplements increase the formation of red blood cells and, consequently, hemoglobin levels. It is required to take a minimum of 90 tablets during pregnancy (Indonesia Ministry of Health, 2018). Due to the generally low level of knowledge, the village health centers, through cadres or midwives, should provide education and information on aspects of Fe supplementation that the respondents did not fully understand.

Types of attitudes

Table 1 shows that about one-third of the respondents (32.2%) had positive attitudes toward Fe supplementation as a preventive measure against stunting. This result is different from a previous study in Kuala Terengganu (Terengganu, Malaysia), where more than half of the respondents (54.2%) had positive attitudes toward taking Fe supplements (Theng et al., 2017). Differences or variations in the attitudes might stem from different levels of concern or awareness. Details on the observed aspects of attitudes and the respondents' degrees of (dis)agreement are shown in Table 3.

Table 3. Responses to questions on attitudes toward Fe supplementation

Statement/Question	Response				
	Strongly agree (%)	Agree (%)	Neither agree nor disagree (%)	Disagree (%)	Strongly disagree (%)
Pregnant women need blood supplement tablets.	63.2	33.6	0.7	2.6	0.0
The recommended number of blood supplement tablets to take*	22.4	50.7	15.1	11.8	0.0
Benefits of blood supplement tablets	40.1	41.4	9.9	7.9	0.7
Foods high in iron	21.7	39.5	25.0	13.8	0.0
Benefits of blood supplement tablets*	5.9	14.5	10.5	57.9	11.2
Impact of anemia on fetal growth*	7.9	10.5	11.8	53.9	15.8
Impact of anemia on pregnant women and babies*	7.2	19.1	3.9	50.0	19.7
Impact of anemia on babies	10.5	32.2	32.2	22.4	2.6
The purpose of the government's specific intervention that provides blood supplement tablets for pregnant women	50.7	44.7	0.7	3.3	0.7
People who need iron the most*	15.1	28.3	5.9	47.4	3.3

Notes: *negative statements/questions

The respondents strongly agreed that pregnant women needed to take blood supplement tablets (63.2%) but did not strongly agree with the statement on the quantity of blood supplement tablets to take throughout pregnancy (22.4%). In addition, about 15.1% strongly agreed that women did not need more iron intake before pregnancy and at least 90 blood supplement tablets during pregnancy (Indonesia Ministry of Health, 2018). Accordingly, it is necessary to increase the knowledge of iron requirements among pregnant women, which is expected to encourage positive attitudes toward Fe supplementation for stunting prevention.

Relationship between demographic characteristics and knowledge of Fe supplementation for stunting prevention

Table 4 shows that 14.3% of respondents in the adolescence group and 28.1% in the adult age group had good knowledge of Fe supplementation. For this demographic variable, the chi-square analysis produced a p-value of 0.444 (<0.05), indicating a statistically significant correlation between age and the knowledge level. This corresponds to a previous study that found a substantial link between age and the degree of awareness of Fe supplementation (Galaupa & Supriani, 2019). Ways of thinking, learning, and understanding ideas develop with age, suggesting that knowledge accumulates over time (I Nengah et al., 2020).

Table 4. Relationship between demographic characteristics and knowledge of Fe supplementation for stunting prevention

Variable	Good		Poor		P-value	OR
	N	%	N	%		
Age						
Adolescents (17–25 years old)	9	14.3	54	85.7	0.044	0.427
Adults (26–45 years old)	25	28.1	64	71.9		
Education						
Nine years of compulsory education	13	16.9	64	83.1	0.100	0.522
> Nine years of compulsory education	21	28.0	54	72.0		
Obstetric history (gravidity)						
G1–2	17	17.5	80	82.5	0.057	0.475
≥G3	17	30.9	38	69.1		

The well-informed respondents accounted for 16.9% of those with nine years of compulsory education and 28.0% with higher educational attainment. With a p-value of 0.100 (>0.05), education level is not significantly correlated with the knowledge of Fe supplementation for stunting prevention. This contradicts a previous study at the Jatibening Public Health Center (West Java, Indonesia), which detected a significant relationship between both variables (Galaupa & Supriani, 2019). According to Notoatmojo 2012, the level of knowledge can be seen from the level of education and other factors, the higher the level of education, the better the level of knowledge and the quicker you can receive information (Notoatmodjo, 2012). This is likely because there is no motivation to look for information regarding the use of Fe supplements or is hindered by other activities so that the level of education does not correlate with knowledge of the use of Fe supplements.

Furthermore, respondents with a good comprehension of Fe supplementation constituted 17.5% of those with an obstetric history of G1–2 and 30.9% with ≥G3. The chi-square test showed a p-value of 0.057 (>0.05), suggesting no significant correlation between obstetric history and the knowledge level. Previous research at the Kramat Public Health Center stated that parity had no significant relationship with knowledge of Fe supplementation (Setiowati, 2021). This could possibly happen because information at the beginning of the first pregnancy was not very extensive and good regarding the use of Fe supplements as a prevention of stuting so that knowledge would be repeated in subsequent pregnancies.

Relationship between demographic characteristics and attitudes toward Fe supplementation for stunting prevention

Table 5 shows that respondents who generally agreed with Fe supplements as a preventive measure against stunting accounted for 30.2% of the adolescent group and 33.7% of the adult group. With a p-value of 0.645 (>0.05), there is no correlation between age and attitudes toward Fe supplementation. This contradicts previous research at the Banyuasin Public Health Center (Purworejo, Indonesia) that found a correlation between both variables (Setyorini & Atiqoh, 2018).

Furthermore, respondents with positive attitudes comprised 32.5% of those with nine years of compulsory education and 32.0% of those attaining higher education levels. The p-value was 0.951 (>0.05), meaning that educational attainment is not significantly correlated with attitudes toward Fe supplementation. On the contrary, research at the Banyuasin Public Health Center (Purworejo, Indonesia) found a relationship between both variables (Setyorini & Atiqoh, 2018).

According to Azwar 2013, attitudes can change in each individual because attitudes can be learned and changed due to several circumstances. Factors that can influence attitudes include the influence of other people or the environment and surrounding culture. So it is possible that age and education level do not have a significant correlation because there are other factors such as the surrounding environment (Azwar, 2013).

Table 5. Relationship between demographic characteristics and attitudes toward Fe supplementation for stunting prevention

Variable	Positive		Negative		P-value	OR
	N	%	N	%		
Age						
Adolescents (17–25 years old)	19	30.2	44	69.8	0.645	0.849
Adults (26–45 years old)	30	33.7	59	66.3		
Education						
Nine years of compulsory education	25	32.5	52	67.5	0.951	1,.022
> Nine years of compulsory education	24	32.0	51	68.0		
Obstetric history (gravidity)						
G1–2	32	33.0	65	67.0	0.792	1.100
≥G3	17	30.9	38	69.1		

About one-third of respondents with an obstetric history of G1–2 (33.0%) and G3 (30.9%) showed positive attitudes toward Fe supplementation. However, because the p-value was 0.792 (>0.05), there is no statistically significant relationship between the two variables. These results contradict the theory that considers a person's experience as a factor of their attitude (Azwar, 2013) but correspond to a previous study that found no relationship between gravidity and compliance with taking Fe tablets in the third trimester among pregnant women in the Sedayu II Public Health Center (Bantul, Indonesia) (Sariyati, 2022). The possibility of other factors such as previous experience in consuming iron tablets, namely the presence of side effects that arise when consuming iron tablets such as nausea, constipation, frustration and fear of having a big baby, is one of the factors that can reduce and also influence the attitude of pregnant women consuming Fe tablets. So it is necessary to carry out further research with other variables to strengthen the cause of there being no correlation between these 2 variables.

In this study, patients with a medical background or from families who worked in medicine were not excluded, which is a weakness of this study. The variables examined in this research are limited so further research is needed with more varied variables so that the possibility that some variables are not correlated in this research can be proven or answered.

CONCLUSION

Knowledge of Fe supplementation as a preventive measure against stunting is significantly related to age but not to education and obstetric history. There is no significant relationship between the three demographic characteristics (age, education, and obstetric history) and attitudes toward Fe supplementation. The results of this research can become a roadmap for future research, it can be further developed to find out other demographic characteristics that correlate with the level of knowledge and attitudes towards using Fe supplements to prevent stunting as well as the hemoglobin value of pregnant women. Apart from that, related parties can improve communication and provide information regarding the use of Fe as a stunting prevention action

ACKNOWLEDGMENT

The authors would like to thank the Sadananya Public Health Center in Ciamis Regency (Indonesia) and the Pharmacy Department at Ahmad Dahlan University, Yogyakarta (Indonesia) for supporting this research.

REFERENCES

Al Amin, M., & Juniati, D. (2017). Klasifikasi kelompok umur manusia berdasarkan analisis dimensi. *Jurnal Ilmiah Matematika*, *2*(6), 1–10.

Aryunita. (2022). The relationship between knowledge of pregnant momen about anemia and Prevention of Folic Acid Consumption During Pregnancy. *International Journal of Public Health Excellence (IJPHE)*, *1*(1), 60–63. https://doi.org/10.55299/ijphe.v1i1.14

Azwar, S. (2013). *Sikap manusia: teori dan pengukurannya*. Pustaka Pelajar. Yogyakarta.

Azzahra, S. (2014). *Gambaran pengetahuan, sikap dan tindakan ibu Hamil terhadap pentingnya mengkonsumsi tablet zat besi Selama Kehamilannya Di Puskesmas Layang Makassar Tahun 2014.Bachelor's Thesis*. Alauddin State Islamic University. Makassar.

I. Nengah, B. S., F. A, Ahmad, R., Chrysella, Ayu S., D., K, Farah., Fitria, F., N. E. S., Happy., A. N. U., Hieronimus, N, Safiinatunnajah, A. D., Wahyu, A, Yunita, & Rahem, A. (2020). Hubungan usia dengan pengetahuan dan perilaku penggunaan suplemen pada mahasiswa institut Teknologi Sepuluh Nopember. *Jurnal Farmasi Komunitas*, *7*(1), 1. https://doi.org/10.20473/jfk.v7i1.21657

Ciamis Health Services. (2022). *Publikasi data stunting hasil Bulan Penimbangan Balita (BPB) Agustus 2022.No 444.1/1321-Dinkes.03/2022*.

Darmawati, I., Marfuah, D., & Nurleli, L. (2023). Knowledge is not related to iron tablets consumption compliance in pregnant women. *Jurnal Keperawatan Komprehensif (Comprehensive Nursing Journal)*, *9*(2). https://doi.org/10.33755/jkk.v9i2.481

Galaupa, R., & Supriani, T. (2019). Evaluasi pengaruh pengetahuan ibu hamil dalam pengkonsumsian tablet Fe. *Jurnal Antara Kebidanan*, *2*(2), 96–103. https://doi.org/10.37063/ak.v2i2.43

Indonesia Ministry of Health. (2018). *Pedoman penatalaksanaan pemberian tablet tambah darah*. Kemenkes RI,. https://promkes.kemkes.go.id/download/fpck/files51888Buku Tablet Tambah darah 100415.pdf

Indonesia Ministry of Health. (2021). *Penurunan prevalensi stunting tahun 2021 sebagai modal menuju generasi emas indonesia 2045*.

Kadir, N. A., Rahim, N. A. A., Mangantig, E., Lah, N. A. Z. N., & Ahmad, A. H. (2021). Knowledge of oral iron consumption among pregnant women at Hospital Universiti Sains Malaysia. *Malaysian Journal of Medicine and Health Sciences*, *17*(9), 107–117.

Notoatmodjo, S. (2012). *Promosi kesehatan & ilmu perilaku*. Jakarta: Rineka Cipta.

Ramayulis, R., Kresnawan, T., Iwaningsih, S., & Rochani, N. S. (2018). *Stop stunting dengan konseling gizi*. Penebar Plus. Jakarta.

Rizkiana, E. (2022). Pengetahuan dan sikap remaja putri terhadap konsumsi tablet tambah darah (Ttd) Sebagai Pencegahan Stunting. *Jurnal Ilmu Kebidanan*, *9*(1), 24–29. https://doi.org/10.48092/jik.v9i1.183

Sariyati, S. (2022). Hubungan umur, pendidikan, gravida dengan kepatuhan minum tablet besi (Fe) pada ibu hamil di wilayah kerja Puskesmas Sedayu II. *Proceeding of The Conference on Multidisciplinary Research in Health Sceince and Technology*.

Setiowati, W. (2021). *Gambaran tingkat pengetahuan ibu hamil tentang konsumsi tablet Fe di Puskesmas Kramat, Kecamatan Kramat. (Tugas Akhir).* Politeknik Harapan Bersama.

Setyorini, A., & Atiqoh, U. (2018). Faktor-faktor yang berhubungan gengan Sikap Ibu Hamil Mengkonsumsi Tablet Fe Di Puskesmas Banyuasin Kabupaten Purworejo. *Komunikasi Kesehatan*, *IX*(2), 58–64.

Theng, C. E., Zakaria, N. S., & Yusof, H. M. (2017). Knowledge and attitude on consumption of

iron supplement among pregnant women in Kuala Terengganu, Terengganu. *Malaysian Applied Biology*, *46*(3), 105–112.

Word Health Organization (WHO). (2020). Levels and trends in child malnutrition, 2020 editio*n.* ISBN 978-92-000357-6, 2-15. WHO

Pharmaciana
Vol.14, No.2, July 2024, Page. 173-182
ISSN: 2088 4559; e-ISSN: 2477 0256
DOI: 10.12928/pharmaciana.v14i2.26359

Antibacterial activity of guava *(Psidium guajava* L.*)* leaf ethanolic extract nanosuspension against *Escherichia coli* bacteria

Lusi Nurdianti[1]*, Anna Yuliana[2], Euis Raras[1], Fajar Setiawan[1], Winda Trisna Wulandari[2], Ardianes Firmansya[1]

[1]Departement of Pharmaceutics, Faculty of Pharmacy, University of Bakti Tunas Husada, Jl. Letjen Mashudi No. 20, Tasikmalaya, West Java, Indonesia
[2]Departement of Pharmacochemistry Faculty of Pharmacy, University of Bakti Tunas Husada, Jl. Letjen Mashudi No. 20, Tasikmalaya, West Java, Indonesia

Submitted: 05-06-2023 ***Reviewed: 19-01-2024*** ***Accepted: 28-06-2024***

ABSTRACT

Diarrhea is a condition where a person has bowel movements three or more times a day, with consistent stools. One of the common bacteria that causes diarrhea is *Escherichia coli.* Empirical and preclinical studies have demonstrated the effectiveness of guava leaves *(Psidium guajava* L.*)* in treating diarrhea due to their tannin content. Nanosuspension formulations can be created to simplify the use of guava leaves for medicinal purposes. This study aims to investigate the efficacy of guava leaf extract, both in its natural form and as a nanosuspension preparation, against *Escherichia coli*. Additionally, the study aims to characterize the guava leaf extract nanosuspension used in the experiment. The technique used to make nanosuspension involves ionic gelation methods by using chitosan as a polymer, and subsequent characterization of the resulting product includes organoleptic testing, specific weight, pH, sedimentation volume, and viscosity. After the characterization of the guava leaf nanosuspension, it was found that the optimal formula had a particle size of 245.7 nm at a concentration of 0.01%, a polydispersion index of 0.406, and a zeta potential of +26.9 mV. Guava leaf ethanol extract 1% has a diameter of the inhibitory zone of 4.05±0.45 mm. However, the nanosuspension form of *P. guajava* L at a concentration of 0.01% has an inhibitory zone diameter of 11.45±0.64 mm. The nanosuspension formulation using *P. guajava* L has met the evaluation requirements and has antibacterial activity against *E. coli* bacteria.

Keywords: *Escherichia coli*, guava leaf ethanolic extract, ionic gelation method.

Corresponding author:
Lusi Nurdianti
Departement of Pharmaceutics, Faculty of Pharmacy, University of Bakti Tunas Husada, Tasikmalaya
Jl. Letjen Mashudi No. 20, Tasikmalaya, West Java, Indonesia
Email:lusinurdianti@universitas-bth.ac.id

INTRODUCTION

Diarrhea poses a considerable health challenge and stands as a prominent cause of illness and death among children across numerous nations, including Indonesia. It is characterized by the occurrence of three or more liquid bowel movements within a day or night. Children are particularly susceptible to diarrhea due to their less robust immune systems (Friedel & Cappell, 2023).

Escherichia coli is a bacterium known to trigger diarrhea, often spread through direct contact, and is particularly prevalent in regions with inadequate sanitation. Guava leaves, rich in compounds such as alkaloids, flavonoids, tannins, phenolics, quinones, and saponins, offer the potential to manage diarrhea. Then, guava ethanol extract with an extract solution concentration of 250 mg/mL has a MIC value of 4.3944 mg/mL against *E. coli* bacteria (Maysarah & Apriani, 2016). Furthermore, a 50% guava extract concentration showed antibacterial properties, effectively inhibiting *E. coli* with an inhibition zone diameter of 10.17±0.24 mm (Farhana et al., 2017).

Nanosuspension preparations offer a convenient means of utilizing guava leaves for medicinal purposes. This technology presents various benefits, including the alteration of surface properties and particle size of herbal remedies, facilitating precise delivery to targeted organs like the brain, lungs, kidneys, and digestive tract with enhanced selectivity, effectiveness, and safety. Furthermore, it enables the controlled release of active compounds, thus reducing potential side effects (Al-Kassas et al., 2017; Alaei et al., 2016; Du et al., 2015; Jahan et al., 2016; Wang et al., 2013). Nanosuspension is widely recommended for herbal medicines because it can reduce drug side effects by using smaller doses compared to conventional doses and improve the physical and chemical stability of drugs (Ansari et al., 2012; Narasaiah et al., 2010). Moreover, augmented particle surface area and solubility can result in heightened bioavailability and absorption of active components. Additionally, the size of the nanoparticles tends to prolong residence times in the GI tract (Ahmad et al., 2015).

The method used to prepare the guava leaf nanosuspension is the ionic gelation method. It uses bottom-up technology to create nanoparticles from a molecular solution by controlling their characteristics, such as size and morphology, for example, using solvent evaporation (Du et al., 2016). Chitosan is used as a polymer that has properties bioactive, biocompatible, chelating, antibacterial, and biodegradable properties. Nonetheless, chitosan's rapid water absorption and significant swelling propensity in aqueous environments limit its suitability for biological and medical applications as a drug delivery and release system. Hence, incorporating sodium tripolyphosphate becomes essential to generate chitosan derivatives with heightened biocompatibility and reduced swelling characteristics (Karimirad et al., 2020). Employing sodium tripolyphosphate as a cross-linking agent at a minimal dosage prevents excessive bonding between the TPP polyanion and chitosan's amino groups. This technique, known as the ionic gelation method, combines chitosan polymer and sodium tripolyphosphate. The formation mechanism of chitosan nanoparticles hinges on the electrostatic interaction between chitosan's amino groups and the negative groups of a polyanion, such as tripolyphosphate (Diniatik et al., 2019).

MATERIALS AND METHOD

Equipment

The experiments utilized an analytical balance (Mettler Toledo), macerator, incubator (Memmert IN 55), autoclave (Biobase), rotary evaporator (Ika), vortex (MixMat), magnetic stirrer with heater (model 79-1), oven (B-one), micropipette (Socorex), DelsaTM Nano C particle Analyzer (Beckman Coulter), and standard laboratory glassware.

Materials

Guava leaves (*P. guajava* L.) comes from the Wado Sumedang area with evidence of plant identification No.189/HB/11/2018 from the Jatinangor Herbarium of the Plant Taxonomy Laboratory (Department of Biology, FMIPA, Padjadjaran University), Ethanol 96% (PT. DPH), Muller Hinton Agar (MHA) media (PT. DPH), *E. coli* bacteria (ATCC 25922), NaCl 0,9% (Otsuka), Acetic acid 1% (Merck),

Chitosan (Sigma Aldrich), Sodium tripolyphosphate (Merck), PGS (Pulvis Gummosus) (PT. DPH), Methylparaben (PT. DPH), Simple syrup, Mint flavor (PT. DPH), Aquadest (PT. DPH), Aqua deionization (PT. Jayamas Medica Industri) and reagents required for screening are Ammonia, Chloroform (Merck), H2SO4 (Merck), Dragendorff reagent (PT. DPH), Mayer reagent (PT. DPH), Wagner reagent (PT. DPH), Magnesium metal (Merck), Zinc, HCl 5N, Amyl alcohol (Merck), Ether, Liebermann burchard reagent, FeCl3 (Merck) and Gelatin 1% (Brataco).

Methods

Sample preparation

Initially, guava leaves underwent a powdering process. They were cleansed with water and then dried in an oven at 40°C for 5 days. After drying, the guava leaves were finely ground into powder and filtered through an 80-mesh sieve.

Extraction preparations

The 500 g of the powdered guava leaves were placed in a maceration container and then soaked in 1.5 liters of 96% ethanol for 3 days while stirring several times. The resulting maceration was then filtered to separate the ethanol liquid from the residue. The liquid extract was concentrated using a rotary evaporator.

Characterization of the simplicia and extract

The simplicia and extract were characterized using organoleptic tests, assessing color, odor, and taste. Phytochemical screening was conducted, involving tests for alkaloid, flavonoid, saponin, tannin, and polyphenol content and the determination of total ash content. Additionally, the ethanol-soluble extract content, water-soluble extract content, and water content were determined using the azeotropic distillation method (Harborne, 1996; Departemen Kesehatan RI, 2000).

Antibacterial activity testing methods

The antibacterial testing was carried out using the diffusion method. 20 mL of Muller Hinton Agar (MHA) media was placed in a sterilized petri dish, and 200 µl of bacterial suspension was added. The dish was then swirled to distribute the media and bacteria and allowed to solidify evenly. Four holes were then made with equal spacing between them. In addition, *E. coli* bacteria from the stock were taken and mixed with 0.9% NaCl, then homogenized. The bacterial suspension was then standardized using the McFarland standard solution, and 50 µl of the extract was poured into the prepared wells. The petri dish was then incubated for 16 to 18 hours at 35±2℃; ambient air (CLSI, 2012).

Antibacterial activity of guava leaf extract

Testing for the antibacterial activity of guava leaf extract involves diluting the extract to assess its inhibitory zone activity against bacteria. The concentrations used in this test were 0%, 1%, 2%, 3%, 4%, 5%, 6%, 7%, 8%, 9%, and 10%. The antibacterial testing was carried out using the diffusion method. 20 mL of Muller Hinton Agar (MHA) media was placed in a sterilized petri dish, and 200 µl of bacterial suspension was added. The dish was then swirled to distribute the media and bacteria and allowed to solidify evenly. Four holes were made with equal spacing, and different extract concentrations were placed in each well. The petri dish was then incubated for 24 hours at 37°C. After that, bacterial growth was observed, and the inhibition zone diameter was measured.

Nanoparticle preparation (ionic gelation method)

Approximately 4 mL of a 0.01% guava leaf extract solution in a 1% acetic acid solvent is placed into a vial. Subsequently, 1 mL of a 0.25% chitosan solution is added to the vial using a 1% acetic acid solvent. The mixture is stirred using a magnetic stirrer for 10 minutes until all components of the guava leaf extract are entirely dissolved. Then, 4 mL of a 0.1% sodium tripolyphosphate solution, prepared with deionized water, is added dropwise at a rate of 1 drop per second. This addition of sodium

tripolyphosphate is carried out on the magnetic stirrer with a speed of 500 rpm for 1 hour. Subsequently, particle size and zeta potential are measured using a DelsaTM Nano C Particle Analyzer (Beckman Coulter (Woranuch & Yoksan, 2013). The composition of guava leaf extract nanoparticles is detailed in Table 1.

Table 1. Guava leaf extract nanoparticle composition

Formula	The ethanolic extract of guava leaf	Chitosan (0.25%)	Sodium tripolyphosphate (0.1%)
F I			
The ethanolic extract of guava leaf 0.05%	4 mL	1 mL	5 mL
F II			
The ethanolic extract of guava leaf 0.01%	4 mL	1 mL	5 mL

Preparation of nanosuspension formulation of guava leaf extract

PGS (*Pulvis Gummosus*) and water are combined in a mortar and crushed until a homogeneous mixture is obtained. Meanwhile, methylparaben is dissolved in hot water in a glass beaker while stirring until completely dissolved. Subsequently, the dissolved methylparaben, simple syrup, mint flavoring, and guava leaf extract nanoparticles are added into the mortar and crushed until homogeneous. Then, distilled water is added to reach a total volume of 100 mL. The formulation details of the guava leaf extract nanosuspension are provided in Table 2.

Table 2. Nanosuspension formulation of guava leaf extract

Composition	Formula I	Formula II
Guava Leaf Extract	8.3%	-
Guava Leaf Extract Nanosuspension	-	8.3%
PGS (Pulvis Gummosus)	1%	1%
Methylparaben	0.1%	0.1%
Simple syrup	25%	25%
Mint Flavour	qs	qs
Aquadest ad	60 mL	60 mL

Evaluation of Guava Leaf Extract Nanosuspension

Guava leaf extract nanosuspension evaluation includes organoleptic, specific gravity, pH, sedimentation volume, and viscosity testing.

Organoleptic test

Organoleptic test including color, odor, and taste.

Specific gravity test

A pycnometer is weighed and recorded as A grams. It is then filled with water up to the brim and weighed again, recording the weight as A1 grams. The nanosuspension is put into an empty pycnometer, weighed, and recorded as A2 grams. The specific gravity of the nanosuspension is then calculated (Emilia et al., 2013).

pH test

The nanosuspension is put into a beaker, and the pH meter is inserted to measure the pH. The results are recorded.

Sedimentation volume test

The nanosuspension is put into a measuring glass of up to 50 mL and left for approximately 1 hour until two phases form. The sedimentation volume is observed and recorded.

Viscosity test

The viscosity test involves transferring the nanosuspension into a beaker and configuring a viscometer to a predetermined speed for viscosity measurement using a Brookfield Viscometer. Subsequently, the recorded results are documented.

Antibacterial Activity of Guava Leaf Extract Nanosuspension

The method is the same as the antibacterial activity testing methods.

RESULT AND DISCUSSION

The phytochemical screening and characterization of simplicia and ethanolic extract of guava leaf

The outcomes of the phytochemical screening conducted on both the simplicial form and the extract yielded identical results concerning the secondary metabolite content yang, as seen in Table 3. This implies that the extraction method did not eliminate the available secondary metabolites in their original form within the simplicia. The non-specific characteristic testing conducted on both the simplicia form and the extract complied with the standards outlined in the Indonesian Herbal Pharmacopoeia (Kementerian Kesehatan RI, 2017). Furthermore, the extract formulation exhibited a decrease in total ash content, indicating a reduction in impurities. Moreover, there was an elevation in the concentration of water-soluble and ethanol-soluble compounds, signifying an enhanced concentration of compounds in the extract formulation compared to the simplicia form. The results of testing non-specific characteristics of simplisia and guava leaf ethanol extract are presented in Table 4.

Table 3. Results of phytochemical screening of guava leaves

Secondary Metabolite	Simplicia	Extract
Flavonoid	+	+
Tannin/Polyphenol	+	+
Saponin	+	+
Quinon	+	+
Steroid/Triterpenoid	+	+
Alkaloid	+	+

Information:
(+) Positive Results; (-) Negative Results

Table 4. Non-specific characteristics of simplicia & guava leaf ethanol extract

Characteristic	Simplicia (%)	FHI Parameters	Extract (%)	FHI Parameters
Water Content	4.00% ± 0.00	<10%	8.00 ± 0.00	<10%
Ash Content	8.84% ± 0.21	<9%	1.64 ± 0.82	<6.1%
Water Soluble Extract Content	24.48% ± 0.01	>18.2%	49.46 ± 0.39	>18.2%
Ethanol Soluble Extract Content	22.60% ± 0.24	>15%	72.45 ±0.86	>15%
Yields			9.506%	

The antibacterial activity of the guava leaf ethanolic extract

At a concentration of 10%, the ethanolic extract from guava leaves maintains its antibacterial effectiveness, confirming the presence of antibacterial properties within the extract. Identifying the

active extract involves establishing its Minimum Inhibitory Concentration (MIC), which gauges the extract's potency against the test bacteria until reaching the lowest effective concentration. Therefore, the MIC is determined at concentrations ranging from 0% to 10% with a concentration variation interval of 1. Several factors can affect the inhibition of test bacteria by antibacterial compounds, including the thickness of the medium bacteria (Maysarah & Apriani, 2016). The results of the antibacterial activity test of guava leaf ethanolic extract are presented in Table 5.

Table 5. The results of the antibacterial activity of the guava leaf ethanolic extract

Concentration (%)	Inhibition zone (mm) ± SD
0	-
1	4.05 ± 0.45
2	4.30 ± 0.30
3	4.72 ± 0.92
4	5.20 ± 0.50
5	6.35 ± 0.55
6	6.45 ± 0.35
7	6.50 ± 0.50
8	6.55 ± 0.15
9	6.65 ± 0.55
10	6.75 ± 0.15

Optimization of nanoparticle preparation

The optimization of nanoparticle production aims to determine an appropriate formula to obtain an optimal result. The optimization includes the amount of chitosan polymer, cross-linking agent sodium tripolyphosphate, stirring time, rotation speed, and dripping speed. Chitosan is a polymer that includes cationic polymers with a high electric charge at pH <6.5 so that it adhesives to the negative surface and chelate metal ions. The highly reactive hydroxyl and amino groups in chitosan play a role in chemical reactions and salt formation. Amino groups allow chitosan interaction with anionic systems, resulting in changes in the physicochemical characteristics of such combinations (Gomes et al., 2017). Tripolyphosphates in multi-ion crosslinked nanoparticles are used as ion pairs of chitosan. The reason for using tripolyphosphate is its nature as a multivalent anion that can form cross-linked bonds with chitosan to produce nanoparticles that are more stable and have better membrane penetration characteristics (Shi et al., 2011). The formation mechanism of chitosan nanoparticles arises from the electrostatic interaction between the amine group of chitosan and the negative groups of polyanions like tripolyphosphate (Matalqah et al., 2020). The results of the nanoparticles of guava leaf extract can be seen in Figure 1.

Figure 1. Nanoparticles of guava leaf extract

The determination of particle size, polydispersity index, and zeta potential

The polydispersity index is a numeric gauge of nanoparticle size distribution within a formulation. A lower polydispersity index implies greater long-term stability of the dispersion system. When the

index approaches 0, it signifies a uniformly dispersed formulation, while a value surpassing 0.5 indicates notable heterogeneity (Desmiaty et al., 2017). Both formulations yielded particle sizes within the nanoparticle range, typically spanning 10-1000 nm. Nanoparticle size can be influenced by factors such as polymer concentration, crosslinker drip rate, and rotational speed during manufacturing.

The polydispersity index findings reveal favorable values of 0.489 and 0.406 for both formulations, respectively. These values fall below 0.5, indicating that the formulations belong to the monodispersed category. In this category, the narrow distribution of nanoparticle particles promotes even dispersion and greater stability compared to polydisperse formulations. Apart from particle size, zeta potential is a crucial characteristic of nanoparticles. Zeta potential testing is conducted to anticipate the stability of colloidal solutions, where particle interactions significantly influence colloidal stability. Zeta potential quantifies the repulsive forces between particles (Ubgade et al., 2021).

Zeta potential testing was only conducted on formulation II because it had the smallest particle size. The zeta potential measurement result for formulation II yielded a value of +26.9 mV, indicating that the nanoparticles in the formulated colloid suspension are approaching stability as they are close to the value of 30 mV. This result can be seen in Table 6.

Table 6. The characterization of guava leaf nanoparticle preparations *(P. guajava* L.*)*

Formula	Size Particle (nm)	Polydispersity Index	Zeta Potential (mV)
I	451.1	0.489	-
II	245.7	0.406	+ 26.9

The evaluation of nanoparticle guava leaf ethanolic extract preparations

The assessment findings of the nanosuspension formulation revealed a milky white appearance, a mint aroma, and a bitter taste. The specific gravity test aimed to compare the final specific gravity of the formulation with the theoretical specific gravity of the suspension. This test, commonly employed for liquids, relies on comparing the weight of a substance in air at 25°C with the weight of water at the same volume and temperature. In suspensions, when water is used as the carrier, the resulting specific gravity typically exceeds that of the carrier (Wang et al., 2013). The specific gravity of the nanosuspension formulation was determined using a pycnometer, yielding results of 1.263 g/mL, 1.0334 g/mL, and 1.0343 g/mL, as illustrated in Table 7.

Table 7. Evaluation of nanosuspension guava ethanolic extract preparations

Parameters	Formula		
	Blank	I	II
Color	White	White	White
Odor	Mint	Mint	Mint
Flavor	Bitter	Bitter	Bitter
Specific gravity	1.2630 g/mL	1.0334 g/mL	1.0343 g/mL
pH	5.6	6.2	5.4
Viscosity	246.7 cP	214.0 cP	241.3 cP

The pH analysis was carried out to assess the acidity level of the completed formulation. Findings revealed that the formula blank exhibited a pH of 5.6, while formula I displayed a pH of 6.2, and formula II had a pH of 5.4. Viscosity testing was conducted to evaluate the consistency and flow characteristics of the final suspension. Per the national standard (SNI), suspension viscosity typically ranges from 37 to 396 cP. The examination outcomes indicated that the suspension's viscosity fell within the established range documented in the literature. These findings are summarized in Table 8.

Table 8. The sedimentation test of nanosuspension guava leaf ethanolic extract

Evaluation Time		Formula		
		Blank	**I**	**II**
	Vo	50 mL	50 mL	50 mL
15,30,40,60 minutes	**Vu**	50 mL	50 mL	50 mL
1 – 5 days	**F**	**1**	**1**	**1**

Information:
Vo = Initial volume; Vu = Final volume of the precipitate; F= Sedimentation volume

The sedimentation volume assessment aimed to ascertain the sedimentation volume of the completed formulation by comparing it with the expected value. Sedimentation volume is determined as the ratio of the final sedimentation volume (Vu) to the initial suspension volume (Vo) (Syamsuni, 2006). When F = 1 signifies flocculation equilibrium, the suspension is deemed satisfactory. If F>1 indicates a very loose and fine floc, resulting in Vu>Vo. Evaluation findings for the three suspension formulations revealed an F value of 1, suggesting these formulations are well-prepared suspensions.

The activity of nanosuspension guava leaf extract preparations

The activity test results conducted on Formula II, which is the nanosuspension, showed the largest inhibition zone of 11.45±0.64 mm, while Formula I showed 8.40±0.35 mm. This indicates that nanosuspension is more effective, in line with the advantages of nanosuspension, which can deliver drugs more effectively to small units in the body and increase drug delivery efficiency by improving solubility in water, can be targeted to reduce toxicity and increase drug distribution efficiency, improve the delivery of bioengineered drugs through various extreme body anatomy such as the brain barrier. Then, particle size testing can show that particle size influences the antibacterial activity of the preparation. Nanosuspensions with smaller particle sizes and large surface areas are able to increase the rate of dissolution and absorption of drugs (Patel & Agrawal, 2011). The results can be seen in Table 9.

Table 9. The activity of nanosuspension guava leaf ethanolic extract preparations against *Escherichia coli*

Formula	Inhibition Activity (mm)
I	8.40 ± 0.35
II	11.45 ± 0.64

CONCLUSION

According to the research findings, the ethanolic extract of guava leaf demonstrated an inhibition zone of 4.05±0.45mm at a concentration of 1%. Conversely, the nanosuspension of guava leaf extract, at a much lower concentration of 0.01%, exhibited a notably larger inhibition zone value of 11.45±0.64mm. The characterization results for the optimized formula of guava leaf nanosuspension at the 0.01% concentration revealed a particle size of 245.7 nm, a polydispersity index of 0.406, and a zeta potential of +26.9 mV.

REFERENCE

Ahmad, J., Amin, S., Rahman, M., Rub, R., Singhal, M., Ahmad, M., Rahman, Z., Addo, R., Ahmad, F., Mushtaq, G., Kamal, M., & Akhter, S. (2015). Solid matrix based lipidic nanoparticles in oral cancer chemotherapy: applications and pharmacokinetics. *Current Drug Metabolism*, *16*(8), 633–644. https://doi.org/10.2174/1389200216666150812122128

Alaei, S., Ghasemian, E., & Vatanara, A. (2016). Spray drying of cefixime nanosuspension to form stabilized and fast dissolving powder. *Powder Technology*, *288*, 241–248. https://doi.org/10.1016/j.powtec.2015.10.051

Al-Kassas, R., Bansal, M., & Shaw, J. (2017). Nanosizing techniques for improving bioavailability of drugs. *Journal of Controlled Release*, *260*, 202–212. https://doi.org/10.1016/j.jconrel.2017.06.003

Ansari, S. H., Islam, F., & Sameem, M. (2012). Influence of nanotechnology on herbal drugs: A Review. *Journal of Advanced Pharmaceutical Technology and Research*, *3*(3), 142–146. https://doi.org/10.4103/2231-4040.101006

CLSI. (2012). Performance standards for antimicrobial disk susceptibility tests; approved standard—eleventh edition. In *Clinical and Laboratory Standards Institute (CLSI)* (Vol. 32, Issue 1, pp. 11–44). Clinical and Laboratory Standards Institute. www.clsi.org.

Departemen Kesehatan RI. (2000). *Parameter standar umum ekstrak tumbuhan obat* (1st ed.). Direktorat jenderal pengawasan obat dan makanan direktorat pengawasan obat tradisional.

Desmiaty, Y., Rahmat, D., & Afifah, H. (2017). Preparation of nanoparticles containing soursop (*Annona Muricata* L.) leaves extract using gelation ionic method and determination of its antioxidant activity. *Research Journal of Pharmaceutical, Biological and Chemical Sciences*, *8*(1), 275–279.

Diniatik, Kusumawati, A., Siswanto, A., Imtihan, Z. F., & Wahyudi, A. (2019). Formulation of nanoparticles of ethanol extract of garcinia mangostana l. Leaves as antioxidant with pectin as cross-linker and chitosan variation as polymer. *International Journal of Recent Technology and Engineering*, *8*(2 Special Issue 9), 779–783. https://doi.org/10.35940/ijrte.B1162.0982S919

Du, J., Li, X., Zhao, H., Zhou, Y., Wang, L., Tian, S., & Wang, Y. (2015). Nanosuspensions of poorly water-soluble drugs prepared by bottom-up technologies. *International Journal of Pharmaceutics*, *495*(2), 738–749. https://doi.org/10.1016/j.ijpharm.2015.09.021

Du, J., Zhou, Y., Wang, L., & Wang, Y. (2016). Effect of PEGylated chitosan as multifunctional stabilizer for deacetyl mycoepoxydience nanosuspension design and stability evaluation. *Carbohydrate Polymers*, *153*, 471–481. https://doi.org/10.1016/j.carbpol.2016.08.002

Emilia, Taurina, W., & Fahrurroji, A. (2013). Formulasi dan evaluasi stabilitas fisik suspensi Ibuproen dengan menggunakan natrosol HBr sebagai bahan pensuspensi. *Media Farmasi Indonesi*, *8*(2), 585–595.

Farhana, J., A, Hossain, M. F., & Mowlah, A. (2017). Antibacterial effects of Guava *(Psidium guajava* L.*)* extracts against food borne pathogens. *International Journal of Nutrition and Food Sciences*, *6*(1), 1–5. https://doi.org/10.11648/j.ijnfs.20170601.11

Friedel, D. M., & Cappell, M. S. (2023). Diarrhea and Coronavirus Disease 2019 Infection. *Gastroenterology Clinics of North America*, *52*(1), 59–75. https://doi.org/10.1016/j.gtc.2022.11.001

Gomes, L. P., Paschoalin, V. M. F., & Del Aguila, E. M. (2017). Chitosan nanoparticles: production, physicochemical characteristics and nutraceutical applications. *Revista Virtual de Quimica*, *9*(1), 387–409. https://doi.org/10.21577/1984-6835.20170022

Harborne, J. B. (1996). *Metode fitokimia : Penuntun Cara Modern Menganalisis Tumbuhan diterjemahan oleh Kosasih Padmawinata dan Iwang Soediro* (S. Niksolihin, Ed.). Penerbit ITB.

Jahan, N., Aslam, S., Rahman, K. ur, Fazal, T., Anwar, F., & Saher, R. (2016). Formulation and characterization of nanosuspension of herbal extracts for enhanced antiradical potential. *Journal of Experimental Nanoscience*, *11*(1), 72–80. https://doi.org/10.1080/17458080.2015.1025303

Karimirad, R., Behnamian, M., & Dezhsetan, S. (2020). Bitter orange oil incorporated into chitosan nanoparticles: Preparation, characterization and their potential application on antioxidant and antimicrobial characteristics of white button mushroom. *Food Hydrocolloids*, *100*. https://doi.org/10.1016/j.foodhyd.2019.105387

Kementerian Kesehatan RI. (2017). *Farmakope Herbal Indonesia* (II). Direktorat jenderal kefarmasian dan alat kesehatan.

Matalqah, S. M., Aiedeh, K., Mhaidat, N. M., Alzoubi, K. H., Bustanji, Y., & Hamad, I. (2020). Chitosan Nanoparticles as a Novel Drug Delivery System: A Review Article. *Current Drug Targets*, *21*(15), 1613–1624. https://doi.org/10.2174/1389450121666200711172536

Maysarah, H., & Apriani, R. (2016). Antibacterial activity test of ethanol extract of white and red flesh from guava leaf (*Psidium guajava*. L) against *Staphylococcus aureus* and *Escherichia coli*. *Jurnal Natural*, *16*(1), 11–12. https://doi.org/10.24815/jn.v16i1.4818

Narasaiah,V, L., ReddyB, K., Kumar M, R., RaoP, S., & ReddyB, V. (2010). Enhanced dissolution rate of atorvastatin calcium using solid dispersion with PEG 6000 by dropping method. *Journal of Pharmaceutical Sciences and Research*, *2*(8), 484–491.

Patel, V., & Agrawal, Y. (2011). Nanosuspension: An approach to enhance solubility of drugs. *Journal of Advanced Pharmaceutical Technology & Research*, *2*(2), 81. https://doi.org/10.4103/2231-4040.82950

Shi, L.-E., Fang, X.-J., Xing, L.-Y., Chen, M., Zhu, D.-S., Guo, X.-F., Zhao, L.-M., & Tang, Z.-X. (2011). Chitosan Nanoparticles as Drug Delivery Carriers for Biomedical Engineering. *J.Chem.Soc.Pak*, *33*(6), 929–934.

Syamsuni, H. (2006). *Farmasetika Dasar dan Hitungan Farmasi* (S. Winny R, Ed.). EGC.

Ubgade, S., Bapat, A., & Kilor, V. (2021). Effect of various stabilizers on the stability of lansoprazole nanosuspension prepared using high shear homogenization: Preliminary investigation. *Journal of Applied Pharmaceutical Science*, *11*(9), 085–092. https://doi.org/10.7324/JAPS.2021.110910

Wang, Y., Zheng, Y., Zhang, L., Wang, Q., & Zhang, D. (2013). Stability of nanosuspensions in drug delivery. *Journal of Controlled Release*, *172*(3), 1126–1141. https://doi.org/10.1016/j.jconrel.2013.08.006

Woranuch, S., & Yoksan, R. (2013). Eugenol-loaded chitosan nanoparticles: I. Thermal stability improvement of eugenol through encapsulation. *Carbohydrate Polymers*, *96*(2), 578–585. https://doi.org/10.1016/j.carbpol.2012.08.117

Pharmaciana
Vol.14, No.2, July 2024, Page. 183-194
ISSN: 2088 4559; e-ISSN: 2477 0256
DOI: 10.12928/pharmaciana.v14i2.26359

The effect of syrup simplex concentration on the physicochemical stability of Gembili's inulin (*Dioscorea esculenta* (Lour.) Burkill) nanosilver colloid

Dian Eka Ermawati*, Yavi Hanuriansyah
Department of Pharmacy, Vocasional School, Universitas Sebelas Maret,
Jl Ir. Sutami 36 A, Kentingan, Surakarta, Central Java, Indonesia

Submitted: 29-06-2023 ***Reviewed: 23-01-2024*** ***Accepted: 28-06-2024***

ABSTRACT

Gembili (*Dioscorea esculenta)* tuber's inulin is a successful bioreductor agent that forms a nanosilver with a size of 481.4 nm and is stable for 30 days at 4 °C storage. That nanosilver has immunomodulatory activity and is proven safe from the results of acute toxicity tests at a dose of 4 mg/kgBW. However, a drug delivery system is needed to be developed as a supplement product. The syrup was chosen because alcohol free, has a better taste, measured dose, and stable to maintain of the active substance compared to elixir, solution, and suspension. Syrup simplex as a syrup base affects stability because it has the potential to form crystals during storage. This research aims to determine the effect of syrup simplex concentration on the physicochemical stability of nanosilver colloid. The research was conducted with the biosynthesis process using gembili's inulin, nanosilver characteristic, modified syrup formula, and stability test. Nanosilver syrup was prepared by modifying the syrup simplex concentration of 20%, 40%, and 60%. Optimum dose of nanosilver as imunomodulator was added, then tested the physicochemical; stability, including organoleptic, pH, and viscosity, before and after storage with temperature variations of 4 °C and 40 °C for six cycles. The choosen formula then analysis using FT-IR and sugar reduction content. Data analysis using SPSS 21.0 Windows with One-way ANOVA. The results showed that the concentration of syrup simplex affected consistency, pH, and viscosity. The syrup simplex concentration of 60% met the requirement with a medium thick consistency, pH 5.25±0.03, a viscosity of 92±2.6 cps, reducing sugar content was 20.59% ±0.002, and the FTIR profile showed that it still contained nanosilver which was indicated by the presence of Ag-N groups compared to silver nitrate solution.

Keywords: nanosilver; syrup simplex, immunostimulant, gembili's inulin, physicochemical stability

Corresponding author:
Dian Eka Ermawati
Universitas Sebelas Maret
Jl. Ir Sutami 36 A Kentingan, Jebres, Surakarta, Central Java, Indonesia
Email: dianekae@staff.uns.ac.id

INTRODUCTION

Nanosilver is a product based on nanotechnology. Currently, nanosilver is developed as a medical agent and has been tested. Silver ions can cause toxicity to the body's tissues because they produce a high affinity for thiols in the liver and other organs (Tiwari et al., 2011). When silver is made into nanoparticles, there is an increase in the contact area with bacteria which causes more effective antibacterial activity and reduces toxicity (Ahmed et al., 2018). In addition to antibacterial activity, nanosilver has antiviral activity (Pulit-Prociak et al., 2015). According to (Harso, 2017), nanosilver is a catalyst for the body's immune system to kill viruses, pathogens, and bacteria in humans.

Biosynthesis of silver nanoparticles using plant extracts is safer for the environment than physical and chemical methods. The polysaccharide group can be a reducing and nanosilver-capping agent. Gembili tubers are local tubers that contain inulin oligosaccharides which can enhance the body's defense mechanism (immunomodulator) (Shafie et al., 2022). Inulin is a carbohydrate that contains fiber from plants and is widely used in the world of health as a source of prebiotics to increase body immunity (Azhar, 2009). Gembili's inulin can be an ion silver bioreductor with immunomodulatory activity. In synergy with this, the nanosilver can increase the solubility of gembili's inulin (Ermawati et al., 2021). Gembili's Inulin, a silver bioreductor, produces particle sizes in the nanometer range (12.4−48.0 nm) with a spherical shape. Intense antibacterial activity against gram-positive and weak against gram-negative bacteria (Ermawati, 2017).

The silver used as medical treatment is silver nitrate (AgNO3), not silver ion (Ag+). The toxicity effect of silver nitrate after being made in nanoparticle form is lower, and the effectivity as an antibacterial agent is increased. The maximum concentration of nanosilver in the human body is 10 mg/Kg BW (Pulit-Prociak et al., 2015). So, the concentration of nanosilver used in this research is safe for humans, which is also supported by further research, namely the immunomodulator test and toxicity test.

The immunomodulator test of gembili's inulin nanosilver based on the Immunoglobulin G (IgG) profile on the serum's tested animal, which was induced by the vaccine at a dose of 4 mg/kgBW, with the ELISA reader method had the highest Optical Density value compared to other doses. The comparison with synthetic immunostimulants produced sig. 0.13>0.05, which means not significantly different and effective as an immunomodulator with immunostimulating activityactivity. The nanosilver solution was stable for 30 days of testing at an optimum pH of 8 (Nurani, 2022). The results of the acute toxicity test of Gembili's inulin nanosilver showed no toxicity symptoms in the first 4 hours of treatment and 24 hours of observation. They had not yet reached the LD50 value. Observations on the semiquantitative histological profile of the kidneys and liver showed reversible damage in congestion and intratubular bleeding at a dose of 254 mg/kgBW (Setianingsih, 2020).

Based on the facts of previous research, gembili’s inulin nanosilver will be developed as a supplement product. The syrup was chosen because alcohol free, has a better taste, measured dose, and stable to maintain of the active substance compared to elixir, solution, and suspension. Simplex syrup as a syrup base affects stability because it has the potential to form crystals during storage. The effect of adding sugar on the characteristics of red dragon fruit syrup with concentration ratios of added sugar of 50, 55, and 65%. Dragon fruit syrup produced by adding 50% sugar has met the SNI (2013) syrup quality standard: a reduced sugar content of 65.7%. According to (Fickri, 2019), the quality requirement in making syrup is the maximum concentration of sugar solution in syrup at room temperature of 65%. If it is higher, crystallization will occur, but if it is lower than 60%, the syrup will be contaminated by microbes. Nanosilver syrup formulation has been carried out before giving nanosilver syrup to honeybees at a dose of 25 ppm, or the equivalent of 25 mg/L nanosilver can improve the health of bees (Grzegorz et al., 2013).

This study will incorporate gembili's inulin nanosilver into syrup preparations. The process of making nanosilver syrup was carried out by adding gembili's inulin of 4 mg/kgBW by modifying the concentration of simplex syrup to 20%, 40%, and 60%, then evaluated on physicochemical properties. This study aims to determine the effect of simplex syrup concentration on the stability of nanosilver

syrup preparations which are expected to accept by patients of various ages for immunomodulatory supplements.

MATERIALS AND METHOD

Materials

Gembili tubers, Cepogo, Central Java, Indonesia (*Dioscorea esculenta* (Lour.) Burkill) with document number of 130/UN27.9.6.4/Lab/2022; silver nitrate (AgNO, Merck KgaA, Germany); 30% ethanol (repackaged by Toko Saba Kimia, Surakarta; simplex syrup (repackaged by PT. Agung Jaya Indonesia); propylene glycol (repackaged by PT. Agung Jaya Indonesia); Na benzoate (repackaged by Toko Saba Kimia, Surakarta); aquadest (Repackaged by PT. Agung Jaya Indonesia), Anhydrous glucose pro analysis Specification 1.08337.11000 (Repackaged by Planet Kimia, Jakarta), Nelson reagent (Repackaged by CV Muda Berkah, Yogyakarta), Arsenomolybdate reagent (Packaged repeated by CV Adi Mandiri, East Java. Instrument: Oven (Mermmet UN110, Germany); pH meter Eutech CyberScan pH 300 (OHAUS Starter 300); Viscometer Rion VT-04F (Japan); UV Visible Spectrophotometer (Genesys 150, USA); FTIR (Shimadzu); Centrifuge (Thermo Scientific, German).

Methods

Gembili's inulin preparation

Determination of gembili tubers was carried out at the Biology Laboratory of the Faculty of Mathematics and Natural Sciences, Universitas Sebelas Maret, Surakarta, Indonesia. Gembili tuber flour is dried in an oven at 40 °C and dissolved in hot water for 30 minutes. The volume of the resulting filtrate was measured, then ethanol 30% was added to 30% of the total filtrate volume. The solution was stored in a freezer at -10 °C for 18 hours until a precipitate was obtained. The inulin precipitate is dried using an oven (Fera & Masrikhiyah, 2019).

Biosynthesis process and characterization of nanosilver

Gembili inulin of 10 grams was dissolved in 250 mL of distilled water at 40 °C and stirred until dissolved. The solution was filtered using Whatman No.1 paper (solution a). Silver nitrate of 85 mg dissolved in 500 mL distilled water at 40 °C (solution b). Solution a (7.0 mL) and solution b (36.0 mL) were incubated at 60 °C for 15 minutes. The biosynthetic solution was deposited for 24 hours to maximize the biosynthetic process. The solution after biosynthesis process were scanning at the maximum wavelength of SPR range of nanosilver using a UV-Vis spectrophotometer, and aquadest was used as a blanko (Ermawati et al., 2021). The biosynthetic solution was deposited for 24 hours to maximize the biosynthetic process. The biosynthesis results were then read at the maximum wavelength using a UV-Vis spectrophotometer, and aquadest was used as a blanko (Ermawati, 2017). Nanosilver characterization was carried out using a Particle Size Analyzer (PSA) to determine the size distribution and uniformity of the particles. The data obtained from this measurement are Z-average, PI (Polydisperse Index), and potential zeta.

Nanosilver syrup was made by carefully weighing the ingredients (Table 1). In the first stage, Na benzoate was dissolved in half of the propylene glycol. Nanosilver was dissolved with the part propylene glycol until dissolved, added with simple syrup until all the ingredients were dissolved, and added aquadest to a volume of 60 mL (Sugarda et al., 2019).

Stability test

The stability test was accelerated in this study by the method cycling test. Syrups were tested on day 0 and after six cycles. One cycle consists of storage at 4±2 °C and 40±2 °C for 24 hours, respectively. Physicochemical evaluation, including organoleptic tests, pH, F value, and viscosity of syrup preparations (Reiger, 2000).

Organoleptic observations of syrup preparations included changes in color, aroma, consistency, and the appearance of gas or crystals. pH meter calibrated with standard pH solutions 4 and 10 before it

uses to measure the pH of syrups. The pH meter was placed in a bottle containing nanosilver syrup until the pH value was constant. Then the results are recorded and replicated three times. Viscosity measurement was done by dipping the spindle into the syrup preparation, the viscometer was turned on until the spindle was completely submerged and the measurement was constant. The syrup was put into the centrifugation tube, and then the centrifuge was operated at 3000 rpm for 10 minutes. Observation of the occurrence of phase separation was carried out. The F value was calculated by dividing the separation height with the total phase height (Ermawati, 2017).

Formula of nanosilver syrup

Table 1. Formula of nanosilver syrup with variation of syrup simplex concentration

Ingredients	Function	Weight (gram)		
		Formula 1 (20% of syrup base)	Formula 2 (40% of syrup base)	Formula 3 (60% of syrup base)
Gembili's inulin nanosilver	Immunomodulator agent	0.36	0.36	0.36
Simplex syrup	Syrup base	12	24	36
Propylene glycol	Co-solvent	4.8	4.8	4.8
Na benzoate	preservative	0.06	0.06	0.06
Distilled water add	solvent	60 mL	60 mL	60 mL

Reduction glucose test

A standard glucose solution with a concentration of 0.04 mg/mL was taken and 1.0 mL of this solution was added to 1.0 mL of Nelson's reagent. The resulting mixture was then heated at 100 °C for 20 mins. After cooling, 1.0 mL of arsenomolybdate reagent and 7.0 mL of distilled water were added and vortexed until homogeneous. The absorbance of the resulting mixture was then measured at a wavelength ranging from 640-840 nm (Al-kayyis & Susanti, 2016). To create a standard curve, a total of 1.0 mL of glucose standard solutions with concentrations of 0.01, 0.02, 0.025, 0.03, 0.035, 0.04, and 0.05 mg/mL were added to volumetric flasks. Furthermore, 1.0 mL of Nelson's reagent was added, followed by heating at 100 °C for 20 mins and cooling. After cooling, 1.0 mL of arsenomolybdate reagent was vortexed until all precipitate dissolved. Subsequently, 7.0 mL of distilled water was added and shaken until homogeneous, and the absorption of each solution was measured at the maximum wavelength. A standard curve was constructed to show the relationship between the standard glucose concentration and the absorbance. For the analysis of nanosilver syrup choosen formula, a 1.0 mL solution with a concentration of 1.0 mg/mL was prepared and placed in a volumetric flask. In addition, 1.0 mL of Nelson's reagent was added, and the mixture was heated at 100 °C for 20 mins and cooled according to the procedure for determining the maximum wavelength.

FT-IR analysis

FTIR was carried out to find information on the chemical bonds in the sample base syrup, nanosilver, and selected nanosilver syrup preparations, which can be seen from the wave number indicating the presence of functional groups. A typical infrared scan is produced in the mid-infrared region of the light spectrum. The mid-infrared region is a 400-4000 cm^{-1} wave number, with the same wavelength of 2.5-25 microns (10-3 mm) (Sanjiwania & Sudiarsa, 2021). FT-IR analysis ensured that the inulin nanosilver was still in the syrup preparation. (Melanie et al., 2015) state that wave numbers below 900 cm-1 are characteristic of inulin carbohydrates.

Data Analysis

Data from the physicochemical properties test for nanosilver syrup between formulas were analyzed using the SPSS 21 program through the Shapiro-Wilk test. If the data were normally distributed, proceed with the One-Way ANOVA test to determine a significant difference between the three formulas. The One-Way ANOVA test data results showed that significant differences would be continued with the Post Hoc test. The results of the physicochemical properties for each formula after the stability test were analyzed using the SPSS 21 program through the Paired Samples T-Test to determine a significant difference.

RESULT AND DISCUSSION

Determination is carried out to prove the correctness of the sample used for research. Determination Results with letter No. 130/UN27.9.6.4/Lab/2022 stated that the tubers used in this study were true yam tubers of the species *Dioscorea esculenta* (Lour.) Burkill.

Biosynthesis or green synthesis is an environmentally friendly and safe silver nitrate synthesis method using biological materials, microorganisms, and plants. This method is safer, more cost-effective, and environmentally friendly than physical and chemical methods. Biosynthesis using plant extracts is simpler than microorganisms because there is no need to prepare microorganism media or cell culture (Pulit-Prociak et al., 2015). Silver metal's physical method is breaking metal solids into small nano-sized particles, while the chemical method is carried out by forming nanoparticles through chemical reactions (Lembang, 2013). Using chemical-reducing agents has disadvantages, such as producing hazardous waste, expensive reducing agents, and being toxic. The nanosilver formed is also unstable because no capping agent can be adsorbed or bind to the surface of the nanoparticles to prevent agglomeration (Abou El-Nour et al., 2010). Development of bioreduction methods using plant extracts as an alternative to those two methods (Lengke et al., 2007).

Characteristic of Gembili's inulin nanosilver

The biosynthesis process was carried out at 60 °C for 15 minutes. The optimal temperature determines the size of the nanosilver formed (Ermawati et al., 2021). Biosynthesis at 60 °C for gembili's inulin nanosilver, the reaction will be completed more quickly, and the resulting particle size is smaller than the biosynthetic process carried out at room temperature. The presence of groups –OH contained in inulin acts as a capping agent, reducing Ag+ to Ag°, thus producing a stable nanosilver. Nanosilver synthesis produces a brownish solution color (Figure 1); this change indicates a reduction process (Ag+) when bound to the -OH functional group contained in the compound in inulin in Gembili tuber. The ability of compounds in plants to reduce (Ag+) into Ag° nanoparticles is the working principle of plants in reducing nanosilver. The maximum wavelength obtained from UV-Vis spectrophotometric characterization is 440 nm. These results indicate that nanosilver has been formed because nanosilver produces absorbance peaks in the SPR (Surface Plasmon Resonance) range of 400-500 nm (Kumar & Yadav, 2009).

Particle Size Analyzer (PSA) to determine particle size distribution and uniformity. The data obtained from this measurement are Z-average, PDI (Polydisperse Index), and potential zeta. Z-average is the average particle diameter, and PDI is the magnitude of the particle size distribution distance. PDI shows that the distribution distance of the sample is wide and has more than one peak; the particle size is varied or heterogeneous (Murano, 1998). Zeta potential is a parameter of the electric charge between colloidal particles (Ozturkoglu-Budak et al., 2019).

The Z-average of the gembili's inulin nanosilver is 109.3-128.9 nm. According to (Nagpal et al., 2010), nanoparticles are solid colloidal particles with a 1-1000 nm diameter. The results indicate that the size of the gembili's inulin nanosilver met the range of nanoparticles. The PI value <0.5 indicates that the resulting nanosilver has a homogeneous particle size distribution. Furthermore, the zeta potential values obtained are -29.1 to -28.4 mV. Zeta potential value indicates that the strength of the particles to repel each other is getting stronger to produce a stable dispersion of the preparation. The

zeta potential value of a stable preparation is more than +25 mV or less than -25 mV. The zeta potential value in this study is less than -25 mV indicating that the resulting nanosilver is stable.

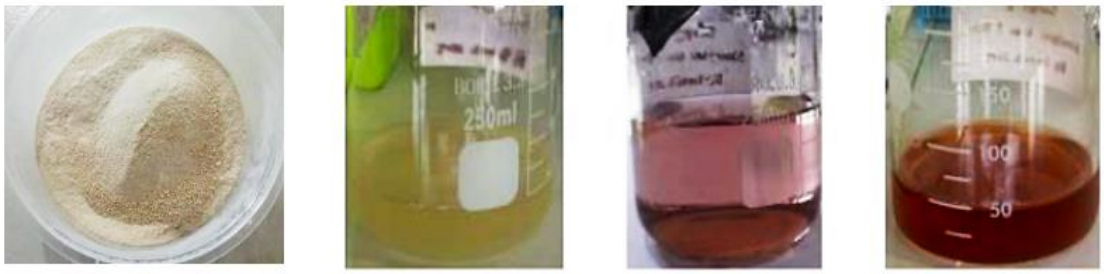

Figure 1. The results of gembili's inulin powder (a); gembili's inulin solution at 40 °C (b); silver nitrate solution (c); and gembili's inulin nanosilver at 60 °C (d)

Inulin's nanosilver effective dose

This study converted a 4 mg/kgBW dose into a 70 kg human dose. The 4mg/kgBW dose was based on Nuraini's research (2022), which found an effective dose of inulin's nanosilver as an immunostimulator. (Nathaya, 2023) carried out an acute toxicity test at this inulin's nanosilver dose to obtain the LD50 value using the Thompson-Weil method. During observation, 24 hours after administration of the sample, it did not show the achievement of 50% mortality in the test animals. The number of deaths of the test animals shows that the f factor was not obtained from the Thompson-Weil table, so the LD50 value could not be calculated. This means that it is safe to take orally at a dose of 4 mg/kgBW.

Nanosilver syrup is formulated for health supplements. Health supplements are products intended to supplement nutritional needs, maintain health, and have nutritional value and physiological effects. Supplement products also contain vitamins, minerals, amino acids, and other non-plant ingredients that can be combined with plants. The rules for using this nanosilver syrup preparation are 5 mL once a day. The minimum use of nanosilver is 10 mg/kgBW or equivalent to 78 mg after being converted to a 70 kg human. A study by (Grzegorz et al., 2013) proved that giving honeybees nanosilver syrup containing 25 mg/L nanosilver could improve bees' health. Based on the results of the preparation stability test, it was found that the best formula was F3 with a 60% simplex syrup concentration.

Stability test of Gembili's inulin nanosilver syrup

Syrup simplex is a sweetener as an additive in syrup, and a sweetener is added to give a sweet taste to the syrup. Stabilizers are meant to keep the syrup stable; examples of stabilizers are antioxidants, buffers, and complexes (Fickri, 2019). The higher the concentration of simplex syrup used, the higher the consistency of the resulting preparation. The addition of the concentration of the simplex syrup used did not affect the color of the nanosilver syrup but could affect the clarity of the color (Figure 2). The odor parameter produced from the nanosilver syrup preparation comes from the sweetener of simplex syrup, which is typical and pungent, so the increase in the concentration of simplex syrup does not affect the odor. The taste produced from the nanosilver syrup preparation comes from the sweet simplex syrup sweetener, so the increase in the concentration of simplex syrup in the nanosilver syrup formula does not affect the taste of the preparation.

Table 2. The result of physicochemical stability test of gembili's inulin nanosilver syrup during the various temperature (4°C and 40°C) for six cycle

Physicochemical test	Cycling test at 4±2°C and 40±2°C for six cicle					
	Formula 1 (20% of simplex syrup)		Formula 2 (40% of simplex syrup)		Formula 3 (60% of simplex syrup)	
	before	after	before	after	before	after
pH	4.87±0.02	4.74±0.04[a]	5.17±0.02	5.08±0.04[b]	5.25±0.03	5.17±0.05
Viscosity (cps)	66±2.1	60±1.5[c]	78±2.5	71±2.1	92±2.6	84±2.6[d]
Reduction glucose (%)	13.88±0.002	12.21±0.002	11.74±0.001	16.41±0.002[e]	13.68±0.002	20.59±0.002[f]

*mean±SD, replication three times; [a,b,c,d,e,f] significant different

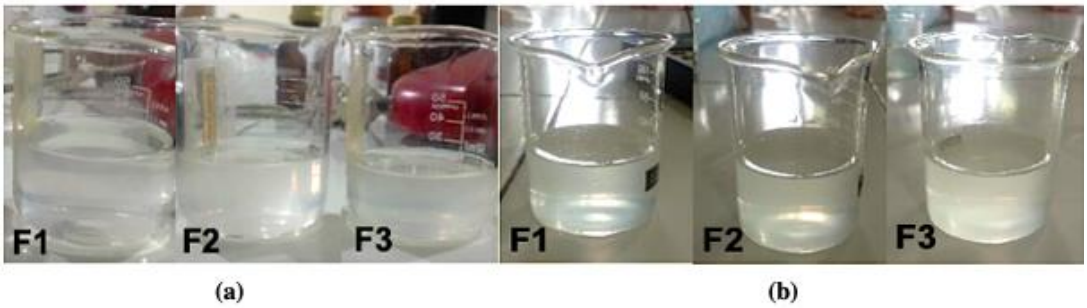

Figure 2. The result of organoleptic evaluation of gembili's inulin nanosilver syrup before (a) and after (b) cycling test. Where F1 (20% of simplex syrup), F2 (40% of simplex syrup), and F3 (60% simplex syrup)

The recommended pH value for syrup preparations is 4–8 (Kementrian Kesehatan RI, 2014). It is necessary to observe the pH because if the syrup formed is too acidic, it can irritate the stomach, while if it is too alkaline, it will cause a bitter taste. The pH of simplex syrup is around 7, so formula 3 has a higher pH than formula 1 and formula 2 (Table 2). Changes in pH in three formulas still meet the requirements. The pH value has decreased but no more than 50% during storage (Deviarny et al., 2013). After stability testing on storage, the three formulas with temperature variations of 4°C and 25°C showed the same pH value based on the recommended syrup pH range according to the Indonesian Pharmacopeia (Kementerian Kesehatan RI, 2014), which requires a pH of 4 – 8. Based on the test results, it can be concluded that an increase in the concentration of simplex syrup does not affect the pH of the nanosilver syrup preparation. Analysis of the homogeneity of variance test obtained a significance value of >0.05 (p-value = 0.763), meaning there is a variance similarity between groups. The One-way ANOVA test obtained a significance value of <0.05 (p-value = 0.000). There is a significant difference between groups in the pH stability test of the preparation.

The viscosity of preparation is also influenced by mixing or stirring factors during the formulation process. The stirring of syrup causes the droplet particles colloide to move freely so that the homogeneity of active substance increases. The joining of droplet particles will result in the contact area between droplet particles becoming weaker. The consistency that decreases in the system will result in a decrease in viscosity in the system during storage (Ozturkoglu-Budak et al., 2019). The difference in viscosity values can be affected by the amount of added solid particles (sugar) in the media. The higher the number of sugar particles, the greater the viscosity value of the syrup (Fajri et al., 2017). According to (Ozturkoglu-Budak et al., 2019), viscosity has a relationship that is directly proportional to the total amount of dissolved sugar. Syrup viscosity can occur because of the strong bonds between particles; the stronger the bonds between particles, the higher the viscosity value. The presence of hydrogen bonds between the hydroxyl groups (OH) on the sugar molecules and the water

molecules causes the high viscosity of the syrup (Grzegorz et al., 2013). These results follow the standard syrup preparation, which is determined to have a viscosity of 27 cPs - 396 cPs (Kementrian Kesehatan RI, 2014). Nanosilver syrup with a greater concentration of simplex syrup has a higher viscosity. The homogeneity of variance test analysis obtained sig > 0.05 (p-value = 0.876). Which means there is a similar variance between groups. One way ANOVA test obtained a significance value of <0.05 (p-value = 0.000). There is a significant difference between the viscosity and the formula. So, this shows that variations in the concentration of simplex syrup affect the viscosity value of nanosilver syrup preparations.

Reduction glucose of nanosilver syrup

Reducing sugar test for nanosilver syrup preparations with the Nelson-Somogyi method, using Spectrophotometer UV-VIS. The principle of the Nelson-Somogyi method is one method of testing glucose concentration with the mechanism of the Nelson reagent will oxidize glucose and then form a molybdenum complex that is blue green after adding arsenomolybdate reagent (Razak et al., 2012). The intensity of the color formed indicates the amount of reducing sugar present in the sample, and this is because the concentration of reduced arsenomolybdate is proportional to the concentration of copper (1) oxide (Cu2O), while the concentration of Cu2O is proportional to the concentration of reducing sugar (Al-kayyis & Susanti, 2016). The maximum wavelength in this research was carried out in the wavelength range of 400-800 nm. In measuring the maximum wavelength of the standard glucose solution, a maximum wavelength of 758 nm was obtained, which was then carried out to determine the standard glucose curve and to analyze the concentration of the nanosilver syrup. Research conducted by (Sari, 2019) obtained a maximum wavelength of 761 nm. This difference still meets the requirement of the tolerance limit, which is approximately 1-3 nm (Kementerian Kesehatan RI, 2014).

The standard curve results obtained by the equation y = 0.0309x - 0.097 are used to calculate the reducing sugar content in the nanosilver syrup sample where (y) is the absorbance value, and (x) is the reducing sugar content in the sample. The correlation coefficient (r2) obtained is 0.9465, which indicates a linear relationship between concentration and absorbance. A good value of r2 close to 1 indicates a linear correlation between concentration and absorbance. The percentage of reducing sugar of formula 2 and formula 3 increased after stability test, the increase in reducing sugar levels is due to the inverse process of sucrose, and the process into reducing sugar increases when the concentration of sucrose increases, besides that during heating, the process of hydrolysis of sucrose into reducing sugars (glucose and fructose) occurs (Table 2) (Shafie et al., 2022).

FT-IR Analysis

Fourier Transform Infrared (FTIR) is a tool used to detect the functional groups of a compound. The working principle of FTIR is to collect infrared light, which is spread on the surface of the sample to determine the frequency of the absorbed waves, which will then be interpreted to determine the specific group of the sample. This study evaluated the chemical interaction between inulin and $AgNO_3$ using FTIR spectroscopy at wavenumber 500−4000cm^{-1}. FTIR analysis was carried out on samples of biosynthetic solutions inulin-$AgNO_3$ (nanosilver), selected nanosilver syrup preparations, and syrup preparations without nanosilver. The interpretation of the FTIR spectrum results is then assisted by a correlation table (Table 3) showing the type of functional group from the range of wavenumbers.

There is a similarity in the absorption peaks between the nanosilver inulin solution and the nanosilver syrup. In nanosilver inulin solution, there is an absorption peak of 1616.42 cm^{-1} (C=C) which is also present in nanosilver syrup of 1628.95 cm^{-1} (C=C) (Figure 3). (Melanie et al., 2015) stated that inulin derived from dahlia tubers has identical FTIR spectra with chicory inulin and artichoke inulin, which is characterized by the appearance of an O−H stretching absorption peak at wave number 3300 cm-1, which is a characteristic of inulin. In the nanosilver syrup sample, there was an absorption peak of 425.32; 447.50 cm^{-1} (Ag-N); 535.27 cm^{-1} (pyranose ring), which was also

present in the inulin's nanosilver of 412.78; 451.326 cm^{-1} (Ag-N); 552.63 cm^{-1} (pyranose ring). Ag-N groups (silver ions) exist in nanosilver solution and nanosilver syrup because silver ions (Ag+) are the basic material used to produce nanosilver particles. These results prove that nanosilver syrup still contains nanosilver characterized by the presence of Ag-N groups. In nanosilver biosynthesis, the reducing agents, such as organic compounds or compounds from plant extracts, can interact with silver ions (Ag+) and form AgN groups. These compounds act in reducing silver ions into nanosilver particles. There are wave shifts in the nanosilver solution, and nanosilver syrup samples indicate that there has been an interaction between the functional groups and the silver nanoparticles, which may affect adding ingredients. This interaction will produce a combination of properties (new properties) that are different from the properties of the original material.

Table 3. The result of functional group of silver nitrate solution, syrup base and nanosilver syrup by FT-IR analysis

Functional group	Wave Number (cm^{-1})		
	Silver nitrate Solution	Syrup base	Gembili's Inulin Nanosilver Syrup
Ag-N	451.326; 412.78		447.50; 425.32
Pyranose ring	552.63		535.27
C-C vibration	702.12	717.55	716.59
OH- bending	-	1384.95	1385.91
C-O-C	1169.88	-	922.98; 841.00
OH-bending	-	-	1082.11; 1042.57; 994.35
NO_2	-	-	1268.25; 1205.56
C=C	1616.42	1637.64	1628.95
O=C=O stratching	2374.47; 2306.00	2356.15	2355.19; 2312.75; 2108.29
C-H stratching	2939.64; 2868.27	-	2924.21; 2886.60; 2854.77
O-H stratching	3396.79; 3249.23	3451.76	3534.71; 3421.8

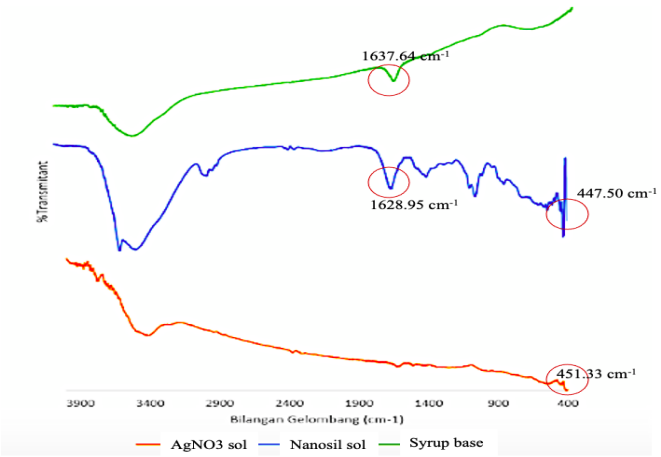

Figure 3. The FT-IR spectra of silver nitrate solution, syrup base and nanosilver syrup where x= wave number (cm^{-1}) and y= % transmitant

CONCLUSION

The results showed that the concentration of simplex syrup affected consistency, pH, and viscosity. The simplex syrup concentration of 60% met the requirement with a medium thick consistency, pH 5.25±0.03, a viscosity of 92±2.6 cps, reducing sugar content was 20.59% ±0.002, and the FTIR profile showed that it still contained nanosilver which was indicated by the presence of Ag-N groups compared to silver nitrate solution.

ACKNOWLEDGEMENT

This research was funded by RKAT PTNBH Universitas Sebelas Maret Fiscal Year 2024 through the Research Scheme RESEARCH GRANT RESEARCH A (HGR-UNS) with Research Assignment Agreement Letter Number: 194/UN27.22/PT.01.03/2024.

REFERENCES

Abou El-Nour, K. M. M., Eftaiha, A., Al-Warthan, A., & Ammar, R. A. A. (2010). Synthesis and applications of silver nanoparticles. *Arabian Journal of Chemistry*, *3*(3), 135–140. https://doi.org/10.1016/j.arabjc.2010.04.008

Ahmed, H. B., Emam, H. E., Mashaly, H. M., & Rehan, M. (2018). Nanosilver leverage on reactive dyeing of cellulose fibers: Color shading, color fastness and biocidal potentials. *Carbohydrate Polymers*, *186*, 310–320. https://doi.org/10.1016/j.carbpol.2018.01.074

Al-kayyis, H. K., & Susanti, H. (2016). Perbandingan metode somogyi-nelson dan anthrone-sulfat pada penetapan kadar gula pereduksi dalam umbi Cilembu (*Ipomea batatas* L.). *Journal of Pharmaceutical Sciences and Community*, *13*(02), 81–89. https://doi.org/10.24071/jpsc.2016.130206

Azhar, M. (2009). Inulin sebagai prebiotik. *Sainstek*, *12*(1), 1–8.

Deviarny, C., Lucida, H., & Safni, S. (2013). Uji stabilitas kimia natrium askorbil fosfat dalam mikroemulsi dan analisisnya dengan HPLC. *Jurnal Farmasi Andalas*, *1*(1).

Ermawati, D E, Yuniastuti, A., & Fadjrin, H. I. (2021). Effectiveness of Nanosilver Biosynthesis using Inulin Gembili Tuber (Dioscorea esculenta L.) on Variation of Inulin Solution Towards Particle Sizes and Antibacterial Activities. *Journal of Physics: Conference Series*, *1912*(1), 012042. https://doi.org/10.1088/1742-6596/1912/1/012042

Ermawati, Dian Eka. (2017). Optimization emulgator composition of water in oil emulsion of strawberry fruits (Fragaria vesca L.) based on simplex lattice design method. *JPSCR : Journal of Pharmaceutical Science and Clinical Research*, *2*(02), 78–89. https://doi.org/10.20961/jpscr.v2i02.14398

Fajri, A., Herawati, N., & Yusmarini, Y. (2017). Penambahan karagenan pada pembuatan sirup dari bonggol Nanas. *Jurnal Online Mahasisawa (JOM)*, *4*(2), 1–12.

Fera, M., & Masrikhiyah, R. (2019). Ekstraksi inulin dari Umbi Gembili (Discorea esculenta L) dengan pelarut etanol. *Jurnal Pangan Dan Gizi*, *9*(2), 156–161. https://doi.org/10.26714/jpg.9.2.2019.110-116

Fickri, D. Z. (2019). Formulasi dan uji stabilitas sediaan sirup anti alergi dengan bahan aktif Chlorpheniramin maleat (CTM). *Journal of Pharmaceutical Care Anwar Medika*, *1*(1). https://doi.org/10.36932/j-pham.v1i1.4

Grzegorz, B., Paleolog, J., Olszewski, K., & Strachecka, A. (2013). Laboratory assessment of the effect of nanosilver on longevity, sugar syrup ingestion, and infection of honeybees with Nosema spp. *Medycyna Weterynaryjna*, *69*(12), 730.

Harso, A. (2017). Nanopartikel dan dampaknya bagi kesehatan manusia. *OPTIKA: Jurnal Pendidikan Fisika*, *1*(1), 20–26.

Kementerian Kesehatan RI. (2014). *Farmakope Indonesia Edisi V, Direktorat Jendral Bina Kefarmasian dan Alat Kesehatan*.

Kumar, V., & Yadav, S. K. (2009). Plant-mediated synthesis of silver and gold nanoparticles and their

applications. *Journal of Chemical Technology & Biotechnology*, *84*(2), 151–157. https://doi.org/10.1002/jctb.2023

Lembang, E. Y. (2013). *Sintesis nanopartikel perak dengan metode reduksi menggunakan Bioreduktor ekstrak daun ketapang (Terminalia catappa). (Desertasi).* Universitas Hasanuddin.

Lengke, M. F., Fleet, M. E., & Southam, G. (2007). Biosynthesis of silver nanoparticles by filamentous Cyanobacteria from a silver(I) nitrate complex. *Langmuir*, *23*(5), 2694–2699. https://doi.org/10.1021/la0613124

Melanie, H., Susilowati, A., Iskandar, Y. M., Lotulung, P. D., & Andayani, D. G. S. (2015). Characterization of Inulin from Local Red Dahlia (Dahlia sp. L) Tubers by Infrared Spectroscopy. *Procedia Chemistry*, *16*, 78–84. https://doi.org/10.1016/j.proche.2015.12.027

Murano, E. (1998). Use of natural polysaccharides in the microencapsulation techniques. *Journal of Applied Ichthyology*, *14*(3–4), 245–249. https://doi.org/10.1111/j.1439-0426.1998.tb00650.x

Nagpal, K., Singh, S. K., & Mishra, D. N. (2010). Chitosan nanoparticles: a promising system in novel drug delivery. *Chemical and Pharmaceutical Bulletin*, *58*(11), 1423–1430. https://doi.org/10.1248/cpb.58.1423

Nathaya, J. N. S. (2023). *Acute toxicity test of nanosilver using Gembili's Inulin (Dioscorea esculenta L.) as Bioreductor, observation of toxic symptoms and semiquantitative histological profile of kidney organs. (Thesis).* Universitas Sebelas Maret : Surakarta.Unpublised.

Nurani, P. I. (2022). *Efektivitas dosis imunomodulator nanosilver hasil biosintesis inulin terhadap kadar imunoglobulin G Mencit yang diinduksi vaksin dengan pembanding imunostimulan herbal.(Tugas Akhir).* Universitas Sebelas Maret: Surakarta. Unpublised.

Ozturkoglu-Budak, S., Akal, H. C., Buran, İ., & Yetişemiyen, A. (2019). Effect of inulin polymerization degree on various properties of synbiotic fermented milk including Lactobacillus acidophilus La-5 and Bifidobacterium animalis Bb-12. *Journal of Dairy Science*, *102*(8), 6901–6913. https://doi.org/10.3168/jds.2019-16479

Pulit-Prociak, J., Stokłosa, K., & Banach, M. (2015). Nanosilver products and toxicity. *Environmental Chemistry Letters*, *13*(1), 59–68. https://doi.org/10.1007/s10311-014-0490-2

Razak, A. R., Sumarni, N. K., & Rahmat, B. (2012). Optimalisasi hidrolisis sukrosa menggunakan resin penukar kation tipe sulfonat. *Jurnal Natural Science*, *1*(1), 119–131.

Reiger, M. M. (2000). *Moisturizers and humectants. Rieger MM. Harry's Cosmeticology. 8th ed.* Chemical Publishing Co.

Sanjiwania, N. M. S., & Sudiarsa, I. W. (2021). Analisis gugus fungsi obat sirup batuk dengan fourier transform infrared. *Jurnal Emasains: Jurnal Edukasi Matematika Dan Sains*, *10*(2), 339–345. https://doi.org/10.5281/zenodo.5643634

Sari, N. (2019). The use of glucose syrup as product of selulosa hidrolyze from the Jackfruit Rags (Artocarpus heterophylus Lamk) as Sweetner on Candies production from the Coconut Plam (Cocos Nucifera L). *Journal of Pharmaceutical And Sciences*, *2*(1), 17–23. https://doi.org/10.36490/journal-jps.com.v2i1.12

Setianingsih, D. (2020). *Uji toksisitas akut dan pengamatan gejala ketoksikan akut nanosilver dengan Bioreduktor inulin umbi Gembili (Discorea esculenta L.). (Skripsi).* Universitas Sebelas Maret: Surakarta. Unpublished.

Shafie, M. H., Kamal, M. L., Zulkiflee, F. F., Hasan, S., Uyup, N. H., Abdullah, S., Mohamed Hussin, N. A., Tan, Y. C., & Zafarina, Z. (2022). Application of Carrageenan extract from red seaweed (Rhodophyta) in cosmetic products: A review. *Journal of the Indian Chemical Society*, *99*(9), 100613. https://doi.org/10.1016/j.jics.2022.100613

Sugarda, W. O., Dewi, K. D. C., Putra, K. W. A., Yogiswara, M. B., Sukawati, C. B. A. C., Sutresna, P. A. R., Dewi, N. L. G. J., Arisanti, C. I. S., & Yustiantara, P. S. (2019). Formulasi sediaan sirup peningkat imunitas dari Herba Meniran (*Phyllanthus niruri* L.). *Jurnal Kimia*, *13*(2), 125–233. https://doi.org/10.24843/JCHEM.2019.v13.i02.p03

Tiwari, D. K., Jin, T., & Behari, J. (2011). Dose-dependent in-vivo toxicity assessment of silver nanoparticle in Wistar rats. *Toxicology Mechanisms and Methods*, *21*(1), 13–24.

https://doi.org/10.3109/15376516.2010.529184

Pharmaciana
Vol.14, No.2, July 2024, Page. 195-208
ISSN: 2088 4559; e-ISSN: 2477 0256
DOI: 10.12928/pharmaciana.v14i2.27851

In-vivo study of oleic acid and tween-80 on patch transdermal *A.paniculata* as anti-diabetic

Nur Aini Fadilah, Iis Wahyuningsih*, Wahyu Widyaningsih
Faculty of Pharmacy, Universitas Ahmad Dahlan,
Jl. Prof. Dr. Soepomo, SH, Warungboto, Umbulharjo, Yogyakarta, Indonesia

Submitted: 10-12-2023 ***Reviewed: 31-03-2024*** ***Accepted:15-07-2024***

ABSTRACT

Sambiloto (*A.paniculata*) is known empirically as a plant that could effectively treat diabetes mellitus. The substance of andrographolide in *A.paniculata* is able to increase insulin secretion, therefore, inhibiting alpha-glucosidase and alpha-amylase. The substances themselves have the ability to reduce blood glucose levels. Poor bioavailability due to pharmacokinetic interactions in the form of metabolism by the enzyme p-glycoprotein and CYP3A4 as well as poor physicochemical properties of water reduces bioavailability in oral administration which results in a decrease in pharmacological activity. The transdermal patch dosage form is chosen since it is considered capable of increasing the effectiveness of andrographolide in ethanol extract of sambiloto (EES). However, the challenge in transdermal preparations is the stratum corneum, which is the main barrier in transdermal drug delivery. Enhancers become a critical point in transdermal delivery. Oleic acid and tween-80 are enhancers that are widely used in transdermal patch preparations. The aim of this study was to determine the comparison of concentrations of oleic acid and tween-80 on the characteristics of transdermal patches. The transdermal patches were made using the solvent casting method with various concentration ratios of oleic acid enhancer and tween F1 (1:1), F2 (1:3), and F3 (1:2). Then, all of the formulas were tested for patch characteristics while also being tested via *in-vivo* antidiabetic activity using diabetic male rat. All of the formulas meet the requirements of patch characteristics. Differences in the concentration of enhancer combinations affect patch characteristics in terms of patch weight and thickness, where F2 has a greater thickness and weight than other formulas. F2 is a formula that has a greater activity than F1 and F3. F2 blood glucose level value on the fifteenth day was 105 ±2.42 mg/dL. Although subcutaneous administration of insulin is quicker in diminishing blood glucose levels, the EES F2 transdermal fix can be compelling in decreasing blood glucose levels.

Keywords: *A.paniculata*, oleic acid, tween-80, patch transdermal, anti-diabetic

Corresponding author:
Iis Wahyuningsih
Fakultas Farmasi Universitas Ahmad Dahlan
Jl. Prof. Dr. Soepomo, S.H, Warungboto, Umbulharjo, Yigyakarta, Indonesia
Email: iis.wahyuningsih@pharm.uad.ac.id

INTRODUCTION

Sambiloto (*Andrographis paniculata*) has been known empirically as a plant that has benefits as a traditional antidiabetic Javanese medicine known as jamu pahitan which is used to treat diabetes mellitus (DM). The main compound contained in sambiloto is andrographolide which induced a hypoglycemia effect through the mechanism of increasing insulin secretion and inhibiting alpha-glucosidase and alpha-amylase. Besides that, andrographolide contained in sambiloto has the ability to increase glucose utilization in streptozotocin-induced rat muscle through the stimulation of GLUT-4 transporters (Sari et al., 2015). According to Hidayat & Wulandari (2021), oral administration of extract ethanolic of *A. paniculata* at the dose of 200 mg/Kg BW can reduce levels SOD catalase, GSH activity in rats and reduces levels of malondialdehyde significantly in the kidney of STZ-diabetics.

Andrographolide is a diterpene lactone group compound that has a low solubility in water and poor bioavailability due to biotransformation by P-glycoprotein in the intestinal tract which causes andrographolide to metabolize more quickly in the duodenum and jejunum (Keerthana et al., 2022). In addition, andrographolide compounds are inhibitors of CYP3A4 and CYPC29 enzymes which cause pharmacokinetic interactions if given together with synthetic drugs such as glipizide, thereby reducing the bioavailability of glipizide (Sundhani et al., 2022). To overcome this, ethanol extract of sambiloto (EES) was defined within the shape of transdermal patches.

Transdermal patch is a systemic drug delivery through penetration of the stratum corneum found in the skin layers of the epidermis to the dermis (Nurahmanto, 2016). The advantages of transdermal preparations as a non-invasive therapeutic agent are significant in preventing first-pass effects (Jafri et al., 2019), chemical degradation in the gastrointestinal environment, and easy access because the skin provides a large surface area and ease of dose setting (Prasetyo et al., 2018).

The challenge in making transdermal arrangements itself is the stratum corneum which may be a boundary to drugs that are administered transdermal (Zaki et al., 2022). The formulation in transdermal preparations such as the selection of polymers, plasticizers, and enhancers can affect the characteristics of transdermal patch preparations which affect the pharmacological activity of transdermal patch preparations. The critical point of transdermal patch preparation is the selection of enhancers which is one of the compounds that increase the penetration of active substances in the skin by disrupting the permeability of the stratum corneum, through intercellular protein bond interactions (Haq et al., 2020).

Oleic acid is a fatty acid enhancer that has a mechanism of action as an enhancer through interaction by reducing the permeability of the stratum corneum. Oleic acid is an enhancer that is widely used in transdermal drug delivery (El-Say et al., 2021). The use of oleic acid in promethazine transdermal patch preparations has the ability to increase promethazine permeation better than propylene glycol and isopropyl alcohol (Nurahmanto, 2016). The use of unsaturated fatty acids such as oleic acid as an enhancer can potentially irritate the skin. Based on clinical research conducted in humans, it was found that the combination of oleic acid at a concentration of 5% and propylene glycol as an enhancer can irritate the skin. This is because oleic acid can increase the production of inflammatory cells such as interleukin-1 alpha and the production of cytokines which are mediators of inflammation that cause inflammation (Moore et al., 2020).

Tween 80 is an enhancer from the non-ionic surfactant group that works by increasing the permeation of active substances through interaction and binding to keratin filaments that interfere with corneocyte permeability (Budhathoki et al., 2016). The use of 1% tween-80 as an enhancer in diazepam transdermal preparations can increase the level of diazepam permeation in the skin. Tween-80 is a non-ionic enhancer that is inert and does not irritate the skin (Pandey, 2014). The use of a combination of oleic acid and tween-80 as an enhancer within the preparation of transdermal patches of EES is expected to increase the permeation of sambiloto extract (*A. paniculata*) so as to increase the viability of sambiloto extract as antihyperglycemic in transdermal delivery. The use of tween-80 as a co-enhancer in an EES transdermal patch is expected to increase the permeation effectiveness of andrographolide contained in the EES compared to the use of single oleic acid (Saitoh et al., 2023).

Physically good patch character must be flexible, thin, smooth, homogeneous, and have a low moisture content. Based on Saitoh et al. (2023) research on the combination of tween 80 and oleic acid in disulfiram patch transdermal demonstrates the increased permeation of disulfiram transdermal patch compared with the use of a single oleic acid. The combination of tween-80 and oleic acid is expected to obtain optimal patch characteristics. The aim of this research is to determine the effect of variations in the combination of tween 80 and oleic acid as an enhancer on the physical characteristics of EES patches (weight, thickness, moisture content, pH, and folding endurance) and the effectiveness as an antidiabetic transdermal patch in diabetic rats.

MATERIALS AND METHOD

Materials

Herba sambiloto simplicia from Merapi Farma, Yogyakarta (determined in Biology Laboratory Universitas Ahmad Dahlan, No. 447/lab.Biologi/B/XI/2023), Glassware (Iwaki), patch mold (Iwaki), aluminum foil, andrographolide (Sigma), desiccator (Pyrex), glucometer (easy touch glucometer), vernier scale, analytical digital balance (Ohaus Adventurer), oven (Memmert), pH meter (Ohaus), soxhlet extractor (Iwaki-pyrex), hotplate stirrer (IKA-CMAG7), rotary evaporator set (Heidolph), waterbath (Memmert), hair razor, silica gel F_{254} plate, ethanol 70% (Brataco), ethanol 96% (Brataco), HPMC (Sarda, Taiwan), oleic acid (AppliChem), tween-80 (Amresco), PEG 400 (Japan Bio Science Laboratory), PVP K-30 (JHNH Life Sciences), aquadest (Otsuka), and streptozotocin (Bioworld), methanol (merck), chloroform (merck), disposable syringe 1 mL (Onemed), buffer citrate solution pH 4.5 (Merck), sodium benzoic (Gloria InterChem).

Methods

Extraction of sambiloto

The extraction of sambiloto was carried out using ethanol 96% solvent with the soxhletation method. A total of 100 grams of powdered sambiloto was wrapped using filter paper and then put into the lead. The extraction process was carried out for 3-4 hours at a temperature of 40-50°C. The extract obtained is evaporated and thickened (Garg et al., 2016).

Phytochemical screening of andrographolide

Phytochemical screening of andrographolide compounds is tested with Thin Layer Chromatography (Rais, 2014). The first step is preparing the test solution of sambiloto extract in the amount of 10 mg/mL. The mobile phase used was chloroform: methanol P (9:1) with the stationary phase silica gel 60 F_{254} using a 20 µL sample and 2 µL as comparison solution (andrographolide solution). The observation was carried out at light UV_{254}.

Formulation of a base patch of EES

The transdermal patch base formulation can be seen in Table 1 of the formula based on the research of (Saitoh et al., 2023) where in this formula there are modifications. The evaluation of the patch characteristics includes patch weight uniformity, patch thickness, patch pH, patch durability value, and moisture content. The method of making patch bases uses the solvent casting method. For the formulation of the patch, preparation is listed in Table 1.

Polyvinyl Pyrrolidone K-30 (PVP-K30) was dissolved in 70% ethanol, then HPMC was dissolved in 70% ethanol. After that, the PVP-K30 and HPMC solutions were mixed and stirred using a hotplate stirrer. A total of 200 mg of herbal sambiloto extract was dissolved with ethanol 70% in 1 mL. PEG 400 was added to the polymer solution and then stirred as mixture 1. Enhancer in the form of tween-80 and oleic acid was mixed and then added to the extract as mixture 2. Mixture 2 is then added to mixture 1, then stirred for 20 minutes until homogeneous, then poured into a patch mold and allowed to stand for 15 minutes at room temperature. The patch was then placed in an oven at 40-45°C for 24-72 hours until

a film layer was formed, the film layer of the patch was then removed from the mold wrapped in aluminum foil, and stored in a desiccator.

Table 1. Formulation of patch transdermal EES with variations of oleic acid and tween 80

Name of Ingredient	Function	Oleic acid: tween 80		
		F1(1:1)	F2(1:3)	F3(1:2)
EES (mg)	Active ingredient	200	200	200
Oleic acid (gram)	Enhancer	0.15	0.15	0.075
Tween 80 (gram)	Enhancer	0.15	0.45	0.15
HPMC (gram)	Polymer	0.25	0.25	0.25
PVP-K30 (gram)	Polymer	0.5	0.5	0.5
PEG 400 (gram)	Plasticizer	0.075	0.075	0.075
Sodium Benzoic (mg)	Preservative agent	15	15	15
Ethanol 70% (mL)	Solvent	Add 15	Add 15	Add 15

Evaluation of transdermal patch EES

Visual appearance

The patches were evaluated visually for color, odor, and texture of the patches.

The thickness of the matrix patches

The thickness of the transdermal patches was measured using vernier calipers at five different places, and the mean value along with Standard Deviation (SD) was calculated (Shivalingam et al., 2021).

Weight uniformity

The weights of five patches were taken and the weight variation was calculated as mean and standard deviation (Shivalingam et al., 2021).

Surface pH

The evaluation of pH patches is tested with a pH meter. The test is carried out using 10 mL of CO_2 free water added to a beaker glass that contains the patch and then allowed to stand for 1 hour. The criteria for the pH range is 4.5-6.5 (Pratiwi et al., 2021).

Determination of folding endurance

The folding endurance test points to decide the folding capacity of the patch. The folding endurance test is carried out by more than once folding the patch at the same point until it breaks (Hartesi et al., 2021).

Percentage of moisture content

The prepared patches were marked, then weighed one by one, and stored in a desiccator containing active silica at room temperature for 24 hours. The patch was weighed more than once until a consistent weight was obtained. The percentage of water content is determined as the difference between the initial and final weight to the final weight (Francis, 2016).

In vivo evaluation of transdermal patches

Animals

The animals used for antihyperglycemic studies were male albino rats (weighing 100-250 g) provided by the animal house, Faculty of Medicine and Health Sciences University of Muhammadiyah

Yogyakarta. The animals were kept and maintained under standard laboratory conditions of temperature and humidity within 12 h day; and 12 h night cycle, and also allowed water consumption *ad libitium* (Hadebe et al., 2014). All the protocols followed for animal studies were reviewed and approved by the Research Ethics Committee of Ahmad Dahlan University, Yogyakarta (Ethical Approval number: 012311289).

Induction of diabetes

Diabetes was induced by streptozotocin-(STZ) (35 mg/kg BW, i.p) (Mostafavinia et al., 2016) in citrate buffer 0.1 M (pH 4.5) (Mostafavinia et al., 2016). The diabetic state was confirmed 72h after STZ injection by hyperglycaemia. Surviving rats with fasting blood glucose levels higher than 200 mg/ dL (Premanath & Nanjaiah, 2015).

Hypoglycaemic study of EES patch transdermal

Rats were shaved on the abdominal region 1-2 days prior to the application of EES patch transdermal (Hendriati et al., 2021). Rats were divided into six groups (n=5). The first group was given the EES Formula 1 (F1) transdermal patch, the second group was given the EES patch transdermal Formula 2 (F2), the third group was given the EES patch transdermal Formula 3 (F3) the patch was given twice a day, the negative group was given blank patches, the positive group was given injected SC insulin short acting novorapid (0.2 mL/200 g), and healthy group was not induced by STZ (Ahmed et al., 2014). Blood glucose levels (BGL) were measured after 24 hours by taking blood through a vein in the rat's tail.

Data Analysis

Data are communicated as mean ± SD and statically analyzed by one-way ANOVA taken after by Tukey's comparisons test with a 95% certainty level for the values of the characteristic fix.

RESULT AND DISCUSSION

Extraction of ethanolic sambiloto

Preparation of the extract by soxhlation with 96% ethanol solvent for four hours at 50^0C. Soxhlet extraction is a method of extraction that is able to extract more of the target compound than any other extraction method. The selection of solvents and temperatures used in the process of the extraction method is key in the secretion of the desired target compounds such as andrographolide (Liang et al., 2023). The solvent used in the herbal extraction method is ethanol with an ethanol concentration of 96% according to Yuan et al. (2017). Ethanol is a solvent that has a lower level of toxicity compared to other organic solvents. The 96% ethanol solvent was chosen based on its ability to draw a certain number of active compounds from the plant while minimizing as little as possible of the unwanted elements. The selection of extraction methods using the Soxhlet method is able to produce extract yields while noting more. The yield of the extract obtained is 220.71 grams with a yield percentage of 16.22% according to DepKes RI (2017). The yield of the extract is not less than 9.6% so the percentage of yield obtained in the extraction meets the requirements. A yield percentage value of more than 10% is a very good value so that the extract of sambiloto obtained is eligible to be continued at the patch formulation stage.

Phytochemical screening of andrographolide

The phytochemical screening of andrographolide on the EES was performed qualitatively using the thin-layer chromatography (TLC) method according to Rais (2014). The purpose of the test is to ensure that the extract contains andrographolide qualitatively. The test solution is prepared by dissolving the extract in a solution of ethanol pro-analyte at a concentration of 10 mg/mL, which is then compared with a 0.1 mg/mL andrographolide (sigma Aldrich) as a comparator. The mobile phase used is chloroform: methanol P (9:1) with the still phase of silica gel 60 F254 and observations are made in UV254. The results of TLC observations can be seen in Figure 1. The Rf values obtained from the test

and comparator solutions are respectively 0.2 and 0.2. The Rf value and the comparator test solution have the same value; this indicates that the test solution is an ethanol extract while still containing andrographolide qualitatively (Ramadhani et al., 2021).

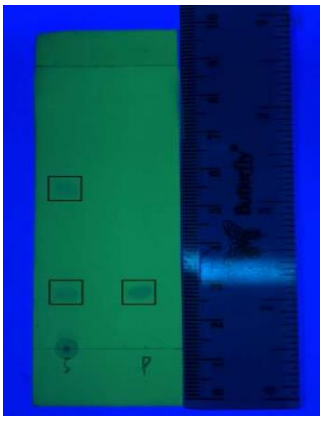

Figure 1. Result of chromatography thin layer of EES, S: sample, P: andrographolide standard solution (mobile phase used is chloroform: methanol P (9:1) in the silica gel 60 F_{254})

The Formulation and Fabrication of EES transdermal patch

The formulation of the EES transdermal patch is carried out by solvent casting technique. HPMC and PVP-K30 are selected as the polymers in the patch manufacturing of EES, which can produce patches with uniform thickness and are able to increase the permeation of the active substance (Kumar et al., 2018). According to Kemala (2016), the use of HPMC as a hydrophilic polymer can provide a clear patch layer while in addition, the use of HPMC either alone or in combination with ethyl cellulose as a polymer can provide good penetration in transdermal patch preparations. The use of a combination of HPMC and PVP-K30 patch characteristics is optimal both in terms of appearance, weight uniformity, percentage of moisture content, and folding endurance, and is able to increase the percentage of the release of pioglitazone hydrochloride (Francis, 2016).

Mixture 1 is a subsequent polymer blend, then added with a PEG 400 plasticizer. The use of PEG 400 as a plasticizer is able to increase the elasticity and folding resistance (Hartesi, et al, 2021). The use PEG 400 in transdermal patches of EES is expected to produce a smooth and elastic patch characteristic. The use of PEG 400 as a plasticizer resulted in the appearance of the EES patches transdermal having a smooth texture. According to Kemala (2016), not only does the PEG 400 increase the flexibility of the glibenclamid patch but also makes a soft patch in the transdermal texture.

Furthermore, an enhancer solution in the form of oleic acid and tween-80 is mixed in a solution of EES while being in the still phase. The use of oleic acid enhancers as promethazine transdermal patches can increase promethazine permeation to a greater extent than propylene glycol and isopropyl alcohol (Nurahmanto, 2016). Tween 80 is an enhancer classified as a class of nonionic surfactants that works by increasing the permeation of the active substance through interaction and binding through keratin filaments that disrupt the permeability of corneocytes. The use of tween-80 1% as an enhancer in diazepam transdermal preparations is able to increase the permeability of diazepam to the skin. Tween-80 is one of the nonionic enhancers that is innate and does not irritate the skin (Pandey, 2014). The herbal ethanol extract solution is then mixed with the enhancer mixture solution. The patch is then placed in an oven at 40-45^{o}C for 24-72 hours until a film is formed and kept in desiccator with aluminum foil.

Evaluation of patch transdermal EES

The visual of both the aroma and texture of the patch EES is evaluated. The visual display of the test results of the patch transdermal EES displays a dark-green-color-like with the distinctive bitter aroma

of the EES. The results of the visual display patch test are shown in Figure 2. Evaluation of the transdermal patch preparation includes testing for weight consistency, thickness uniformity, pH, folding endurance, and percentage moisture content are shown in Table 2.

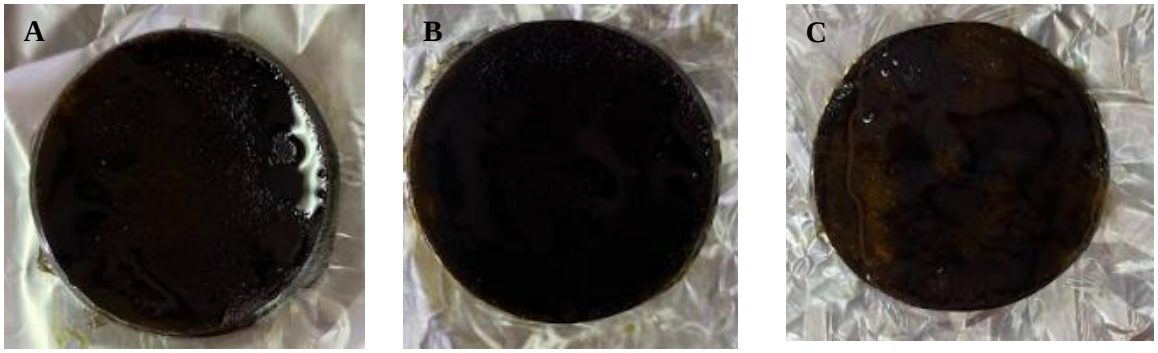

Figure 2. Visual appearance of patch transdermal EES with variations formulas of oleic acid: tween 80 (A) F1 (1:1), (B) F2 (1:3), (C)F3 (1:2)

Table 2. Result of evaluation patch transdermal of EES with variations formulas

Formula (Oleic acid: tween 80)	Thickness (mm)	Weight Uniformity (gram)	Surface pH	Folding Endurance	Moisture Content (%)
F1 (1:1)	0.34 ± 0.01	1.68 ± 0.03	5.32 ± 0.01	315 ± 1.58	2.50 ± 0.75
F2 (1:3)	0.36 ± 0.02	1.85 ± 0.04	5.32 ± 0.01	300 ± 2.70	2.52 ± 0.71
F3 (1:2)	0.32 ± 0.01	1.73 ± 0.02	5.33 ± 0.01	323 ± 1.92	2.86 ± 1. 07

Weight uniformity testing aims to affirm the weight of the patch produced by each uniform formula. Uniformity of the weights may affect the uniformity of the content of the patch. The results of the weight uniformity testing showed the average weight of the three patch formulations ranged from 1.68 to 1.85 grams. The largest average value of patch weights is derived from F2, where the average patch weight on F2 is 1.85 ± 0.04 grams. According to Kemala (2016), the difference in patch weight values in each formula is due to imperfect evaporation of the solvent and uneven dilution of the patch-based liquid in the mold. According to Shivalingam et al. (2021), the value of One-way ANOVA analysis obtained a significance value of 0.000 < 0.05 which shows a significant difference in the patch weight. This is due to the use of a large concentration of tween-80 in the F2 formula, where tween-80 is one of the non-volatile solvents of the surfactant group. In addition, tween-80 has a high viscosity in a larger patch weight (Baranauskaite et al., 2021). The comfort of using a transdermal patch is determined by the weight of the patch matrix. The lighter the patch matrix produced, the more comfortable the patch is to use. Therefore, it will not interfere with activities and provide an aesthetically beautiful patch appearance (Setyawan, 2015).

The thickness of the patches was found to be in the range of 0.32 ± 0.01 to 0.36 ± 0.02. The thickness of the patches depends on the concentration of the enhancer. The higher the concentration of the enhancer, the thicker and heavier the patch will be. Similarly, with the weight of transdermal patches. The variations in thickness may be due to different concentrations of enhancer formulations. According to Soral et al., (2021), the use PVP-K30 in large concentrations can increase the rebeprazol transdermal patch. The other reasons may be due to the need of temperature control which has influenced the controlled dissipation of solvent from the damp film surface. There's a relationship between the weight of the patch and drug substance (Francis, 2016). A suitable thickness of patch size is in the range of 0.5-1.00 mm. From the analysis by one-way ANOVA, a significance value of 0.003 < 0.05 which shows a

significant difference in the patch thickness. This is due to the fact that the heavier the patch weight, the thicker the patch is. The use of tween-80 as an enhancer and PEG 400 as a plasticizer increases the thickness of the patch preparation. The greater the concentration of tween-80 used, the thicker the patch is. EES patch thickness uniformity values of formula F1, F2, and F3 belong to the category of good patch size (Francis, 2016). The comfort of using a transdermal patch is influenced by the physical characteristics of the patch matrix, one of which is the thickness of the patch matrix. The thinner the patch matrix produced, the more comfortable the patch is to use, as it will not interfere with activities and provide an aesthetically beautiful patch appearance (Setyawan et al., 2015).

The surface pH of all the formulations was found to be in the range of 5.32 ± 0.01 to 5.33 ± 0.01, which coincides with a pH range of skin and hence can be concluded that no skin irritation should be occurring (Ravindra et al, 2022). Based on a one-way ANOVA value of sig 0.163 > 0.05, there is no difference between the value of the pH influence enhancer. The results show that the EES patch has a relatively acidic pH, where the acidic pH of the patch can effectively prevent and reduce bacterial growth (Pratiwi et al., 2021).

The folding endurance of transdermal patches was measured manually. The folding endurance of the patches was found to be in the range intended. The patches would not break and would retain their integrity with general skin folding when applied to the skin. The good patches transdermal is more 100-300 times fold resistance (Solanke et al., 2018). PEG 400 is a plasticizer that is widely used in transdermal patch preparations. PEG 400 and PVP-K30 can increase the flexibility and elasticity of the atorvastatin transdermal patch preparation, thereby preventing cracking of the transdermal patch preparation (Castañeda et al., 2017) The folding endurance values of the three formulas meet the requirements, although in F2 the value is smaller than F1 and F3, this is due to the different percentage value of enhancer content between EES transdermal patch formulas, as well as the process of making transdermal patches that should consider humidity conditions and temperature stability during the process of drying (Budhathoki et al., 2016).

The percentage of the moisture content of patches transdermal is around 2.50 ± 0.75 to 2.86 ± 1.07. The low percentage of moisture content in formulations could help them to remain stable and prevent them from being completely dried. The percentage of moisture content of the patches plays a role in maintaining the physical stability of the patch matrix because a small percentage of moisture content of patches will make the physical patch remain flexible and not brittle, resulting in the patch still being comfortable when used (Setyawan et al., 2015). In formula F3, the average %MC value is greater than in formulas F2 and F1, this is due to the drying process not being optimal so that the water content in the EES transdermal patch does not evaporate optimally, causing the water content in the patch to be greater (Ermawati & Prilantari, 2019). Several factors that can increase the %MC value in transdermal patch preparations are the use of hygroscopic transdermal patch ingredients such as the hydrophilic polymer PVP-K30 (Tripathi, 2022). Based on data from testing using one-way ANOVA, the %MC statistical test results show a sig value of 0.759 > 0.05, which means there is no significant difference in %MC between the three EES transdermal patch formulations.

The effectiveness of the patch is not only determined by the physicochemical properties of the active ingredients but is also determined by the composition of the excipients that form it. One of the excipients commonly used in transdermal patch formulations is permeation enhancer. The results of this research show that the characteristics of EES transdermal patches were affected by the ratio of tween-80 and oleic acid as the enhancers. The use of enhancers with non-volatile ingredients can increase the weight and thickness of the transdermal patch. This affects the weight and thickness of the patches produced (Francis, 2016). According to Jafri et al., (2019), The use of single oleic acid as an enhancer with a concentration of 0.5-2% does not affect the weight of the lamotrigine transdermal patch. The combination of oleic acid enhancer and tween-80 in various ratios affects the characteristics of the EES transdermal patch on the weight and thickness of the EES transdermal patch. This was caused by being influenced by the increase in tween-80 concentration in F2.

In vivo study of patch transdermal EES

The application of the EES transdermal patch to the rat was carried out by attaching the EES transdermal patch to the rat's abdomen (Hendriati et al., 2021). Rats that had been induced with STZ were then tested for blood glucose levels (BGL). After day 3 of post-induction, the rats that had been induced with STZ were then tested for BGL. The rats within the BGL range of ≥200 mg/dL were used in this study (Premanath & Nanjaiah, 2015). The experiment was carried out for 15 days. Blood samples were taken via the tail vein of the rats. Testing was carried out for 15 days, then observations were carried out on days 3, 5, 7, 9, 11, 13, and 15 (Perada & Murthy, 2022). The effect of EES patch transdermal in diabetic rats is shown in Figure 3. In the EES transdermal patch hypoglycemic activity test on the third day after STZ induction, the average BGL of the mice ranged from 230-245 mg/dL, according to the American Diabetes Association, (2024), if the BGL is ≥ 200 mg/dL then it has been declared to be in the diabetes phase.

The EES transdermal patch was administered twice a day after 24 hours of testing for BGL of 2-13 mg/dL (Hadebe et al., 2014), where positive control in the form of short-acting insulin novorapid provided a greater reduction in blood glucose levels from 225 mg/dL ± 3.94 to 202 mg/dL ± 1.85 followed, F1 245 mg/dL ± 1.72 to 240 mg/dL ± 1.72, F3 245 mg/dL ± 3.01 to 240 mg/dL ± 3.12 and F2 230 mg/dL ± 2.65. Measurement of BGL on the fifth day showed a decrease in BGL ranging from 2-13 mg/dL. The positive control group showed a greater reduction in BGL from 225 mg/dL ± 3.94 to 202 mg/dL ± 1.85 followed, by F1 245 mg/dL ± 1.72 to 240 mg/dL ± 1.72, F3 245 mg/dL ± 3.01 to 240 mg/dL ± 3.12 and F2 230 mg/dL ± 2.65. Insulin aspart is a short-acting insulin with a working mechanism of inhibiting glucose, fat, and peripheral glucose absorption, especially in muscle and fat with an onset of 3-5 hours (Haahr & Heise, 2020).

On the seventh day of observation, treatment groups F2 and F3 experienced a greater reduction in BGL than the other treatment groups by 10 and 15 mg/dL. The decrease in BGL from the F2 and F3 formula groups shows that EES is effective in the form of a transdermal patch dosage form. Andrographolide from EES was known for its action in bringing down BGL through a few mechanisms such as increased GLUT-4 protein in soleus muscle for glucose take-up, moved forward pancreatic islet, expanded beta-cell density, and expanded pancreatic insulin substance (Sari et al., 2015). An oral concentration of andrographis paniculata extract of 200 mg was able to reduce BGL in rats induced by STZ (Hidayat & Wulandari, 2021), this dose is used in all three transdermal patch formulas. Even though the three formulas have the same dosage, the difference in enhancer concentration affects the activity of reducing rat's BGL. Enhancers influence the effectiveness of the EES transdermal patch as an anti-diabetic.

Enhancers influence the effectiveness of the EES transdermal patch on the pharmacological effects of active substances made in transdermal preparations (Kumar et al., 2015). Observations on the eleventh day in the F2 group show that the average BGL in the mice showed a value of 186 mg/dL, while the treatment groups in F1 and F3 were still above 200 mg/dL. The average BGL value in the F2 group mice was almost close to the BGL value in the positive group. Observation of BGL on the 15th day of the treatment group given EES Formula 1-3 transdermal patches and the positive control group value ranged from 100-130 mg/dL, where the positive control group had a smaller BGL value of 100 mg/dL then the treatment group F2 is 105 mg/dL.

The results of testing the BGL activity of the three EES transdermal patch formulas with a combination of oleic acid enhancer and tween-80 in various comparisons showed that formula F2 was the EES transdermal patch formula which had greater BGL-reducing activity compared to the F1 and F3 groups. Based on one-way ANOVA statistical testing, the resulting significance value is 0.000 < 0.005. There were significant differences between each treatment group.

Enhancers are a critical point in the delivery of transdermal preparations with various mechanisms of action on the stratum corneum, thereby increasing the permeation of active substances that influence pharmacological effectiveness (Haq et al., 2020). The combination of oleic acid and tween-80 can provide a synergistic effect of the EES transdermal patch preparation (Bigucci et al., 2015). Oleic acid

is one of the enhancers of the unsaturated fatty acid group (Nurahmanto, 2016). In the atorvastatin polymethacrylate transdermal patch preparation, the use of an oleic acid enhancer can increase the permeation of atorvastatin as an anti-dyslipidemia (El-Say et al., 2021). Oleic acid is able to increase the permeation of ketorolac fourteen times compared to pure ketorolac (Kumar et al., 2015). At a concentration of 1-3%, the use of oleic acid in the transdermal lornoxicam preparation was able to increase the anti-inflammatory activity in rats induced by carrageenan compared to administration of the oral preparation (Hashmat et al., 2020).

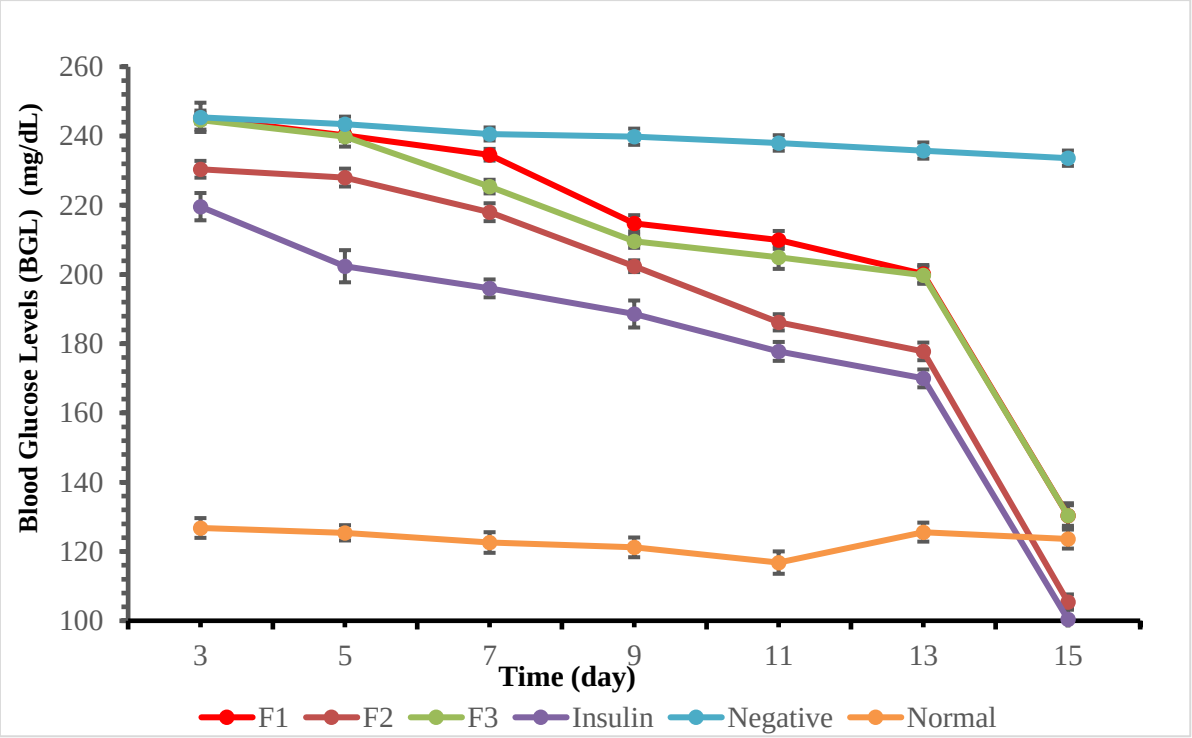

Figure 3. Effect of transdermal patch on blood glucose levels in diabetic rats treated by F1, F2, F3, positif control, negative control and normal

Tween-80 is an enhancer from the non-ionic surfactant group. The use of tween-80 at low concentrations can form lipid emulsification in the stratum corneum thereby increasing the permeability of the active substance. The choice of enhancers in the form of oleic acid and tween-80 in making EES transdermal patches is to provide a synergistic effect of enhancers in increasing the permeation of andrographolide in the bitter extract as an antidiabetic. According to Bigucci et al., (2015), using oleic acid combined with tween-80 through extensive testing in-vitro provides a better permeation effect on the propranolol HCl transdermal patch compared to the propranolol HCl transdermal patch which only uses a single enhancer of oleic acid and a single tween-80. The structure of the stratum corneum consists of parts that are lipophilic and hydrophilic, so the use of a combination of enhancers that have hydrophilic properties such as tween-80 and lipophilic properties such as oleic acid makes it easier for the active substances to penetrate optimally thereby increasing greater permeability (Saitoh et al., 2023).

Based on testing the characteristics of the patch and testing the BGL lowering activity of the EES transdermal patch, it was found that the F2 formulation was the optimal formula both in terms of characteristics and testing the blood glucose lowering activity in STZ-induced rats. The use of a combination of 1% oleic acid enhancer and 3% tween-80 is able to increase the permeation of

andrographolide contained in the EES. According to Zaki et al., (2022), a concentration of 1% oleic acid in the tacrolimus nanovesicles transdermal gel preparation is able to increase the permeation of the preparation. Tacrolimus transdermal gel is 3.6 times higher than tacrolimus oral suspension preparation.

The use of 1% oleic acid concentration in transdermal lornoxicam preparations can increase the permeation of lornoxicam (Hashmat et al., 2020). Tween-80 concentration of 3% can increase the permeation of ketoprofen by nine times compared to the standard (Mita et al., 2018). The use of oleic acid and tween-80 as enhancers in the EES transdermal patch with a ratio of 1% and 3% can increase the effectiveness of the EES transdermal patch preparation as an antidiabetic.

This is in accordance with Saitoh et al. (2023) research, the use of a combination of oleic acid and tween-80 in the disulfiram transdermal patch preparation was able to increase disulfiram permeation better than the use of oleic acid alone. The combined application of oleic acid and tween 80 significantly increased the amount of drug that permeated into the skin. Oleic acid may progress the fluidity of intercellular lipids within the stratum corneum and tween 80 may move forward the skin permeability of the drug by increasing the solubility.

CONCLUSION

The characteristics of EES transdermal patches were affected by the ratio of tween-80 and oleic acid as the enhancers. The combination of oleic acid and tween 80 as a permeation enhancer has an influence on the physical characteristics (weight and thickness) and BGL lowering activity of EES patches.

ACKNOWLEDGEMENT

The authors sincerely thank to DRTPM program PTM NOMOR: 049/PPS-PTM/LPPM UAD/VI/2023 for funding this research.

REFERENCES

Ahmed, O. A. A., Ahmed, T. A., Abdel-Naim, A. B., Khedr, A., Banjar, Z. M., & Afouna, M. I. (2014). Enhancement of in vitro skin transport and in vivo hypoglycemic efficacy of glimepiride transdermal patches. *Tropical Journal of Pharmaceutical Research*, *13*(8), 1207–1213. https://doi.org/10.4314/tjpr.v13i8.

American Diabetes Association. (2024). 2. Diagnosis and Classification of Diabetes: Standards of Care in Diabetes—2024. *Diabetes Care*, *47*(January), S20–S42. https://doi.org/10.2337/dc24-S002

Baranauskaite, J., Ockun, M. A., Uner, B., Tas, C., & Ivanauskas, L. (2021). *Effect of the amount of polysorbate 80 and oregano essential oil on the emulsion stability and characterization properties*. https://doi.org/https://doi.org/10.3390/ molecules26206304

Bigucci, F., Abruzzo, A., Cerchiara, T., Gallucci, M. C., & Luppi, B. (2015). Formulation of cellulose film containing permeation enhancers for prolonged delivery of propranolol hydrocloride. *Drug Development and Industrial Pharmacy*, *41*(6), 1017–1025. https://doi.org/10.3109/03639045.2014.925914

Budhathoki, U., Gartoulla, M. K., & Shakya, S. (2016). Formulation and evaluation of transdermal patches of atenolol. *Indonesian Journal of Pharmacy*, *27*(4), 196–202. https://doi.org/10.14499/indonesianjpharm27iss4pp196

Castañeda, P. S., Escobar-Chávez, J. J., Aguado, A. T., Cruz, I. M. R., & Melgoza Contreras, L. M. (2017). Design and evaluation of a transdermal patch with Atorvastatin. *Farmacia*, *65*(6), 908–916.

DepKes RI. (2017). Formularies. *Farmakope Herbal Indonesia Edisi II*, 213–218. https://doi.org/10.1201/b12934-13

El-Say, K. M., Ahmed, T. A., Aljefri, A. H., El-Sawy, H. S., Fassihi, R., & Abou-Gharbia, M. (2021). Oleic acid–reinforced PEGylated polymethacrylate transdermal film with enhanced antidyslipidemic activity and bioavailability of atorvastatin: A mechanistic ex-vivo/in-vivo analysis. *International Journal of Pharmaceutics*, *608*(August). https://doi.org/10.1016/j.ijpharm.2021.121057

Ermawati, D. E., & Prilantari, H. U. (2019). Pengaruh kombinasi polimer hidroksipropilmetilselulosa dan natrium karboksimetilselulosa terhadap sifat fisik sediaan matrix-based patch ibuprofen. *JPSCR : Journal of Pharmaceutical Science and Clinical Research*, *4*(2), 109. https://doi.org/10.20961/jpscr.v4i2.34525

Francis, D. J. E. (2016). Development and evaluation of matrix type transdermal patches of pioglitazone hydrochloride. *Universal Journal of Pharmaceutical Research*, *1*(1), 31–37. https://doi.org/10.22270/ujpr.v1i1.r5

Garg, C., Sharma, P., Satija, S., & Garg, M. (2016). Stability indicating studies of Andrographis paniculata extract by validate HPTLC protocol. *Journal of Pharmacognosy and Phytochemistry*, *5*(6), 337–344.

Haahr, H., & Heise, T. (2020). Fast-acting insulin aspart: a review of its pharmacokinetic and pharmacodynamic properties and the clinical consequences. *Clinical Pharmacokinetics*, *59*(2), 155–172. https://doi.org/10.1007/s40262-019-00834-5

Hadebe, S. I., Ngubane, P. S., Serumula, M. R., & Musabayane, C. T. (2014). Transdermal delivery of insulin by amidated pectin hydrogel matrix patch in streptozotocin-induced diabetic rats: Effects on some selected metabolic parameters. *PLoS ONE*, *9*(7). https://doi.org/10.1371/journal.pone.0101461

Haq, A., Chandler, M., & Michniak-Kohn, B. (2020). Solubility-physicochemical-thermodynamic theory of penetration enhancer mechanism of action. *International Journal of Pharmaceutics*, *575*(August 2019), 118920. https://doi.org/10.1016/j.ijpharm.2019.118920

Hartesi, B., Sagita, D., Andriani, L., Angke, T., & Natalia, S. (2021). Patch transdermal dari fraksi N-Heksan ekstrak ruku- ruku (Ocimum Tenuiflorum L.) sebagai antiinflamasi. *Jurnal MIPA*, *9*(2), 60. https://doi.org/10.35799/jmuo.9.2.2020.28709

Hashmat, D., Shoaib, M. H., Ali, F. R., & Siddiqui, F. (2020). Lornoxicam controlled release transdermal gel patch: Design, characterization and optimization using co-solvents as penetration enhancers. *PLoS ONE*, *15*(2), 1–23. https://doi.org/10.1371/journal.pone.0228908

Hendriati, L., Hamid, I. S., Widodo, T., Surya, R. H., Wahyudi, A. E., & Rasdianto, D. D. (2021). Analgesic activity of transdermal patch ethanol extract Piper Nigrum L Fructus with some enhancers on Mice. *Jurnal Farmasi Sains Dan Praktis*, *7*(1), 67–73. https://doi.org/10.31603/pharmacy.v7i1.4033

Hidayat, R., & Wulandari, P. (2021). Effects of Andrographis paniculata (Burm. F.) extract on diabetic Nephropathy in Rats. *Reports of Biochemistry and Molecular Biology*, *10*(3), 445–454. https://doi.org/10.52547/rbmb.10.3.445

Jafri, I., Shoaib, M. H., Yousuf, R. I., & Ali, F. R. (2019). Effect of permeation enhancers on in vitro release and transdermal delivery of lamotrigine from Eudragit®RS100 polymer matrix-type drug in adhesive patches. *Progress in Biomaterials*, *8*(2), 91–100. https://doi.org/10.1007/s40204-019-0114-9

Keerthana, A., Sunilchandra, U., Nb, S., M, V. K., B, K. R., Sheela, P., & Srinivasan, G. (2022). *Pharmacokinetic evaluation of single oral dose of meloxicam with or without co-administration of andrographolide or bromelain in rats*. *11*(5), 349–354.

Kemala, N. I. W. (2016). *Glibenklamid Menggunakan Hydroxy Propyl Methyl Cellulose (Hpmc) K15M Sebagai Polimer (Skripsi)*, Universitas Islam Indonesia, 1–121.

Kumar, M., Trivedi, V., Shukla, A. K., & Dev, S. K. (2018). Effect of polymers on the physicochemical and drug release properties of transdermal patches of atenolol. *International Journal of Applied Pharmaceutics*, *10*(4), 68–73. https://doi.org/10.22159/ijap.2018v10i4.24916

Kumar, P., Singh, S., Mishra, D., & Girotra, P. (2015). Enhancement of ketorolac tromethamine permeability through rat skin using penetration enhancers: An ex-vivo study. *International Journal of Pharmaceutical Investigation*, *5*(3), 142. https://doi.org/10.4103/2230-973x.160850

Liang, D., Zhang, W.-M., Liang, X., Tian, H.-Y., Zhang, X.-M., Li, X., & Gao, W.-Y. (2023). A review on the extraction and separation of andrographolide from Andrographis paniculata: extraction

selectivity, current challenges and strategies. *Traditional Medicine Research*, *8*(7), 38. https://doi.org/10.53388/tmr20230107001

Mita, S. R., Musfiroh, I., SK, I., & MF, D. (2018). Study in vitro of Ketoprofen patch with tween 80 as enhancer. *International Research Journal of Pharmacy*, *9*(7), 111–115. https://doi.org/10.7897/2230-8407.097134

Moore, E. M., Wagner, C., & Komarnytsky, S. (2020). The enigma of bioactivity and toxicity of botanical oils for skin care. *Frontiers in Pharmacology*, *11*(May), 1–17. https://doi.org/10.3389/fphar.2020.00785

Mostafavinia, A., Amini, A., Ghorishi, S. K., Pouriran, R., & Bayat, M. (2016). The effects of dosage and the routes of administrations of streptozotocin and alloxan on induction rate of type1 diabetes mellitus and mortality rate in rats. *Laboratory Animal Research*, *32*(3), 160. https://doi.org/10.5625/lar.2016.32.3.160

Nurahmanto, D. (2016). Formulasi dan evaluasi sediaan patch transdermal prometazin HCL sebagai pengobatan morning sickness. *South African Medical Journal*, *101*(2003), 16.

Pandey, A. (2014). Role of surfactants as penetration enhancer in transdermal drug delivery system. *Journal of Molecular Pharmaceutics & Organic Process Research*, *02*(02). https://doi.org/10.4172/2329-9053.1000113

Perada, S., P. N. Murthy. (2022). Design, development and evaluation of transdermal drug delivery system for treatment of diabetes. *Journal of Pharmaceutical Negative Results*, *13*(8), 3610–3617. https://doi.org/10.47750/pnr.2022.13.s08.448

Prasetyo, B. F., Wientarsih, I., Sajuthi, D., & Juniantito, V. (2018). Formation of Andrographlolide-BetaCyclodextrin Inclusion to Increase Solubility and Dissolution Rate. *Indonesian Journal of Pharmaceutical Science and Technology*, *5*(2), 49. https://doi.org/10.24198/ijpst.v5i2.14995

Pratiwi, G., Susanti, S., & Shiyan, S. (2021). *Application of factorial design for optimization of PVC-HPMC polymers in matrix film ibuprofen patch-transdermal drug delivery system*. *1*(1), 11–21.

Premanath, R., & Nanjaiah, L. (2015). Antidiabetic and antioxidant potential of Andrographis paniculata Nees. leaf ethanol extract in streptozotocin induced diabetic rats. *Journal of Applied Pharmaceutical Science*, *5*(1), 069–076. https://doi.org/10.7324/JAPS.2015.50113

Rais, I. R. (2014). Ekstraksi androgafolid dari Andrographis paniculata (Burm.f.) Nees menggunakan ekstraktor soxhlet. *Pharmaciana*, *4*(1), 85–92. https://doi.org/10.12928/pharmaciana.v4i1.402

Ramadhani, M. A., Hati, A. K., Jusman, A. H., Farmasi, P. S., Kesehatan, F., Waluyo, U. N., Insulin, N. D., & Glukosa, P. (2021). *Perbandingan aktivitas penurunan glukosa pada ekstrak dan nanoekstrak daun Insulin (Tithonia diversifolia) dengan metode in vitro*. *1*(2), 28–36.

Saitoh, H., Takami, K., Ohnari, H., Chiba, Y., Ikeuchi-Takahashi, Y., & Obata, Y. (2023). Effects and mode of action of oleic acid and tween 80 on skin permeation of disulfiram. *Chemical and Pharmaceutical Bulletin*, *71*(4), 289–298. https://doi.org/10.1248/cpb.c22-00821

Sari, K. R. P., Sudarsono, & Nugroho, A. E. (2015). Effect of herbal combination of Andrographis paniculata (Burm.f) Ness and Gynura procumbens (Lour.) Merr ethanolic extracts in alloxan-induced hyperglycemic rats. *International Food Research Journal*, *22*(4), 1332–1337.

Setyawan E.I, Warditiani N.K, D. S. . (n.d.). *Pengaruh penggunaan propilenglikol dan mentol terhadap matrik patch transdermal ekstrak air Herba Sambiloto (Andrographis paniculata (burm. F.) Nees*.

Shivalingam, M. R., Balasubramanian, A., & Ramalingam, K. (2021). Formulation and evaluation of transdermal patches of pantoprazole sodium. *International Journal of Applied Pharmaceutics*, *13*(5), 287–291. https://doi.org/10.22159/ijap.2021v13i5.42175

Solanke, P. N., Ambekar, A. W., & Chemate, S. (2018). *Formulation , development and characterization of transdermal drug delivery system for antidiabetic drug*. *4*(5), 668–672.

Soral, M., Nanjappa, S. H., & Alayadan, P. (2021). Formulation and evaluation of transdermal patch of rabeprazole sodium. *Journal of Reports in Pharmaceutical Sciences*, *10*(2), 240–246. https://doi.org/10.4103/jrptps.JRPTPS_126_20

Sundhani, E., Nugroho, A. E., Nurrochmad, A., Puspitasari, I., Prihati, D. A., & Lukitaningsih, E.

(2022). *Pharmacokinetic herb-drug interactions of glipizide with*. https://doi.org/https://doi.org/10.3390/ molecules27206901

Tripathi, R, Singh, A., & Sahu, N. (2022). *Formulation and evaluation of transdermal patches*. *11*(17), 49–68. https://doi.org/10.20959/wjpr202217-24471

Yuan, Y., Win Aung, K. K., Ran, X. K., Wang, X. T., Dou, D. Q., & Dong, F. (2017). A new sesquiterpene lactone from yacon leaves. *Natural Product Research*, *31*(1), 43–49. https://doi.org/10.1080/14786419.2016.1212028

Zaki, R. M., Ibrahim, M. A., Alshora, D. H., & Abou El Ela, A. E. S. (2022). Formulation and evaluation of transdermal gel containing tacrolimus-loaded spanlastics: in vitro, ex vivo and in vivo studies. *Polymers*, *14*(8). https://doi.org/10.3390/polym14081528

.

Pharmaciana
Vol.14, No.2, July 2024, Page. 209-219
ISSN: 2088 4559; e-ISSN: 2477 0256
DOI: 10.12928/pharmaciana.v14i2.28653

Effects of *Piper crocatum* leaf extract-based ointments on bacteria associated with diabetic ulcers: an *in vitro* study

Yudha Rizky Nuari*, Mila Abusri, Wahyu Yuntari, Oca Maharani Tryadi, Fiarriescha Marra Ardhiana
Faculty of Pharmacy, Universitas Ahmad Dahlan
Jl. Prof. Dr.Soepomo, S.H., Warungboto, Umbulharjo, Yogyakarta, Indonesia

Submitted: 02-04-2024 ***Reviewed: 08-07-2024*** ***Accepted: 16-07-2024***

ABSTRACT

Diabetic patients with poor blood glucose control are highly susceptible to developing secondary infections, which can lead to the development of prolonged diabetic ulcers. Therefore, a suitable medication that may effectively prevent the occurrence of secondary infections is crucial to shorten the closure of diabetic ulcers. Red betel leaf (*Piper crocatum* Ruiz & Pav) is reported to possess antimicrobial activity due to the presence of flavonoids. This study aimed to evaluate the effect of ethanolic extract of red betel leaf (EERBL) ointments against the most prevalent bacteria associated with diabetic foot ulcers (DFU): *Staphylococcus aureus* and *Pseudomonas aeruginosa*. The EERBL was prepared by macerating powdered red betel leaf with 96% ethanol and was screened for the presence of flavonoids and the determination of total flavonoid content (TFC) by thin layer chromatography and UV-Vis spectrophotometry, respectively. This study examined three hydrophilic-based ointments containing 10%, 20%, and 30% EERBL, respectively, followed by characterization for pH, spreadability, adhesivity, and viscosity. The EERBL ointments' effect on the bacteria was evaluated using the well-diffusion method by observing inhibition zone formation after 24-hour incubation. The results showed that varying the EERBL concentrations in the formulations led to different spreadability, adhesivity and viscosity ($p<0.05$). Furthermore, all EERBL ointments demonstrated the formation of an inhibition zone on cultured media, indicating the presence of antimicrobial activity. The ointment with 30% EERBL had the largest diameter of the inhibition zone against both bacteria ($p<0.05$). The findings suggest a higher antimicrobial activity was observed with an increase in the concentration of EERBL within the ointments.

Keywords: Red betel leaf (*Piper crocatum*), flavonoids, ointment, antimicrobial activity, diabetic ulcers

Corresponding author:
Yudha Rizky Nuari
Department of Pharmaceutics, Faculty of Pharmacy, Universitas Ahmad Dahlan
Jl. Prof. Dr.Soepomo, S.H., Warungboto,Umbulharjo,Yogyakarta, Indonesia
Email: yudha.nuari@pharm.uad.ac.id

INTRODUCTION

In 2021, Indonesia was among the top ten countries worldwide with the highest occurrence of diabetes with approximately 11 million cases (Hidayat et al., 2022; Tanoey & Becher, 2021). Diabetes is a chronically persistent disease that ranked as the third leading cause of mortality in Indonesia, as reported in 2017 (Hidayat et al., 2022). Inadequate management and poorly controlled diabetes over a long period can result in several severe complications, such as macroangiopathy, diabetic retinopathy, diabetic nephropathy, and diabetic neuropathy, including diabetic foot ulcers (Beulens et al., 2021; Farmaki et al., 2020).

Diabetic foot ulcer (DFU) is considered the most severe complication of diabetes mellitus that is linked to significant illness, death, and a decrease in quality of life, which continues to increase in prevalence over time (Cho et al., 2018). A diabetic foot ulcer is described as a deep wound located below the ankle in individuals with diabetes and may lead to a devastating long-term complication of non-traumatic lower limb amputation, especially in diabetic patients with poorly managed, chronically infected diabetic foot ulcers (Jupiter et al., 2016). Patients diagnosed with diabetes have a one-fourth probability of developing Diabetic Foot Ulcers (DFU) during the course of their lives, and the prevalence of DFU-related amputation is virtually every half minute globally (Chammas et al., 2016). Diabetic foot ulcers (DFU) are a prevalent reason for hospitalization among diabetic patients and have a notable socioeconomic effect (Ha et al., 2021). Patients with DFU experience a mortality rate that is more than double that of diabetic patients without ulcers, with approximately 40% of the five-year mortality rates after ulceration (Jupiter et al., 2016; Rubio et al., 2020). Additionally, the DFU and its long-term consequences are responsible for both direct healthcare expenses and extended periods of disability (Ha et al., 2021; Rubio et al., 2020).

Diabetic patients with ulcers are susceptible to developing secondary infections DFU due to delayed wound healing (Matheson et al., 2021; Sadeghpour et al., 2019). Gram-positive bacteria, such as Staphylococcus aureus, and gram-negative bacteria, including Pseudomonas aeruginosa, are the most responsible colonies that cause secondary infections in DFU, as observed from the bacterial cultures of patient samples globally (Datta et al., 2019; Sadeghpour et al., 2019). These bacteria on the surface wound create a favorable niche for further invasion, resulting in chronic infected DFU (Li et al., 2022). This infection increases the likelihood of multi-drug resistance and ultimately prolongs the wound-healing process (Datta et al., 2019; Yan et al., 2022).

Piper crocatum Ruiz & Pav (*P. crocatum*), or red betel, is a well-known traditional herbal remedy from Indonesia (Setyawati et al., 2023). This easily cultivated plant is readily available, and its leaf has been traditionally and empirically used as herbal medicine to treat wounds for generations in Indonesia (Suri et al., 2021). According to numerous studies, red betel leaves are composed of tannins, polyphenols, saponins, and flavonoids (Januarti et al., 2019; Rahma, 2022; Setyawati et al., 2021; Suri et al., 2021). In addition, flavonoids reportedly exhibit antibacterial properties and may serve as a viable alternative source of treatment for infections manifested in diabetic ulcers (Farhadi et al., 2019; Ibrahim et al., 2018; Shamsudin et al., 2022).

The current study focuses on formulating and characterizing topical ointments containing ethanolic extract of red betel leaf (EERBL) using a hydrophilic ointment base with variations of EERBL concentrations of 10%, 20%, and 30% b/b. The ointment base is selected due to its ability to form a physical barrier, which enables protection from potential bacterial infections in the wound area and provides moisture to facilitate growth factors to migrate and diffuse to the wound during the closure (Hoekstra et al., 2017; Taddese et al., 2021). This study aims to assess the effects of the EERBL ointments against the two most prevalent DFU-associated bacteria, namely *Staphylococcus aureus* and *Pseudomonas aeruginosa*, as compared to positive control (mupirocin topical cream) and placebo (the ointment base). Ultimately, the EERBL ointment with the largest inhibitory zone diameter, which signifies antimicrobial activity, will be selected for further in vivo investigation using diabetic animal models in future experiments.

MATERIALS AND METHOD

Materials

Piper crocatum (red betel leaves) was obtained from Bantul while ethanol 96%, toluene, ethyl acetate, formic acid, $AlCl_3$, $FeCl_3$, Na-acetate, NaOH, HCl, and silica gel 60 254 were purchased from Merck®. In addition, methyl paraben, propyl paraben, stearyl alcohol, and white vaseline were purchased from PT Brataco whereas sodium lauryl sulphate, propylene glycol, quercetin standard, and Dragendorff reagent were from Sigma Aldrich®. Furthermore, nutrient broth and Mueller Hinton were acquired from Oxoid®, and distilled water, Mayer's reagent, NaCl 0.9%, Mupirocin ointment were purchased from PT Widatra, Labchem®, Otsuka®, and PT Etercon Pharma, respectively. For antimicrobial activity evaluation, *Staphylococcus aureus* (ATCC 25923) and *Pseudomonas aeruginosa* (ATCC 27853) were employed in this study.

Methods

Sample preparation

Red betel leaves (*Piper crocatum* Ruiz & Pav) were collected from Bantul and were initially subjected to a determination test for plant identification at the Biology Laboratory, Faculty of Applied Science and Technology, the University of Ahmad Dahlan, Yogyakarta, Indonesia (ID no:142/Lab.Bio/B/III/2024). The red betel leaves were freshly sorted and rinsed to remove dirt and dust by flowing water before being dried at room temperature. The dried leaves were then blended and milled into small pieces and fine powder (Safithri et al., 2023).

Extract preparation and characterization

Ethanolic extract of red betel leaf (EERBL) was prepared by weighing the powdered red betel leaves for 350 g and macerated using 1400 mL of 96% ethanol in a glass jar for 24 hours with occasional stirring. After 24 hours, the filtrate and the residue were separated; the latter was re-macerated for another 24 hours with a similar protocol for two rounds. The filtrates from maceration and re-maceration were collected and evaporated for one hour at 60°C in a rotary evaporator (Heidolph®). Following this, the filtrates were then dried on a waterbath (Memmerth®) until a viscous extract was observed (Navirius et al., 2023; Puspita et al., 2019). The crude extracts were afterward characterized for organoleptic properties, % yield, and water content by the toluene distillation method with the equation (1) (Kemenkes RI, 2017):

$$\text{Water content } (\%) = \frac{\text{Water Volume (mL) x 1 gram/mL}}{\text{Sample weight (gram)}} \; x \; 100\% \quad \text{.....(1)}$$

Phytochemical screening

A qualitative phytochemical screening test was performed on the concentrated EERBL for flavonoids, alkaloids, saponin, tannin, triterpenoids, and steroids (Puspita et al., 2019). In addition, thin-layer chromatography (TLC) was employed to ensure the presence of flavonoids within the ethanolic extracts with quercetin as a biomarker according to the Indonesian Herbal Pharmacopeia Edition II (Kemenkes RI, 2017). A mixture of toluene P, ethyl acetate P, and formic acid P (7:2.5:0.5) was used as a mobile phase while a silica gel 60 F254 was used as a stationary phase (Kemenkes RI, 2017).

Determination of total flavonoid content

Total flavonoid content was determined by UV-Vis spectrophotometry (Shimadzu®) using a quercetin standard. The standard solutions were prepared at 5, 10, 25, 50, 75, and 100 mg/L dissolved in ethanol with the addition of 0.1 mL of 10% $AlCl_3$ and 1 mL of 1M Na-acetate prior to measurement at a wavelength of 438 nm. For sample analysis, 0.5 mL of each concentrated ethanolic extract was added with 1.5 mL of ethanol, 0.1 mL of 10% $AlCl_3$, and 1 mL of 1M Na-acetate and was read at the

same wavelength as the standards (Nerdy et al., 2022). The flavonoid content was calculated and expressed as quercetin equivalent (mg QE/g) with the equation (2) (Kemenkes RI, 2017):

$$\text{Total Flavonoid (QE)} = c\,(V/m) \quad \ldots\ldots\ldots\ldots (2)$$

QE = quercetin equivalent
c = total flavonoid concentration from quercetin standard curve (mg/l)
V = volume of sample
m = weight of sample (gram)

Preparation of ointment of ethanolic Extract of Red Betel Leaf (EERBL Ointment)

An ointment is generally a favorable topical preparation for diabetic ulcer treatment (Agharazi et al., 2022; Salahi et al., 2024; Zhao et al., 2023). In this study, the EERBL ointments were prepared through a fusion method. Firstly, methylparaben, propylene glycol, sodium lauryl sulfate, and water were mixed in an evaporating porcelain dish and heated at 60℃ until partly melted; this mixture was referred to as mixture one. Additionally, a second mixture consisting of white vaseline, propylparaben, and stearyl alcohol was prepared and subjected to the same temperature as the previous mixture; this mixture was referred to as mixture two. Subsequently, mixture one was introduced into mixture two; both mixtures were homogeneously mixed. Ultimately, the EERBL was added and constantly stirred using a stirring rod until a homogenous ointment was formed (USP, 2007). All ointments were prepared according to the following formulations (Table 1).

Table 1. Formulations of ethanolic extract of red betel leaf ointments

Ingredients	Ointment Formulations (gram)		
	F1	F2	F3
Ethanolic extract of Red Betel Leaf (EERBL)	10	20	30
Methyl paraben	0.025	0.025	0.025
Propyl paraben	0,015	0.015	0.015
Sodium Lauryl Sulfate	0.7	0.7	0.7
Propyleneglycol	8.5	8,5	8.5
Stearyl alcohol	15	15	15
White vaseline	20	20	20
Aquadest (distilled water)	ad 100	ad 100	ad 100

Characterization of ointment

The EERBL ointments were subjected to characterization for pH, spreadability, adhesivity, and viscosity (Maulina & Sugihartini, 2015). Firstly, the pH was measured by mixing 2.5 grams of the ointment with 50 mL of aquadest. The mixture was then heated up to 60-70℃ until homogenously mixed, following measurement with a digital pH meter. Secondly, the spreadability was determined by applying 0.5 grams of the ointments onto a round glass plate, with a second glass plate was placed on top of it. A weight of 100 grams was allowed to remain on the top glass plate for one minute. The diameter of the circle was measured after the ointment was widely spread. Thirdly, the adhesivity was conducted by placing one gram of the ointment on a glass plate that was subsequently covered with another glass plate, with a weight of one kg was added on top of it for 5 minutes. Afterward, the squeezed glass was released, and the adhesiveness was evaluated by measuring the time required to separate both glasses using a stopwatch. Lastly, the viscosity test was carried out using Rheosys Merlin VRII (Scientex®) using a cone and plate 2°/30mm spindle with 0.5 gram of sample of each run.

Antibacterial activity

Nutrient Broth (NB) media was used to propagate pure cultures of DFU-associated bacteria: *Staphylococcus aureus* (ATCC 25923) and *Pseudomonas aeruginosa* (ATCC 27853). The cultured media was placed into an incubator (Binder® Series E/B 28) for 24-hour incubation. Following this, 0.9% NaCl was mixed with bacterial cultures on the NB media, and the level of turbidity was standardized using Mc Farland 0.5. The standardized turbidity level bacterial cultures were uniformly swabbed on the surface of a Mueller Hinton Agar (MHA) media and allowed to sit for 5 minutes. The antibacterial activity assay was performed by means of the well-diffusion method by filling the reservoirs in the MHA media with 0.02 grams of 10%, 20%, and 30% EERBL ointments (F1, F2, and F3), 2% mupirocin ointment (positive control) and placebo (ointment base only). The MHA media was incubated at 37°C for 24 hours. After incubation, a calliper was used to measure the formation of the inhibition zone diameter (Balouiri et al., 2016; Blando et al., 2019; Puspita et al., 2019).

Data Analysis

The data collected from this study were statistically analyzed utilizing the one-way ANOVA and the Tukey test with a significance level of $p<0.05$.

RESULT AND DISCUSSION

Characterization of EERBL

The concentrated ethanolic extract of red betel leaves (*Piper crocatum* Ruiz & Pav) (EERBL) was subjected to characterization, including organoleptic properties, % yield, and water content. The crude extracts were observed as a thick, dark brown-reddish-colored extract with a bitter flavor and typical aroma of red betel leaf. Furthermore, the total weight of the crude concentrated EERBL was 98.12 grams from 350 grams of powdered red betel leaf used, resulting in a yield of 28.03%. Subsequently, the water content was also determined to ensure the risk of potential bacterial or microorganism growth during the storage is low, thereby not affecting the quality and safety of the product. The water content was 7.51% ± 0.286, as determined by the toluene distillation method (Kemenkes RI, 2017). All these evaluated characteristics were in line with the compendial criteria suggested in the Indonesian Herbal Pharmacopeia Edition II and are presented in Table 2.

Table 2. Attributes of crude ethanolic extract derived from red betel leaves

Parameter	Result	Requirement*
Color	Dark brown-reddish	Dark brown-reddish
Taste	Bitter	Bitter
Odor	Distinctive aroma of red betel leaf	Distinctive aroma of red betel leaf
Yield	28.03%	> 17%
Water Content	7.51% ± 0.286**	< 10%

*Compendial requirement as described in the Indonesian Herbal Pharmacopeia Edition II for red betel leaf extract
**data are shown as mean ± SD (n=3)

Phytochemical screening & total flavonoid content

Preliminary phytochemical screenings were performed on the extracts prior to ointment preparations (Puspita et al., 2019). According to the Indonesian Herbal Pharmacopeia Edition II, the red betel leaf extract is known to contain flavonoids with quercetin used as a marker to identify the flavonoid content in the extract (Kemenkes RI, 2017). The results suggest the presence of flavonoids, alkaloids, phenols, steroids, triterpenoids, and tannins with an absence of saponins in the extracts as screened through a qualitative phytochemical screening test (Table 3). These findings are in line with previous studies (Heliawati et al., 2022; Puspita et al., 2019; Suri et al., 2021). In addition, a thin-layer chromatography test on the extract was also performed to ensure the flavonoid content as compared to the quercetin standard with a theoretical Rf value of 0.38 for identification (Kemenkes RI, 2017). The result showed that both the extract and the quercetin standard had the same Rf value at around 0.38,

establishing the presence of quercetin in the extract (Figure 1). Ultimately, total flavonoid content (TFC) in EERBL was also determined via UV-Vis spectrophotometry using a quercetin standard with a result of 78.14 ± 7.63 mg QE/g (n=5).

Figure 1. Thin layer chromatography analysis of quercetin standard (A) vs EERBL (B) with identical RF values, suggesting the presence of flavonoid quercetin in the EERBL

Table I. Preliminary phytochemical screenings on the red betel leaf ethanolic extracts

Secondary Metabolite	Test	Result
Flavonoids	Bate Smite-Metcalfe's test	+
	NaOH 10%	+
Alkaloids	Deagendorff's test	+
	Mayer's test	+
Saponins	Frothing test	-
Tannins	Ferric Chloride test	+
Triterpenoids	Liebermamn's test	+
Steroids	Liebermamn's test	+
Phenols	Ferric Chloride test	+

Key = + present, - absent

Preparation and characterization of ointment

Three different formulations were employed for preparing the hydrophilic-based ointments with variations on the concentration of ethanolic extract of red betel leaf (EERBL): 10%, 20%, and 30%, respectively. A hydrophilic base was selected as the ointment base due to its ability to facilitate good absorption while providing optimum viscosity for better spreadability and adhesivity to the skin upon application (Shigeyama et al., 1999).

Table 4. Characterization data of the red betel leaf ethanolic extracts ointments

Parameter	F1	F2	F3
pH	4.81 ± 0.14^{a}	5.12 ± 0.21^{ab}	5.28 ± 0.18^{b}
Spreadability (cm)	5.52 ± 0.24^{a}	4.89 ± 0.19^{b}	4.37 ± 0.19^{c}
Adhesivity (seconds)	32.43 ± 1.8^{a}	54.18 ± 2.6^{b}	63.71 ± 1.4^{c}
Viscosity (cP)	8367 ± 373^{a}	$10{,}453 \pm 910^{b}$	$13{,}551 \pm 794^{c}$

Key: EERBL = Ethanolic Extract of Red Betel Leaf; data are shown as mean ± SD (n=3); values within a row with different superscripts are significantly different according to the Tukey test ($p < 0.05$)

After preparation, the EERBL ointments were characterized for pH, spreadability, adhesivity, and viscosity. The measured pH of the ointments ranged between 4.81 to 5.28. The spreadability of the ointments was at 4.65 to 5.20 cm, while the adhesivity ranged from 32 to 63 seconds among the three formulations, respectively. Ultimately, the viscosity of the ointments was also evaluated with Rheosys Merlin VRII (Scientex®) using a cone and plate 2°/30mm spindle with a 0.5 gram sample for each measurement. The data of the ointment's characterization is presented in Table 5.

From Table 4, the pH of the ointments met the criteria of the ideal pH ointment for human skin, which is 4.5-6.5. For spreadability, Formulation 1 showed the highest value with an average spread of 5.22 cm, while for the adhesivity parameter, Formulation 3 had the longest adherence with 63.71 seconds, slightly longer than Formulation 2. The same trend was also observed in the viscosity, where Formulation 3 demonstrated the most viscous ointment with 11,851 cP. The viscosity of all groups was still within the range of compendial viscosity for an ointment, which is around 2000 to 50,000 cP (Anonim, 2020). Consistency of the ointments might be responsible for these findings as a result of different ratios between aqueous and non-aqueous components in each formulation which determines the liquidity of the ointments, leading to different spreadability, adhesivity, and viscosity (Conti-Silva et al., 2018; Herbig et al., 2023). Of the three formulations, Formulation 1 contains the highest amount of water within its formulation, while Formulation 3 is the opposite. This implies that Formulation 1 became easily spread ointment while Formulation 3 was the stickiest and most viscous ointment. Despite these results, all the parameters above follow the ideal criteria for ointments.

Antibacterial activity

Previous studies showed that ethanolic fraction of red betel leaf extract was able to exert antimicrobial activity against several bacteria (Candrasari, et al., 2012; Purba et al., 2022; Puspita et al., 2019; Rachmawaty et al., 2018). Therefore, this study focuses on evaluating the antimicrobial activity of the EERBL with different concentrations within the ointment. The antibacterial activity of the EERBL ointments was evaluated by means of determining the inhibition zone diameter on the two most common bacteria associated with diabetic foot ulcer (DFU): *Staphylococcus aureus* and *Pseudomonas aeruginosa* (Sadeghpour et al., 2019). Mupirocin ointment was used as a positive control as it is widely used clinically as a broad-spectrum topical antibiotic for ulcers (Dallo et al., 2023; Ishikawa & Horii, 2005). The diameter zone of inhibition was examined using the well-diffusion method. Data on the diameter of the inhibition zone is displayed in Table 5.

Table 5. Inhibition zone diameter of the red betel leaf ethanolic extracts ointments

Formulation	Diameter of Inhibition Zone (mm)	
	Staphylococcus aureus	***Pseudomonas aeruginosa***
F1 (10% EERBL)	10.4 ± 0.60^{a}	8.1 ± 0.40^{a}
F2 (20% EERBL)	12.6 ± 0.63^{b}	9.8 ± 0.35^{b}
F3 (30% EERBL)	14.8 ± 0.98^{c}	12.7 ± 0.55^{c}
Positive Control*	36.4 ± 0.65^{d}	32.1 ± 0.93^{d}
Placebo**	0 ± 0^{e}	0 ± 0^{e}

Key = EERBL = Ethanolic Extract of Red Betel Leaves; *Mupirocin cream (2%); **ointment base only; Data are shown as mean ± SD (n=3); values within a column with different superscripts are significantly different according to the Tukey test ($p < 0.05$)

The antimicrobial activity in this study was determined by the ability to form an inhibition zone in the cultured media after 24-hour incubation. As depicted in Table 5, all placebo groups - containing only ointment base - showed no inhibitory activity, while positive controls exhibited the largest inhibition zone diameter in both groups. This is reasonable since mupirocin is a broad-spectrum topical antibiotic that can clinically constrain a wide range of bacterial growth by blocking bacterial RNA and protein synthesis, including Gram-positive *Staphylococcus aureus* and Gram-negative *Pseudomonas aeruginosa* (Dallo et al., 2023; Erwin, 2024; Ishikawa & Horii, 2005). In addition, the

formation of an inhibition zone was observed in all EERBL ointment groups. Formulation 1 exhibited a weak antimicrobial activity in both bacteria while Formulation 3 had the largest diameter with a moderate activity against both bacteria. Even though the magnitude of the constrained activity was approximately a third lower than that of the control group, all EERBL ointments (10-30%) were able to exert antimicrobial activity against *Staphylococcus aureus* and *Pseudomonas aeruginosa*, the most common bacteria isolated from diabetic foot ulcer samples (Sadeghpour et al., 2019). The statistical analysis of ANOVA and Tukey test revealed that all groups were significantly different ($p<0.05$).

As shown in Table 5, the antimicrobial activity is higher with an increase in the concentration of EERBL within the ointments. Such inhibition activity is likely due to the flavonoid content of EERBL in the EERBL ointments. In general, the inhibitory activity of the EERBL ointments against *Staphylococcus aureus* is slightly greater than *Pseudomonas aeruginosa* as evaluated by the inhibition diameter zone. These results are in agreement with other studies that report similar findings (Hartini & Nugroho, 2020; Puspita et al., 2019; Rachmawaty et al., 2018). Flavonoids are effectively able to affect bacterial cell membrane integrity and biofilm formation, leading to bacterial growth suppression (Heliawati et al., 2022; Kaul et al., 2013; Puspita et al., 2019; Shamsudin et al., 2022).

CONCLUSION

The EERBL ointments exhibit antimicrobial activity by forming an inhibitory zone against DFU-associated bacteria: *Staphylococcus aureus* and *Pseudomonas aeruginosa*. The EERBL ointment with 30% EERBL content - provides the second-largest inhibition zone diameter after the control group with moderate activity to both bacteria. Diabetic patients with poor blood glucose management are at high risk of acquiring secondary infections that may delay wound closure. Such delay in wound healing may develop minor injuries into diabetic ulcers if not properly treated. Regarding this, therefore, the EERBL ointment is likely to be developed as a candidate for DFU topical treatment as it exerts flavonoid-related antimicrobial activity that may prevent secondary infection, leading to shortened closure of DFU. However, further experiments are needed to evaluate the effectiveness of the EERBL ointment for DFU in diabetic animal models.

ACKNOWLEDGEMENT

The authors sincerely thank the Institute for Research and Community Service of Universitas Ahmad Dahlan (LPPM-UAD) for providing financial support to this research with reference number PD-064/SP3/LPPM-UAD/VIII/2023.

REFERENCES

Agharazi, M., Gazerani, S., & Huntington, M. K. (2022). Topical Turmeric Ointment in the Treatment of Diabetic Foot Ulcers: A Randomized, Placebo-Controlled Study. *The International Journal of Lower Extremity Wounds*, 15347346221143222. https://doi.org/10.1177/15347346221143222

Anonim. (2020). *Farmakope Indonesia Edisi VI*. Kemenkes RI.

Balouiri, M., Sadiki, M., & Ibnsouda, S. K. (2016). Methods for in vitro evaluating antimicrobial activity: A review. *Journal of Pharmaceutical Analysis*, *6*(2), 71–79. https://doi.org/10.1016/j.jpha.2015.11.005

Beulens, J. W. J., Yauw, J. S., Elders, P. J. M., Feenstra, T., Herings, R., Slieker, R. C., Moons, K. G. M., Nijpels, G., & van der Heijden, A. A. (2021). Prognostic models for predicting the risk of foot ulcer or amputation in people with type 2 diabetes: a systematic review and external validation study. *Diabetologia*, *64*(7), 1550–1562.

Blando, F., Russo, R., Negro, C., De Bellis, L., & Frassinetti, S. (2019). Antimicrobial and antibiofilm activity against Staphylococcus aureus of Opuntia ficus-indica (L.) Mill. Cladode Polyphenolic Extracts. *Antioxidants (Basel, Switzerland)*, *8*(5). https://doi.org/10.3390/antiox8050117

Candrasari, A., Romas, M., & Astuti, O. (2012). Uji daya antimikroba ekstrak etanol daun sirih merah (Piper Crocatum Ruiz & Pav.) Terhadap pertumbuhan Staphylococcus aureus ATCC 6538,

Eschericia coli ATCC 11229 dan Candida albicans ATCC 10231 secara *in vitro*. *Biomedika*, *4*(1), 9–16. https://doi.org/10.23917/biomedika.v4i1.258

Chammas, N. K., Hill, R. L. R., & Edmonds, M. E. (2016). Increased mortality in diabetic foot ulcer patients: the significance of ulcer type. *Journal of Diabetes Research*, *2016*, 2879809. https://doi.org/10.1155/2016/2879809

Cho, N. H., Shaw, J. E., Karuranga, S., Huang, Y., da Rocha Fernandes, J. D., Ohlrogge, A. W., & Malanda, B. (2018). IDF Diabetes Atlas: Global estimates of diabetes prevalence for 2017 and projections for 2045. *Diabetes Research and Clinical Practice*, *138*, 271–281. https://doi.org/10.1016/j.diabres.2018.02.023

Conti-Silva, A. C., Ichiba, A. K. T., Silveira, A. L. da, Albano, K. M., & Nicoletti, V. R. (2018). Viscosity of liquid and semisolid materials: Establishing correlations between instrumental analyses and sensory characteristics. *Journal of Texture Studies*, *49*(6), 569–577. https://doi.org/10.1111/jtxs.12358

Dallo, M., Patel, K., & Hebert, A. A. (2023). Topical antibiotic treatment in dermatology. *Antibiotics (Basel, Switzerland)*, *12*(2). https://doi.org/10.3390/antibiotics12020188

Datta, P., Chander, J., Gupta, V., Mohi, G. K., & Attri, A. K. (2019). Evaluation of various risk factors associated with multidrug-resistant organisms isolated from diabetic foot ulcer patients. *Journal of Laboratory Physicians*, *11*(1), 58–62. https://doi.org/10.4103/JLP.JLP_106_18

Erwin DZ, C. P. (2024). Mupirocin. [Updated 2024 Jan 11]. In: StatPearls [Internet]. Treasure Island (FL): StatPearls Publishing; 2024 Jan. In *StatPearls*. https://www.ncbi.nlm.nih.gov/books/NBK599499/

Farhadi, F., Khameneh, B., Iranshahi, M., & Iranshahy, M. (2019). Antibacterial activity of flavonoids and their structure-activity relationship: An update review. *Phytotherapy Research : PTR*, *33*(1), 13–40. https://doi.org/10.1002/ptr.6208

Farmaki, P., Damaskos, C., Garmpis, N., Garmpi, A., Savvanis, S., & Diamantis, E. (2020). Complications of the Type 2 Diabetes Mellitus. *Current Cardiology Reviews*, *16*(4), 249–251. https://doi.org/10.2174/1573403X1604201229115531

Ha, J. H., Jin, H., & Park, J.-U. (2021). Association between socioeconomic position and diabetic foot ulcer outcomes: a population-based cohort study in South Korea. *BMC Public Health*, *21*(1), 1395. https://doi.org/10.1186/s12889-021-11406-3

Hartini, Y. S., & Nugroho, L. H. (2020). Antibacterial effect of red betel (Piper crocatum) extract in combination with vancomycin against staphylococcus aureus. *Biodiversitas*, *21*(7), 3271–3274. https://doi.org/10.13057/biodiv/d210750

Heliawati, L., Lestari, S., Hasanah, U., Ajiati, D., & Kurnia, D. (2022). Phytochemical Profile of Antibacterial Agents from Red Betel Leaf (Piper crocatum Ruiz and Pav) against Bacteria in Dental Caries. *Molecules (Basel, Switzerland)*, *27*(9). https://doi.org/10.3390/molecules27092861

Herbig, M. E., Evers, D.-H., Gorissen, S., & Köllmer, M. (2023). Rational Design of Topical Semi-Solid Dosage Forms-How Far Are We? *Pharmaceutics*, *15*(7). https://doi.org/10.3390/pharmaceutics15071822

Hidayat, B., Ramadani, R. V., Rudijanto, A., Soewondo, P., Suastika, K., & Siu Ng, J. Y. (2022). Direct Medical Cost of Type 2 Diabetes Mellitus and Its Associated Complications in Indonesia. *Value in Health Regional Issues*, *28*, 82–89. https://doi.org/10.1016/j.vhri.2021.04.006

Hoekstra, M. J., Westgate, S. J., & Mueller, S. (2017). Povidone-iodine ointment demonstrates in vitro efficacy against biofilm formation. *International Wound Journal*, *14*(1), 172–179. https://doi.org/10.1111/iwj.12578

Ibrahim, N. 'Izzah, Wong, S. K., Mohamed, I. N., Mohamed, N., Chin, K.-Y., Ima-Nirwana, S., & Shuid, A. N. (2018). Wound Healing Properties of Selected Natural Products. *International Journal of Environmental Research and Public Health*, *15*(11). https://doi.org/10.3390/ijerph15112360

Ishikawa, J., & Horii, T. (2005). Effects of Mupirocin at Subinhibitory Concentrations on Biofilm Formation in Pseudomonas aeruginosa. *Chemotherapy*, *51*(6), 361–362. https://doi.org/10.1159/000088962

Januarti, I. B., Wijayanti, R., Wahyuningsih, S., & Nisa, Z. (2019). Potensi Ekstrak Terpurifikasi Daun Sirih Merah (Piper crocatum Ruiz &Pav) Sebagai Antioksidan Dan Antibakteri. *JPSCR: Journal of Pharmaceutical Science and Clinical Research*, *4*(2), 60–68. https://doi.org/http://dx.doi.org/10.20961/jpscr.v4i2.27206

Jupiter, D. C., Thorud, J. C., Buckley, C. J., & Shibuya, N. (2016). The impact of foot ulceration and amputation on mortality in diabetic patients. I: From ulceration to death, a systematic review. *International Wound Journal*, *13*(5), 892–903. https://doi.org/10.1111/iwj.12404

Kaul, K., Tarr, J. M., Ahmad, S. I., Kohner, E. M., & Chibber, R. (2013). *Introduction to Diabetes Mellitus BT - Diabetes: An Old Disease, a New Insight* (S. I. Ahmad (ed.); pp. 1–11). Springer New York. https://doi.org/10.1007/978-1-4614-5441-0_1

Kemenkes RI. (2017). *Farmakope Herbal Indonesia Edisi 2*. 561.

Li, Y., Ju, S., Li, X., Li, W., Zhou, S., Wang, G., Cai, Y., & Dong, Z. (2022). Characterization of the microenvironment of diabetic foot ulcers and potential drug identification based on scRNA-seq. *Frontiers in Endocrinology*, *13*, 997880. https://doi.org/10.3389/fendo.2022.997880

Matheson, E. M., Bragg, S. W., & Blackwelder, R. S. (2021). Diabetes-related foot infections: diagnosis and treatment. *American Family Physician*, *104*(4), 386–394.

Maulina, L., & Sugihartini, N. (2015). Formulasi gel ekstrak etanol kulit buah Manggis (Garcinia mangostana L.) dengan variasi gelling agent sebagai sediaan luka bakar. *Pharmaciana*, *5*(1), 43–52. https://doi.org/10.12928/pharmaciana.v5i1.2285

Navirius, F. J., Pamudji, G., & Herowati, R. (2023). Effect of red betel (Piper crocatum) leaf ethanol extract on increased creatinine and ureum levels in white rat wistar strain induced Streptozotosin-Nikotinamid. *Media Farmasi: Jurnal Ilmu Farmasi*, *20*(2), 57. https://doi.org/10.12928/mf.v20i2.25457

Nerdy, N., Barus, B. R., El-Matury, H. J., Ginting, S., Zebua, N. F., & Bakri, T. K. (2022). Comparison of flavonoid content and antioxidant activity in calyces of two roselle varieties (Hibiscus sabdariffa L.). *IOP Conference Series: Earth and Environmental Science*, *956*(1). https://doi.org/10.1088/1755-1315/956/1/012001

Purba, M. R., Wijaya, S., & Kasuma, A. (2022). Potential of red betel leaf extract (Piper crocatum) and Siwak (Salvadora persica) against Staphylococcus Aureus bacteria. *Bioscientia Medicina : Journal of Biomedicine and Translational Research*, *6*(5), 1728–1731. https://doi.org/https://doi.org/10.37275/bsm.v6i5.504

Puspita, P. J., Safithri, M., & Sugiharti, N. P. (2019). Antibacterial activities of Sirih Merah (*Piper crocatum*) leaf extracts. *Current Biochemistry*, *5*(3), 1–10. https://doi.org/10.29244/cb.5.3.1-10

Rachmawaty, F. J., Akhmad, M. M., Pranacipta, S. H., Nabila, Z., & Muhammad, A. (2018). Optimasi ekstrak etanol daun Sirih Merah (Piper Crocatum) sebagai antibakteri terhadap bakteri Staphylococcus Aureus. *Mutiara Medika: Jurnal Kedokteran Dan Kesehatan*, *18*(1), 13–19. https://doi.org/10.18196/mm.180109

Rahma, W. (2022). Uji aktivitas ekstrak etanol daun Sirih Merah (Piper crocatum) terhadap bakteri Propionibacterium acnes. *Jurnal Mahasiswa Kesehatan*, *4*(1), 53–61. https://doi.org/10.30737/jumakes.v4i1.2033

Rubio, J. A., Jiménez, S., & Lázaro-Martínez, J. L. (2020). Mortality in patients with diabetic foot ulcers: causes, risk factors, and their association with evolution and severity of ulcer. *Journal of Clinical Medicine*, *9*(9). https://doi.org/10.3390/jcm9093009

Sadeghpour, F. H., Zakrzewski, M., Vickery, K., Armstrong, D. G., & Hu, H. (2019). Bacterial diversity of diabetic foot ulcers: current status and future prospectives. *Journal of Clinical Medicine*, *8*(11). https://doi.org/10.3390/jcm8111935

Safithri, M., Andrianto, D., Gaisani Arda, A., Hawa Syaifie, P., Mardia Ningsih Kaswati, N., Mardliyati, E., Ramadhan, D., Miftah Jauhar, M., Wahyu Nugroho, D., Anggraini Septaningsih, D., Tria Melati, L., Hudayanti, M., Sarah, E., Alifibi Putera Irsal, R., & Taufiqu Rochman, N. (2023). The effect of red betel (Piper crocatum) water fraction as tyrosinase inhibitors: In vitro, molecular

docking, and molecular dynamics studies. *Journal of King Saud University - Science*, *35*(10), 102933. https://doi.org/10.1016/j.jksus.2023.102933

Salahi, P., Nasiri, M., Yazdanpanah, L., Khosravi, S., & Amini, M. R. (2024). Short-term effect of dressing with Dermaheal ointment in the treatment of diabetic foot ulcer: A double-blinded randomized controlled clinical trial. *Health Science Reports*, *7*(2), e1868. https://doi.org/10.1002/hsr2.1868

Setyawati, A., Sri, M., Wahyuningsih, H., Aris, D., Nugrahaningsih, A., Effendy, C., & Ibeneme, S. (2023). Piper crocatum Ruiz & Pav as a commonly used typically medicinal plant from Indonesia: What do we actually know about it? scoping review. *Indonesian Contemporary Nursing Journal*, *7*(2), 61–78.

Setyawati, A., Wahyuningsih, M. S. H., Nugrahaningsih, D. A. A., Effendy, C., Fneish, F., & Fortwengel, G. (2021). Piper crocatum Ruiz & Pav. ameliorates wound healing through p53, E-cadherin and SOD1 pathways on wounded hyperglycemia fibroblasts. *Saudi Journal of Biological Sciences*, *28*(12), 7257–7268. https://doi.org/10.1016/j.sjbs.2021.08.039

Shamsudin, N. F., Ahmed, Q. U., Mahmood, S., Ali Shah, S. A., Khatib, A., Mukhtar, S., Alsharif, M. A., Parveen, H., & Zakaria, Z. A. (2022). Antibacterial effects of flavonoids and their structure-activity relationship study: a comparative interpretation. *Molecules (Basel, Switzerland)*, *27*(4). https://doi.org/10.3390/molecules27041149

Shigeyama, M., Ohgaya, T., Kawashima, Y., Takeuchi, H., & Hino, T. (1999). Mixed base of hydrophilic ointment and purified lanolin to improve the drug release rate and absorption of water of minocycline hydrochloride ointment for treatment of bedsores. *Chemical & Pharmaceutical Bulletin*, *47*(6), 744–748. https://doi.org/10.1248/cpb.47.744

Suri, M. A., Azizah, Z., & Asra, R. (2021). A Review: Traditional Use, Phytochemical and Pharmacological Review of Red Betel Leaves (Piper Crocatum Ruiz & Pav). *Asian Journal of Pharmaceutical Research and Development*, *9*(1), 159–163. https://doi.org/10.22270/ajprd.v9i1.926

Taddese, S. M., Gurji, T. B., Abdulwuhab, M., & Aragaw, T. J. (2021). Wound healing activities of hydromethanolic crude extract and solvent fractions of bersama abyssinica leaves in mice. *Evidence-Based Complementary and Alternative Medicine : ECAM*, *2021*, 9991146. https://doi.org/10.1155/2021/9991146

Tanoey, J., & Becher, H. (2021). Diabetes prevalence and risk factors of early-onset adult diabetes: results from the Indonesian family life survey. *Global Health Action*, *14*(1), 2001144. https://doi.org/10.1080/16549716.2021.2001144

USP. (2007). *Hydrophilic Ointment: In United States Pharmacopeia Convention Committee of Revision (Ed.), United States Pharmacopeia* (29-NF4 ed.). In united states pharmacopeial convention committee of revision (Ed.).

Yan, X., Song, J.-F., Zhang, L., & Li, X. (2022). Analysis of risk factors for multidrug-resistant organisms in diabetic foot infection. *BMC Endocrine Disorders*, *22*(1), 46. https://doi.org/10.1186/s12902-022-00957-0

Zhao, Y., Dai, X., Sun, X., Zhang, Z., Gao, H., & Gao, R. (2023). Combination of Shengji ointment and bromelain in the treatment of exposed tendons in diabetic foot ulcers: study protocol for a non-blind, randomized, positive control clinical trial. *BMC Complementary Medicine and Therapies*, *23*(1), 359. https://doi.org/10.1186/s12906-023-04128-z

Pharmaciana
Vol.14, No.2, July 2024, Page. 220-232
ISSN: 2088 4559; e-ISSN: 2477 0256
DOI: 10.12928/pharmaciana.v14i2.28399

The effect of recompression and concentration of polyvinylpyrrolidone (PVP) K-30 on the quality of paracetamol tablets

Desak Made Rachel Angelina, Agatha Budi Susiana Lestari*
Faculty of Pharmacy, Sanata Dharma University
Paingan, Maguwoharjo, Depok, Sleman, Yogyakarta, Indonesia

Submitted: 11-02-2024 ***Reviewed: 03-04-2024*** ***Accepted: 28-06-2024***

ABSTRACT

Quality control during production is a critical process that ensures the quality of the tablets until they reach the consumer. In the pharmaceutical industry, reworking is possible, including tablet recompression. Nevertheless, the recompression process may have affected the potential of PVP K-30 as a binder to reunite the particles of tablet ingredients. However, the difference in PVP K-30 concentration might result in differences in granule and tablet characteristics. This study aims to determine whether there is an effect of recompression and the difference in PVP K-30 on the quality of paracetamol tablets. The effect of recompression and the difference in PVP K-30 was seen based on whether there is a significant difference in the physical properties of the mixture of tablet ingredients (mixture's flow rate and compressibility) and the tablets (compactibility, tablet hardness, friability, and disintegration time) from the formula with a concentration of 2% w/w and 4% w/w PVP K-30 after experiencing 2 times of recompression. Paracetamol tablets were made by the wet granulation method through the stages of granulation, lubrication, physical properties testing of the mixture, tablet compression, physical properties testing of tablets, crushing, and recompression. Data analysis was performed statistically using the Shapiro-Wilk normality test, followed by a two-way analysis of variance (ANOVA), or Kruskal-Wallis test, and post-hoc Mann-Whitney test. The results showed there was an effect of recompression and different concentrations of PVP K-30 on the potential of PVP K-30 as a binder, as seen from the significant differences in the physical properties of the mixture and tablets in each test group.

Keywords: recompression, polyvinylpyrrolidone (PVP) K-30, paracetamol tablets, wet granulation.

Corresponding author:
Agatha Budi Susiana Lestari
Faculty of Pharmacy, Sanata Dharma University
Paingan, Maguwoharjo, Depok, Sleman, Yogyakarta, Indonesia
Email: a_budi@usd.ac.id

INTRODUCTION

Tablet pharmaceutical dosage forms are a widely used and generally preferred pharmaceutical solid dosage form. Tablets are easy and convenient to use, more accurate in dosage, and more stable in storage and distribution (Al-Zoubi et al., 2021). In addition to active pharmaceutical ingredients, tablets also contain excipients such as filler, binder, lubricant, disintegration, and if required a sweetening agent, flavoring agent, and coloring agent (Iqubal et al., 2014). Paracetamol is a drug with antipyretic and anti-inflammatory indications (Sugiyono et al., 2017). This active pharmaceutical ingredient has poor flow and compressibility characteristics, it had a wide particle size distribution (PSD) of irregular particles, which caused poor flowability and a high difference between bulk and tapped densities (Šimek et al., 2017). One way to improve these characteristics of paracetamol, is to produce paracetamol tablets using the wet granulation method. The wet granulation method is carried out by granulating the tablet ingredients with a liquid binder (Hiremath et al., 2019). Particle size enlargement and a more uniform shape of particles caused by granulation improve tablet materials' flow and compressibility characteristics.

Binders ensure that tablets, powders, granules and others can be formed with the required mechanical strength. Polyvinylpyrrolidone (PVP) K-30 is one of the binders that is commonly used in tablet manufacturing. In the tablet formulation, PVP K-30 as a binder was added at a concentration of 0.5-5% w/w (Sheskey et al., 2017). As a binder, PVP K-30 can produce granules with better flow characteristics, as well as higher binding strength and lower friability (Hiremath et al., 2019).

The quality of the tablet material mixture affects the quality of the tablet produced (Janssen et al., 2023). Evaluation of the mixture includes flow rate, compressibility, and compactibility. Besides, the quality of tablets is generally evaluated by their organoleptic, weight uniformity, hardness, friability, disintegration, and dissolution time profiles. The binder, as one of the essential components of the tablet, may influence the quality of the tablet. The amount of binder added to a tablet formula influences the physical characteristics of the granules and tablets produced. The addition of a large amount of binder produces tablets with high hardness characteristics and slow disintegration and dissolution times. Otherwise, a small amount of binder produces tablets with high friability characteristics (Puspita et al., 2022).

In tablet manufacturing, tablet quality is monitored from the material in the process to the finished product. However, occasionally the pharmaceutical industry faces problems related to the quality of tablets that do not meet the specifications required. To overcome the problem, the pharmaceutical industry could take reworking action against the problematic batch (BPOM, 2018). These processes are taken to obtain pharmaceutical dosage forms that fulfill quality criteria. During tablet manufacturing, the reworking action that could be carried out is recompression.

Recompression is the repeated compression of tablets under the same conditions as the first compression (Rojas et al., 2015). Nevertheless, crushing and recompression might alter of the mixtures and tablets physical characteristics. Related research that was conducted by (Rojas et al., 2015) shows that recompression caused a decrease in particle size, reduced porosity, increased compactibility, and decreased flow rate of the tablet material mixture. Otherwise, (Gamlen et al., 2015) conducted similar research that showed repeated compression and precompression did not affect the tensile strength of Avicel PH 101 tablets, although there was a small effect on the friability and disintegration time of the tablets. Moreover, there is an effect that decreased the tensile strength and increased the disintegration time of dicalcium phosphate dihydrate (DCP) tablets but improved the tensile strength and friability of Starch 1500 tablets. This study aims to determine whether there is an effect of recompression on the quality of paracetamol tablets.

MATERIALS AND METHOD

Materials

The materials that are used are paracetamol pharmaceutical grades, polyvinylpyrrolidone (PVP) K-30 pharmaceutical grades, lactose pharmaceutical grades, croscarmellose sodium pharmaceutical grades, talc pharmaceutical grades, magnesium stearate pharmaceutical grades, and aquadest.

Instruments

The instruments that are used are analytical balances Pioneer PA213 (OHAUS Stuccler, Putian, China), all-purpose machine GmBH AR 401(Erweka, Langen, Germany), sieve (cust, Indotest Multi Lab), flowability tester GmBH (Erweka, Langen, Germany), tap density volumizer HY-100B (Wincom Company Ltd., Changsha, China), drying cabinet, single punch tablet press machine (Korsch Maschinefabrik Berlin), vacuum (Chefinox Boombastic), friability tester CS-2 (Lorderan, Shanghai, China), hardness tester (Pharma Test PTB 302), disintegration tester Develop BJ-2 (Laboao International, Zhengzhou, China), Spectrophotometer UV-Vis (Shimadzu), mortar and stamper.

Methods

Preparation of PVP K-30 solution

This study used two levels of PVP K-30 concentration which are 2% w/w as formula 1 and 4% w/w as formula 2. PVP K-30 solution was prepared by dissolving PVP K-30 powder in aquadest solvent at concentration of 10% w/v for formula 1 and 20% w/v for formula 2.

Granulation method

Paracetamol, lactose, and ⅓ amount of croscarmellose sodium (Table 1) were weighing and mixed in a cube mixer with the mixer running for 15 minutes. The mixture was granulated by adding PVP K-30 solution little by little, up to 90 mL. The wet mass was milled to form granules through a sieve manually.

The wet granules were dried in the drying cabinet at a temperature of 50ºC. The moisture content of granules was checked every 24 hours, and the moisture content was calculated by the following Equation 1.

$$\%\ Moisture\ content = 100 \times \left(\frac{weight\ of\ wet\ granules - weight\ of\ dry\ granules}{weight\ of\ dry\ granules}\right) \quad \text{.....(1)}$$

The required moisture content of dried granules is not more than 5% (Crouter&Briens, 2013). Afterwards, the dried granules were sieved with 12/50 number mesh of sieve.

Lubrication method

Granules, ⅔ amount of croscarmellose sodium, and talc were mixed by mixer for 5 minutes. After the first mixing, magnesium stearate was added to the mixture, and the mixer was running for 5 minutes.

Mixture characteristic evaluation

Flowrate test

A total of 100 g of the mixture was loaded into the hopper of the flowability tester and the "START" button was pressed. The flow rate of the mixture tested was shown on the instrument screen. The requirement for a free to flow rate is > 10 g/s (Setyono & Purnawiranita, 2021). This measurement was taken 3 times.

Compressibility test

A total of 40 g of the mixture was loaded into the 100mL graduated cylinder without any tapping and then tapping 500 times using a tap volumeter. The closest scale of the graduated cylinder where the top of the mixture stuck before tapping was noted as starting volume (V_0) while after tapping it was noted as final volume (V_f). The compressibility of the mixture was determined by calculating the compressibility index using the following Equation 2.

$$compressibility\ index = 100\ x\ (\frac{V_0 - V_f}{V_0}) \quad \text{.....(2)}$$

If the mixture has excellent compressibility, it is indicated by a compressibility index <10%. This measurement was taken 3 times.

Table 1. The formula of paracetamol tablet

Ingredients	Function	Composition (mg)	
		Formula 1	Formula 2
Paracetamol	API	300	300
Lactose	Filler	238	226
PVP K-30	Binder	12	24
Aquadest	Binder solvent	90	90
Croscarmellose sodium	Disintegrant	20	20
Talc	Glidant	27	27
Magnesium Stearate	Lubricant	3	3

Notes:
Formula 1: formula with the concentration of 2% w/w PVP K-30
Formula 2: formula with the concentration of 4% w/w PVP K-30

Compactibility test

A portion of the mixture was compressed into tablets with various compression pressures by downscaling the upper punch scale from 1 mm, 2 mm, 3 mm, 4 mm, 5 mm, 6 mm, 7 mm, 8 mm, and 9 mm. Compactibility was measured according to the hardness of the tablet that was able to be compressed at each pressure applied, this measurement was taken three times.

Tablet compression

The mixture was compressed into tablets using a single-punch tablet press machine. The compression pressure was set based on the results of the previous orientation to produce tablets with a weight of 600 mg and a hardness in the range of 4-8 kg which is the upper punch with downscaling at 11 mm and the lower punch at 13 mm. The mixture was compressed with the same compression pressure for each formula.

Tablet characteristic evaluation

Organoleptic test

Tablets from each formula and each compression were tested organoleptically through sensory testing including tablet shape, color, and odor.

Weight uniformity test

One tablet taken randomly from each formula at each compression was determined for its assay using a UV spectrophotometer. The A value is calculated as the percentage of the measured amount of active ingredient content over the amount indicated in the etiquette. A total of 10 random tablets from each formula at each compression were weighted (w_i) and the average weight was calculated (w bar). The estimated content (X_i) of each tested tablet unit was calculated by the following Equation 3.

$$X_i = w_i \times (\frac{A}{\overline{W}}) \quad \text{.....(3)}$$

The weight variation was determined by calculating the acceptance value (NP) by the following Equation 4.

$$NP = \left|M - \bar{X}\right| + ks \quad \text{..... (4)}$$

Where M is the reference value, X is the average of the estimated contents of each unit of tablet tested, k is the acceptability constant (if n = 10, then k = 2.4; if n = 30, then k = 2.0), and s is the standard deviation. Weight variation is fulfilled if the acceptance value of the first 10 tablet units is not more than or equal to L1%. If the acceptance value is greater than L1%, then the weight variation test is applied to an additional 20 units of tablets (Direktorat Jenderal Kefarmasian dan Alat Kesehatan, 2020).

Hardness test

A total of five tablets taken randomly from each formula at each compression and recompression were placed on the pressing pad, and then the "START" button was pressed to operate the hardness tester. The hardness result (kg) of the tested tablets will be shown on the screen of the hardness tester instrument. Tablet hardness measurement was done three times with the requirement of good tablet hardness between 4-8 kg (Rori et al., 2016).

Friability test

A total of 20 tablets randomly chosen from each formula in each compression and recompression were weighed after removing any loose dust from those tablets first. The weight result was determined as the initial weight. The tablets were put into the friability tester and operated with 100 rotations. The tablets were removed from the instrument and dedusted again. Twenty tablets were weighed, and the weight result was determined as the final weight. Tablet friability was evaluated based on its percentage friability which was measured by the following Equation 5.

$$\%\ friability = \frac{initial\ weight - final\ weight}{initial\ weight} \times 100\% \quad \text{....(5)}$$

The requirement for good friability is % friability of no more than 1% (Rori et al., 2016). The measurement was taken 3 times.

Disintegration test

One tablet taken randomly from each formula at each compression and recompression was placed in each of the six tubes in the basket. The basket was dipped in a medium of water at a temperature of 37±2°C, then the disintegration tester was turned on. The requirement for a good tablet disintegration time is that the tablet be destroyed in no more than 15 minutes (Rori et al., 2016).

Crushing

All tablets remaining after the physical characteristics testing were crushed using a mortar and stamper with a constant crushing force. The mixture was sieved using a sieve with a mesh number 12/50. Crushing was repeated twice for each formula.

Tablet recompression

The sieved mixture from the crushing step was recompressed using a single punch tablet compression machine with the same compression method as the first tablet compression. Recompression was done twice for each formula.

Data Analysis

The data obtained were the results of the physical characteristics testing of the mixture, including flow rate, compressibility, and compactibility of the mixture; and the physical characteristics of the tablets, including hardness, friability, and disintegration time of the tablets. The data distribution was tested with the Shapiro-Wilk normality test. If the data is normally distributed, statistical analysis of the data is continued using the two-way analysis of variance (ANOVA) test, if it is not normally distributed, it is continued using the Kruskal-Wallis test with a confidence level of 95% and a p-value <0.05. Kruskal-Wallis's analysis then continued with the post-hoc Mann-Whitney test to find out the differences between the data groups. Significant differences between the data groups shown statistically identify the effect of re-compression and concentration of PVP K-30 on the physical characteristics of the mixture and the tablets produced.

RESULT AND DISCUSSION

In this study, binder concentrations of 2% and 4% were used, taking into consideration that the concentration range of PVP K30 as a binder was 0.5-5%, so concentrations of 2% and 4% could be used to see the effect of different PVP concentrations on the physical properties of the paracetamol tablet. The granules were tested for moisture content using the gravimetric method, and the moisture content of the formula 1 granules was 2.92% and the formula 2 granules was 3.77%. The mixture is a combination of granules and powders of disintegrant, and lubricant material mixed at the lubrication step. Testing of the physical characteristics of the mixture was carried out on the initial mixture before compression (mixture I), the mixture of crushed tablets from the first compression (mixture II), and the mixture of crushed tablets from the first re-compression (mixture III). Before testing, the whole mixture was sieved first with a 12/50 mesh sieve. Testing of the physical properties of tablets was performed on the first compressed tablet (tablet I), the first re-compressed tablet (tablet II), and the second re-compressed tablet (tablet III). Recompression of the tablet was conducted twice because of the lack of a tablet machine, that couldn't compress for the third recompression.

Physical characteristics testing of mixtures

The physical characteristics of the mixture are observed based on the flowability and compactibility of the mixture. Good mixture flow is necessary to ensure uniform filling into the die hole, which directly determines the weight variation of the tablets. The flow characteristics of the mixture was performed by measuring the flow rate and compressibility of the mixture as shown in Table 2.

Flow rate through an orifice is generally measured as the mass of material per unit time flowing from any of several types of containers (cylinders, funnels, hoppers). It is thought to be a more direct measure of flow than measurements such as angle of repose (Amidon et al, 2017). Shape, size, and size distribution factors greatly influence the flow characteristics of the mixture. A spherical particle shape will improve the flow of the mixture (Chen et al., 2019). However, in this study, the particle shape of the mixture was not examined in detail, so it could not be ascertained how it looked before and after crushing.

Table 2. The flow characteristic of the powder mixture in each formula

The parameter of flow characteristics	Formula 1			Formula 2		
	Mixture I	Mixture II	Mixture III	Mixture I	Mixture II	Mixture III
Flow rate (g/s) $\bar{X} \pm$ SD	42.9±2.2	32.7±1.6	29.2±1.8	47.0±2.6	39.0±0.9	31.7±2.4
Carr index (%) $\bar{X} \pm$ SD	3.3±0.04	8.4±1.01	7.4±0.1	6.0±0.7	7.8±1.1	7.1±0.1

Notes:

$\bar{X}$: average of 3 measurements

SD : standard deviation
Formula 1 : formula with the concentration of 2% w/w PVP K-30
Formula 2 : formula with the concentration of 4% w/w PVP K-30
Mixture I : initial mixture
Mixture II : the mixture of crushed tablets from the first compression
Mixture III: the mixture of crushed tablets from the first re-compression

The results showed that the flow rate and compressibility index of the mixture of both formulas before and after compression-recompression were > 10 grams/second and < 10%, respectively, so the mixture was classified as having good flow characteristics. The results of Kruskal-Wallis's analysis showed p-values of 0.009 and 0.014 respectively, for the test groups of flow rate and compressibility of the mixture. Mann-Whitney follow-up test showed that there was an effect of re-compression and different concentrations of PVP K-30 on the flow rate and compressibility of the mixture. In this research, the recompression process was still carried out, even though the powder mixture profile and physical properties of the tablets had met the requirements, considering that this research aimed to see the effect of recompression on the quality of the paracetamol tablet. One of the limitations of this research is that the crushing process was carried out manually, not using a special machine. This can affect the particle size distribution of the granules produced and the flow characteristics of the granules after recompression.

The mixture of formula 2 with a higher concentration of PVP K-30 has a faster flow rate than the mixture of formula 1. The higher the concentration of binders, the greater the cohesiveness of the powder to form granules and the larger the granule's size (Köster & Kleinebudde, 2024). Research conducted by (Puspita et al., 2022) showed similar results whereby a large granule size reduces friction between particles and the hopper wall. In addition, the gravity increases as the granule size increases, making the mixture's flow easier (Schlick-Hasper et al., 2022).

In contrast, crushing after compression and re-compression caused a decrease in flow rate and an increase in the compressibility index of the mixture, although it was still within the required range. The manual crushing technique with an attempted constant crushing force could not guarantee the same force at each crushing. Overpowering crushing produces small particles or fines, while underpowering produces large particles. Although the size distribution is maintained by sieving, there is an increase in fines due to crushing.

Small particle size creates a larger specific surface area and increases interaction between the mixture particles and the hopper surface, which prevents the flow of the mixture (Syukri, 2018). Small particles tend to fill up the large particle pores, increasing the volume reduction and thus increasing the compressibility index of the mixture (Ulusoy, 2023). The initial mixture before the first compression has the highest flow rate and the smallest compressibility index value because its particles have better uniform shape, size, and size distribution. The lesser inter-particle interaction causes the mixture to flow and settle more easily (Khaidir et al., 2015).

Compactibility is the ability of a material to form tablets of sufficient tensile strength under the effect of densification and is strongly correlated with the strength of interparticulate bonds in the compact (bonding strength) (Apeji et al, 2019). The parameter of the mixture's compactibility is the hardness of the tablet compressed with various compression pressures (Huda & Sari, 2021). The mixture that can form hard tablets under applied pressure without showing a tendency to caping possesses good compactibility. Table 3 shows the hardness results of the compactibility test with a 10 mm lower punch.

Fines increased due to crushing will fill the pores between particles thus the porosity decreases and the hardness and compactibility of the mixture increase (Solikhati et al., 2022. The increased compactibility of mixtures II and III is indicated by an increase in tablet hardness on the same punch scale as mixture I. Meanwhile, the mixture that became tighter as recompression led to the machine's

inability to compress the tablets with higher pressure. At the upper punch downscale of 8 mm (except mixture I of formula 1) and downscale of 9 mm, all mixtures could not be compressed due to the machine jamming and releasing a loud noise. Recompression caused increased compactibility of the mixtures, resulting in increased hardness of the tablets at each compression.

Table 3. The compactibility of the powder mixture in each formula

Downscaling upper punch (mm)	Tablet's hardness (kg)					
	Formula 1			Formula 2		
	Mixture I	Mixture II	Mixture III	Mixture I	Mixture II	Mixture III
1	*	*	*	*	*	*
2	*	*	*	*	*	*
3	*	*	*	*	*	*
4	*	*	*	*	*	*
5 ± SD	0.05±0.01	0.46±0.05	1.06±0.12	0.07±0.01	0.39±0.04	1.68±0.19
6 ± SD	0.16±0.05	3.46±0.24	4.59±0.31	0.77±0.23	4.58±0.28	5.56±0.44
7 ± SD	2.28±0.50	5.66±0.06	6.97±0.25	3.8±0.08	7.47±0.42	9.29±0.23
8 ± SD	4.66±0.28	#	#	#	#	#
9	#	#	#	#	#	#

Notes:
The result is an average of 3 measurement
* : the mixture could not yet compress
# : the machine cannot compress the mixture
Formula 1 : formula with the concentration of 2% w/w PVP K-30
Formula 2 : formula with the concentration of 4% w/w PVP K-30
Mixture I : initial mixture
Mixture II : the mixture of crushed tablets from the first compression
Mixture III : the mixture of crushed tablets from the first re-compression

The mixture of formula 2 with 4% w/w PVP K-30 produced tablets with higher hardness than the mixture of formula 1 with 2% w/w PVP K-30 at the same punch scale. This indicates that the concentration of binder could affect the tablet hardness (Mahours et al, 2017). Binders play a role in forming compact tablets through compression.

Kruskal-Wallis statistical analysis was applied to the 5 mm and 6 mm compactibility test groups, with p-value of 0.006 for both test groups. The follow-up Mann-Whitney test showed that there was an effect of recompression action and different concentrations of PVP K-30 on the compactibility of the mixture. Meanwhile, the 7 mm compactibility test group was statistically analysed with the two-way Anova test and obtained a p-value <0.001 for the formula and compression variables, and p value of 0.069 for the interaction between formula and compression. In compactibility analysis, a different statistical method is used because the data is not normally distributed, so two-way anova analysis cannot be used, and must use Kruskal-Wallis's analysis.

Physical characteristics testing of tablets

Tablets from both formulas as a result of each compression had an organoleptic round shape, white in colour (Figure 1 and 2) and were odourless. However, caping occurred in the tablets from the first and second re-compression of formula 1 (Figure 1). One of the causes of caping is the lack of binding agent concentration in tablets (Mashabai et al., 2022). Besides, increased fines can lead to caping because there is air entangled between the fines in the mixture which expands when the compression pressure is released. The presence of capping in the recompression process can be caused by

differences in particle size distribution that are too large, resulting in a void volume containing air. As a result, when it is compressed, the air trapped in the powder will try to escape, causing tablet to cap.

Figure 1. The organoleptic of paracetamol tablet resulted from Formula 1 (A) first compression tablet (B) first recompression tablet (C) second recompressed tablet

Figure 2. The organoleptic of paracetamol tablet resulted from Formula 2 (A) first compression tablet (B) first recompression tablet (C) second recompressed tablet

Tablet compression pressure influences the physical properties of the tablets produced. In this study, the tablet compression pressure was kept the same for each compression and recompression so that the physical properties of the tablets produced could be compared. However, as the study goes on, the reality is that crushing, and recompression cause the physical properties of the mixture to change. These changes caused the machine to be unable to recompress the tablets at the initial pressure. Nonetheless, the compression pressure was kept the same for each compression as much as possible, considering the ability of the tablet compression machine to lower the pressure when required. Table 4 shows the physical characteristics of the tablet.

Weight variation for tablets with active ingredient content > 25% of tablet weight is taken to ensure uniformity of active ingredient content in tablets. Weight variation is strongly influenced by the flow characteristics of the mixture, the more uniform the amount of mixture that enters the die hole resulting the more uniform the tablet weight (Puspita et al., 2022). The results in Table IV show that the tablets of both formulas in each compression and recompression have met the requirements of the weight variation acceptance criteria, which is NP of the first 10 tablet units is maximum 15. All mixtures still qualify for good flow characteristics so weight variation can still be achieved.

Tablet hardness describes the overall resistance of the tablet to mechanical stresses such as cracking and breaking of the tablet. Tablet hardness increases with the amount of recompression applied. The greater the number of compressions, the denser the particles of the crushed tablet mixture. In the second compression, the tablet was compressed twice and crushed twice so that the particles of the mixture were more compact, and the tablets produced had the highest hardness. Only

tablet III did not meet the hardness requirement of 4-8 kg. Meanwhile, the higher the concentration of binder, the harder the tablet produced (Osman et al., 2019). Tablets of formula 2 have a higher hardness than tablets of formula 1.

Table 4. Physical characteristics testing of paracetamol tablets

Physical characteristics	Tablet					
	Formula 1			Formula 2		
	I	II	III	I	II	III
Weight variation (NP)	2.9	2.33	4.95	8.05	3.03	3.38
Hardness (kg) $\bar{X}$ ±SD	4.4±0.04	5.4±0.09	6.6±0.07	4.5±0.03	7.01±0.11	13.3±0.09
Friability (%) $\bar{X}$ ± SD	0.58±0.16	6.32±0.15	5.72±0.64	0.48±0.02	2.97±0.28	1.09±0.11
Disintegration time (minutes) $\bar{X}$ ± SD	0.75±0.16	1±0,03	1.28±0.03	1.40±0.02	2.37±0.06	2.54±0.03

Notes :

NP : acceptance value

$\bar{X}$: average of 3 measurements

SD : standard deviation

Formula 1 : formula with the concentration of 2% w/w PVP K-30

Formula 2 : formula with the concentration of 4% w/w PVP K-30

I : tablet from first compression

II : tablet form first recompression

III : tablet from second recompression

Tablet friability describes the resistance of the tablet surface to friction or scraping (Osei-Yeboah & Sun, 2015). The results showed that only the first compressed tablets from both formulas met the requirements of good tablet friability of < 1%. The increase in friability in tablets from re-compression may be due to crushing after compression, which has created a new surface on the mixture particles that may not contain a binder. It decreases the binding force between particles so that the resistance on the tablet surface decreases and the friability increases (Suhery et al., 2016). However, there was a decrease in the % friability of the tablets from the second re-compression compared to the first recompressed tablets. This was probably due to an increase in hardness, where the harder the tablet, the lower the friability (Khaidir et al., 2015). In general, an increase in tablet hardness is accompanied by a decrease in tablet friability. In this study, the increase in tablet hardness was accompanied by an increase in friability as well. This can be caused by differences in particle distribution that are too large, so that the presence of fine-sized particles will increase the brittleness of the tablet when compressed.

In addition, the fines that caused the capping of the re-compressed tablets from Formula 1 resulted in the highest % friability of the tablets. Tablets of Formula 2 did not have capping which resulted in a smaller % friability because the binder reduced the friability of the tablets produced. Polyvinylpyrrolidone (PVP) K-30 as a binder produces fewer fines (Putra et al., 2019).

Tablet disintegration time describes the time required for a tablet to disintegrate after contact with the gastrointestinal fluid (Khaidir et al., 2015). All tablets had a good disintegration time of no more than 15 minutes. The re-compression action and higher concentration of PVP K-30 led to an increase in tablet disintegration time. The porosity of the tablets that decreased along with the number of recompressions caused the tablets to absorb water slower, and the longer it took for the tablets to

disintegrate (Rahayu & Anisah, 2021). Meanwhile, higher concentrations of binders produce stronger granule bonds and harder tablets that prevent the tablets from disintegrating easily.

Two-way ANOVA statistical analysis was applied to the tablet hardness, friability, and disintegration time test data groups. All test data groups produced p values <0.001 in the variable's formula, number of compressions, and interaction between formula and number of compressions. These results mean that there is an effect of different concentrations of PVP K-30 and re-compression, and there is a relationship between different concentrations of PVP K-30 and re-compression on the physical properties of tablet hardness, friability, and disintegration time.

CONCLUSION

It can be concluded that there is a significant effect of recompression and different concentrations of PVP K-30 on the physical properties of the mixture (flow rate, compressibility, and compactibility of the mixture) and the physical properties of paracetamol tablets (tablet hardness, friability, and disintegration time).

ACKNOWLEDGEMENT

The authors would like to thank to PT. Konimex, for the support of research material and LPPM Sanata Dharma University, for the support of research funding.

REFERENCES

Al-Zoubi, N., Gharaibeh, S., Aljaberi, A., & Nikolakakis, I. (2021). Spray drying for direct compression of pharmaceuticals. *Processes*, *9*(2), 267. https://doi.org/10.3390/pr9020267

Amidon, G. E., Meyer, P. J., & Mudie, D. M. (2017). Chapter 10—Particle, Powder, and Compact Characterization. In Y. Qiu, Y. Chen, G. G. Z. Zhang, L. Yu, & R. V. Mantri (Eds.), *Developing Solid Oral Dosage Forms (Second Edition)* (pp. 271–293). Academic Press. https://doi.org/10.1016/B978-0-12-802447-8.00010-8

Apeji, Y. E., Olayemi, O. J., Anyebe, S. N., Oparaeche, C., Orugun, O. A., Olowosulu, A. K., & Oyi, A. R. (2019). Impact of binder as a formulation variable on the material and tableting properties of developed co-processed excipients. *SN Applied Sciences*, *1*(6), 561. https://doi.org/10.1007/s42452-019-0585-2

BPOM. (2018). *Pedoman cara pembuatan obat yang baik (CPOB)*. Direktorat Pengawasan Produksi Obat, Narkotika, Psikotropika, dan Prekursor Badan Pengawas Obat dan Makanan.

Chen, K., Hou, B., Wu, H., Huang, X., Li, F., Xiao, Y., Li, J., Bao, Y., & Hao, H. (2019). Hollow and solid spherical azithromycin Particles Prepared by Different Spherical Crystallization Technologies for Direct Tableting. *Processes*, *7*(5), 276. https://doi.org/10.3390/pr7050276

Crouter, A., & Briens, L. (2013). The Effect of Moisture on the Flowability of Pharmaceutical Excipients. *AAPS PharmSciTech*, *15*(1), 65–74. https://doi.org/10.1208/s12249-013-0036-0

Direktorat Jenderal Kefarmasian dan Alat Kesehatan. (2020). *Farmakope Indonesia (Edisi VI)*,. Jakarta: Kementrian Kesehatan Republik Indonesia.

Elisabeth, V., Y., P. V., YamLean, & Supriati, H. S. (2018). Formulasi sediaan granul dengan bahan pengikat pati kulit pisang Goroho (*Musa Acuminafe* L.) dan pengaruhnya pada sifat fisik granul. *Pharmacon*, *7*(4), 1–11. https://doi.org/10.35799/pha.7.2018.21416

Gamlen, M. J. D., Martini, L. G., & Al Obaidy, K. G. (2015). Effect of repeated compaction of tablets on tablet properties and work of compaction using an instrumented laboratory tablet press. *Drug Development and Industrial Pharmacy*, *41*(1), 163–169. https://doi.org/10.3109/03639045.2013.850715

Hiremath, P., Nuguru, K., & Agrahari, V. (2019). Material attributes and their impact on wet granulation process performance. In *Handbook of Pharmaceutical Wet Granulation* (pp. 263–315). Elsevier. https://doi.org/10.1016/B978-0-12-810460-6.00012-9

Huda, C., & Sari, T. A. (2021). *Buku ajar teknologi sediaan Solida*. Media Nusa Creative (MNC

Publishing).
Iqubal, M. K., Singh, P. K., Shuaib, M., Iqubal, A., & Singh, M. (2014). Recent advances in direct compression technique for Pharmaceutical tablet formulation. *International Journal of Pharmaceutical Research and Development*, *6*(1), 49–57.
Janssen, P. H. M., Fathollahi, S., Bekaert, B., Vanderroost, D., Roelofs, T., Vanhoorne, V., Vervaet, C., & Dickhoff, B. H. J. (2023). Impact of material properties and process parameters on tablet quality in a continuous direct compression line. *Powder Technology*, *424*, 118520. https://doi.org/10.1016/j.powtec.2023.118520
Khaidir, S., Murrukmihadi, M., & Kusuma, A. P. (2015). Formulasi tablet ekstrak kangkung air (*Ipomoea aquatica* F.) dengan variasi kadar amilum manihot sebagai bahan penghancur. *Jurnal Ilmiah Farmasi*, *11*(1), 1–8. https://doi.org/10.20885/jif.vol11.iss1.art1
Khairnar, R.G., Darade, A.R., Tasgaonkar R.R. (2024). A review on tablet binders as a pharmaceutical excipient. *World Journal of Biology Pharmacy and Health Sciences, 17(03),* 295-302. https://doi.org/10.30574/wjbphs.2024.17.3.0142
Köster, C., & Kleinebudde, P. (2024). Evaluation of binders in twin-screw wet granulation – Optimization of tabletability. *International Journal of Pharmaceutics*, *659*, 124290. https://doi.org/10.1016/j.ijpharm.2024.124290
Mahours, G. M., Shaaban, D. E. Z., Shazly, G. A., & Auda, S. H. (2017). The effect of binder concentration and dry mixing time on granules, tablet characteristics and content uniformity of low dose drug in high shear wet granulation. *Journal of Drug Delivery Science and Technology*, *39*, 192–199. https://doi.org/10.1016/j.jddst.2017.03.0014
Mashabai, I., Ruspendi, R., & Syauqi, M. I. (2022). Analisa permasalahan sticking pada tablet XYZ menggunakan metode PDCA di PT. Sunthi Sepuri. *Jurnal Pendidikan Dan Aplikasi Industri UNISTEK*, *9*(1), 19–27. https://doi.org/10.33592/unistek.v9i1.2067
Osei-Yeboah, F., & Sun, C. C. (2015). Validation and applications of an expedited tablet friability method. *International Journal of Pharmaceutics*, *484*(1), 146–155. https://doi.org/10.1016/j.ijpharm.2015.02.061
Osman, Z., Adam, N. S., Hassan, H. A., & Nur, A. O. (2019). Influence Of Binding Solution Concentration, Drying Duration And Drying Temperature On Physiochemical Performance Of Norfloxacin Granules And Tablets. *International Journal of Pharmacy and Pharmaceutical Sciences*, 71–79. https://doi.org/10.22159/ijpps.2019v11i10.17612
Puspita, O. E., G. Ebtavanny, T., & A. Fortunata, F. (2022). Studi pengaruh jenis bahan pengikat sediaan tablet dispersi Solid Kunyit terhadap profil disolusi ekstrak Kunyit (*Curcuma domestica*). *Pharmaceutical Journal of Indonesia*, *8*(1), 95–102. https://doi.org/10.21776/ub.pji.2022.008.01.10
Putra, D. J. S., Antari, N. W. Y., Putri, Arisanti, C. I. S., & Samirana, P. O. (2019). Penggunaan polivinill pirolidon (PVP) sebagai bahan pengikat pada formulasi tablet ekstrak Daun Sirih (*Piper betle* L.). *Jurnal Farmasi Udayana*, *8*(4), 14. https://doi.org/10.24843/JFU.2019.v08.i01.p03
Rahayu, S., & Anisah, N. (2021). Pengaruh variasi konsentrasi amprotab sebagai desintegrant terhadap sifat fisik tablet ekstrak Buah Pare *(Momordica charantia* L.). *Jurnal Ilmiah Ibnu Sina (JIIS): Ilmu Farmasi Dan Kesehatan*, *6*(1), 39–48. https://doi.org/10.36387/jiis.v6i1.572
Rojas, J., Zuluaga, C., & Cadavid, A. (2015). Effect of reprocessing and excipient characteristics on ibuprofen tablet properties. *Tropical Journal of Pharmaceutical Research*, *14*(7), 1145. https://doi.org/10.4314/tjpr.v14i7.4
Rori, W. M., Y.Yamlean, P. V., & Sudewi, S. (2016). Formulasi dan evaluasi sediaan tablet ekstrak daun Gedi Hijau (*Abelmoschus manihot*) dengan metode Granulasi Basah. *Pharmacon*, *5*(2), 243–250. https://doi.org/10.35799/pha.5.2016.12212
Schlick-Hasper, E., Bethke, J., Vogler, N., & Goedecke, T. (2022). Flow properties of powdery or granular filling substances of dangerous goods packagings—Comparison of the measurement of the angle of repose and the determination of the Hausner ratio. *Packaging Technology and Science*, *35*(10), 765–782. https://doi.org/10.1002/pts.2678
Setyono, B., & Purnawiranita, F. A. (2021). Analysis of Flow Characteristics and Paracetamol Tablet

Hardness Using 2D Double Mixer of Design Drum Type with Rotation and Mixing Time Variations. *Journal of Mechanical Engineering, Science, and Innovation*, *1*(2), 38–48. https://doi.org/10.31284/j.jmesi.2021.v1i2.2282

Sheskey, P. J., Cook, W. G., & Cable, C. G. (2017). *Handbook of Pharmaceutical Excipients (8th edition)*. London: Pharmaceutical Press.

Šimek, M., Grünwaldová, V., & Kratochvíl, B. (2017). Comparison of compression and material properties of differently shaped and sized paracetamols. *KONA Powder and Particle Journal*, *34*, 197–206. https://doi.org/10.14356/kona.2017003

Solikhati, A., Rahmawati, R. P., & Kurnia, S. D. (2022). Analisis mutu fisik granul ekstrak kulit manggis dengan metode granulasi basah. *Indonesia Jurnal Farmasi*, *7*(1), 1. https://doi.org/10.26751/ijf.v7i1.1421

Sugiyono, Komariyatun, S., & Hidayati, D. N. (2017). Formulasi tablet parasetamol menggunakan tepung bonggol pisang kepok (*Musa paradisiaca* cv. Kepok) sebagai bahan pengikat. *Media Farmasi Indonesia*, *12*(1), 1156–1166.

Suhery, W. N., Fernando, A., & Giovanni, B. (2016). Perbandingan metode Granulasi basah dan kempa langsung terhadap sifat fisik dan waktu hancur orally disintegrating tablets (ODTs) Piroksikam. *Jurnal Sains Farmasi & Klinis*, *2*(2), 138. https://doi.org/10.29208/jsfk.2016.2.2.65

Syukri, Y. (2018). *Teknologi sediaan obat dalam bentuk solid*. Universitas Islam Indonesia.

Ulusoy, U. (2023). A review of particle shape effects on material properties for various engineering applications: from macro to nanoscale. *Minerals*, *13*(1), 91. https://doi.org/10.3390/min13010091

Pharmaciana
Vol.14, No.2, July 2024, Page. 233-241
ISSN: 2088 4559; e-ISSN: 2477 0256
DOI: 10.12928/pharmaciana.v14i2.25827

Phytochemical and antibacterial analyses of essential oils extracted from the leaves of *Euodia suaveolens* Scheff

Boy Rahardjo Sidharta[1*], Patricius Kianto Atmodjo[2]
[1]Biology Study Program, Faculty of Biotechnology, Universitas Atma Jaya Yogyakarta, Jl. Babarsari 44, Yogyakarta, Indonesia
[2]Biotechno-Industry Research Group, Faculty of Biotechnology, Universitas Atma Jaya Yogyakarta, Jl. Babarsari 44, Yogyakarta, Indonesia

Submitted: 10-02-2023 ***Reviewed: 24-07-2023*** ***Accepted: 21-05-2024***

ABSTRACT

Euodia suaveolens is one of the plants that ancient people in Indonesia used due to its manifold benefits. Earlier research on this plant was mostly done on its potency as a mosquito repellent. This present study aims to determine the phytochemical and antibacterial analyses of the essential oils (EOs) extracted from the leaves of *E. suaveolens*. The EOs of the leaves of *E. suaveolens* were extracted by steam distillation method and were analyzed phytochemically utilizing the GC-MS technique to determine the chemical constituents. The chemical components were tested on four pathogenic bacteria *Escherichia coli*, *Pseudomonas aeruginosa*, *Staphylococcus aureus*, and *Staphylococcus epidermidis* utilizing the diffusion agar method. The results showed that the main compounds extracted from the EOs were α-curcumene, evodone, globulol, limonene, linalool, longipinenepoxide, menthofuran, and p-mentha-1,8-diene. The antibacterial analysis of these compounds showed potential activities to inhibit the growth of four pathogenic bacteria tested, but the inhibition zones formed were still lower compared to commercial antibiotic kanamycin. *E. suaveolens* EOs exhibited diameter of zone of inhibition as follows 2.03±0.22, 0.50±0.49, 1.38±0.10, 1.40±0.27 cm to *E. coli*, *P. aeruginosa*, *S. aureus*, and *S. epidermidis* while kanamycin showed 3.43±0.08, 3.25±0.08, 3.38±0.12, and 3.18±0.24 cm respectively. These results recommend that the main compounds extracted from the EOs of the leaves of *E. suaveolens* be explored further to determine their potencies as new antibiotic medications.

Keywords: *E. suaveolens*, essential oils (EOs), steam distillation, antibacterial potency

Corresponding author:
Boy Rahardjo Sidharta
Faculty of Biotechnology, Universitas Atma Jaya Yogyakarta
Jl. Babarsari 44, Yogyakarta, Indonesia
Email: boy.sidharta@uajy.ac.id

INTRODUCTION

Resistance of some bacteria to antibiotics has been increasing for the last few years and it has also forced healthcare practitioners to find new antibiotic medications. Antibiotic or antimicrobial resistance (AMR) has become a big threat to medical, food safety, and nation-building (World Health Organization., 2019). Malpractice of antibiotic usage in third-world countries such as Indonesia has weighted the problems, such as the increase in TB (tuberculosis), pneumonia, gonorrhea, and salmonellosis infections, infectious diseases are harder to eradicate; longer stay in hospitals; health costs and death cases increase (Davies & Davies, 2010; Zaman et al., 2017). The new antibiotic is hoped to suppress health costs due to the high price of antibiotics prescribed. New antibiotics can also decrease the length of stay in hospitals and increase workforce productivity (World Health Organization., 2019).

Indonesia which is located in the tropical area is known as a megadiversity country which has been utilized since their prehistoric ancestors for daily life needs, including bacterial infectious disease cures. Some of the medicinal plants in Indonesia have been known and utilized by people from other countries. *Euodia suaveolens* Scheff. (syn. *Euodia hortensis* Forster & Forster; vernacular name "zodia") is originally coming from West Papua and some researchers have been trying to find bioactive compounds from the plant to solve health problems in Indonesia (Maryuni et al., 2008; Romulo et al., 2018; Simaremare & Lestari, 2017). Furano monoterpenes (evodene) and prenylated acetophenones have been extracted from *E. suaveolens* leaves, and essential oil (EO) containing a-copaene, ar-curcumene, and caryophyllene have also been extracted from the flowers of this plant (Brophy et al., 1985; Lemmens & Bunyapraphatsara, 2003).

Research and application of the bioactive compounds of this plant as mosquito repellent has been done by many (Budiman & Rahmawati, 2015; Mirawati et al., 2018; Simaremare et al., 2017; Simaremare & Lestari, 2017; Widawati & Santi, 2013). To increase its mosquito-repellent potency, the plant extract was mixed with other plant extracts such as lemon grass (*Cymbopogon citratus*) (Mirawati et al., 2018) or rosemary (*Rosmarinus officinalis*) (Widawati & Santi, 2013). The plant extract has been utilized to eradicate warehouse insect pest *Tribolium castaneum* (Cameron et al., 2016), has been tested for its toxicity to *Artemia salina* larvae (Lestari et al., 2015), has been tested as an antiretroviral agent (Larson et al., 2014) and has also been applied as an anticancer agent (Sanora et al., 2019).

However, research on the phytochemical and antibacterial analyses of the EOs of *Euodia suaveolens* is lacking. Antibacterial potency of the compounds of the EOs of the plant against pathogenic Gram-negative bacteria *Escherichia coli* and *Pseudomonas aeruginosa*, as well as Gram-positive bacteria *Staphylococcus aureus* and *Staphylococcus epidermidis* has never been published. The ability of the bioactive compounds has never been compared to antibiotics commonly prescribed in health care practices, such as kanamycin. Therefore, this present research aims to analyze: 1) the bioactive compounds of the EOs extracted from the leaves of the plant and 2) the potencies of the bioactive compounds of the EOs against four selected pathogenic bacteria such as *Escherichia coli*, *Pseudomonas aeruginosa*, *Staphylococcus aureus*, and *Staphylococcus epidermidis*.

MATERIALS AND METHOD

Materials

Euodia sauveolens leaf samples were collected from a plant collector in Sleman, Yogyakarta Special Province, Indonesia. The plant leaf samples were described and identified by a plant taxonomist at the Faculty of Biotechnology, Universitas Atma Jaya Yogyakarta. The plant samples were deposited in the herbarium at the Faculty of Biotechnology, Universitas Atma Jaya Yogyakarta. The plant leaves were selected based on good quality sample standards such as green in color, fresh condition, no insect bites, and clean (no dirt).

The GCMS-QP2010S Shimadzu equipment (Shimadzu Ltd., Japan) was utilized in the present research with the following settings: carrier gas: Helium, column type Rtx 5, column flow: 0.55

ml/min, column length: 30 m, column oven temperature: 50.0 °C, detector gain mode: Absolute, detector gain: 1.50 kV, film: 0.25 µm, flow control mode: pressure, injection temperature: 300.0 °C, injection mode: split, ion source temperature: 250.00 °C, ionizer: EI 70 Ev, pressure: 13.0 kPa, interface temperature: 300.00 °C, linear velocity: 26.8 cm/sec, purge flow: 3.0 mL/min, split ratio: 139.0, solvent cut time: 3.00 min, total flow: 79.3 mL/min, threshold: 0.

Methods

Plant sample preparation

Ten kilograms of *E. sauveolens* fresh leaves samples were rinsed with tap water thoroughly and discharged to reduce the water. The samples were distilled utilizing the steam distillation method for four hours. The samples were then put into a biomass holding chamber of the distillation apparatus. The water steam was gained by heating the water in a vessel and the steam flowed into a holding chamber where the leaf samples were put. The water steam passed across the leaves and produced vapor, which then condensed and flowed into a clean Erlenmeyer flask. The EOs layer was separated and kept in a clean flacon bottle (Božović et al., 2017; Rassem et al., 2016).

Phytochemical analysis

Several 3.5 ml of the EOs extracted were analyzed utilizing GCMS-QP2010S Shimadzu equipment. The chemical compounds of the EOs were identified by contrasting the results of the chromatogram and retention time with the reference from the mass spectra library (Wiley229. LIB) (Ghimire et al., 2017; Handayani & Nurcahyanti, 2015). While another 3.5 mL of the EOs was utilized for the antibacterial analysis.

Antibacterial analysis

The antibacterial analysis was done utilizing the diffusion agar method to determine the potency of the EOs against four selected pathogenic bacteria. Pure cultures of four selected pathogenic bacteria were inoculated at nutrient agar plates, each plate with one culture. Every 20 µl of the EOs was poured into a well in the nutrient agar plate and another well was filled with commercial antibiotic kanamycin 50 µg/ml (Kimia Farma Inc., Indonesia). All the agar plates were incubated at 37 ^{o}C for 24 hours and then the diameters of the inhibition zones found were quantified utilizing a caliper (Simaremare & Lestari, 2017; Solórzano-Santos & Miranda-Novales, 2012).

Data Analysis

The experimentations were done in quintuplicates and data obtained were analyzed utilizing analysis of variance (ANOVA) procedure statistical method at $p<0.05$.

RESULT AND DISCUSSION

Phytochemical analysis

The chemical compounds of the EOs extracted were put in sequence based on the percentage of chromatogram area as follows linalool (1.40 %), longypynenepoxyde (1.66 %), globulol (1.88 %), α-curcumene (4.65 %), evodone (5.55 %), limonene (10.99 %), p-mentha-1,8-diene (14.34 %), and menthofuran (50.38 %) (Table 1). The total chemical compounds revealed were 25, but 18 other compounds with smaller percentage area (Figure 1).

There were similarities and differences compared to previous research findings, both the kinds of and the percentage area of each chemical compound revealed. Menthofuran was the compound with the highest percentage area extracted from the EOs as reported by (Brophy et al., 1985; Chand et al., 2016; Maryuni et al., 2008). In general, menthofuran and furans are chemical substances that are vulnerable to oxidative metabolism by cytochrome P450 enzymes (Khojasteh et al., 2010). More recent research shows that menthofuran can inhibit severe acute respiratory syndrome coronavirus (SARS-CoV-2) replication in the infected cells (Sanja et al., 2022). Menthofuran is highly demanded

in the aroma industry and estimated that the demand for menthofuran is 150–200 mt/year (Kumar et al., 2014). Other EO compounds that were found in the plant were limonene, evodone, α-curcumene, and linalool (Brophy et al., 1985; Chand et al., 2016; Maryuni et al., 2008), while longypynenepoxide, globulol, and p-mentha-1,8-diene have never been reported by any researchers who were working with *E. suaveolens*.

The difference in terms of the percentage area of every EO compound was due to the difference in distillation and analysis methods utilized (Dhifi et al., 2016; Lahlou, 2004). Some researchers noticed that the difference was influenced by the origin (geographical), environmental condition (ecological), growth condition (physiological) (Chand et al., 2016; Maharaj et al., 2016), and the species or subspecies or varieties of the plant used (Lemmens & Bunyapraphatsara, 2003).

Table 1. Characteristics of the essential oils compounds extracted from the plant

Peak#	R Time	Area	Area %	Compound Name
1	13.111	119467	0.29	β-myrcene
2	14.598	5893898	14.34	p-mentha-1,8-diene
3	19.454	20706148	50.38	menthofuran
4	20.472	243132	0.59	β-pinene
5	24.951	2281197	5.55	evodone
6	25.118	387444	0.94	1,4-heptadiene, 3-methyl
7	25.823	135389	0.33	α-copaene
8	26.740	4516886	10.99	limonene
9	26.958	283879	0.69	1-p-menthen-9-al
10	27.136	257174	0.63	β-caryophyllene
11	27.358	106995	0.26	carvyl acetate
12	28.098	309811	0.75	α-humulene
13	28.550	347119	0.84	α-farnesene
14	28.668	1912747	4.65	α-curcumene
15	28.998	145463	0.35	gurjunene
16	29.303	682229	1.66	longipinenepoxide
17	31.159	176347	0.43	β-cyclocitral
18	31.300	159377	0.39	β-terpinyl butanoate
19	31.491	576708	1.40	linalool
20	31.592	109121	0.27	tetradecane, 3-phenyl
21	31.814	292934	0.71	caryophyllene epoxide
22	32.173	165927	0.40	patchulane
23	32.552	773805	1.88	globulol
24	33.907	343305	0.84	geraniol
25	47.681	173741	0.42	3,5-dodecadiene, 2-methyl
		41100243	100.00	

Antibacterial analysis

The antibacterial analysis was done utilizing the agar well diffusion method instead of the agar disk diffusion method because the present research makes use of four pathogenic bacteria with different traits, specifically aerobic and anaerobic. In the agar well diffusion method, the antibacterial substances tested were placed into a well and diffused throughout the agar media, thus it will reach both the aerobic and anaerobic part of the media. In the agar disk diffusion method, the antibacterial substances were absorbed by the paper disk and then placed on top of the media, hence the antibiotic substances were mostly diffused horizontally (Balouiri et al., 2016).

.

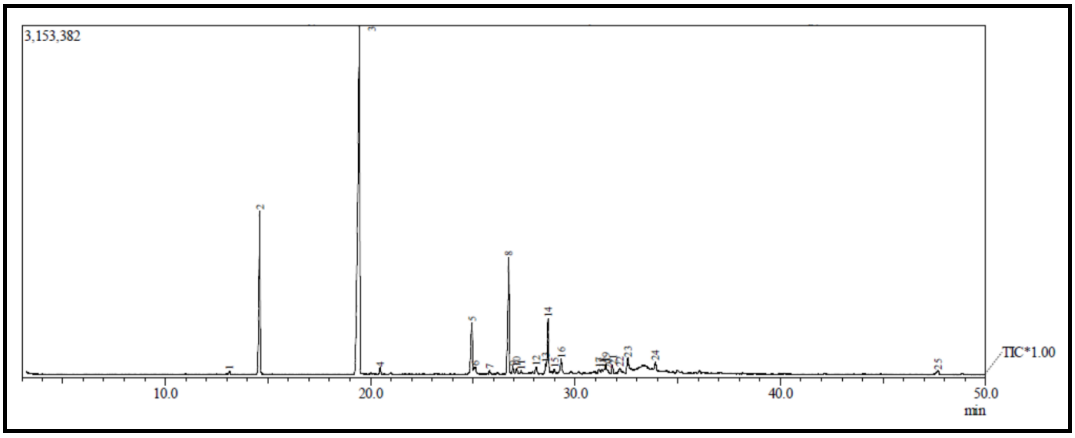

Figure 1. Chromatogram profile of the EO compounds extracted from *E. suaveolens* leaves

The EOs extracted from the leaf of the plant showed clear inhibition zones against four pathogenic bacteria tested (Table 2, Figure 2). *E. coli* showed the highest diameter of inhibition zones compared to the other three bacteria, while *P. aeruginos*a was the least. The diameter of the inhibition zones of *S. aureus* and *S. epidermidis* was not significantly different. All of the diameter of inhibition zones formed by the EOs extracted was still lower than commercial antibiotic kanamycin.

E. coli was higher in terms of diameter of inhibition zones compared to *P. aeruginosa*, though the two bacteria were grouped as Gram-negative, but differ in oxygen demand. *E. coli* is considered aerobic, while *P. aeruginosa* is an anaerobic bacterium (Andrade et al., 2014; Maharaj et al., 2016). Therefore, *E. coli* was more inhibited by the chemical compounds in the EOs which were also known as volatile compounds and tend to diffuse to the surface of the agar plate (Maharaj et al., 2016; Solórzano-Santos & Miranda-Novales, 2012). The diameter of the inhibition zones of *S. aureus* and *S. epidermidis* was not significantly different, since the two bacteria were the same genus. Bacteria with close phylogenetic relationships show higher similarities, including the ability to respond to the chemical compounds of the EOs extracted (Solórzano-Santos & Miranda-Novales, 2012). Similar findings were reported by Swamy et al., 2016 that Gram-negative bacteria were more sensitive toward the EOs of thyme (*Thymus vulgaris*).

The effect of the EOs on microorganisms may be due to the synergistic effects of the compounds which become more effective in the inhibition of a particular species of microorganisms either by causing cell lysis or death or by inhibiting the cell wall synthesis (Mahmoud et al., 2016). The plausible inhibition mechanisms showed by the EOs to the bacteria include: a) the EOs will spread on the cell wall of the bacteria, increase its permeability, and cause the loss of important compounds in the cell, b) increase the acidity inside the cell, thus ATP productions are inhibited, and c) damages of cell genetic materials which leads to the cell death (Andrade et al., 2014; Bach & Bach, 2021; Li et al., 2014; Saad et al., 2013; Turgis et al., 2009; Turina et al., 2006). One of the important characteristics of EOs is their hydrophobicities which make them easily bind to lipids in the cell membrane and mitochondria, disturb the structure, and increase membrane permeability (Chouhan et al., 2017; Lopez-Romero et al., 2015; Solórzano-Santos & Miranda-Novales, 2012).

Antibacterial activities of the EOs extracted from the plant leaf are smaller compared to kanamycin (Table 2, Figure 2). The diameter of inhibition zones of the four pathogenic bacteria tested is significantly different statistically compared to kanamycin. Kanamycin is known as a wide-spectrum antibiotic that is capable of inhibiting both Gram-negative and positive bacteria (Maharaj et al., 2016; Solórzano-Santos & Miranda-Novales, 2012). However, the potential of the chemical compounds of the EOs extracted from *E. suaveolens* as an antibacterial agent is still promising to be explored in the future.

Table 2. Diameter (cm) of inhibition zones of the EOs to the pathogenic bacteria

Sample	Pathogenic Bacteria			
	E. coli	***P. aeruginosa***	***S. aureus***	***S. epidermidis***
Essential Oils	2.03 ± 0.22^{c}	0.50 ± 0.49^{a}	1.38 ± 0.10^{b}	1.40 ± 0.27^{b}
Positive Control (kanamycin)	3.43 ± 0.08^{d}	3.25 ± 0.08^{d}	3.38 ± 0.12^{d}	3.18 ± 0.24^{d}

Note: numbers are mean ± SD from quintuplicates, numbers with the same alphabet in the row show no significant difference statistically ($p<0.05$)

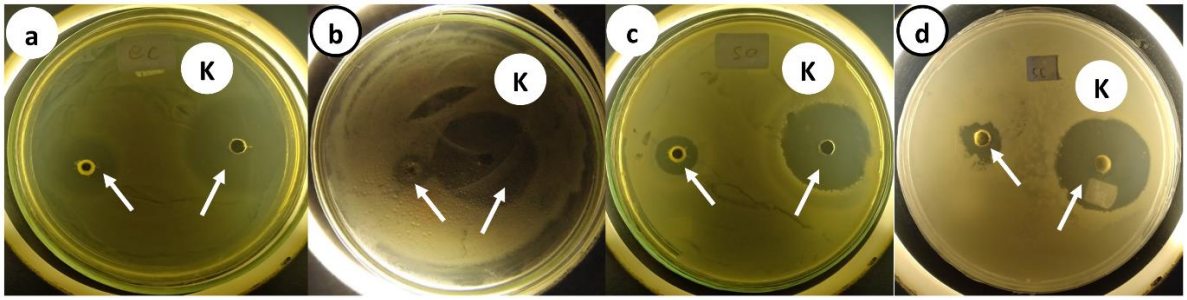

Figure 2. Inhibition zones of the EOs against a) *E. coli*, b) *P. aeruginosa*, c) *S. aureus*, and d) *S. epidermidis*. K is antibiotic kanamycin treatment. Arrows show the inhibition zones on the agar plate

CONCLUSION

The main chemical compounds revealed from the EOs extracted from the *E. suaveolens* leaves are menthofuran, p-mentha-1,8-diene, limonene, evodone, α-curcumene, globulol, longipinenepoxide, and linalool. The chemical compounds from the EOs extracted showed the ability to inhibit three pathogenic bacteria namely *Escherichia coli*, *Staphylococcus aureus*, and *Staphylococcus epidermidis*, but with low inhibition against *P. aeruginosa*.

ACKNOWLEDGEMENT

This research project was funded by the Research and Community Service Institute of Universitas Atma Jaya Yogyakarta, Indonesia. The authors are thankful to Ms. Sri Wahyuni and Ms. Christiana Asmaranti Kirana Putri, for their assistance during the data gathering in the laboratory.

REFERENCES

Andrade, B. F. M. T., Nunes Barbosa, L., da Silva Probst, I., & Fernandes Júnior, A. (2014). Antimicrobial activity of essential oils. *Journal of Essential Oil Research*, *26*(1), 34–40. https://doi.org/10.1080/10412905.2013.860409

Bach, H., & Bach, H. (2021). Antimicrobial and anti-inflammatory activities of commercial aromatizing fragrances. *Future Science OA*, *7*(6). https://doi.org/10.2144/fsoa-2020-0194

Balouiri, M., Sadiki, M., & Ibnsouda, S. K. (2016). Methods for in vitro evaluating antimicrobial activity: a review. *Journal of Pharmaceutical Analysis*, *6*(2), 71–79. https://doi.org/10.1016/j.jpha.2015.11.005

Božović, M., Navarra, A., Garzoli, S., Pepi, F., & Ragno, R. (2017). Esential oils extraction: a 24-hour steam distillation systematic methodology. *Natural Product Research*, *31*(20), 2387–2396.

https://doi.org/10.1080/14786419.2017.1309534
Brophy, J. J., Rahmani, M., Toia, R. F., Croft, K. D., & Lassak, E. V. (1985). The volatile oils of Euodia hortensis forma hortensis. *Flavour and Fragrance Journal*, *1*(1), 17–20. https://doi.org/10.1002/ffj.2730010105
Budiman, B., & Rahmawati, R. (2015). Perbandingan efektivitas ekstrak Zodia (Evodia sauveolens) dan Serai (Cymbopogan citratus) sebagai Repellent (Penolak) Nyamuk. *Higiene Jurnal Kesehatan Lingkungan*, *1*(2), 67–74.
Cameron, R. R., Arinafril, A., & Mulawarman, M. (2016). Uji bioaktivitas ekstrak daun Zodea (Evodia suaveolens Sheff)terhadap hama gudang Tribolium castaneum(Coleoptera: Tenebrionidae)Herbst. *Jurnal Agroekoteknologi Tropika (Journal of Tropical Agroecotechnology)*, *5*(3), 222–231.
Chand, R., Jokhan, A. D., & Gopalan, R. D. (2016). Bioactivity of selected essential oils from medicinal plants found in Fiji against the Spiralling whiteflies (Aleurodicus dispersus Russell). *Advances in Horticultural Science*, *30*(3), 165–174. https://doi.org/10.13128/ahs-20279
Chouhan, S., Sharma, K., & Guleria, S. (2017). Antimicrobial activity of some essential oils—present status and future perspectives. *Medicines*, *4*(3), 58. https://doi.org/10.3390/medicines4030058
Davies, J., & Davies, D. (2010). Origins and evolution of antibiotic resistance. *Microbiology and Molecular Biology Reviews*, *74*(3), 417–433. https://doi.org/10.1128/MMBR.00016-10
Dhifi, W., Bellili, S., Jazi, S., Bahloul, N., & Mnif, W. (2016). Essential oils' chemical characterization and investigation of some biological activities: a critical review. *Medicines*, *3*(4), 25. https://doi.org/10.3390/medicines3040025
Ghimire, B. K., Yoo, J. H., Yu, C. Y., & Chung, I.-M. (2017). GC–MS analysis of volatile compounds of Perilla frutescens Britton var. Japonica accessions: Morphological and seasonal variability. *Asian Pacific Journal of Tropical Medicine*, *10*(7), 643–651. https://doi.org/10.1016/j.apjtm.2017.07.004
Handayani, P. A., & Nurcahyanti, H. (2015). Ekstraksi minyak Atsiri daun Zodia (Evodia suaveolens) dengan metode maserasi dan distilasi air. *Jurnal Bahan Alam Terbarukan*, *3*(1), 1–7.
Khojasteh, S. C., Oishi, S., & Nelson, S. D. (2010). Metabolism and toxicity of menthofuran in Rat liver slices and in Rats. *Chemical Research in Toxicology*, *23*(11), 1824–1832. https://doi.org/10.1021/tx100268g
Kumar, B., Mali, H., & Gupta, E. (2014). Genetic variability, character association, and path analysis for economic traits in menthofuran rich half-Sib seed progeny of Mentha piperita L. *BioMed Research International*, *2014*, 1–7. https://doi.org/10.1155/2014/150830
Lahlou, M. (2004). Methods to study the phytochemistry and bioactivity of essential oils. *Phytotherapy Research*, *18*(6), 435–448. https://doi.org/10.1002/ptr.1465
Larson, E. C., Hathaway, L. B., Lamb, J. G., Pond, C. D., Rai, P. P., Matainaho, T. K., Piskaut, P., Barrows, L. R., & Franklin, M. R. (2014). Interactions of Papua New Guinea medicinal plant extracts with antiretroviral therapy. *Journal of Ethnopharmacology*, *155*(3), 1433–1440. https://doi.org/10.1016/j.jep.2014.07.023
Lemmens, R. H. M. ., & Bunyapraphatsara, N. (2003). *Plant resources of south-east Asia 12(3), Medicinal and poisonous plants 3* (R. H. M. . Lemmens & N. Bunyapraphatsara (eds.)). Backhuys Publishers, Leiden.
Lestari, M. S., Himawan, T., Abadi, A. L., & Retnowati, R. (2015). Toxicity and phytochemistry test of methanol extract of several plants from Papua using Brine Shrimp Lethality Test (BSLT). *Journal of Pharmaceutical Research*, *7*(4), 866–872.
Li, Y., Fabiano-Tixier, A.-S., & Chemat, F. (2014). *Essential oils as reagents in green chemistry*. Springer International Publishing. https://doi.org/10.1007/978-3-319-08449-7
Lopez-Romero, J. C., González-Ríos, H., Borges, A., & Simões, M. (2015). Antibacterial effects and mode of action of selected essential oils components against Escherichia coli and Staphylococcus aureus. *Evidence-Based Complementary and Alternative Medicine*, *2015*, 1–9.

https://doi.org/10.1155/2015/795435
Maharaj, P. P. P., Devi, R., & Prasad, S. (2016). Antimicrobial effect of essential oils of some Fijian medicinal plant leaves on pathogenic bacteria. *The South Pacific Journal of Natural and Applied Sciences*, *34*(2), 35. https://doi.org/10.1071/SP16005
Mahmoud, A. M., El-Baky, R. M. A., Ahmed, A. B. F., & Fadl, G. (2016). Antibacterial activity of essential oils and in combination with some standard antimicrobials against different pathogens isolated from some clinical specimens. *American Journal of Microbiological Research*, *4*(1), 16–25. https://doi.org/10.12691/ajmr-4-1-2
Maryuni, A. E., Bintang, M., & Poeloengan, M. (2008). *Isolasi dan identifikasi senyawa antibakteri Minyak Atsiri Daun Zodia (Evodia sp). (Thesis).* Sekolah Pascasarjana, Institut Pertanian Bogor, Bogor, Indonesia.
Mirawati, P., Simaremare, E. S., & Pratiwi, R. D. (2018). Uji efektivitas Repellent sediaan lotion kombinasi minyak Atsiri daun Zodia (Evodia suaveolens Scheff) dan minyak Atsiri batang Serai (Cymbopogon citratus) terhadap nyamuk Aedes aegypti L. *PHARMACY: Jurnal Farmasi Indonesia (Pharmaceutical Journal of Indonesia)*, *15*(1), 1. https://doi.org/10.30595/pharmacy.v15i1.2286
Rassem, H. H. A., Nour, A. H., & Yunus, R. M. (2016). Techniques for extraction of essential oils from plants: a review. *Australian Journal of Basic and Applied Sciences*, *10*(16), 117–127.
Romulo, A., Zuhud, E. A. M., Rondevaldova, J., & Kokoska, L. (2018). Screening of in vitro antimicrobial activity of plants used in traditional Indonesian medicine. *Pharmaceutical Biology*, *56*(1), 287–293. https://doi.org/10.1080/13880209.2018.1462834
Saad, N. Y., Muller, C. D., & Lobstein, A. (2013). Major bioactivities and mechanism of action of essential oils and their components. *Flavour and Fragrance Journal*, *28*(5), 269–279. https://doi.org/10.1002/ffj.3165
Sanja, Ć. Z., Schadich, E., Džubák, P., Hajdúch, M., & Tarkowski, P. (2022). Antiviral activity of Selected Lamiaceae essential oils and their Monoterpenes against SARS-Cov-2. *Frontiers in Pharmacology*, *13*. https://doi.org/10.3389/fphar.2022.893634
Sanora, G. D., Mastura, E. Y., Handoyo, M. O. M., & Purnama, E. R. (2019). Identification of anticancer active compound from GC-MS test results of Zodia Leaves (Evodia suaveolens) ethanol extract. *Jurnal Biota*, *5*(2), 89–95. https://doi.org/10.19109/Biota.v5i2.3374
Simaremare, E. S., & Lestari, F. D. (2017). Uji potensi minyak Atsiri daun Zodia (Evodia suaveolens Scheff.) sebagai insektisida nyamuk Aedes aegypti L dengan metode elektrik. *Pharmacy*, *14*(1), 1–10.
Simaremare, E. S., Sinaga, D. I., & Agustini, V. (2017). Sabun Zodia Sebagai Repellent Terhadap Nyamuk Aedes aegypti mosquitoes. *Pharmaceutical Journal of Indonesia*, *3*(1), 11–16. https://doi.org/10.21776/ub.pji.2017.003.01.2
Solórzano-Santos, F., & Miranda-Novales, M. G. (2012). Essential oils from aromatic herbs as antimicrobial agents. *Current Opinion in Biotechnology*, *23*(2), 136–141. https://doi.org/10.1016/j.copbio.2011.08.005
Swamy, M. K., Akhtar, M. S., & Sinniah, U. R. (2016). Antimicrobial properties of plant essential oils against Human pathogens and their mode of action: an updated review. *Evidence-Based Complementary and Alternative Medicine*, *2016*, 1–21. https://doi.org/10.1155/2016/3012462
Turgis, M., Han, J., Caillet, S., & Lacroix, M. (2009). Antimicrobial activity of mustard essential oil against Escherichia coli O157:H7 and Salmonella typhi. *Food Control*, *20*(12), 1073–1079. https://doi.org/10.1016/j.foodcont.2009.02.001
Turina, A. de. V., Nolan, M. V., Zygadlo, J. A., & Perillo, M. A. (2006). Natural terpenes: Self-assembly and membrane partitioning. *Biophysical Chemistry*, *122*(2), 101–113. https://doi.org/10.1016/j.bpc.2006.02.007
Widawati, M., & Santi, M. (2013). The effectiveness of fixative addition on Zodia (Evodia suaveolens S.) and Rosemary (Rosmarinus officinalis l.) Gel against Aedes aegypti. *Health Sciences Journal of*

Indonesia, *4*(2), 103–106.

World Health Organization. (2019). *Situational analysis of antimicrobial resistance in the South-East Asia Region, 2018*.

Zaman, S. Bin, Hussain, M. A., Nye, R., Mehta, V., Mamun, K. T., & Hossain, N. (2017). A review on antibiotic resistance: alarm bells are ringing. *Cureus*. https://doi.org/10.7759/cureus.1403

Pharmaciana
Vol.14, No.2, July 2024, Page. 242-250
ISSN: 2088 4559; e-ISSN: 2477 0256
DOI: 10.12928/pharmaciana.v14i2.27137

The optimation of fermentation time, antibacterial activity, and profiling secondary metabolite of symbiont fungi from Sponge *Gelliodes fibulata*

Siska Rusmalina[1], Mahfur[2]*, Nunung Hasanah[3], Mochamad Ardy Wiyono[2], Nonik Nur Ekayanti[2], Jacinda Caroline Nathania[1]

[1]Diploma Program of Pharmacy, Faculty of Pharmacy, Pekalongan University, Jl. Sriwijaya No 3, Pekalongan, Indonesia
[2]Bachelor Program of Pharmacy, Faculty of Pharmacy, Pekalongan University, Jl. Sriwijaya No 3, Pekalongan, Indonesia
[3]Ners Professional Study Program, Faculty of Health Sciences, Pekalongan University, Jl. Sriwijaya No 3, Pekalongan, Indonesia

Submitted: 05-09-2023 ***Reviewed: 24-04-2024*** ***Accepted: 28-06-2024***

ABSTRACT

Symbiont fungi are organisms that live in sponges tissue. Sponges are known to contain many metabolites which have the potential to be used as raw materials for medicine. Sponge *Gelliodes fibulata* belongs to the category demospongiae. The purpose of this study was to determine the optimal time to obtain the best secondary metabolite profile results in the sponge symbiont fungus *Gelliodes fibulata*. This research is included in experimental research. Beginning with the fungi culture of the sponge *Gelliodes fibulata*. Time variations 2, 4, 6, 8, 10, 12, and 14 are used to see differences in secondary metabolite production. A liquid extraction process is carried out to obtain secondary metabolites produced during fermentation. The final stage is to carry out qualitative analysis with TLC and antibacterial testing with the well-diffusion method. The results obtained indicate that the length of fermentation time influences the secondary metabolites obtained and automatically influences their antibacterial activity. The profile of secondary metabolites from TLC showed that the 10th day of fermentation had the secondary metabolites with high complexity and the highest yield 0.086%. The results of antibacterial activity showed that the 10th day of fermentation had the largest inhibition zone with 7.75 ± 0.44 mm compared to the other days of fermentation.

.

Keywords: *Antibacterial, Gelliodes fibulata, fermentation, Sponge, Symbiont fungi*

Corresponding author:
Mahfur
Bachelor Program of Pharmacy, Faculty of Pharmacy, Pekalongan University, Pekalongan, Indonesia
Jl. Sriwijaya no. 3, Bendan, Pekalongan, Central of Java, Indonesia
Email: Mahfur.isfa@gmail.com

INTRODUCTION

Symbiont fungi are one of the microbes that live in sponge tissue. A symbiotic relationship of mutualism occurs between the symbiont fungus and its host, the sponge. This symbiotic mutualism occurs when the sponge obtains nutritional derivatives and active compounds from the symbiont fungus, while the fungus obtains nutrients from the metabolic products of the sponge (Leal et al., 2014). Symbiont fungi residing in the sponge can produce possible compounds that are the same or different from the original sponge, with varying properties (Webster & Thomas, 2016). The contribution of symbiont fungi in producing secondary metabolites in their host or sponge is very large, especially in producing compounds that have certain characteristics. These compounds have great potential as medicinal compounds, including alkaloids, terpenoids, steroids, quinones, and phenols (Freeman et al., 2020).

Sponges are one type of biological natural resource, their habitat in the sea reaches 830 species consisting of three classes, namely Calcarea, Demospongiae, and Hexactinellidae (Braekman & Daloze, 2004; Marzuki, 2018). Sponges are known to contain many metabolite compounds that have the potential as medicinal raw materials (Mahfur, Setyowati, et al., 2022; Mahfur, Wahyuono, et al., 2022). *Gelliodes fibulata* sponge is a sponge from the Demospongiae class, this class is the largest class that covers 90% of all sponge species (Setyowati et al., 2017). However, the *Gelliodes fibulata* sponge itself has not been widely studied and utilized and also for microorganisms associated with the sponge. Biotechnology is studying microorganisms that are widely used in fermentation.

A fermentation process is a form of biotechnology used to increase the production of secondary metabolites in microorganisms such as symbiont fungi (Mahfur et al., 2023; Samirana et al., 2021). Fermentation will produce secondary metabolite products in large quantities and have good quality. The process of forming fermentation products is influenced by many factors, one of which is the time or length of the fermentation process (Setyowati et al., 2018). Environmental factors in mushroom growth have an impact on the amount and variety of secondary metabolites produced, so it is necessary to optimize growing conditions. Optimization is the first step of fungus cultivation in producing bioactive secondary metabolite compounds (Freeman et al., 2020).

Research on the effect of fermentation time on secondary metabolite profiles and antibacterial activity in *Gelliodes fibulata* symbiont fungus has never been done before, so this research is very relevant. This study aims to determine the optimal time for fermenting the symbiont fungus from the sponge *Gelliodes fibulata*. The selection of optimal time is based on the metabolite profile produced, and antibacterial activity against *Escherichia coli*.

MATERIALS AND METHOD

Materials

Gelliodes fibulata sponge from Gili layar, West Lombok, Nusa Tenggara Barat (NTB). *Escherichia coli* bacteria, Himedia brand Sabouraud Dextrose Agar (SDA) media, Himedia brand Sabouraud Dextrose Broth (SDB), Himedia brand Muller Hinton Agar (MHA), Aquadest, Natural Sea Salt, NaCl infusion, Ciprofloxacin injection (HJ), GF 254 silica gel plate (Merck), 70% alcohol (Onemed), Pro analysis Ethyl acetate (Merck), n-hexsan (Merck), Chloroform (Merck), Ethyl acetate (Merck) and Methanol (Merck).

Methods

Sponge identification.

Identification of sponge samples was carried out with the aim of confirm the correctness of the sponge sample. Identification was carried out at the Marine Natural Product Laboratory Diponegoro University, Semarang, Indonesia using reference (Uriz et al., 2003).

Symbiont fungus cultivation and purification

Gelliodes fibulata sponges were cleaned and sprayed on the surface with sterile sea salt water. Cultivation begins with the *Gelliodes fibulata* sponge cut using a sterile cutter longitudinally, then the inside of the sponge is sprayed with sterile sea salt water. The cut results were placed on a petri dish containing saline SDA media with the addition of chloramphenicol as much as 1 mL, with the inside of the sponge facing towards the media. Culture at 37°C storage for 5-7 days to obtain the growth of the sponge symbiont fungus *Gelliodes fibulata* (Purwantini et al., 2016). Cultivation will produce several fungi that grow in saline SDA media. The selected fungi are those that have the most dominant growth in the cultivation. The dominant fungal culture was cultured on saline SDA media with a sterile technique and incubated for 14 days.

Purification and identification of symbiont fungus

The purification procedure was performed according to each colony's unique morphological characteristics. The predominating fungi is called as isolate fungi and are cultured on the media to produce a pure isolate. The symbiotic fungus was examined under macro, micro, and molecular microscopes to identify it. The steps in molecular identification were DNA extraction, PCR process, and the last identification of phylogenetic trees were analyzed using MEGA 7.0 software, while statistical analysis used the Neighbor-Joining method with 1000 bootstrap replication fields (Mahfur et al, 2023).

Fermentation of symbiont fungus

Fermentation was carried out using saline SDB (Suboroud Dextrose Broth) media. Some of the predominating fungus was cultured into 200 mL of saline SDB media. Incubation time was carried out using a variety of days, it is 2, 4, 6, 8, 10, 12, and 14 days. Incubation was carried out using the shaker incubation method at 120 rpm at 37°C (Setyowati et al, 2017).

Extraction of secondary metabolites

Extraction began with the separation of fermentation products between mycelia and supernatant. The supernatant obtained was extracted by liquid-liquid extraction method using ethyl acetate solvent in a 1:1 ratio. The extraction results were evaporated using an evaporator at 60°C (Setyowati et al, 2018). The yield obtained was calculated.

Identification of metabolite profile

Identification of secondary metabolites was carried out using the thin-layer chromatography (TLC) method. The stationary phase used was silica GF_{254} and the mobile phase used was n-hexan: ethyl acetate (1:3). Identification of chemical compound groups using spray reagents. Dragendroff reagent was used for alkaloid identification, cytroborate reagent was used for flavonoid identification, the vanillin-sulfate reagent was used for steroid identification, and $FeCl_3$ reagent was used for phenolic identification (Mahfur et al, 2023; Wulansari et al, 2020).

Antibacterial test of extracts

The test was conducted on Mueller Hinton Agar (MHA) media using the well diffusion method. *E. coli* bacteria that had been inoculated were taken with an ose to make a bacterial suspension with a concentration similarity of 0.5% McFarland. The concentration of the extract used to test was 25 mg/mL with ethyl acetate solvent. Bacterial suspensions were then applied to MHA media. MHA media was prepared in as many as 2 petri dishes, each divided into 4 wells for testing extract samples resulting from variations in fermentation days. Incubation was carried out at 37°C for 24 hours. This bacterial test was repeated 3 times. The clear zone around the wells indicating the absence of bacterial growth was then measured with a caliper and counted (Cita et al., 2017).

Data Analysis

The results of the TLC analysis indicated a change in the color of the spots. The antibacterial assay was repeated three times, and the potential of the antibacterial was expressed as an average of three replications ± Standard Deviation (SD). The test results were statistically analyzed using one-way analysis of variance (ANOVA) SPSS program for Windows version 16.

RESULT AND DISCUSSION

Sponge identification and Cultivation of symbiont fungus

The identification results at the Marine Natural Product Laboratory of Diponegoro University are based on letter no. Idn.201101-Sp showed that the sponge used included the species *Gelliodes fibulata*. Cultivation was done by planting small parts of the sponge on saline SDA media. The cultivation results showed that 4 types of fungi grew in the process (Figure 1). The results of fungal growth were selected with the most dominating colony growth category in the media. then re-cultured into new saline SDA media for purification. The purpose of purification is to separate the dominant symbiont fungi from other fungi so that pure colonies are obtained in each medium (Ginting et al., 2019; Rosmania & Yanti, 2020). Green fungi are fungi that grow dominantly in the cultivation process and are selected to continue in the next test. After re-growing on the media for 14 x 24 hours, pure fungal isolates are obtained, it is fungi that contain one form of the same colony morphology. Pure fungal isolates obtained are continued to the fermentation stage, with to multiply symbiont fungi (Setyowati et al., 2018).

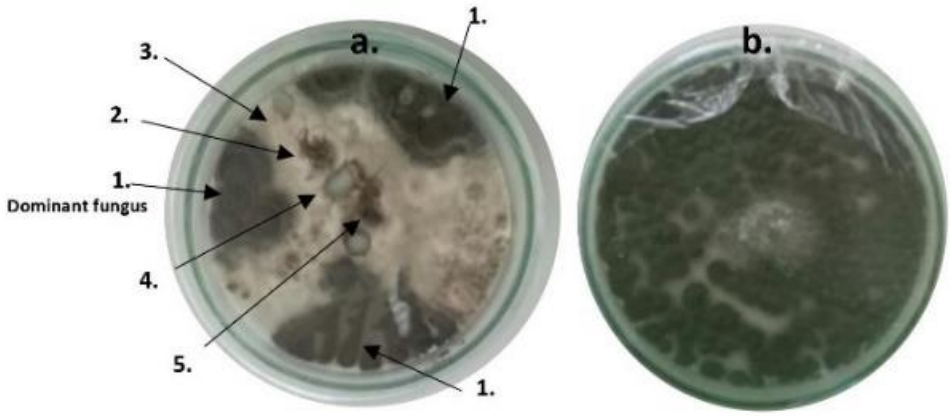

Figure 1. a.) Cultivation results of *Gelliodes fibulata* sponge. b.) symbiont dominant fungus culture. The number 1-5 indicate the types of fungi growing

Identification of fungus symbiont dominant

The aim of the purification procedure is to produce pure isolates according to their morphology. The green mycelium (Figure 1) was identified with micro, macroscopical, and molecular tests. The DNA sequencing was used to identify dominating fungal strains and registered in GenBank (accession numbers OQ451585, www.ncbi.nlm.nih.gov). The isolates showed 99.08% homology and 93% query cover to *Penicillium nalgiovense* (Figure 2). The isolates exhibit a high degree of similarity and are probably members of the same species because the maximum identity value is more than 97%.

Fermentation of symbiont fungi

Fermentation was carried out using saline SDB (Suboroud Dextrose Broth) media. A total of 5 parts of the cultured fungi plots were put into 200 mL of saline SDB media. The incubation time was carried out using a variety of days, it is 2, 4, 6, 8, 10, 12, and 14 days. Shaker incubation at 120 rpm was used at this fermentation stage. The fermentation process using liquid media will make the fungi produce

bioactive compounds. Microorganism fermentation is influenced by physical and chemical factors. Physical factors that affect microorganisms include temperature, pH, and osmotic salinity, while chemical factors consist of carbon, nitrogen, and nutrient sources in the culture medium (Setyowati et al., 2018). Based on several studies, simple carbon sources such as glucose and dextrose greatly influence the growth of fungi associated with marine environments and can also influence the production of secondary metabolites that influence their biological activity (Anuhya et al., 2017; Mahapatra & Banerjee, 2013). SDB liquid media contains dextrose, carbohydrates, and nitrogen, and has a pH of 5-6, making it suitable for fungal growth media (Rendowaty et al., 2017). Fermentation time is an independent variable, it is days 2 to 14 with a difference of 2 days. The time variable is based on the growth phases that occur in microorganisms. The growth phase of microorganisms is divided into several parts, lag phase, log phase, stationary phase, and death phase. The lag phase is the growth phase of the fungi adapting to its environmental conditions. The log phase of fungi growth generally occurs from day 7th to day 14th, in the log phase there is an increase in the amount of biomass. In the next phase, if carbon as an important source of energy or nutrients has been used up, it does not mean that growth stops. The growth phase can continue due to the lysis of dead cells used as a source of nutrients (Carranza et al., 2017). This is the basis for the selection of fermentation time to see which time is the most optimum to get good results based on metabolites and antibacterial activity. The predominant fungi associated with fermented *Gelliodes fibulata* is *Penicillium nalgiovense* which has a growth phase where 150 hours is the most optimal growth time in the growth process (Papagianni & Sergelidis, 2014).

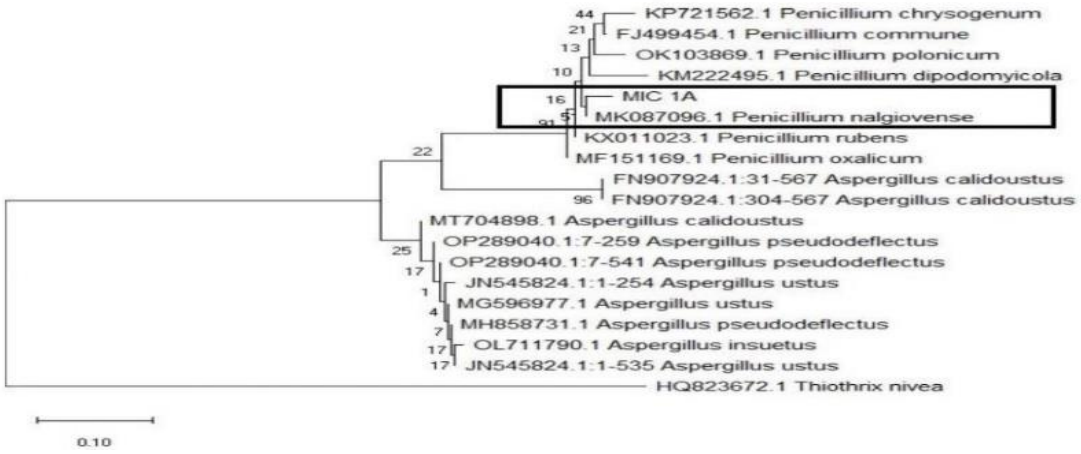

Figure 2. phylogenetic tree of predominating fungi on sponge *Gelliodes fibulata*

Extraction of secondary metabolites

The fermentation stage will obtain 2 parts, biomass (mycellium) and supernatant, a better extraction process is to use both parts. This is because the active compounds are not clearly known, whether they are inside the cells or outside the cells. therefore, the use of extraction processes for both parts results in optimal extraction (Samirana et al., 2021). In this study, the supernatant part was used for extraction like in some previous studies (Rendowaty et al., 2017). Extraction of symbiont fungal isolates from *Gelliodes fibulata* sponge aims to separate the active compounds present in the supernatant. Extraction is done by liquid-liquid extraction method from the supernatant of fermentation results. The extraction results obtained yields on each day of fermentation in succession are as follows, day 2 gets a yield of 0.018% b/v, day 4 as much as 0.041% b/v, day 6 as much as 0.041% b/v, day 8 as much as 0.059% b/v, day 10 as much as 0.086% b/v, day 12 as much as 0.071% b/v and day 14 as much as 0.046% b/v can seen Figure 3. The yield results obtained illustrate that fermentation time affects the amount of yield. This is clearly due to the growth phase of the fungi. The peak growth of the *Gelliodes fibulata* symbiont fungi

fermentation can be concluded to occur on day 10th when viewed from the resulting yield. The following days 12th and 14th, experienced a decrease in yield and it can be concluded that growth has entered the stationary phase and the death phase. The extraction yield is a description of the amount of metabolites produced, the more yield obtained, the more secondary metabolites contained in the extract (Samirana et al., 2021).

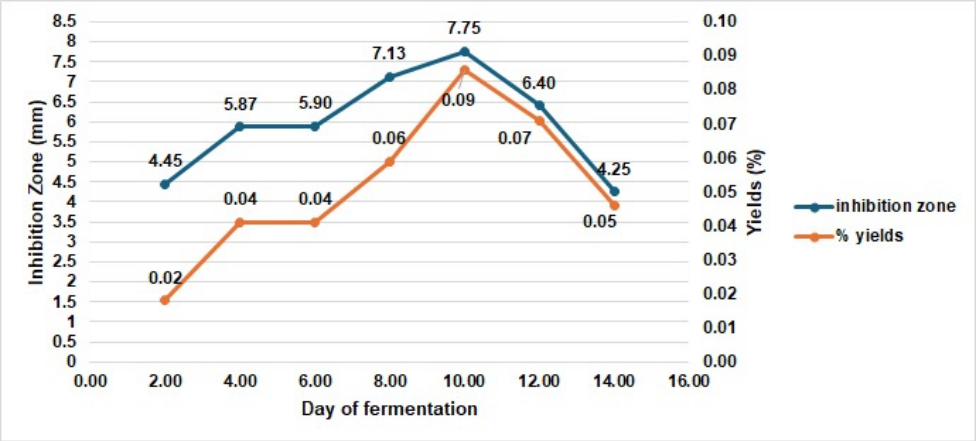

Figure 3. The curve of the effect of fermentation time with inhibition zone and % yield produced

Identification of metabolite profiles

The results of the identification of the secondary metabolite content of ethyl acetate extract of symbiont fungi show that the extract contains several classes of chemical compounds. The identification of chemical compound groups analyzed using spray reagents for each group of chemical compounds obtained results as in Table 1. The TLC profile of each extract from the fermentation time showed different results, which showed that fermentation time affected the content of secondary metabolites produced (Figure 4). The longer the fermentation time, the more the TLC profile shows the compound content. Starting from day 8th untile day 12th fermentation looks to have a more complex profile than other fermentation times. Clearly seen from the results of the TLC profile with vanillin sulfate reagent under visible light. On the day 8th and 10th fermentation had spots with blue-green color, and on day 12th fermentation the color of the spots became thinner, but other spots with purple appeared and then on the 14th day of fermentation all the spots were not visible. This indicates that the production of secondary metabolites in the fermentation phase occurs in accordance with the growth phase of the fungi.

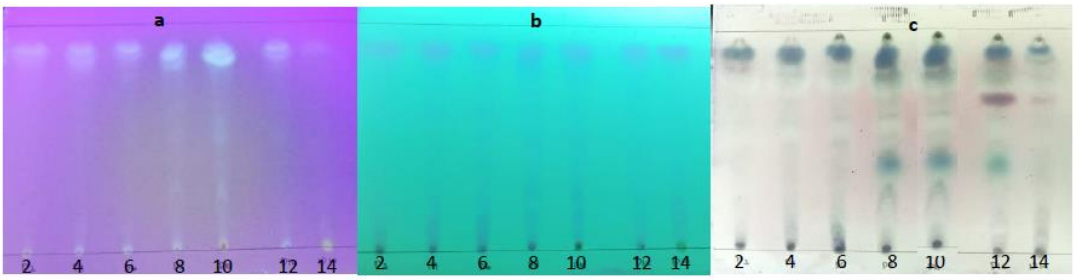

Figure 4. The TLC results of ethyl acetate extract of the sponge symbiont fungus *Gelliodes fibulata*. a) UV 366 b) UV 254 c) vanillin- Sulfate reagent under visible light

Antibacterial test of extracts

Antimicrobial activity test against *E. coli* ATCC 25922 was conducted using the well diffusion method. The diffusion method was chosen because it has several advantages compared to other methods including the amount of substance used can be adjusted, the time is shorter, easy to apply, and simpler

(Tumiwa et al., 2019). Antimicrobial testing aims to determine the activity of inhibiting bacterial growth from extracts of symbiont fungi associated with the sponge *Gelliodes fibulata*. Antibacterial activity arises because the ethyl acetate extract of symbiont fungi contains alkaloid, terpenoid, phenolic, and flavonoid compounds (Table 1). Terpenoid compounds are able to damage porins due to disruption of membrane and cell wall formation in bacteria (Wulansari et al., 2020). Flavonoid compounds have a mechanism of inhibition of DNA and RNA formation, cell membrane function, and oxygen utilization by bacteria. Alkaloids have a mechanism of action by disrupting the constituent components of peptidoglycan so that the cell wall layer is not formed intact and causes cell death (Amalia et al., 2017). While phenol compounds are bactericidal, the antibacterial activity of phenol compounds plays a role in damaging the cell wall and enzymes in the plasma membrane of microorganisms (Bouarab-Chibane et al., 2019).

Table 1. Identification results of secondary metabolite compound classes of ethyl acetate extract of the sponge symbiont fungus *Gelliodes fibulata*

Name of compound	Reagent	Observation result	appearance
Alkaloid	Dragendrof	+	orange red spot
Flavonoid	Cytroborate	+	Yellow spot
Steroid/Triterpenoid	Vanilin-sulfate	+	Blue green spot
Phenolic	$FeCl_3$	+	purple spot

+ showed has chemical compound class

The results obtained in antibacterial testing against *E-coli* are indicated by the creation of clear zones around the wells. This indicates that there is growth inhibitory activity on *E-coli* bacteria from fungi extracts isolated from sponges. The results of antibacterial testing of ethyl acetate extract from day 2 to day 14 of fermentation successively showed an inhibition zone of 4.45 ± 0.38 mm, 5.87 ± 0.32 mm, 5.90 ± 0.53 mm, 7.13 ± 0.35 mm, 7.75 ± 0.44 mm, 6.40 ± 0.60 mm, 4.25 ± 0.22 mm (Table 2). The criteria for antibacterial activity based on the inhibition zone follows the previous classification, where the classification criteria are divided into 4 criteria, namely weak, moderate, strong, and very strong (Tumiwa et al., 2019). The results of antibacterial testing of ethyl acetate extract of symbiont fungi showed 2 criteria, namely moderate criteria and weak criteria. The moderate criteria were the results of fermentation days 4, 6, 8, 10, and 12, while the weak criteria were the results of fermentation days 2, and 14. The 10^{th} day's fermentation has a better inhibition zone compared to other days because fermentation on that day produces complex metabolites. Supported by TLC profile data which shows that the compounds that contribute to increasing activity are terpenoids. The presence of terpenoid compounds can be seen in the results of analysis using vanillin-sulfate reagent with the appearance of a blue green-color spots on TLC which appears on days 8^{th}, 10^{th}, and 12^{th} of fermentation.

Table 2. Antibacterial testing results of ethyl acetate extract of the sponge symbiont fungus *Gelliodes fibulata* against *E-coli*

Fermentation Duration (day)	Inhibition Zone (mm)	Criteria
2	4.45±0.38	Weak
4	5.87±0.32	Moderate
6	5.90±0.53	Moderate
8	7.13±0.35	Moderate
10	7.75±0.44	Moderate
12	6.40±0.60	Moderate
14	4.25±0.22	Weak

Data are presented as mean±SD.

CONCLUSION

From the results, it can be concluded that fermentation time affects the yield of extracts produced and also affects their antibacterial activity. Day 10th fermentation has a complex metabolite profile and more yield and has a better inhibition zone compared to other days.

ACKNOWLEDGEMENT

Thanks are due to Institute for Research and Community Services (LPPM) of Pekalongan University with number 572/B.06.01/LPPM/XI/2022 for providing grant funding for this research.

REFERENCES

Amalia, Al., Sari, I., & Nursanty, R. (2017). *Seminar Nasional Biotik*. 387–391.

Anuhya, G., Jyostna, V., Yvv, A. K., Bodaiah, B., & Sudhakar, P. (2017). Influence Of Physico-chemical Parameters On Secondary Metabolite Production By Marine Fungi. *International Journal of Current Pharmaceutical Research*, *9*(5), 112–119.

Bouarab-Chibane, L., Forquet, V., Lantéri, P., Clément, Y., Léonard-Akkari, L., Oulahal, N., Degraeve, P., & Bordes, C. (2019). Antibacterial properties of polyphenols: Characterization and QSAR (Quantitative structure-activity relationship) models. *Frontiers in Microbiology*, *10*(4), 1–22. https://doi.org/10.3389/fmicb.2019.00829

Braekman, J. C., & Daloze, D. (2004). Chemical and biological aspects of sponge secondary metabolites. *Phytochemistry Reviews*, *3*(3), 275–283. https://doi.org/10.1007/s11101-004-3253-z

Carranza, C. S., Barberis, C. L., Chiacchiera, S. M., & Magnoli, C. E. (2017). Assessment of growth of Aspergillus spp. from agricultural soils in the presence of glyphosate. *Revista Argentina de Microbiología*, *49*(4), 384–393. https://doi.org/10.1016/j.ram.2016.11.007

Cita, Y. P., Suhermanto, A., Radjasa, O. K., & Sudharmono, P. (2017). Antibacterial activity of marine bacteria isolated from sponge Xestospongia testudinaria from Sorong, Papua. *Asian Pacific Journal of Tropical Biomedicine*, *7*(5), 450–454. https://doi.org/10.1016/j.apjtb.2017.01.024

Freeman, C. J., Easson, C. G., Matterson, K. O., Thacker, R. W., Baker, D. M., & Paul, V. J. (2020). Microbial symbionts and ecological divergence of Caribbean sponges: A new perspective on an ancient association. *ISME Journal*, *14*(6), 1571–1583. https://doi.org/10.1038/s41396-020-0625-3

Ginting, E. L., Rangian, L., Wantania, L. L., & Wullur, S. (2019). Isolation of Symbiotic Bacteria with Red Algae from Tongkaina Waters, North Sulawesi. *Jurnal Ilmiah Platax*, *7*(2), 395. https://doi.org/10.35800/jip.7.2.2019.23728

Leal, M. C., Sheridan, C., Osinga, R., Dioníasio, G., Rocha, R. J. M., Silva, B., Rosa, R., & Calado, R. (2014). Marine microorganism-invertebrate assemblages: Perspectives to solve the "supply problem" in the initial steps of drug discovery. *Marine Drugs*, *12*(7), 3929–3952. https://doi.org/10.3390/md12073929

Mahapatra, S., & Banerjee, D. (2013). Optimization of a bioactive exopolysaccharide production from endophytic Fusarium solani SD5. *Carbohydrate Polymers*, *97*(2), 627–634. https://doi.org/10.1016/j.carbpol.2013.05.039

Mahfur, M., Kamila, A., Abidah, J. F., Samirana, P. O., Hikmawan, B. D., & Pratimasari, D. (2023). Antibacterial activity of ethyl acetate extract of symbiont fungus Aspergillus sp. in the sponge Rhabdastrella sp. from Gili Layar Island, Lombok, Indonesia. *Journal of Applied Pharmaceutical Science*, *13*(11), 1–8. https://doi.org/10.7324/JAPS.2023.146303

Mahfur, M., Setyowati, E. P., Wahyuono, S., & Purwantini, I. (2022). Sponge Hyrtios reticulatus : Phytochemicals and Bioactivities. *Research J. Pharm. and Tech.*, *15*(June), 1–7.

Mahfur, M., Wahyuono, S., Purwantini, I., & Setyowati, E. P. (2022). In vitro antiplasmodial activities of the fractions of Hyrtios reticulatus sponge extract. *Journal of Applied Pharmaceutical Science*, *12*(9), 114–120. https://doi.org/10.7324/JAPS.2022.120913

Marzuki, I. (2018). *Eksplorasi Spons Indonesia : Seputar Kepulauan Spermonde* (Vol. 1). https://doi.org/10.17605/OSF.IO/VP369

Papagianni, M., & Sergelidis, D. (2014). Purification and biochemical characterization of a novel

alkaline protease produced by Penicillium nalgiovense. *Applied Biochemistry and Biotechnology*, *172*(8), 3926–3938. https://doi.org/10.1007/s12010-014-0824-3

Purwantini, I., Wahyono, Mustofa, Susidarti, R. A., Sholikhah, E. N., & Hestiyani, R. A. N. (2016). Antiplasmodial activity of endophytic fungi isolated from Artemisia annua, L. *International Journal of Pharmaceutical and Clinical Research*, *8*(5), 341–344.

Rendowaty, A., Djamaan, A., & Handayani, D. (2017). Waktu kultivasi optimal dan aktivitas antibakteri dari ekstrak etil asetat Jamur simbion Aspergillus unguis (WR8) dengan Haliclona fascigera. *Jurnal Sains Farmasi & Klinis*, *4*(1), 49. https://doi.org/10.29208/jsfk.2017.4.1.147

Rosmania, R., & Yanti, F. (2020). Perhitungan jumlah bakteri di Laboratorium Mikrobiologi menggunakan pengembangan metode Spektrofotometri. *Jurnal Penelitian Sains*, *22*(2), 76. https://doi.org/10.56064/jps.v22i2.564

Samirana, P. O., Yosi Bayu, M., Riris Istighfari, J., & Erna Prawita, S. (2021). Marine sponge-derived fungi: fermentation and Cytotoxic activity. *Journal of Applied Pharmaceutical Science*, *11*(01), 21–39. https://doi.org/10.7324/JAPS.2021.110103

Setyowati, E. P., Pratiwi, S. U. T., Purwantiningsih, & Purwantini, I. (2018). In-vitro cytotoxicity and apoptosis mechanism of ethyl acetate extract from Trichoderma reesei strain TV221 associated with marine sponge: Stylissa flabelliformis. *Journal of Applied Pharmaceutical Science*, *8*(9), 151–157. https://doi.org/10.7324/JAPS.2018.8921

Setyowati, E. P., Sudarsono, S., & Murwanti, R. (2017). Penares sp sponge from Menjangan Island-water West Bali National Park: Isolation of Cytotoxic Compounds. *Majalah Obat Tradisional*, *22*(3), 153. https://doi.org/10.22146/mot.31547

Tumiwa, P. I., Yudistira, A., & Wewengkang, D. S. (2019). Aktivitas antimikroba ekstrak etil asetat Jamur laut yang diisolasi dari organisme laut Spons phylospongioa Lamellosa yang Deambil Dari Perairan Desa Tumbak, Kecamatan Pusomaen, Kabupaten Minahasa Tenggara Terhadap Mikroba Staphylococcus Aureus, Escherich. *Pharmacon*, *8*(4), 851. https://doi.org/10.35799/pha.8.2019.29362

Uriz, M., Turon, X., Becerro, M. A., & Agell, G. (2003). Siliceous spicules and skeleton frameworks in sponges: Origin, diversity, ultrastructural patterns, and biological functions. *Microscopy Research and Technique*, *62*(4), 279–299. https://doi.org/10.1002/jemt.10395

Webster, N. S., & Thomas, T. (2016). The sponge hologenome. *MBio*, *7*(2). https://doi.org/10.1128/mBio.00135-16

Wulansari, E. D., Lestari, D., & Khoirunissa, M. A. (2020). Kandungan terpenoid dalam daun Ara (Ficus Carica L.) sebagai agen antibakteri terhadap bakteri Methicillin-Resistant Staphylococcus Aureus. *Pharmacon*, *9*(2), 219. https://doi.org/10.35799/pha.9.2020.29274

Pharmaciana
Vol.14, No.2, July 2024, page. 251-259
ISSN: 2088 4559; e-ISSN: 2477 0256
DOI: 10.12928/pharmaciana.v14i2.27277

Ethanol-based solvent system for recovery antioxidant activity *Centella asiatica* L. Urban and its application in sleep-deprived Rats

Sri Wardatun*, Trirakhma Sofihidayati, Nida Afifah, Juju Juhroh
Pharmacy Program Study, Universitas Pakuan,
Jl. Pakuan,Tegallega, Bogor,West Java, Indonesia

Submitted: 22-09-2023 ***Reviewed: 05-12-2023*** ***Accepted: 29-06-2024***

ABSTRACT

Antioxidants can eliminate free radicals by donating electrons to oxidants. Preclinical and clinical studies show that *Centella asiatica* L. Urban has antioxidant activity. Ethanol was the best solvent for extracting antioxidant compounds from *Centella asiatica* L. Urban. The concentration of ethanol solvents affects the compounds extracted and their antioxidant activities. The study used sleep-deprived rats with glutathione (GSH) concentration parameters to identify ethanol-based solvent systems for the optimum recovery of antioxidant activities and the in vivo antioxidant activity of the most active extract. *C. asiatica* L. Urban powder was macerated with 30, 50, 70, and 96% ethanol, respectively. Using a phosphomolybdate reagent, the extract's antioxidant activity was assessed. In vivo, antioxidant activity was tested on the extract with the highest in vitro antioxidant activity. Ethanol-based solvent systems show different recovery antioxidant activities of *C. asiatica* L. Urban. The antioxidant activity was most recovered in 70% ethanol, with an IC_{50} value of 76.76±25.29 µg/mL. Ethanol 70% *C. asiatica* L. Urban extract given to sleep-deprived rats at 300 mg/kg was not significantly different in glutathione levels from those group rats that received the positive control solution (vitamin C). The *C. asiatica* L. Urban 70% ethanol extract can increase glutathione levels in sleep-deprived rats.

Keywords: *Centella asiatica* L. Urban, antioxidant activity, ethanol, glutathione

Corresponding author:
Sri Wardatun
Pharmacy Program Study, Universitas Pakuan
Jl. Pakuan,Tegallega, Bogor,West Java, Indonesia
Email: sri.wardatun@unpak.ac.id

INTRODUCTION

The plant *Centella asiatica* L. Urban has been utilized for therapeutic purposes for a long time (Gohil et al., 2010). Preclinical and clinical studies show that *C. asiatica* L. Urban has wound healing activity, can be used as a brain stimulant, has cognitive improvement and neuroprotective, antiepileptic, and anticonvulsant activities, antioxidant, anti-gastric ulcer, anti-inflammatory properties, anti-proliferative activity, cardioprotective activity, and antidiabetic activity (Arribas-López et al., 2022; Biswas et al., 2021; Junsi & Siripongvutikorn, 2022; Matthews et al., 2019; Mishra et al., 2022; Ramli et al., 2020; Zweig et al., 2021). There are antiviral, antifungal, and antibacterial properties in *C. asiatica* L. Urban (Biswas et al., 2021). There were 139 secondary metabolites isolated from *C. asiatica* L. Urban (Kunjumon et al., 2022). A compound class of phytochemical constituents has been identified as flavonoids, alkaloids, flavones, glycosides, phenolic acids, saponins, triterpenic acids, sesquiterpenes, monoterpenes, diterpenes, polyacetylenes, amino acids, ketone, sugar, sterols, essential oils, minerals, volatiles, and fatty oils (Biswas et al., 2021). The active ingredients of triterpenoid saponin were asiatic acid, asiaticoside, madekossida, and centelloside (Irham et al., 2019).

The solvent was one of the critical parameters that affected the number of bioactive compounds and activity extracted (Mohapatra et al., 2021; Ng et al., 2020). Solvents also affect cell wall permeability via chemical and physical changes (Oreopoulou et al., 2019). The solvent with different polarities had a significant effect on antioxidant activities. The maceration of *C. asiatica* L. Urban has been carried out using methanol, distilled water, ethyl acetate, and n-hexane as solvents; ethanol has not yet been used (Gunathilake et al., 2019; Ng et al., 2020). The ethanol concentration primarily affects the solvent's polarity and extraction efficiency (Trujillo et al., 2020). Ethanol is a non-toxic organic solvent that is relatively cheap, reusable, environment friendly, and commonly used in the preparation of food or nutraceuticals (Gunathilake et al., 2019; Joshi & Adhikari, 2019). The use of ethanol is expected to increase the extraction efficiency of compounds from *C. asiatica* L. Urban that have antioxidant activity; however, it has been shown that the use of ethanol at high concentrations reduces antioxidant activity (Gunathilake et al., 2019). Thus, it's critical to ascertain how ethanol concentration affects *C. asiatica* L. Urban's antioxidant activities.

Antioxidant activity is defined as the ability to reduce free radicals. Free radicals are highly reactive because their outer electrons are unpaired. Free radicals can impair cells by damaging lipids, proteins, and deoxyribonucleic acid (DNA), which can lead to various chronic and degenerative diseases. Antioxidants can eliminate free radicals; they can donate electrons to oxidants to inhibit their activity (Gulcin, 2020).

This study aimed to extract *C. asiatica* L. Urban used various ethanol concentrations to assess the antioxidant properties of extracts in vitro and in vivo. The phosphomolybdate reagent was utilized to ascertain the in vitro antioxidant activity (Alam et al., 2013). Antioxidant activity in vivo was assessed by quantifying glutathione (GSH) levels. It has been demonstrated that *C. asiatica* L. Urban methanol extract raises GSH levels in vivo; however, 70% ethanol extract has not yet been determined (Arora et al., 2018). GSH in the body has a thiol group or sulfhydryl group derived from cysteine residues, so it can function as an antioxidant capable of lowering nitrogen, reactive oxygen, and electrophiles (Lushchak, 2012).

MATERIALS AND METHOD

Materials

C. asiatica L. Urban was obtained from Bogor, Indonesia, and its identity was determined in the Herbarium Bogoriense, National Research and Innovation Agency, quercetin (Sigma Aldrich, Singapore), ascorbic acid/vitamin C (Merck, Indonesia), and every reagent that was utilized was analytical grade.

Preparation of the extract

The herb was dried, and a powder was prepared. A total of 400 g of dry powder was pretreated with petroleum ether (1:4) for 24 h. The fat-free residue was divided equally by weight and then macerated with 30, 50, 70, or 96% ethanol at 1:10 (v/v), respectively. Then, filtrates were concentrated at 40 °C using a rotary evaporator until a dried extract was obtained. The dried extracts were weighed to obtain yield extract (%), which is determined by weighing the extract in comparison to the weight of *C. asiatica* L. Urban's raw material (Ng et al., 2020).

Preparation of reagents and solutions

To prepare the phosphomolybdate reagent solution, a total of 3.33 mL of sulfuric acid was diluted in 100 mL of aquadest, then 0.4 grams of sodium phosphate and 0.5 grams of ammonium molybdate were added. 30 mM sodium phosphate, 0.6 M sulfuric acid, and 4 mM ammonium molybdate were all present in the reagent solution. Before use, the reagent was always freshly produced (Murtala et al., 2021).

To prepare the quercetin standard solution, 50 mg of quercetin was weighed and dissolved in 50 mL (1,000 µg/mL) of methanol. The following concentrations were then prepared: 50, 60, 70, 80, and 90 µg/mL.

The test solutions were prepared by making stock solutions of extract that had been extracted with 30, 50, 70, and 96% ethanol. The extract was weighed at 50 mg and dissolved in 25 mL of methanol (2,000 µg/mL). Each was then diluted at 600, 400, 200,100, and 100 µg/mL, respectively.

Qualitative in vitro tests of phenolic compound and antioxidant activity

One milliliter of ethanol extract solution was mixed with three drops of a 5% ferric chloride solution. When the extract's color changed to a deep green or bluish-black color, it meant that polyphenolic chemicals were present (Shaikh & Patil, 2020).

To determine the flavonoid components, 1 mL of the extract was heated in 1–2 mL of 50% methanol, added 0.5 g of magnesium powder, and then added with 5–6 drops of chloride acid. Flavones were detected by the formation of an orange-red color and a red color in the extract, respectively (Shaikh & Patil, 2020).

To perform the free radical scavenging test, 0.5 mL of ethanol extract solution and 15 mM DPPH reagent solution were added, respectively. When the samples' color changed from purple to yellow, antioxidant activity was confirmed (Ayoola et al., 2008).

Antioxidant activity test

The antioxidant activity tests were carried out in a test tube after adding one milliliter of phosphomolybdate reagent and one milliliter of extract solution. At 95 ^{0}C, the mixture has been incubated for 60 minutes. The solution was kept at room temperature. Subsequently, 1 mL was taken out of the mixture, and 5 mL of methanol was added. For an optimum incubation time of 30 minutes, the mixture shall be allowed to stand. Using a UV-Vis spectrophotometer (Jasco-V730) at a wavelength of 703.5 nm, the absorbance of the mixture was determined (Alam et al., 2013). The samples were determined to have antioxidant activity when the color changed from yellow to green (Abifarin et al., 2019; Murtala et al., 2021).

In vivo testing

Analysis of glutathione (GSH) levels

Before in vivo testing, a research permit was obtained from the Ethics Commission Faculty of Mathematics and Natural Sciences, Universitas Pakuan, Indonesia, No. 036/KEPHP-UNPAK/11-202. Adult male white Sprague-Dawley rats weighing 180–200 g had been used in this research. The rats were kept in standard cages at 24 ± 1 °C with a 12/12 light/dark cycle, ad libitum for access to water and food. Acclimatization was carried out for one week. Four treatment groups were randomly given to the rats, with six rats in each group. Group 1 was the negative control and was given 1 mL of aquadest.

Group 2 was the positive control and was given ascorbic acid 100 mg/day in 1 mL (Zasowska-Nowak et al., 2021).

Rats in Groups 3 and 4 were given an ethanol extract of *C. asiatica* L. Urban at doses of 300 mg/kg BW and 500 mg/kg BW in 1 mL, respectively (El-Sebaey et al., 2019). After acclimatization, animals were treated with sleep deprivation using gentle handling procedures. This procedure involved brushing fur with a cotton tip applicator, inserting objects into the cage, tapping the cage, and rotating the cage. The test rat group was divided into two batches (Ramanathan et al., 2010). The treatment of each batch was carried out by the same person with the same intensity and duration of treatment. The procedure was carried out for 6 hours (08.00–14.00) for six days and 2 hours on day 7 (08.00–10.00). The handling procedure is carried out for 5 minutes every 30 minutes (Ramanathan et al., 2010; Villafuerte et al., 2015).

One hour after sleep-deprived procedures finished, all group rats were given aquadest, vitamin C solution, or *C. asiatica* L extract, respectively. Administration was performed once (a single dose) using a gastric probe. Two hours after aquadest or ascorbic acid solution or extract has been administered, these animals have been sacrificed. Their livers and kidneys were removed and quickly cut open on ice after being cleaned with previously cold saline. For estimation of GSH content, a mixture of liver (25%) and kidney (10%) homogenates has been prepared and used. Protein in 0.5 mL of mixed tissue homogenate was precipitated with a 20% trichloroacetic acid (125 µL) dilution, incubated for 5 minutes, and then cooled the mixture on ice. After adding 0.6 mL of 5% TCA to the mixture, it was centrifuged at 1,000 rpm for 10 minutes. Next, a 0.2 M phosphate buffer (pH 8.0) solution was mixed with 0.1 mL of the supernatant until 1 mL was obtained. Then 2 mL of freshly made DTNB solution in 0.2 M phosphate buffer was added to supernatant. After 1F0 minutes, the the yellow color of solution was measured using a spectrophotometer at a wavelength of 412 nm (Sheeja & Kuttan, 2006).

Statistical analyses

All measurements were performed in triplicate. The average standard deviation of the results was provided. To assess the importance between groups, statistical analyses have been carried out with ANNOVA. A significance level of 0.05 was chosen for the p-value.

RESULT AND DISCUSSION

The herbal powder was pretreated with petroleum ether to remove fat before being macerated with various concentrations of ethanol. The yield extract is presented in Table 1.

Table 1. Extract yields of *C. asiatica* L. Urban extract using various concentrations of ethanol

Type of solvent Extraction	Yield ± SD (%)
30% ethanol	17.38 ± 1.64
50% ethanol	16.21 ± 0.60
70% ethanol	15.75 ± 0.96
96% ethanol	9.89 ± 1.47

Extraction yields showed the ability of the solvent to obtain a crude extract from dried powders and then use it for further utilization (Azmin & Nor, 2020). Table 1 shows a 30% ethanol extract of *C. asiatica* L. Urban was found to have a higher yield than the others. The increasing extracting yield of *C. asiatica* L. Urban by different concentrations of ethanol solvent was in the following 30% ethanol > 50% ethanol > 70% ethanol > 96% ethanol. The extract shall yield an indicative amount of compounds that have been recovered from the solvent (Oreopoulou et al., 2019; Yeop et al., 2019). The results of extraction yields are proportional to the polarity of the solvent (Ng et al., 2020). The difference in ethanol concentration causes a difference in polarity. The lower concentration of ethanol has a higher polarity because water has a higher polarity than ethanol and can produce a higher extract yield of *C. asiatica* L.

Urban. The solvent will diffuse into plant material during extraction and dissolve compounds according to their polarity (Azmin & Nor, 2020). The 30% ethanol solvent was found to be an efficient solvent for extracting yields. The results are according to Ng et al., 2020, who showed that a solvent with a higher polarity may extract extracts with a higher yield. Generally, the polarity of the solvent can impact to yield of extracts.

The results of preliminary qualitative tests for polyphenols and flavonoids showed that *C. asiatica* L. Urban powder and ethanolic extracts contained polyphenols and flavonoids. The preliminary free radical scavenger test (with the DPPH reagent) and antioxidant activity test (with the phosphomolybdate reagent) showed that powder and ethanol extracts had both antioxidant and free radical scavenging activity. Polyphenols and flavonoids were significant compounds that provided antioxidant activity in *C. asiatica* L. Urban and give a strong correlation to antioxidant activity. The main compounds of polyphenols and flavonoids in *C. asiatica* L. Urban ethanolic extracts are apigenin, rutin, kaempferol, luteolin, quercitrin, quercitin, castilliferol, and chlorogenic acid (Azmin & Nor, 2020; Jhansi & Kola, 2019; Ramli et al., 2020).

Reactive oxidative species (ROS), which cause cell damage, are released when there is an imbalance between oxidants and antioxidants, leading to oxidative stress. ROS can consist of peroxide, hydroxyl ions, and nitric oxide, which form during living metabolism and can cause various diseases like aging, cancer, inflammatory diseases, and cardiovascular diseases. Antioxidants are effective agents to eliminate the action of ROS in the body (Jhansi & Kola, 2019; Ramli et al., 2020). Sources of antioxidant agents can come from herbs, *C. asiatica* L. Urban was one of them (Idris & Mohd Nadzir, 2021). The results of the antioxidant activity assay of *C. asiatica* L. Urban is shown in Table 2. In vitro, antioxidant activity was determined using the phosphomolybdate reagent, which is a mixture of sulfuric acid, ammonium molybdate, and sodium phosphate. The green phosphomolybdate complex is created by the reduction of Mo (VI) to Mo (V) at an acidic pH. This oxidation-reduction reaction is the basis of the phosphomolybdate method (Alam et al., 2013). The 70% ethanol extract was shown to have the strongest antioxidant activity compared to the other extracts. The antioxidant activity of 70% ethanol extract > 96% ethanol extract > 50% ethanol extract > 30% ethanol extract of *C. asiatica* L. Urban (Table 2). The different solvent concentrations show different antioxidant activities. The polarity of the solvent contributed had an impact to the solubility of compounds during extraction. Flavonoids, polyphenol compounds, and other antioxidant agents have different solubility in different ethanol polarities (Azmin & Nor, 2020). This matter causes different ethanol concentrations, resulting in different antioxidant activities. The extract with the highest antioxidant activity was then determined for in vivo testing.

Table 2. Antioxidant activity of *C. asiatica* L. Urban extract which was extracted using various concentrations of ethanol

Type of solvent extraction	IC_{50} ± SD (µg/mL)
quercetin	38.85 ± 13.06
30% ethanol extract	459.74 ± 116.12
50% ethanol extract	364.25 ± 78.13
70% ethanol extract	76.76 ± 25.29
96% ethanol extract	203.95 ± 68.54

Figure 1 shows GSH levels of rats that were treated with positive control solution, negative control solution, or *C. asiatica* L. Urban 70% ethanol extracts with different doses. It can be seen that sleep-deprived rats that received 300 mg/kg of *C. asiatica* L. Urban extract had significantly different GSH levels compared to rats that received a negative control solution (aquadest). In addition, their GSH levels were not significantly different from those of rats that received a positive control solution (oral ascorbic acid).

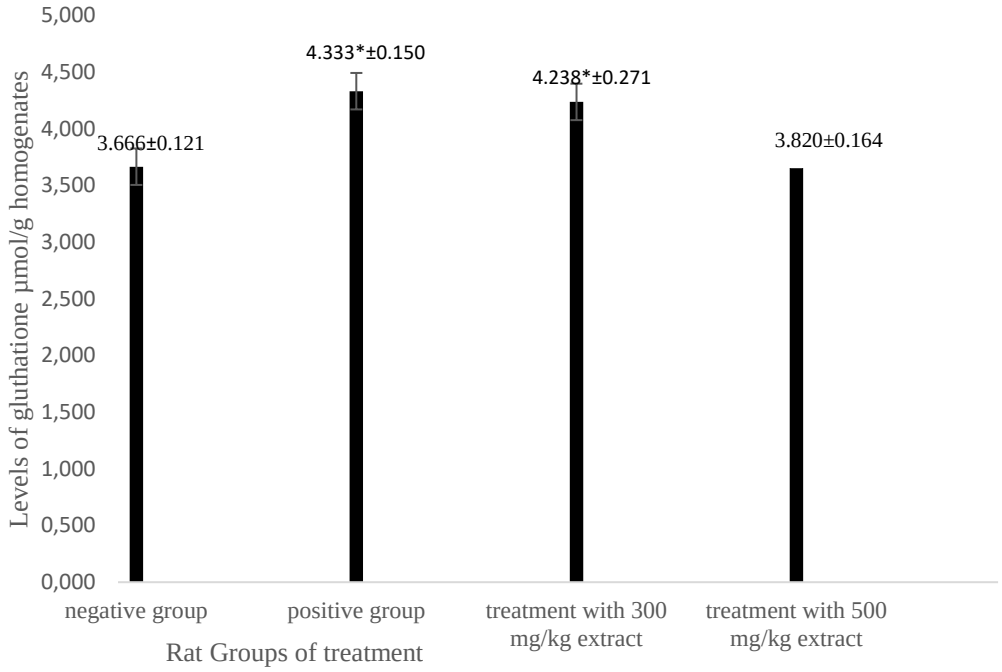

Figure 1. Levels of GSH in a mixture of liver and kidney homogenates of sleep-deprived rats
* Results are significantly different from the negative group ($p < 0.05$)

GSH (glutathione) levels in tissues of treated rats with 70% ethanol extract of *C. asiatica* L. Urban was determined. GSH levels were determined by quantitating the sulfhydryl group (R-SH) present in GSH (Moron et al., 1979). GSH and DTNB react to form the GSH dimer and 2-nitro-5-mercaptobenzoic acid (Appala et al., 2016), a yellow compound (Khan, 2012) that can be detected at 411 nm, which falls within the yellow-green absorption spectrum of 400–435 nm (Shah et al., 2015; Verma & Mishra, 2018). GSH compounds were used as standards in this assay.

Sleep deprivation, or a reduction in sleep time, can promote oxidative stress. When the body's antioxidant systems are overburdened by prooxidants like ROS, oxidative stress results (Villafuerte et al., 2015). Superoxide dismutase (SOD), glutathione peroxidase (GPx), and catalase (CAT) as antioxidant enzymes become less active when ROS production surpasses the antioxidant capacity of the cell and induces oxidative stress. This lowers GSH levels and increases ROS accumulation (Gulcin, 2020). Antioxidants are expected to increase reduced GSH levels because oxidative stress can be overcome by the presence of antioxidants. The activity of *C. asiatica* L. Urban extract was traced, and the results are shown in Figure 1. The research demonstrated that giving sleep-deprived rats 300 mg/kg of *C. asiatica* L. Urban extract produced significantly different GSH levels than rats given aquadest (negative control) and similar GSH levels than rats given oral vitamin C (positive control). Vitamin C has antioxidant activity because it can donate electrons to free radicals and can increase GSH levels in the body (Biswas et al., 2021; Gulcin, 2020). GSH levels were not significantly increased by the 500 mg/kg dose of the extract in comparison to the positive control but above the negative control's GSH levels. This is due to the extract's ingredients having saturated the receptors in the body and preventing them from producing the maximum effect (Pasaribu et al., 2012). Therefore, administering the 70% ethanol extract of *C. asiatica* L. Urban which contained antioxidant compounds for sleep-deprived rats, was found to increase GSH levels in the body.

The increased GSH levels detected in rats administered *C. asiatica* L. Urban extracts were related to the overall activity of the natural materials in the extract. Natural materials can induce Nfr2 pathway

signals (Molaei et al., 2021) and play a role in the inactivation of nuclear factor erythroid 2 (Waz et al., 2021). Nrf2 is an important factor in the transcription process that is encoded by the nuclear factor erythroid 2 leucine 2 (NFE2L2) gene and functions to regulate the expression of gene sequences in antioxidant response element (ARE) and influences the synthesis of GSH, GPx, the thioredoxin system, and enzymes related to phase 1 and phase 2 (Molaei et al., 2021). An increase in GSH levels in the body is advantageous because GSH has antioxidant activity; its thiol group or sulfhydryl group derived from cysteine residues allows it to reduce reactive oxygen or nitrogen compounds and electrophiles (Lushchak, 2012).

CONCLUSION

Of all the studied extracts, 70% ethanol extract *C. asiatica* L. Urban's had the highest antioxidant activity. The GSH levels of sleep-deprived rats treated with 300 mg/kg of the extract were found to be comparable to those of rats given vitamin C. Therefore, in sleep-deprived rats, the 70% ethanol extract of *C. asiatica* L. Urban may raise glutathione levels.

ACKNOWLEDGMENTS

All authors give high gratitude to Universitas Pakuan for the financial support of this research under contract number 70. LPPMVII, 2021.

REFERENCES

Abifarin, T. O., Afolayan, A. J., & Otunola, G. A. (2019). Phytochemical and antioxidant activities of Cucumis africanus L.f.: a wild vegetable of South Africa. *Journal of Evidence-Based Integrative Medicine*, *24*, 2515690X1983639. https://doi.org/10.1177/2515690X19836391

Alam, M. N., Bristi, N. J., & Rafiquzzaman, M. (2013). Review on in vivo and in vitro methods evaluation of antioxidant activity. *Saudi Pharmaceutical Journal*, *21*(2), 143–152. https://doi.org/10.1016/j.jsps.2012.05.002

Appala, R. N., Chigurupati, S., Appala, R. V. V. S. S., Krishnan Selvarajan, K., & Islam Mohammad, J. (2016). A simple HPLC-UV method for the determination of Glutathione in PC-12 Cells. *Scientifica*, *2016*, 1–6. https://doi.org/10.1155/2016/6897890

Arora, R., Kumar, R., Agarwal, A., Reeta, K. H., & Gupta, Y. K. (2018). Comparison of three different extracts of Centella asiatica for anti-amnesic, antioxidant and anticholinergic activities: in vitro and in vivo study. *Biomedicine & Pharmacotherapy*, *105*, 1344–1352. https://doi.org/10.1016/j.biopha.2018.05.156

Arribas-López, E., Zand, N., Ojo, O., Snowden, M. J., & Kochhar, T. (2022). A systematic review of the effect of Centella asiatica on Wound Healing. *International Journal of Environmental Research and Public Health*, *19*(6), 3266. https://doi.org/10.3390/ijerph19063266

Ayoola, G. A., Folawewo, A. D., Adesegun, S. A., & Abioro, O. O. (2008). Phytochemical and antioxidant screening of some plants of apocynaceae from South West Nigeria. *African Journal of Plant Science*, *2*(9), 124–128.

Azmin, S. N. H. M., & Nor, M. S. M. (2020). Chemical fingerprint of Centella Asiatica's bioactive compounds in the ethanolic and aqueous extracts. *Advances in Biomarker Sciences and Technology*, *2*, 35–44. https://doi.org/10.1016/j.abst.2020.10.001

Biswas, D., Mandal, S., Chatterjee Saha, S., Tudu, C. K., Nandy, S., Batiha, G. E., Shekhawat, M. S., Pandey, D. K., & Dey, A. (2021). Ethnobotany, phytochemistry, pharmacology, and toxicity of Centella asiatica (L.) Urban: A comprehensive review. *Phytotherapy Research*, *35*(12), 6624–6654. https://doi.org/10.1002/ptr.7248

El-Sebaey, A. M., Abdelhamid, F. M., & Abdalla, O. A. (2019). Protective effects of garlic extract against hematological alterations, immunosuppression, hepatic oxidative stress, and renal damage induced by cyclophosphamide in rats. *Environmental Science and Pollution Research*, *26*(15), 15559–15572. https://doi.org/10.1007/s11356-019-04993-7

Gohil, K., Patel, J., & Gajjar, A. (2010). Pharmacological review on Centella asiatica: A potential herbal

cure-all. *Indian Journal of Pharmaceutical Sciences*, *72*(5), 546. https://doi.org/10.4103/0250-474X.78519

Gulcin, İ. (2020). Antioxidants and antioxidant methods: an updated overview. *Archives of Toxicology*, *94*(3), 651–715. https://doi.org/10.1007/s00204-020-02689-3

Gunathilake, K. D. P. P., Ranaweera, K. K. D. S., & Rupasinghe, H. P. V. (2019). Response surface optimization for recovery of polyphenols and carotenoids from leaves of Centella asiatica using an ethanol-based solvent system. *Food Science & Nutrition*, *7*(2), 528–536. https://doi.org/10.1002/fsn3.832

Idris, F. N., & Mohd Nadzir, M. (2021). Comparative studies on different extraction methods of Centella asiatica and extracts bioactive compounds effects on antimicrobial activities. *Antibiotics*, *10*(4), 457. https://doi.org/10.3390/antibiotics10040457

Irham, W. H., Tamrin, Marpaung, L., & Marpongahtun. (2019). Bioactive compounds in Pegagan leaf (Centella asiatica L. Urban) for wound healing. *Journal of Physics: Conference Series*, *1232*(1), 012019. https://doi.org/10.1088/1742-6596/1232/1/012019

Jhansi, D., & Kola, M. (2019). The antioxidant potential of Centella asiatica: a review. *Journal of Medicinal Plants Studies*, *18*(2), 18–20. http://dx.doi.org/10.1016/j.etap.

Joshi, D. R., & Adhikari, N. (2019). An overview on common organic solvents and their toxicity. *Journal of Pharmaceutical Research International*, 1–18. https://doi.org/10.9734/jpri/2019/v28i330203

Junsi, M., & Siripongvutikorn, S. (2022). Development of herbal juice from Centella asiatica: antioxidant property, nutritional value and shelf life of product. *Food Science and Technology*, *42*. https://doi.org/10.1590/fst.93722

Khan, H. (2012). Oxidation of glutathione (GSH) in blood plasma due to oxidative stressors: A case study of silver. *African Journal of Pharmacy and Pharmacology*, *6*(21). https://doi.org/10.5897/AJPP11.790

Kunjumon, R., Johnson, A. J., & Baby, S. (2022). Centella asiatica: Secondary metabolites, biological activities and biomass sources. *Phytomedicine Plus*, *2*(1), 100176. https://doi.org/10.1016/j.phyplu.2021.100176

Lushchak, V. I. (2012). Glutathione homeostasis and functions: potential targets for medical interventions. *Journal of Amino Acids*, *2012*, 1–26. https://doi.org/10.1155/2012/736837\

Matthews, D. G., Caruso, M., Murchison, C. F., Zhu, J. Y., Wright, K. M., Harris, C. J., Gray, N. E., Quinn, J. F., & Soumyanath, A. (2019). Centella asiatica improves memory and promotes antioxidative signaling in 5XFAD mice. *Antioxidants*, *8*(12), 630. https://doi.org/10.3390/antiox8120630

Mishra, A., Singh, Y., Singh, R., Kumar, R., Shukla, S., Kumar, R., Prajapati, Aditi, Rawat, N., Kumar, A., & Pol7, S. L. (2022). Ethano-pharmacology activity & Antioxidant activity of Centella asiatica Plant Parts. *Neuroquantology*, *20*(11), 7562–7572. https://doi.org/10.14704/nq.2022.20.11.NQ66753

Mohapatra, P., Ray, A., Jena, S., Nayak, S., & Mohanty, S. (2021). Influence of extraction methods and solvent system on the chemical composition and antioxidant activity of Centella asiatica L. leaves. *Biocatalysis and Agricultural Biotechnology*, *33*, 101971. https://doi.org/10.1016/j.bcab.2021.101971

Molaei, E., Molaei, A., Abedi, F., Hayes, A. W., & Karimi, G. (2021). Nephroprotective activity of natural products against chemical toxicants: The role of Nrf2/ARE signaling pathway. *Food Science & Nutrition*, *9*(6), 3362–3384. https://doi.org/10.1002/fsn3.2320

Moron, M., Depierre, J., & Mannervik, B. (1979). Levels of glutathione, glutathione reductase and glutathione S-transferase activities in rat lung and liver. *Biochimica et Biophysica Acta (BBA) - General Subjects*, *582*(1), 67–78. https://doi.org/10.1016/0304-4165(79)90289-7

Murtala, R., S. I., Alhassan., H.I, Rasheed., S. N., Dalhatu., S.S, Bala., S.A, Idris., & D. C., Anyanaso. (2021). Comparative phytochemical screening and antioxidant activity of lemon grass and sweet

wormwood leaves extract. *International Journal of Advanced Chemistry*, *9*(1), 20–24. https://doi.org/10.14419/ijac.v9i1.31422

Ng, Z. X., Samsuri, S. N., & Yong, P. H. (2020). The antioxidant index and chemometric analysis of tannin, flavonoid, and total phenolic extracted from medicinal plant foods with the solvents of different polarities. *Journal of Food Processing and Preservation*, *44*(9). https://doi.org/10.1111/jfpp.14680

Oreopoulou, A., Tsimogiannis, D., & Oreopoulou, V. (2019). Extraction of polyphenols from aromatic and medicinal plants: an overview of the methods and the effect of extraction parameters. In *Polyphenols in Plants* (pp. 243–259). Elsevier. https://doi.org/10.1016/B978-0-12-813768-0.00025-6

Pasaribu, F., Sitorus, P., & Bahri, S. (2012). The test of ethanol extract of mangosteen rind (Garcinia mangostana L.) to decrease blood glucose level. *Journal of Pharmaceutics and Pharmacology*, *1*(1), 1–8.

Ramanathan, L., Hu, S., Frautschy, S. A., & Siegel, J. M. (2010). Short-term total sleep deprivation in the rat increases antioxidant responses in multiple brain regions without impairing spontaneous alternation behavior. *Behavioural Brain Research*, *207*(2), 305–309. https://doi.org/10.1016/j.bbr.2009.10.014

Ramli, S., Xian, W. J., & Abd Mutalib, N. A. (2020). A review: antibacterial activities, antioxidant properties and toxicity profile of centella asiatica. *Educatum Journal Of Science, Mathematics And Technology*, *7*(1), 39–47. https://doi.org/10.37134/ejsmt.vol7.1.5.2020

Shah, R. ., Shah, R. ., Pawar, R. ., & Gayakar, P. P. (2015). UV-Visible spectroscopy-review. *International Journal of Institutional Pharmacy and Life Science*, *5*(5), 490–505.

Shaikh, J. R., & Patil, M. (2020). Qualitative tests for preliminary phytochemical screening: An overview. *International Journal of Chemical Studies*, *8*(2), 603–608. https://doi.org/10.22271/chemi.2020.v8.i2i.8834

Sheeja, K., & Kuttan, G. (2006). Protective effect of andrographis paniculata and andrographolide on Cyclophosphamide-induced urothelial toxicity. *Integrative Cancer Therapies*, *5*(3), 244–251. https://doi.org/10.1177/1534735406291984

Trujillo, A. S. D., Jiménez Forero, J. A., Pineda Insuasti, J. A., González Trujillo, C. A., & García Juarez, M. (2020). Extracción de sustancias bioactivas de Pleurotus ostreatus (Pleurotaceae) por maceración dinámica. *Acta Biológica Colombiana*, *25*(1), 61–74. https://doi.org/10.15446/abc.v25n1.72409

Verma, G., & Mishra, M. (2018). Development and optimization of UV-Vis spectroscopy - a review. *World Journal of Pharmaceutical Research*, *7*(11), 1170–1180.

Villafuerte, G., Miguel-Puga, A., Murillo Rodríguez, E., Machado, S., Manjarrez, E., & Arias-Carrión, O. (2015). Sleep deprivation and oxidative stress in animal models: a systematic review. *Oxidative Medicine and Cellular Longevity*, *2015*, 1–15. https://doi.org/10.1155/2015/234952

Waz, S., Heeba, G. H., Hassanin, S. O., & Abdel-latif, R. G. (2021). Nephroprotective effect of exogenous hydrogen sulfide donor against cyclophosphamide-induced toxicity is mediated by Nrf2/HO-1/NF-κB signaling pathway. *Life Sciences*, *264*, 118630. https://doi.org/10.1016/j.lfs.2020.118630

Yeop, A., Pang, S. F., Law, W. P., Yusoff, M. M., & Gimbun, J. (2019). Assessment of size reduction and extraction methods on the yield of gallic acid from Labisia pumila leaf via Microstructures analysis. *Materials Today: Proceedings*, *19*, 1280–1286. https://doi.org/10.1016/j.matpr.2019.11.134

Zasowska-Nowak, A., Nowak, P. J., & Ciałkowska-Rysz, A. (2021). High-dose vitamin C in advanced-stage cancer patients. *Nutrients*, *13*(3), 735. https://doi.org/10.3390/nu13030735

Zweig, J. A., Brandes, M. S., Brumbach, B. H., Caruso, M., Wright, K. M., Quinn, J. F., Soumyanath, A., & Gray, N. E. (2021). Loss of NRF2 accelerates cognitive decline, exacerbates mitochondrial dysfunction, and is required for the cognitive enhancing effects of Centella asiatica during aging. *Neurobiology of Aging*, *100*, 48–58. https://doi.org/10.1016/j.neurobiolaging.2020.11.019

Pharmaciana
Vol.14, No.2, July 2024, Page. 260-266
ISSN: 2088 4559; e-ISSN: 2477 0256
DOI: 10.12928/pharmaciana.v14i2.28083

The antiviral activity of *Laportea decumana* Methanolic extract against NDV virus

Tee Albert[1,†], Pho Duc Khiem[2,†], Musung Anastasia Beatrix[1], Wijaya Dorothy[1], Sutejo Richard[1*]
[1]Biomedicine Department, Indonesia International Institute for Life Sciences, Indonesia
Jl. Pulomas Barat Kav 88, Jakarta Timur, DKI Jakarta, Indonesia
[†]Contributed equally as co-first authors
[2]Medical and Pharmaceutical Biotechnology at the University of Pecs, Faculty of Medicine, Hungary

Submitted: 29-12-2023 ***Reviewed: 09-07-2024*** ***Accepted: 17-07-2024***

ABSTRACT

The avian species virus that causes Newcastle disease is an extremely contagious illness. Avian paramyxovirus 1, or Newcastle disease virus (NDV), is a virus that brings harm to poultry's central nervous system and digestive tract. The NDV outbreak was initially documented in 1928 in Java, Indonesia. Newcastle disease does not currently require therapy. One popular and useful strategy for preventing and treating viral infections, such as Newcastle disease, is vaccination. With a variety of native medicinal plants and an abundance of biodiversity, Indonesia presents a promising area for biotechnology and pharmaceutical research. *Laportea decumana*, is a native plant in the Eastern part of Indonesia that contains alkaloids, glycosides, steroids, flavonoids, tannin, and saponin. Its cytotoxic, analgesic, antioxidant, and antibacterial properties have all been demonstrated. The antiviral properties of *L. decumana* have not been extensively researched. Thus, the purpose of this study is to examine L. decumana's antiviral activity, particularly against NDV, using a variety of techniques, including the plaque assay, cytotoxicity test, and gene expression experiment. *L. decumana* extracts at 100 μg/mL or less is a safe concentration to consider, as it still has 65% and above cell viability based on the results of the cytotoxic assay.

Keywords: NDV, *Laportea decumana*, antiviral, plaque assay

Corresponding author:
Richard Sutejo
Indonesia International Institute for Life Sciences
Jl. Pulomas Barat Kav 88, Jakarta Timur, DKI Jakarta, Indonesia
Email: richard.sutejo@i3l.ac.id

INTRODUCTION

Newcastle disease is a highly contagious disease caused by avian viral infection. This virus is known for its harmful effects on the central nervous system and digestive tract of poultry (Butt et al., 2019). NDV is a non-segmented virus structured into six genes that encode various proteins: NP, M, HN, P, L, and F. L is considered a virulence marker of NDV. NDV is a negative-stranded RNA virus (Murulitharan et al., 2013). The NDV outbreak was first reported in Indonesia in 1928, specifically in Java (Dzogbema et al., 2021). Currently, there are no treatments for Newcastle disease (Absalón et al., 2019). Vaccination is a common and effective method to prevent and control viral infections, including Newcastle disease (Ellebedy & Ahmed, 2016).

Due to its wide range of native medicinal plants and rich biodiversity, Indonesia is an ideal area for biotechnology and pharmaceutical research. Moreover, Indonesia is known as a high-humidity country which promotes the growth of natural plants, including Laportea. One of the commonly studied species of Laportea is *Laportea decumana*. This species has been determined to contain alkaloids, steroids, tannins, saponins, flavonoids and glycosides, which have been widely used in many research areas (Thalib et al., 2021). Flavonoids, a type of phenolic compound, have been shown to work as an antiviral agent by inhibiting proteases, DNA/RNA polymerases, and viral neuraminidase (Ninfali et al., 2020). Interestingly, *L. decumana* has been tested for its antioxidant and antibacterial purposes; however, the antioxidant properties of this plant have yet to be investigated (Simaremare et al., 2018; Thalib et al., 2022). Immortalized cell line has been widely used as a host cell in much research since it is shown to provide a reproducible outcome and consistent sample (Kaur & Dufour, 2012). One of the examples of commonly used immortalized cell lines is HeLa cells. Some antiviral studies have shown the use of HeLa cells as host cells, including (Chu et al., 2018), where the influence of NDV on HeLa cells was tested through the MEK/ERK signaling activation.

Hence, the aim of this research is to investigate the antiviral activity of *L. decumana*, especially against NDV in the HeLa cells, by utilizing several methods. A plaque assay was performed to determine the amount of infectious virus in the sample. The cytotoxicity properties of *L. decumana* were then tested using an MTS assay, followed by the determination of the gene expression ability, which was conducted through qRT-PCR towards the NDV gene.

MATERIALS AND METHOD

Materials

The *Laportea decumana* used was purchased from the local market in Papua, marked by being a perennial plant with slightly woody, approximately 2 meters in height, with well-branched stems and leaves densely armed with irritant hairs with lengths of approximately 0.5 to 1 cm. The HeLa cell culture used was obtained from ATCC. NDV virus used in this experiment was a La Sota strain grown in embryonated chicken eggs (Chu et al., 2019; Masoud et al., 2022; Mast et al., 2006).

Methods

Generation of L. decumana methanolic extract

Two hundred grams of *L. decumana* powder were put in two Erlenmeyer, one hundred grams each. The powder was macerated for three days at 180 rpm after being soaked in 500 mL of methanol. A Buchner pump and Whatman filter paper (Grade 1) were used to filter the extract. There were two iterations of the maceration procedure. A Buchi rotary evaporator was employed to concentrate the filtrates at 65°C. After that, the surplus solvent was eliminated using an evaporating dish set over a 50°C water bath under a fume hood for two days or until the weight stabilized and the extract yield could be determined. The extracts were placed in the refrigerator to be used later on and covered with aluminum foil.

HeLa cell culture

HeLa cell lines were grown at 37°C in a 5% CO_2 incubator in a complete Dulbecco's Modified Eagle Medium (DMEM) containing 10% Fetal Bovine Serum (FBS), 3.7 gr/L Sodium Bicarbonate

($NaHCO_3$), and 1% Penicillin-streptomycin. The cells were passaged thrice a week in sterile conditions under a biosafety cabinet.

Cytotoxicity Assay of L. decumana extract

HeLa cell lines were seeded with complete DMEM at a density of 1 x 104cell/well in a 96-well plate and incubated in a 5% CO_2 incubator at 37°C for 24 hours. The cells were then washed and starved for 3 hours in DMEM and treated with different concentrations of *L. decumana* extracts (50, 100, 150, 200, and 250 µg/mL) and incubated for 48 hours. The cells were supplemented with 15 µL MTS reagent. The absorbance of untreated and *L. decumana* treated cells was readed using a microplate reader at 490 nm. The half-maximal inhibitory concentration (IC_{50}) was then assessed using the following equation (Bayer et al., 2023):

$$y = D + \frac{A+D}{1+10^{(x-logC)B}} \quad \text{.....(1)}$$

Plaque assay

The plaque assay had been conducted according to previous methods devised with modification (Chu et al., 2018, 2019). The HeLa cell line was first seeded in a 24-well plate in DMEM and incubated to a confluency of 80-90% in a 37°C incubator with 5% CO2 for 48 hours. The HeLa cells were infected with 200 µL of diluted (10^{-5}) NDV in complete DMEM, and they were incubated for 1 hour. After the incubation, the viral inoculum was taken out, and the cells were then washed with DMEM. 500 µL of semi-solid medium containing the diluted *L. decumana* extracts (20, 40, 60, 80, and 100 µg/mL) mixed with 1.5% Carboxymethylcellulose (CMC) in DMEM supplemented with 2% FBS and 1% Penicillin-Streptomycin were added to the cell monolayers. After being incubated for 72 hours, the cells were stained with 1% crystal violet (100 µL per well) without removing the CMC media and were incubated at room temperature for 15 minutes. After incubation, the dyed medium was removed, and the cells were washed once with PBS. Finally, cells were preserved with 2% formaldehyde. The plaque size measurement was performed after the removal of formaldehyde.

Gene expression analysis

HeLa cell lines were seeded in a 24-well plate and incubated for 24 hours. The cells were then infected with NDV (MOI: 1) for 1 hr before the viral inoculum was removed and treated with 40 µg/mL of *L decumana* for 24 hrs. After 24 hrs, RNA of HeLa cell lines was extracted using GeneAid RNA Extraction Kit based on the provider's protocol. The quality of the RNA was then assessed using a Nanodrop spectrophotometer in which all of the samples had a 260/280 ratio of 2.0 to 2.2 and a 260/230 ratio of 1.8 to 2.1. The cDNA was then synthesized by following the RevertAid First Strand cDNA Synthesis Kit protocol. The qRT-PCR data was generated in TOYOBO Sybr qPCR Mix based on the provider's protocol; the primers to detect NDV virus expression were 5' – AAAGTGGTGACACAGGTCGG-3' as forward and 5'- CCGATGTATTGCCGCTCAAG-3' as reverse (Mao et al., 2022). The data is examined using the $2^{-\Delta\Delta Ct}$ method (Livak & Schmittgen, 2001).

Data Analysis

The quantitative data used in this experiment was analyzed using GraphPad, using two-way ANOVA for statistical significance and Student T-test for pair-to-pair comparison of data.

RESULT AND DISCUSSION

Cytotoxic Activity of L. decumana extract towards HeLa cells using MTS assay

L. decumana exerts a cytotoxic effect on 150 µg/mL, 200 µg/mL, and 250 µg/mL (cell viability of 32.2%, 29.6 %, and 26.5%). At a concentration of 100 µg/mL or lower, L. decumana increased the viability of Hela cells by 65% (Figure 1.) The IC_{50} (50% cytotoxic concentration) for *L. decumana* obtained was at 131 µg/mL.

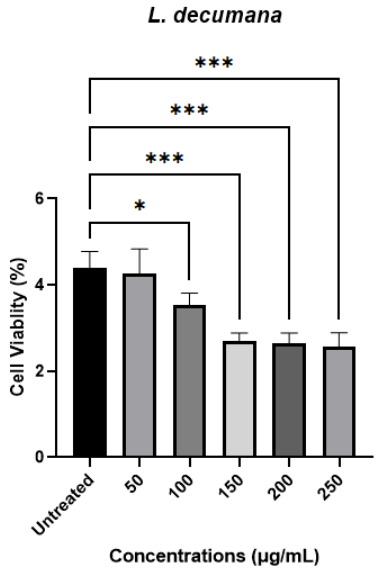

Figure 1. Cytotoxicity result of HeLa cells treated with *L. decumana*. The data presented as mean ± SD (*) P ≤ 0.05 & (***) P ≤ 0.001

In this study, *L. decumana* proved high toxicity at 150 µg/mL and higher concentrations. The IC_{50} of *L. decumana* was approximately 131 µg/mL, which killed 50% of the HeLa cells. The safe concentration to be considered is *L. decumana* at 100 µg/mL or lower since it still has 65% and above cell viability. This *in vitro* study should be investigated further with an *in-vivo* model since the results of the *in vitro* assay do not always match with the results of the *in-vivo* analysis (Di Nunzio et al., 2017).

Assessment of antiviral activity of L. decumana extracts against NDV by plaque assay

The Hela cells infected with NDV under different conditions were observed under the microscope to examine the cell morphology and proliferation. As seen in Figure 2A. and Figure 2B., NDV-infected Hela cells had thinner cell morphology and lower cell density compared to the healthy ones. When being treated with *L. decumana* with a concentration of 20 µg/mL, the infected HeLa cells looked healthier, resulting in similar cell morphology to the negative control but slightly lower in cell density (Figure 2C). Figure 2D indicated a significant improvement in cell morphology and cell proliferation as well as very high cell confluency with monolayer formation by treating the infected cells with 40 µg/mL of *L. decumana* leaf extracts.

HeLa has been reported to be a preferred target by NDV due to its rapidly replicating nature (Chu et al., 2019). Hence, the infection and cytopathic effect (CPE) was observed. After removing the stain and fixing the cells following the plaque-forming assay protocol, the virus growth was measured through the diameter of the plaque (Goh et al., 2016). The plaque sizes were visibly reduced in the 20 µg/ml and 40 µg/mL *L. decumana* extract treated wells compared to the untreated one. By increasing the *L. decumana* extract concentration to 60, 80, and 100 µg/mL, no plaques could be observed anymore. However, it should be noted that there were less visibly stained cells when they were treated with higher concentrations. A higher concentration of *L. decumana* extract could exert growth inhibition of the HeLa cells, marked by a relatively lighter density of stained HeLa cells (Figure 2 B, C, D). Cytotoxicity of plant extracts towards HeLa cells has been demonstrated from various plants as well (Amna et al., 2019; Ismail et al., 2020; Mavrikou et al., 2020).

In this study, to explore whether the treatment had an impact on NDV replication, qPCR was performed with 40 µg/mL of *L. decumana*-treated HeLa cells, and the untreated group served as the control. However, the qPCR results of NDV in HeLa cells were not significant when being treated with 40 µg/mL of *L. decumana* (Figure 3). The non-treated, infected cells still showed CPE, and the *L.*

decumana-treated cells showed less CPE and cell death. This indicates that *L. decumana* extract did not affect the replication activity of NDV. The outcome most likely indicates that the active compound is not a replication-inhibiting agent for viruses. The viral entry, assembly, and release are the most likely targets for the compound, as has been demonstrated on *Polyalthia longifolia*. It is shown that it inhibits viral entry and budding but not attachment and viral RNA replication (Yadav et al., 2020).

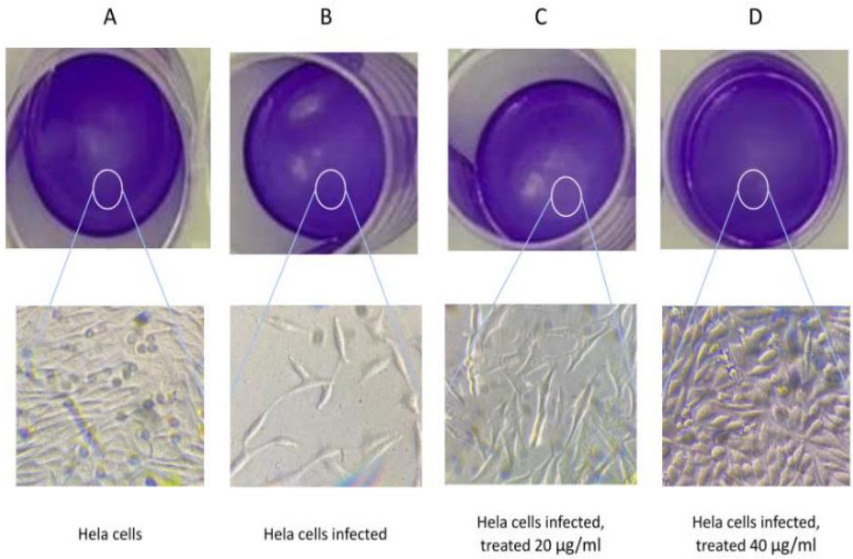

Figure 2. Plaque forming assay result of HeLa cells against NDV (A) HeLa cells without NDV infection and *L. decumana* treatment, (B) infected with NDV and not treated with *L. decumana*, (C) infected with NDV and treated with 20 µg/mL of *L. decumana*, and (D) infected with NDV and treated with 40 µg/mL of *L. decumana*

Viral gene expression analysis

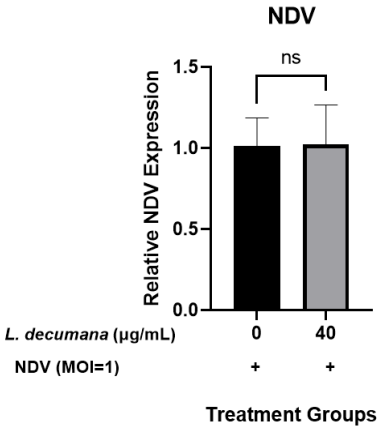

Figure 3. The relative expression of NDV in HeLa cells treated with *L. decumana*.

CONCLUSION

The experimental results show that *L. decumana* extract inhibits NDV production at a dose of 20 µg/mL, with no evidence of viral gene downregulation. It is suggested that the inhibition of *L. decumana* extract occurs at the protein level, where it could produce non-infectious viral particles. Further investigation is necessary to confirm its mechanism.

At a concentrarion of 100 µg/mL, the methanolic extract of *L. decumana* produced above 65% cell viability in HeLa cells. At a dose of 20 µg/mL, the NDV virus plaque assay showed inhibition,

indicating the antiviral activity. The gene expression research revealed no downregulation of viral gene expression, suggesting that other mechanisms, such as entrance, assembly, or budding, are being inhibited rather than viral replication. Mechanistic studies on *L. decumana* methanolic extract can also be done to further elucidate the antiviral activity.

In conclusion, *L. decumana* has proved to produce a high toxicity at 150 µg/mL and higher concentrations where its IC_{50} lies at 131 ug/mL. *L. decumana* also shows an inhibitory effect at the dose of 20 µg/mL, which indicates antiviral activity. However, the gene expression analysis result shows that *L. decumana* could not downregulate the viral gene expression, suggesting that other mechanisms, such as entrance, assembly, or budding, are being inhibited rather than viral replication. Mechanistic studies on *L. decumana* methanolic extract can also be done to further elucidate the antiviral activity.

REFERENCES

Absalón, A. E., Cortés-Espinosa, D. V., Lucio, E., Miller, P. J., & Afonso, C. L. (2019). Epidemiology, control, and prevention of Newcastle disease in endemic regions: Latin America. *Tropical Animal Health and Production*, *51*(5), 1033–1048. https://doi.org/10.1007/s11250-019-01843-z

Amna, U., Halimatussakdiah, Wahyuningsih, P., Saidi, N., & Nasution, R. (2019). Evaluation of cytotoxic activity from Temurui (*Murraya koenigii* [Linn.] Spreng) leaf extracts against HeLa cell line using MTT assay. *Journal of Advanced Pharmaceutical Technology & Research*, *10*(2), 51. https://doi.org/10.4103/japtr.JAPTR_373_18

Bayer, F. P., Gander, M., Kuster, B., & The, M. (2023). CurveCurator: a recalibrated F-statistic to assess, classify, and explore significance of dose–response curves. *Nature Communications*, *14*(1), 7902. https://doi.org/10.1038/s41467-023-43696-z

Butt, S. L., Moura, V. M. B. D., Susta, L., Miller, P. J., Hutcheson, J. M., Cardenas-Garcia, S., Brown, C. C., West, F. D., Afonso, C. L., & Stanton, J. B. (2019). Tropism of newcastle disease virus strains for chicken neurons, astrocytes, oligodendrocytes, and microglia. *BMC Veterinary Research*, *15*(1), 317. https://doi.org/10.1186/s12917-019-2053-z

Chu, Z., Gao, X., Liu, H., Ma, J., Wang, C., Lu, K., Han, Q., Wang, Y., Wang, C., Adam, F. E. A., Wang, X., Xiao, S., & Yang, Z. (2019). Newcastle disease virus selectively infects dividing cells and promotes viral proliferation. *Veterinary Research*, *50*(1), 27. https://doi.org/10.1186/s13567-019-0644-0

Chu, Z., Ma, J., Wang, C., Lu, K., Li, X., Liu, H., Wang, X., Xiao, S., & Yang, Z. (2018). Newcastle disease virus V protein promotes viral replication in HeLa Cells through the activation of MEK/ERK signaling. *Viruses*, *10*(9), 489. https://doi.org/10.3390/v10090489

Di Nunzio, M., Valli, V., Tomás-Cobos, L., Tomás-Chisbert, T., Murgui-Bosch, L., Danesi, F., & Bordoni, A. (2017). Is cytotoxicity a determinant of the different in vitro and in vivo effects of bioactives? *BMC Complementary and Alternative Medicine*, *17*(1), 453. https://doi.org/10.1186/s12906-017-1962-2

Dzogbema, K. F.-X., Talaki, E., Batawui, K. B., & Dao, B. B. (2021). Review on newcastle disease in poultry. *International Journal of Biological and Chemical Sciences*, *15*(2), 773–789. https://doi.org/10.4314/ijbcs.v15i2.29

Ellebedy, A. H., & Ahmed, R. (2016). Antiviral vaccines: challenges and advances. In *The Vaccine Book* (pp. 283–310). Elsevier. https://doi.org/10.1016/B978-0-12-802174-3.00015-1

Goh, K. C. M., Tang, C. K., Norton, D. C., Gan, E. S., Tan, H. C., Sun, B., Syenina, A., Yousuf, A., Ong, X. M., Kamaraj, U. S., Cheung, Y. B., Gubler, D. J., Davidson, A., St John, A. L., Sessions, O. M., & Ooi, E. E. (2016). Molecular determinants of plaque size as an indicator of dengue virus attenuation. *Scientific Reports*, *6*(1), 26100. https://doi.org/10.1038/srep26100

Ismail, I., Suppian, R., Mohamad, H., Radzi, S. A. M., & Abdullah, H. (2020). In vitro cytotoxicity and apoptosis-inducing activity of quercus infectoria extracts in HeLa Cells. *Pharmacognosy Journal*, *13*(2), 401–410. https://doi.org/10.5530/pj.2021.13.51

Kaur, G., & Dufour, J. M. (2012). Cell lines: valuable tools or useless artifacts. *Spermatogenesis*, *2*(1),

`1-5. https://doi.org/10.4161/spmg.19885

Livak, K. J., & Schmittgen, T. D. (2001). Analysis of relative gene expression data using real-time quantitative PCR and the $2^{-\Delta\Delta CT}$ method. *Methods*, *25*(4), 402–408. https://doi.org/10.1006/meth.2001.1262

Mao, Q., Ma, S., Schrickel, P. L., Zhao, P., Wang, J., Zhang, Y., Li, S., & Wang, C. (2022). Review detection of Newcastle disease virus. *Frontiers in Veterinary Science*, *9*. https://doi.org/10.3389/fvets.2022.936251

Masoud, F., Mahmood, M. S., Rahman, S. U., & Abbas, R. Z. (2022). An efficient approach for the recovery of LaSota strain of newcastle disease virus from cloned cDNA by the Simultaneous use of seamless PCR cloning technique and RNA-POL II promoter. *Pakistan Veterinary Journal*, *42*(3), 346–351. https://doi.org/10.29261/PAKVETJ/2022.059

Mast, J., Nanbru, C., Decaesstecker, M., Lambrecht, B., Couvreur, B., Meulemans, G., & van den Berg, T. (2006). Vaccination of chicken embryos with escape mutants of La Sota Newcastle disease virus induces a protective immune response. *Vaccine*, *24*(11), 1756–1765. https://doi.org/10.1016/j.vaccine.2005.10.020

Mavrikou, S., Tsekouras, V., Karageorgou, M.-A., Moschopoulou, G., & Kintzios, S. (2020). Anticancer and biochemical effects of Viscum album L. protein extracts on HeLa cells. *Plant Cell, Tissue and Organ Culture*, *140*, 369–378. https://doi.org/10.1007/S11240-019-01733-0/METRICS

Murulitharan, K., Yusoff, K., Omar, A. R., & Molouki, A. (2013). Characterization of Malaysian velogenic NDV strain AF2240-I genomic sequence: A comparative study. *Virus Genes*, *46*, 431–440. https://doi.org/10.1007/S11262-012-0874-Y/FIGURES/1

Ninfali, P., Antonelli, A., Magnani, M., & Scarpa, E. S. (2020). Antiviral properties of flavonoids and delivery strategies. *Nutrients*, *12*(9), 2534. https://doi.org/10.3390/nu12092534

Simaremare, E. S., Ruban, A., & Runtuboi, D. Y. P. (2018). Aktivitas antibakteri ekstrak etanol daun Gatal (Laportea aestuans (L.) Chew). *Jurnal Biologi Papua*, *9*(1), 1–7. https://doi.org/10.31957/jbp.101

Thalib, A., Masadah, R., Prihartono, P., Hamid, F., Haidir, M., Hasan, H., Keliwawa, S., & Labulawa, I. (2022). Antioxidant activity of *Laportea decumana* (Roxb) wedd ethanol and n-Hexane extracts. *Open Access Macedonian Journal of Medical Sciences*, *10*(A), 590–594. https://doi.org/10.3889/oamjms.2022.8399

Thalib, A., Masadah, R., Prihartono, P., Hamid, F., Hasan, H., Keliwawa, S., & Labulawa, I. (2021). *Laportea decumana* (Robx) Wedd. herbal endemic potential from Indonesia: A literature review. *Open Access Macedonian Journal of Medical Sciences*, *9*(F), 639–643. https://doi.org/10.3889/oamjms.2021.7759

Yadav, P., Choudhury, S., Barua, S., Khandelwal, N., Kumar, N., Shukla, A., & Garg, S. K. (2020). Polyalthia longifolia leaves methanolic extract targets entry and budding of viruses-an in vitro experimental study against paramyxoviruses. *Journal of Ethnopharmacology*, *248*, 112279. https://doi.org/10.1016/j.jep.2019.112279